Investigation of new ways to generate and capture transient cyclic allenes

by

Marius-Georgian Constantin

A thesis submitted in partial fulfillment of the requirements for the degree of

Doctor of Philosophy

Department of Chemistry

University of Alberta

Abstract

Transient cyclic allenes are strained reactive intermediates currently underexploited in the synthetic organic field. Although there are several literature-known ways to generate and capture cyclic allenes, there is still room for new complementary methods to be developed. This thesis will discuss new ways to generate several cyclic allenes through lithium- and magnesium-halogen exchange promoted elimination. A new way of trapping electron-deficient cyclic allenes through a hetero-Diels–Alder cycloaddition will also be presented.

In Chapter 1, cyclic allenes will be discussed in the larger context of reactive intermediates. This review will also introduce notions about the properties, methods to generate and the chemical behavior of cyclic allenes. Several recent results present in the literature will showcase the current research direction in this area.

In Chapter 2, the results regarding new ways to generate several cyclic allenes through lithium- and magnesium-halogen exchange promoted elimination will be discussed. The typical dimerization and trapping of cyclic allenes were examined under these new conditions. Our investigation revealed that lithium-halogen exchange provided access to a series of dimers. Based on the initial findings with lithium halogen exchange, we developed an improved method using magnesium-halogen exchange, which offered access to specific trapping products and dimers.

In Chapter 3, an investigation on the generation of electron-deficient cyclic allenes through base-promoted elimination will be presented. An unprecedented mode of dimerization of cyclic allenes was discovered. We later developed a new way of trapping electron-deficient cyclic allenes with enamines through a hetero-Diels–Alder

cycloaddition. This novel trapping provided access to several structurally complex polycyclic products.

Chapter 4 will discuss the research efforts to find a new method to generate C-acylimine reactive intermediates using a manganese (III) one-electron oxidizing agent. This discussion will focus on obtaining a single diastereomer isolated product during those efforts and my attempt to explain the formation of that product.

Chapter 5 will provide a set of conclusions and possible future research plans for each of the projects presented in this thesis.

Preface

Part of Chapter 2 of this thesis will be published as Constantin, M. G.; Almehmadi, Y. A.; Liu, X.; West, F. G "Generation of cyclic allenes through metal-halogen exchange promoted elimination" manuscript in preparation. I was responsible for the experimental work, the data collection, and characterization of compounds as well as the manuscript composition for compounds **5, 88, 89, 81**. Almehmadi, Y. A. (equal contribution) was responsible for the experimental work, the data collection, and characterization of compounds as well as the manuscript composition for compounds **92**, **87**. Liu, X. (an undergraduate research student mentored by me) was responsible for the experimental work, the data collection, and the characterization of compounds **5**, **87**, **6**, **93**. West, F. G. was the supervisory author involved in concept formation and manuscript composition.

Part of Chapter 3 of this thesis has been published as Wang, B.; Constantin, M. G.; Singh, S.; Zhou, Y.; Davis, R. L.; West, F. G. "Generation and trapping of electron-deficient 1,2-cyclohexadienes. Unexpected hetero-Diels–Alder reactivity" *Org. Biomol. Chem.* **2021**, *19* (2), 399–405. I was responsible for the experimental work, the data collection, and characterization of compounds and the manuscript composition concerning the trapping with enamines part of the paper (I made **49a-g** and **50** as final products and their precursors). Wang, B. was responsible for the experimental work, the data collection, and characterization of compounds, as well as the manuscript composition concerning the dimerization (**37a-c**) and trapping with furan (**30a-d**) and 1,3-diphenylisobenzofuran (**36a-d**). Singh, S. was responsible for the computational calculation part of the paper. Zhou, Y. was responsible for the X-ray crystallography analysis of cycloadduct **49a**, which confirmed the relative stereochemistry assignment for this compound. Davis, R. L. and

West, F. G. were the supervisory authors involved in concept formation and manuscript composition.

Acknowledgements

First of all, I would like to extend my thanks to my supervisor, Professor Frederick G. West, for his continuous support, excellent research guidance, and for letting me embark in his group for my graduate school journey. I have learned a lot about organic chemistry from our interactive research discussions and group meetings. Thank you for bearing with me and help me get to this stage.

Second, I would like to thank all current and former West group members: Kyle and Yaaseen, for great discussions about cyclic allenes and research in general; Yury, Ahmed O., Ahmed E., Maxwell, Natasha, Jenny, Luna, Shaohui, Mandy, Peter, Olivier for being great lab coworkers and good conversation partners. I would like to thank Xinghai for working together for several months on cyclic allenes and his refreshing curiosity about organic chemistry in general. I would like to offer my special thanks to Shorena, who has helped me accommodate to the lab, graduate school, and life in a new environment in general. She provided good advice for developing lab skills and extending my organic chemistry knowledge.

Next, I would like to thank all chemistry support staff for keeping the department running in great shape and always finding solutions for any technical problem a graduate student may have.

Last, I would like to thank my sister for having an almost daily phone conversation and for being willing to listen to my mundane problems. Your moral support over the years helped me a lot during my Ph.D. studies.

For anyone that I might have omitted in here, I will now thank you.

Table of Contents

List of Figures

List of Tables

List of Schemes

List of symbols and abbreviations

^{1}H	proton
^{13}C	carbon 13
β	beta position
σ	sigma bond
º	degree(s)
π	pi bond
Ac	acetyl
appquint	apparent quintet
APT	attached proton test
aq	aqueous
Ar	aryl
calcd.	calculated
COSY	correlation spectroscopy
d	doublet
DABCO	1,4-diazabicyclo[2.2.2]octane
DCM	dichloromethane
dd	doublet of doublets
ddd	doublet of doublets of doublets
dddd	doublet of doublets of doublets of doublets
DMAP	4-(dimethylamino)pyridine
DMF	dimethylformamide
DMS	Doering–Moore–Skattebøl

DMSO	dimethylsulfoxide
DPIBF	diphenylisobenzofuran
dtdd	doublet of triplets of doublets of doublets
EI	electron impact
EDG	electron donating group
equiv.	equivalent(s)
Et	ethyl
ESI	electro spray ionization
EWG	electron withdrawing group
FVP	flash vacuum pyrolysis
hfacac	hexafluoroacetylacetonate
HDDA	hexadehydro-Diels–Alder
HOMO	highest occupied molecular orbital
HRMS	high resolution mass spectrometry
HSQC	heteronuclear single quantum coherence spectroscopy
i-PrMgCl	isopropylmagnesium chloride
IR	infrared spectroscopy
kcal	kilocalorie(s)
KIE	kinetic isotope effect
KO*t*-Bu	potassium *tert*-butoxide
LDA	lithium diisopropylamide
LG	leaving group
LiHMDS	lithium bis(trimethylsilyl)amide

L_n	ligand
LUMO	lowest unoccupied molecular orbital
L-Selectride	lithium tri-*sec*-butylborohydride
M	metal
M^+	molecular ion peak
m	multiplet
Me	methyl
MeLi	methyllithium
min	minute(s)
mmol	millimole(s)
m/z	mass-to-charge ratio
n-BuLi	*n*-butyllithium
NBS	*N*-bromosuccinimide
NMR	nuclear magnetic resonance
Nu	nucleophile
OAc	acetoxy
OTf	triflate
OTs	tosylate
pp	pages
ppm	parts per million
Py	pyridine
q	quartet
R	generic alkyl group

R_f	retention factor
rt	room temperature
s	singlet
s-BuLi	*sec*-butyllithium
SET	single electron transfer
SOMO	singly occupied molecular orbital
t	triplet
TBAF	tetrabutylammonium fluoride
t-BuLi	*tert*-butyllithium
t-BuMgCl	*tert*-butylmagnesium chloride
TEMPO	2,2,6,6-tetramethylpiperidine 1-oxyl
THF	tetrahydrofuran
TMS	trimethylsilyl
TMP	2,2,6,6-tetramethylpiperidinyl
TOCSY	total correlation spectroscopy
TROESY	transverse rotating-frame Overhauser enhancement spectroscopy
Ts	tosyl

1. Generation and trapping of reactive cyclic allenes

1.1 Common reactive intermediates in organic chemistry

1.1.1 Background

Organic chemistry through the study of the compounds containing carbon, the most chemically prolific element, occupies a significant role in the larger field of chemistry. Reactive intermediates have a key role in organic chemistry through their presence in a plethora of reactions. They are short-lived species generated and consumed during specific reactions. Understanding the generation, mechanistic implications, and the chemistry of reactive intermediates allows for more effective exploitation in valuable and novel synthetic transformations that rely on their reactivity; thus their research is of the utmost importance for the continuing development of organic chemistry.[1–3]

During a chemical reaction, when reactants are transforming into products, they go through maximum free energy states, known as transition states (*Figure 1.1*). The transition state has partially formed or broken bonds, and it may violate the valence bond rules for certain atoms. On the other hand, reactive intermediates have fully formed bonds and are transient species present in the reaction for a certain length of time, depending on their stability. They constitute energy minima in-between transition states.[1–3]

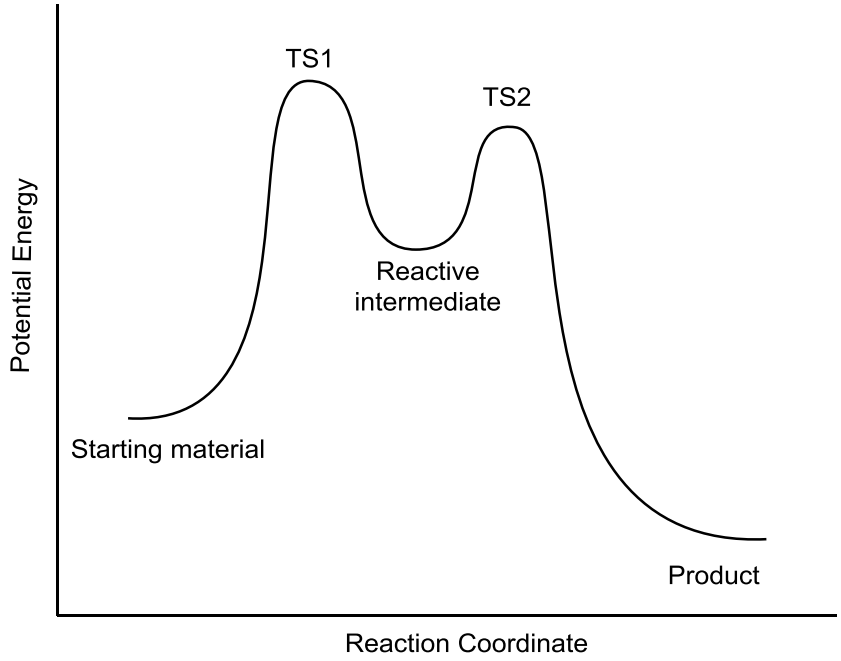

Figure 1.1 Reaction profile involving a reactive intermediate

There are different types of reactive intermediates, which can be categorized by several criteria: the source of their reactivity, the electric charge, or the coordination on the central element.[3] From the source of reactivity, one can distinguish reactive intermediates with incomplete valence shell (carbocations **1**, radicals **2**, carbenes **3**), and complete valence shell (carbanions **4**, strained intermediates) as shown in *Figure 1.2*. There are numerous strained reactive intermediates known in the literature,[4] but the focus in this chapter will be on cyclic allenes **7** and similar species such as benzynes **5** and cycloalkynes **6**. Regarding the electric charge, there are examples of reactive intermediates with positive (carbocations **1**), negative (carbanions **4**), or neutral charges (radicals **2**, carbenes **3**, benzynes **5**, cycloalkynes **6**, cyclic allenes **7**).

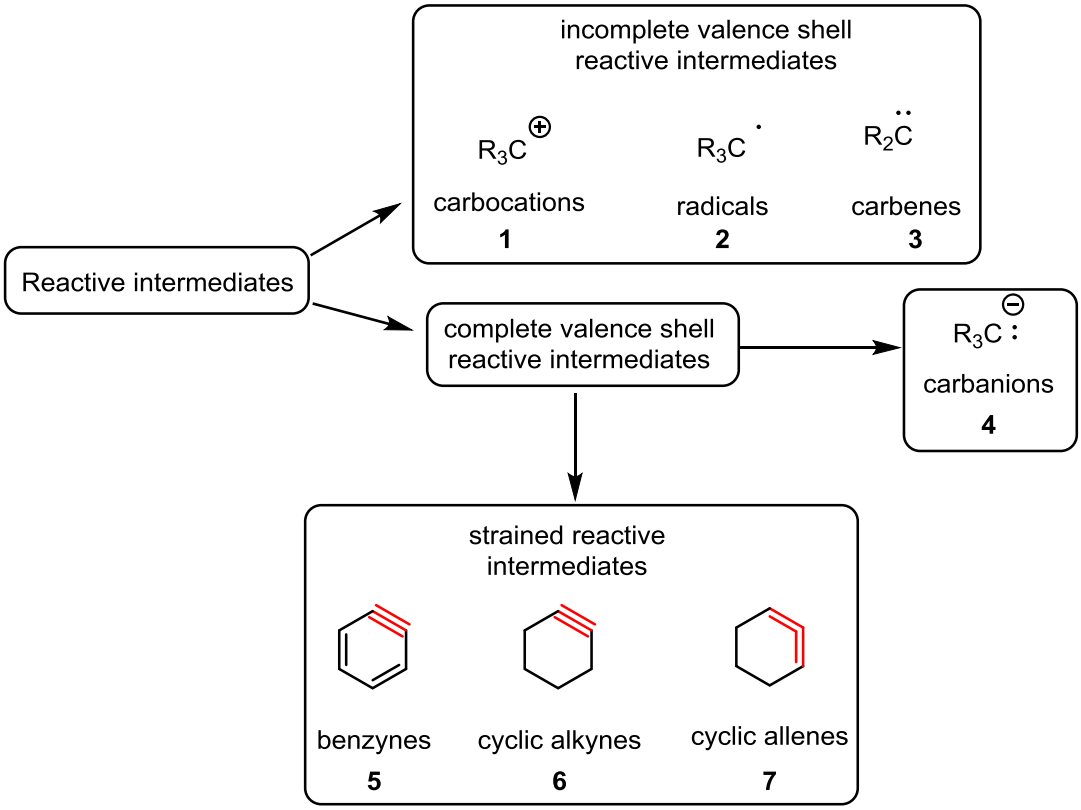

Figure 1.2 Classification of reactive intermediates by the source of their reactivity

Table 1.1 Reactive intermediates categorized by coordination on the central atom

	-onium ion	neutral molecule	radical	anion	-enium ion	-ene
C	$R_5C^{\oplus}$ carbonium ion	R_4C	$R_3C^{\bullet}$ carbon radical	$R_3C:^{\ominus}$ carbanion	$R_3C^{\oplus}$ carbenium ion	$R_2C:$ carbene
N	$R_4N^{\oplus}$ ammonium ion	$R_3N:$	$R_2N^{\bullet}:$ aminyl radical	$R_2N^{\ominus}$ amide anion	$R_2N:^{\oplus}$ nitrenium ion	$RN:$ nitrene
O	$R_3O^{\oplus}:$ oxonium ion	$R_2O:$	$RO^{\bullet}:$ oxyl radical	$RO:^{\ominus}$ alkoxide	$RO:^{\oplus}$ oxenium ion	$O:$ oxene

In terms of coordination on the central atom, one can observe a range of types of reactive species (from carbonium ion to carbene in the case of carbon), which show

different properties depending on the coordination level and the valence shell status (*Table 1.1*).[1,3] Similar ranges of different reactive intermediates can be observed for nitrogen (from ammonium ion to nitrene) and oxygen (from oxonium ion to oxene).

1.1.2 Carbanions

Carbanions are nucleophilic reactive intermediates that have a fundamental role in the advancement of the organic chemistry field. Although they are highly reactive transient species in a plethora of organic reactions, many can be stored for days or weeks, usually in an organometallic form dissolved in an appropriate solvent. The most common organometallics are the commercially available organolithium and Grignard reagents. The stability of different carbanions increases with the *s* character of the orbital containing the pair of electrons (*Figure 1.3*). Therefore an sp^3 carbanion **4** would be less stable than an sp^2 carbanion **8**, which would be less stable than *sp* carbanion **9**.[5,6]

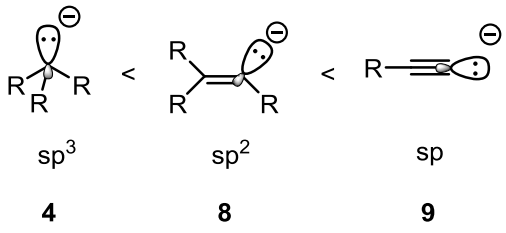

Figure 1.3 The relative stability of carbanions

The sp^3 carbanions can undergo inversion depending on the energy barrier for this process, as shown in *Scheme 1.1*. Methyl anion **10** has a shallow energy barrier for the inversion, while trifluoromethyl anion **11** shows a much higher energy barrier which in this particular case is correlated with the highly electronegative fluorine substituents. Another way to increase the energy barrier is the use of ring strain. For example, the inversion barrier for the cyclopropyl carbanion **12** is 16.3 kcal/mol.[7]

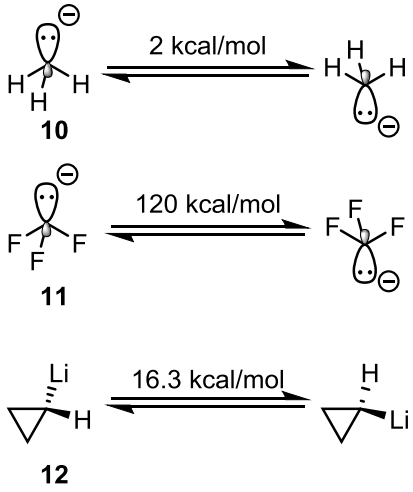

Scheme 1.1 Inversion barriers of several carbanions

1.1.3 Carbocations

Carbocations are representative reactive intermediates known for over 100 years. They are transient species in well-known reactions such as S_N1, E1 and several rearrangements. According to Olah, carbocations should be classified by the coordination number on the positive carbon, as seen with carbenium ions **13** in the case of a coordination number of three and carbonium ions **14** in the case of coordination number of five (or greater for non-classical carbocations) as depicted in *Figure 1.4*. [8–10]

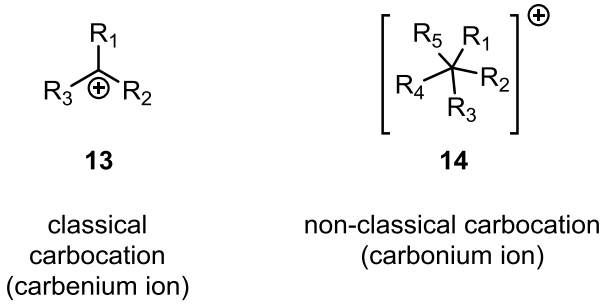

Figure 1.4 Classification of carbocations

Classical carbocations (carbenium ions) **13** are common reactive intermediates in organic chemistry. They possess an sp^2 hybridization on the central carbon with an empty

p orbital **15**, which can engage in hyperconjugation with neighboring sigma bonds when those are properly aligned **16** (*Figure 1.5*). Alkyl substituents have an inductive electronic effect which can increase the electron density on the carbocation and make it more stable. Therefore tertiary carbocations **17a** are more stable than their secondary analogues **17b**, which are more stable than primary carbocations **17c**.

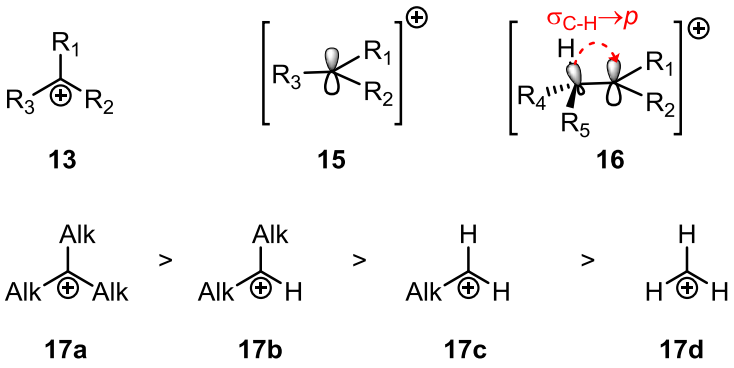

Figure 1.5 Structure and relative stability of carbocations

The proposal of non-classical carbocations evoked intense debate in the organic chemistry community. The question in this debate was if these carbocations were 3-center 2-electron species or if they were a pair of classical carbocations **18a** and **18b** in fast equilibration (*Figure 1.6*). The investigation focused at the beginning on figuring out the structure of the 2-norbornyl cation. Shortly, through the means of ^{13}C NMR spectroscopy at low temperature, it was shown that the two labeled carbons were giving only one signal, which corresponds to the delocalized non-classical carbocation **18** proposal.[11–14]

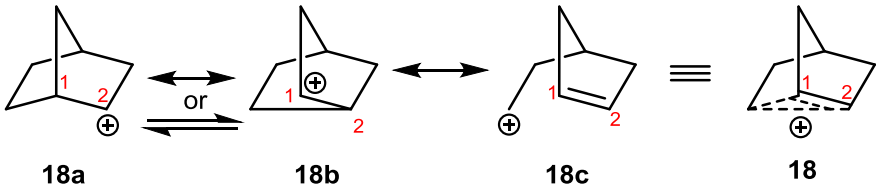

Figure 1.6 The structure of 2-norbornyl carbocation **18**

1.1.4 Radicals

Radicals are common reactive intermediates in organic chemistry that have an unpaired electron. The highest energy occupied orbital of these species is usually referred as SOMO, which stands for singly-occupied molecular orbital. Depending on the nature of the SOMO orbital, there could be π radicals in which the SOMO is a *p*-type orbital and σ radicals where the SOMO is a hybrid orbital (sp^3, sp^2, *sp*) as presented in *Figure 1.7*. Methyl radical **19** is a π-radical with all the substituent hydrogen atoms in the same plane, but depending on the substituents, this type of radical can become through pyramidalization a σ-radical. Electronegative substituents can induce pyramidalization; thus, trifluoromethyl radical **21** is a σ-radical with tetrahedral geometry. Although, in general, the cyclic alkanes give π-radical species as the cyclohexyl radical **20**, cyclopropyl radical **22** is a σ-radical with 3 kcal/mol inversion barrier. Aromatic radicals and vinylic radicals are of σ-radical type and in the case of vinyl radicals **23** and **24** one can observe fast inversions similar to the sp^3 σ-radicals.[15]

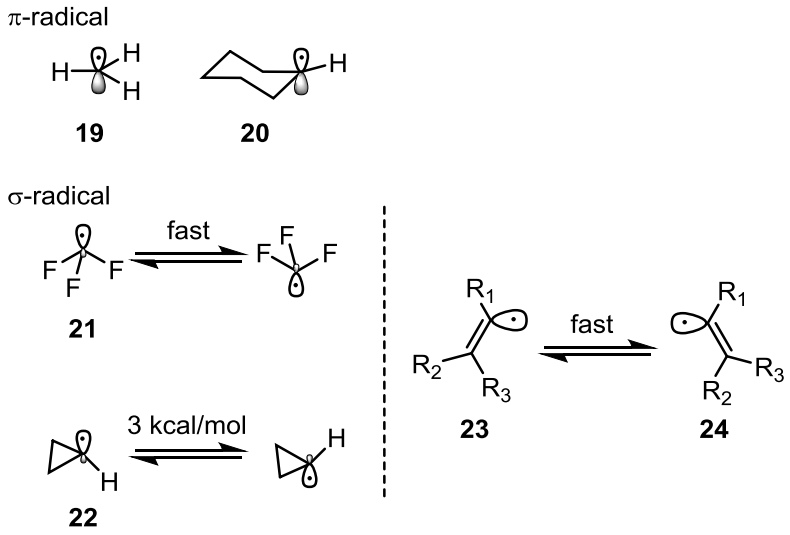

Figure 1.7 Radicals classification based on the nature of SOMO

A more particular case of reactive intermediate species is 1,4-biradicals which are well-studied in the literature.[16–18] A 1,4-diradical reactive intermediate **25** can be generated through different thermal or photochemical processes. Depending on the structural

particularities of the starting material and the reaction conditions used, one could get access to cyclobutanes **26** and **27** and olefin **28** as presented in *Scheme 1.2*. A similar type of transient species was proposed as an intermediate in the mechanism of dimerization of cyclic allenes, which will be discussed further in this chapter.

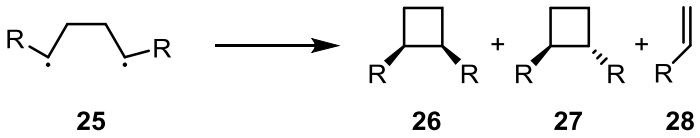

Scheme 1.2 Reactions of 1,4-biradicals

1.1.5 Carbenes

Carbenes, as commonly encountered active intermediates, can be classified as singlet and triplet carbenes. In the singlet carbenes, the two electrons are paired, while in triplet carbenes, the two electrons are unpaired (*Figure 1.8)*. In **29a** singlet configuration of methylidene the two opposite spin electrons are in the sp^2 orbital and the *p* orbital is unoccupied. In the triplet configuration of methylidene shown in **29b**, the two unpaired electrons occupy different orbitals, one in an sp^2 orbital and one in the *p* orbital. Another triplet carbene configuration for methylidene is the *sp* hybridized methylidene **29c** linear carbene, which presents two orthogonal *p* orbital with one electron in each. In general, carbenes are bent, with rare cases of linear carbenes. Carbenes are known as ambiphiles, acting both as a nucleophile or as an electrophile depending on the reaction partner and on the carbene itself.[19–21]

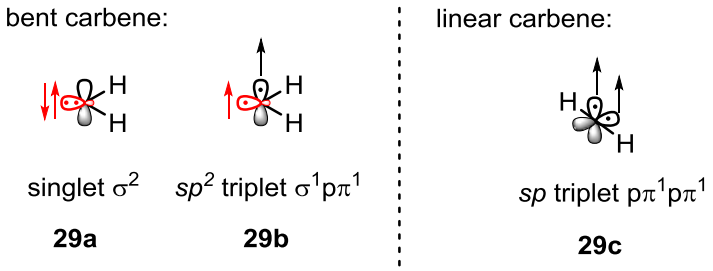

Figure 1.8 Classification of carbenes by electronic configurations

Although the free carbenes have been known as interesting reactive intermediates with exciting potential for synthetic organic chemistry, these intermediates become more commonly used only after the discovery and development of metallocarbenes.[22,23] The use of metallocarbenes allows increased control over these reactive intermediates, most of them being easily generated in situ, or some could be synthesized and isolated as stable reagents (*Scheme 1.3*). In general, a metallocarbenes **32** can be generated from the reaction of a diazo starting material **30** and the corresponding transition metal with release of nitrogen. Depending on the nature of metallocarbenes **32** and other conditions, they can act as an electrophilic carbene **32a** or as a nucleophilic carbene **32b**.[24]

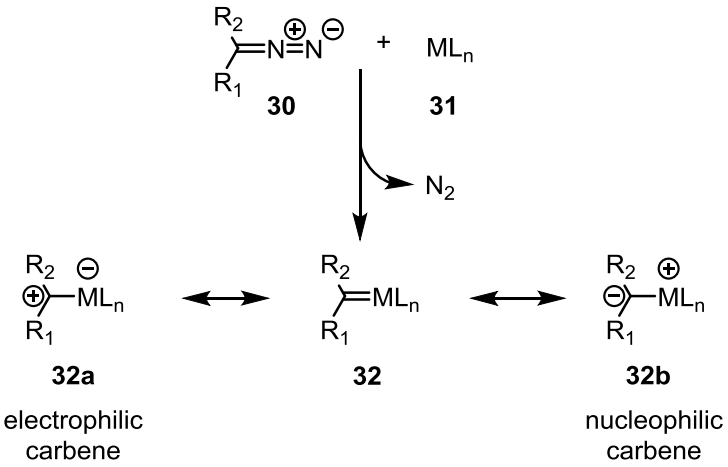

Scheme 1.3 The ambiphilic nature of carbenes

1.1.6 Arynes

Arynes are strained reactive intermediates well studied and known in the organic chemistry field for over a century. [25] During this time, several methods to generate benzyne **5** were developed, as shown in *Scheme 1.4*. Being a well-researched topic, there are currently several comprehensive reviews on aryne chemistry.[26–30] Benzyne **5** can be generated through the decomposition upon heating of certain diazonium starting material **33**.[31] Base promoted elimination methods are available through the use of aryl halide

starting materials **34**.[32,33] A milder way to generate benzyne is the use of fluoride promoted elimination strategy using starting materials as **35a** and **35b**.[34,35] Metal-halogen exchange promoted elimination generation methods were also used in the case of benzynes from starting materials as **36a** and **36b**.[36,37] The hexadehydro-Diels–Alder (HDDA) reaction in between 1,3-diynes **37** and alkynes **38** is also known to generate benzynes.[38]

The Diels–Alder reaction is one of the typical trapping processes where arynes are involved as the dienophile, and the trapping partner is the diene (*Scheme 1.4*). A representative [4+2] cycloaddition is between benzyne **5** and furan **39** where cycloadduct **45** was obtained.[35] Benzyne **5** could be involved in [2+2] cycloaddition, in which it could have as partner an electron-rich olefin as the ketene acetal **40** to obtain benzocyclobutene **46**.[39] In certain conditions, such as in the presence of a palladium (0) catalyst **41**, benzyne **5** can undergo trimerization to get triphenylene **47**.[40] Since benzynes have an electrophilic character they can participate in the nucleophilic addition of different nucleophiles, such as diisopropylamine **42**, obtaining *N,N*-diisopropylaniline **48**.[41] Another interesting reaction observed with benzyne **5** is the insertion in β-keto-ester **43** to obtain ortho-disubstituted arenes **49**.[42] Benzynes also participate in [3+2] cycloadditions, such as the reaction of benzyne **5** with 3-oxo-pyrazolidinium **44** trapping reagents, where structurally complex 1,2-diazetin-3-one cycloadducts **50** can be obtained.[43]

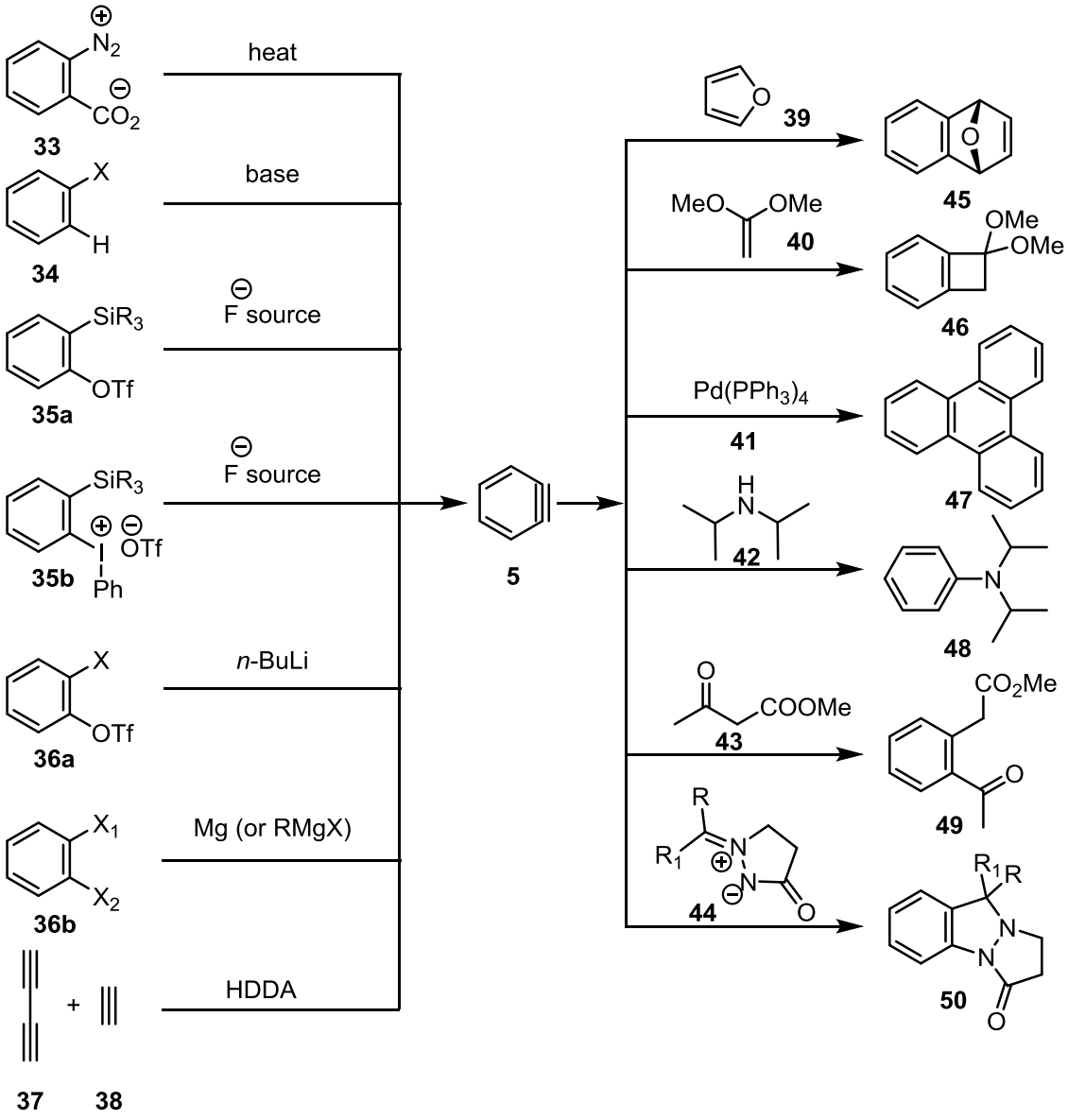

Scheme 1.4 Generation and trapping of benzyne **5**

These reactive intermediates were also used in total synthesis. The Stoltz group generated a benzyne intermediate from starting material **51**, which could insert in beta-keto-ester **52** to furnish the polycyclic skeleton of the natural product in intermediate **53** (*Scheme 1.5*).[44] Ten more steps were performed in the synthetic route to get access to (+) amurensinine **54** eventually.

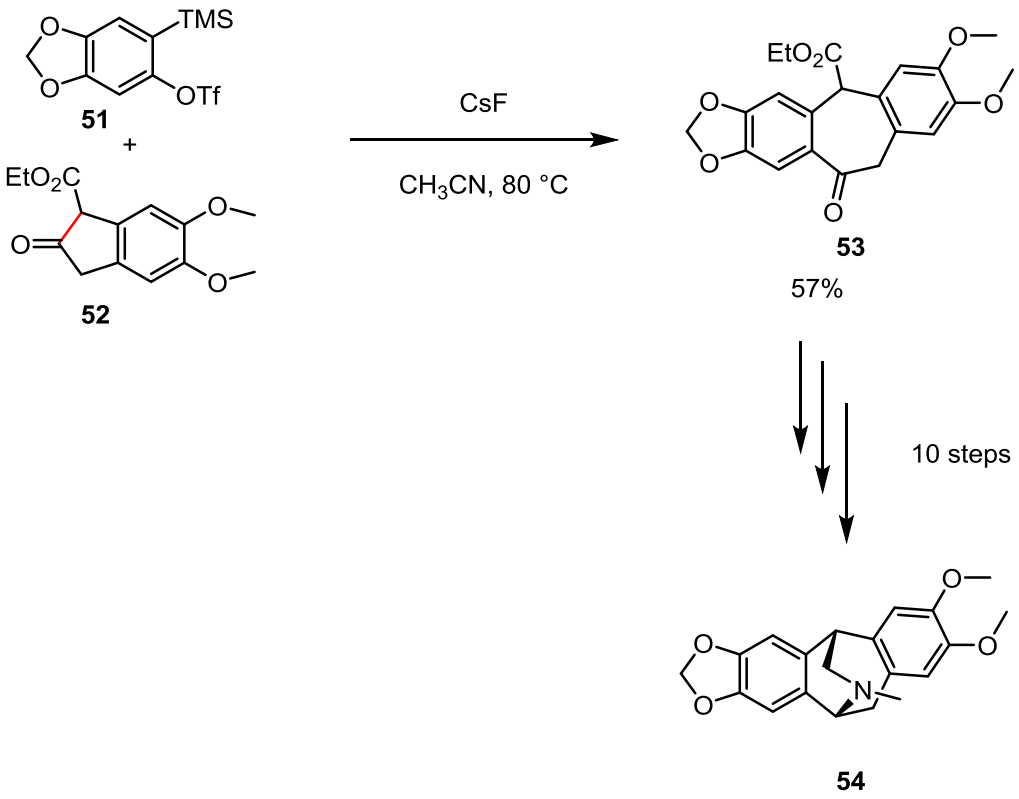

Scheme 1.5 Synthesis of (+) amurensinine **54**

More recent work was done in a series of projects in Hoye's group where they used the hexadehydro-Diels–Alder (HDDA) reaction to generate benzynes and then trap those intramolecularly or intermolecularly. They were able to access a plethora of polycyclic compounds using this method.[38] In this approach, carefully designed starting material such as triyne **55** was involved, which upon heating in chloroform for 18h, underwent the HDDA reaction to generate benzyne **56**. During the reaction, once reactive intermediate **56** is generated, it would react with suitable trapping partners, such as norbornene, to give the *exo* cycloadduct **57** in this particular case.[45]

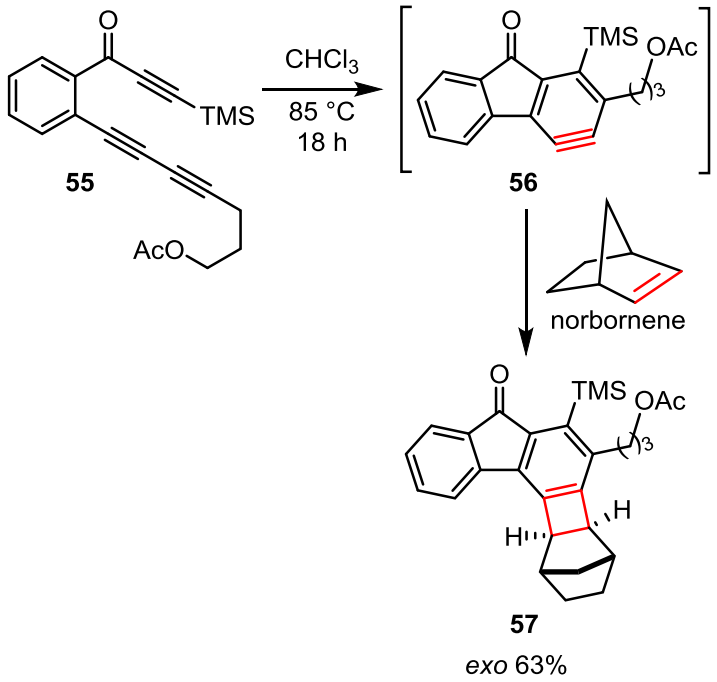

Scheme 1.6 The generation of arynes via HDDA reaction

1.1.7 Cycloalkynes

Cycloalkynes are strained reactive intermediates isomeric with the cyclic allenes, making them of particular interest for our research. The two isomeric species cyclohexyne **6** and 1,2-cyclohexadiene **7** could be generated from halocyclohexenes **58** through base elimination (*Scheme 1.7*). From studying the base elimination using KO*t*-Bu in DMSO for different halocyclohexenes it was found that 1-chlorocyclohexene **58a** gave mostly 1,2-cyclohexadiene **7** (96:4), while using 1-iodocyclohexene **58b** increased the relative amount of cyclohexyne **6** to a 50:50 ratio.[46]

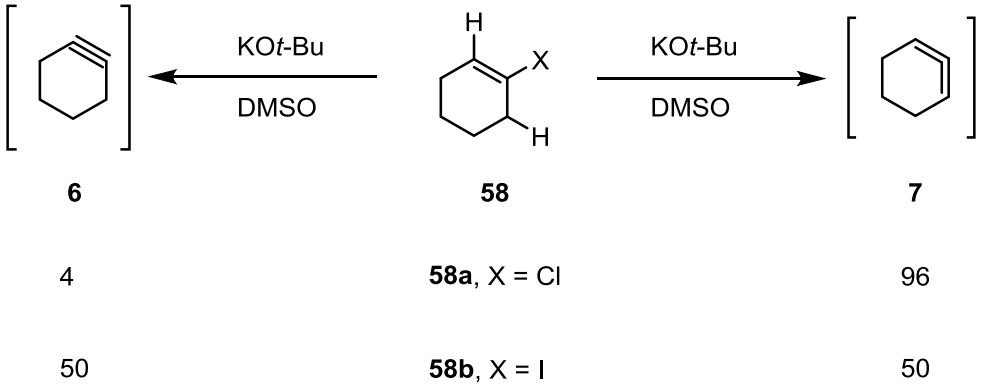

Scheme 1.7 Generation of cyclohexyne **6** versus 1,2-cyclohexadiene **7**

Cycloalkynes present a significantly perturbed geometry of the triple bond compared to the linear geometry of the acyclic alkynes. Bach has calculated the strain energies, bending angles, and bond lengths for several cycloalkynes (*Figure 1.9*).[47] These results also correlate well with other computational studies of cycloalkynes.[48–50] One can easily observe that the strain energy decreases with increasing ring size. While cyclohexyne **6** is a transient species, cycloheptyne **59** has a half-life of one hour at -78 ºC. Cyclooctyne **60** is a more stable compound, which in fact can be isolated. However, due to a considerable ring strain energy of approximatively 20 kcal/mol, it retains some residual reactivity as compared with an unstrained alkyne, which can be exploited in certain transformations.[51,52]

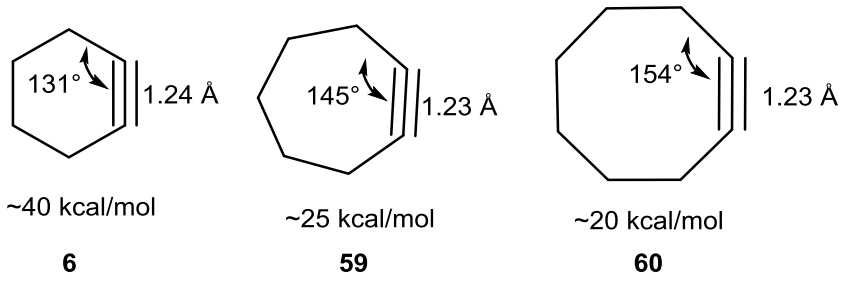

Figure 1.9 Calculated strain energies and bending angles of cycloalkynes **6**, **59** and **60**

A more recent use of cycloalkynes is in biorthogonal chemistry. Bertozzi's group showed that one could use biotin-derived cyclooctynes **61** in reaction with azide modified glycoproteins **62** to furnish triazoles **63** (*Scheme 1.8*).[53] This is an excellent example of how fundamental chemistry discoveries could find application. The [3+2]-cycloaddition of

alkynes with azides initially developed by Huisgen and co-workers was done at high temperatures, thus making this method unsuitable for biological systems.[54] Later, Sharpless and coworkers developed the copper(I) catalyzed version of this reaction, which, although used in many biological applications, still had a severe drawback in terms of the copper toxicity towards bacterial and mammalian cells.[55] The method developed by Bertozzi can now be used in living cells as well since it is a copper-free method, and uses the ring strain of the cyclooctyne **61**.

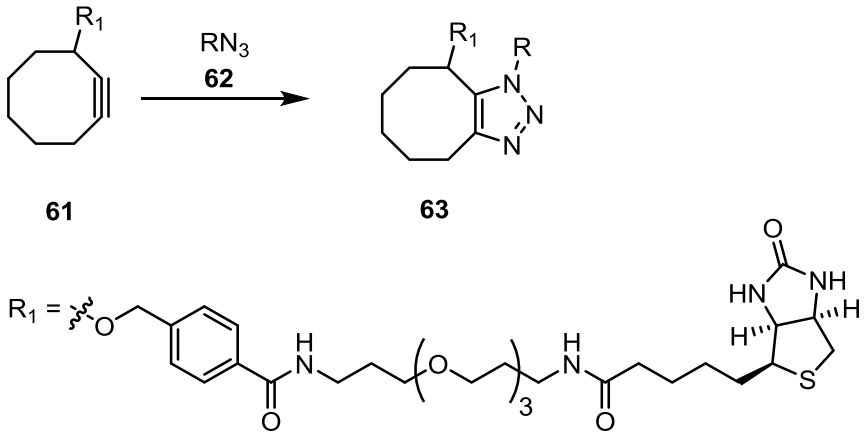

Scheme 1.8 The [3+2] cycloaddition of azide **62** and cyclooctyne **61**

1.1.8 Cyclic allenes

Cyclic allenes are the main focus of my research and the topic of this introductory chapter. It will be discussed more in terms of influential research results in this area over time and recent findings that can open new investigation avenues. Several reviews and book chapters were published on this subject over the years, representing a comprehensive literature review at those dates in time.[56–61]

The reactivity of cyclic allenes is strongly correlated with ring strain energy. The ring strain energy comes from bending and twisting a typical acyclic allene's linear and orthogonal geometry when the two-component double bonds of an allene are set in an appropriate size ring. Several groups studied the geometry and the ring strain energy of the reactive cyclic allenes computationally.[62–65] Studies by the Johnson group showed that the

ring strain energy increases with the decrease of the ring size from just 2 kcal/mol for the 1,2-cyclononadiene **66** up to 32 kcal/mol for 1,2-cyclohexadiene **7** (*Figure 1.10*).[65] Their calculations also revealed that the bending angle of the 3-carbon allene unit increase with ring size from 138º in 1,2-cyclohexadiene **7** to 170º in 1,2-cyclononadiene **66**. Another geometrical parameter calculated was the out-of-plane hydrogen bending angle, which is the angle in between C-H bond and the plane defined by the 3 carbon atoms forming the allene moiety. This angle is 45º for a typical allene **68**. The out-of-plane hydrogen bending angle increases with ring size from 23º in 1,2-cyclohexadiene **7** to 34º in 1,2-cyclononadiene **66**. In order to obtain these results, they performed semiempirical MNDO calculations. [65]

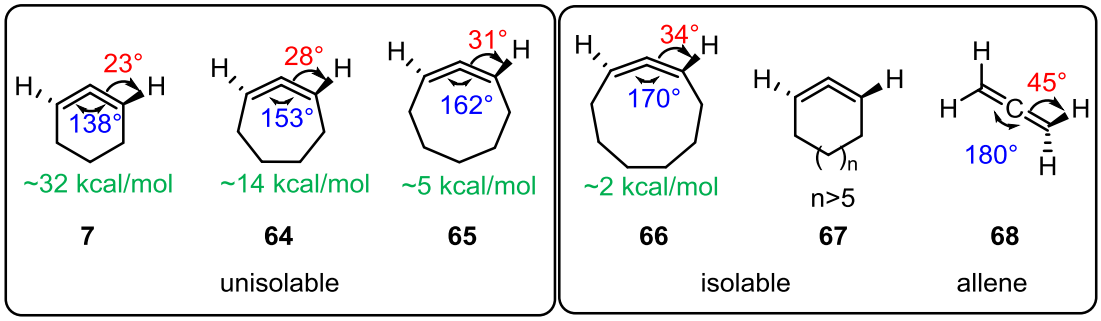

Figure 1.10 Strain energies and bending angles for cyclic allenes

Once the first clear demonstration for the generation of 1,2-cyclohexadiene **7** was achieved, discussions and proposals concerning the structure and the electronic configuration of this transient molecule began. Several proposals were suggested over the years, including two possible zwitterion species **7a** and **7b**, two possible diradical species singlet **7c** and triplet **7d** and the closed-shell allene structure **7**, which is chiral in contrast to the planar species **7a-d**.[65] The discussion resolved when several experimental and theoretical were pointing towards the chiral allene structure **7**. It was found through calculation that the ground state is chiral allene **7** close in energy with the diradical singlet species **7c**.[63] As experimental evidence, the IR absorption recorded by Wentrup's group at 1886 cm-1, which although it was shifted approximatively 70 cm-1 from the typical value for an allene, correlated well with the semiempirical calculations.[66]

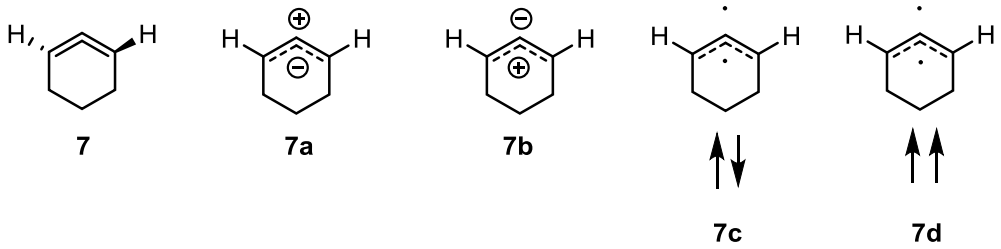

Figure 1.11 Proposed electronic structures of 1,2-cyclohexadiene **7**

During the theoretical studies, it was proposed that the interconversion in between the two possible enantiomers **7P** and **7M** of 1,2-cyclohexadiene **7** would go through the singlet diradical transition state **7c** at around 14-15 kcal/mol higher in energy than the chiral allene **7**.[60] The diradical transition state **69a** for a typical acyclic allene such as 2,3-pentadiene is calculated at around 46 kcal/mol.[68] Although the energy barrier for **7** might not be as high as in typical acyclic allene, it could be enough to keep the chiral properties of the cyclic allene under mild conditions, which would allow chemists to exploit this stereochemical information.

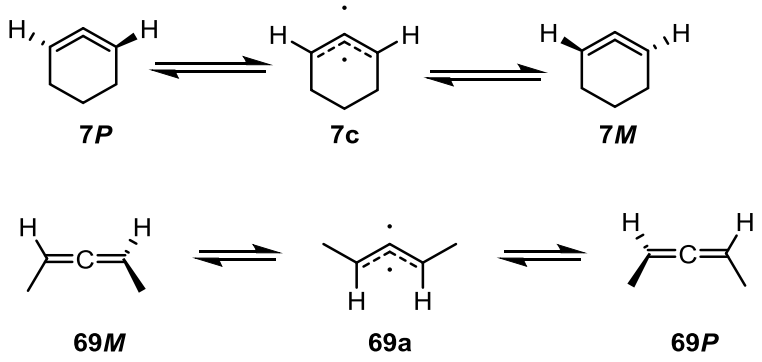

Scheme 1.9 The racemization barrier for **7** and **69**

Balci and Jones generated optically active cyclic allene **7f**, starting from well-designed starting material **70** (*Scheme 1.10*).[69] They exploited the kinetic isotope effect (KIE), by getting selective deprotonation and thus generating an enantioenriched cyclic allene **7f**. The transient species **7f** was captured with DPIBF, and the product cycloadduct **71** was determined to be optically active. This experimental work is quite important since it once again confirmed the chiral, closed-shell nature of 1,2-cyclohexadiene **7**, and demonstrated the potential of cyclic allenes as partners in enantioselective transformations.

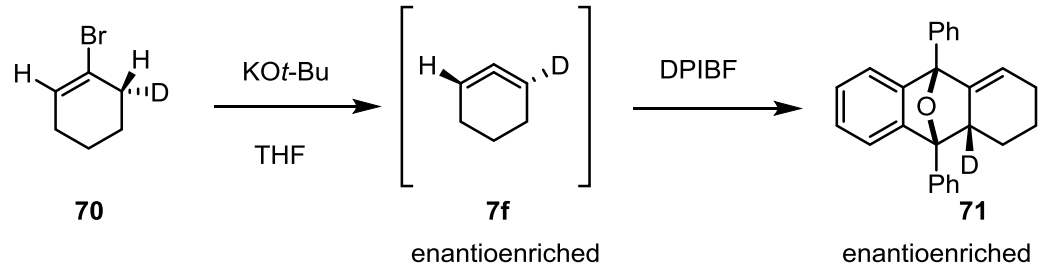

70 **7f** **71**

enantioenriched enantioenriched

Scheme 1.10 Generating and trapping optically active 1,2-cyclohexadiene **7f**

Heterocyclic allenes represent an important direction in the reactive cyclic allene field, which is not fully explored at the moment. When incorporated into the cyclic allene ring, one or more heteroatoms should affect the structure and the electronics of the system, and through those, the reactivity could show new avenues.[56] Boswell and Bass were first to generate aza-3,4-cyclohexadiene **72** and trapped similarly with 1,2-cyclohexadiene **7**.[70] In a more recent study, the Garg group unveiled a range of capturing reactions of this intermediate, which included the generation and trapping of enantioenriched substrates.[71] The isomeric reactive intermediate of **72**, 1-aza-2,3-cyclohexadiene **73**, proved to be an elusive fleeting species with the attempts into its generation performed in Christl group being unsuccessful.[72] However, they were able to generate and trap in a typical manner zwitterion **73a**. Schreck and Christl generated 1-oxa-3,4-cyclohexadiene **74** and studied its chemical behaviour.[73,74] The unsymmetrical isomer of **74**, 1-oxa-2,3-cyclohexadiene **75**, was generated and trapped with typical trapping reagents where a difference in the reactivity of the two double bonds was observed since the electromer effect of the oxygen is increasing the electron density on its neighboring double bond.[75] The substrates with sulphur in the ring 1-thia-3,4-cyclohexadiene **76** and 1-thia-2,3-cyclohexadiene **77** were also studied.[56] The studies of heterocyclic allenes went further in substrates with two or three heteroatoms in the ring as **78**,[76] **79**,[77] **80**,[78] **81**,[79] and **82**.[80,81]

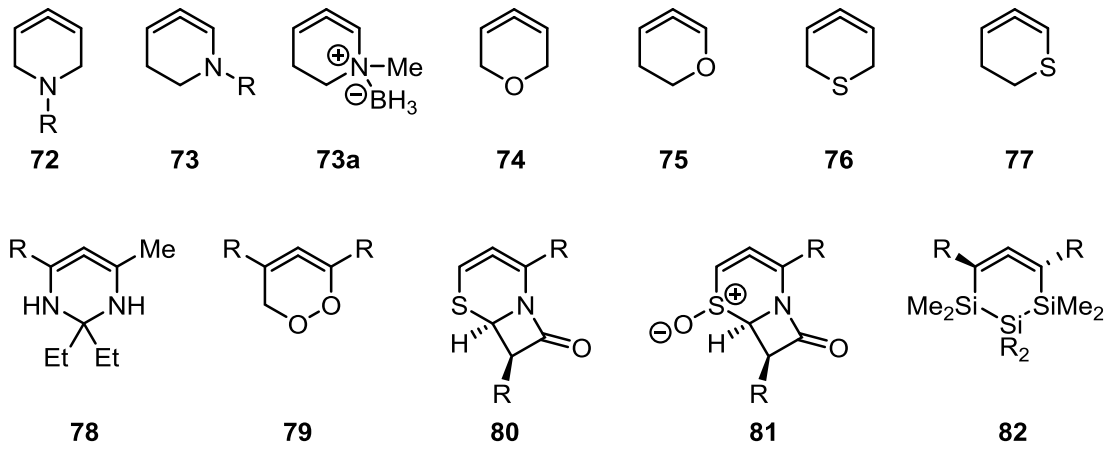

Figure 1.12 Studied 6-membered ring heterocyclic allenes

1.2 Reactive cyclic allenes generation methods

Reactive cyclic allenes such as 1,2-cyclohexadiene **7** started as a curiosity in organic chemistry, but they now capture more attention as a research area. Of course, in order to study reactive cyclic allenes experimentally, one needs to find an appropriate method to generate such reactive intermediates. Thus the question of what methods to generate cyclic allenes are available arises (*Scheme 1.11*). The most common methods to generate reactive cyclic allenes are base elimination,[82,83] Doering–Moore–Skattebøl (DMS) rearrangement,[84,85] and fluoride promoted elimination.[86] The treatment of 1,6-dichlorocyclohexene **86** with magnesium generated **7** as well.[87] Wentrup used flash vacuum pyrolysis (FVP)[66] to generate 1,2-cyclohexadiene **7** through a decarbonylation of **87** followed by a rearrangement of an intermediary carbene. In this subchapter, several approaches to generate cyclic allenes will be discussed. The subchapter will focus only on the methodology to generate cyclic allenes, the synthetic routes towards the precursors, the advantages and the drawbacks of each methodology.

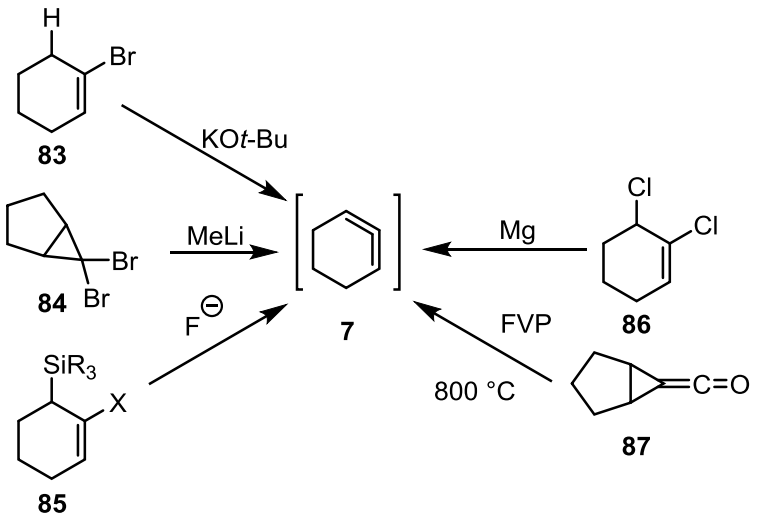

Scheme 1.11 Methods to generate 1,2-cyclohexadiene **7**

1.2.1 Generation of cyclic allenes through base elimination

Although some other work was done towards the generation of 1,2-cyclohexadiene **7** none could prove clearly that this transient species was generated until Wittig and Fritze were able to generate and trap 1,2-cyclohexadiene **7** (*Scheme 1. 12*). [82,83] They developed a base promoted elimination method in which 1-bromocyclohexene **83** in the presence of KO*t*-Bu generated 1,2-cyclohexadiene **7**, which was captured with diphenylisobenzofuran (DPIBF). The Diels–Alder reaction resulted in a mixture of *endo*/*exo* cycloadducts **88** in 38% yield as an outcome of the Diels–Alder trapping process. When they did not use a trapping reagent, they could isolate the dimer product in 7%. As discussed in section 1.1.7, when one uses a base elimination method on 1-halo-cyclohexene substrates, there could be a competing reaction towards cyclohexyne elimination product. Another possible drawback of this method is the harsh base involved in the reaction, which could potentially present incompatibility issues with a more functionalized substrate or some trapping reagents.

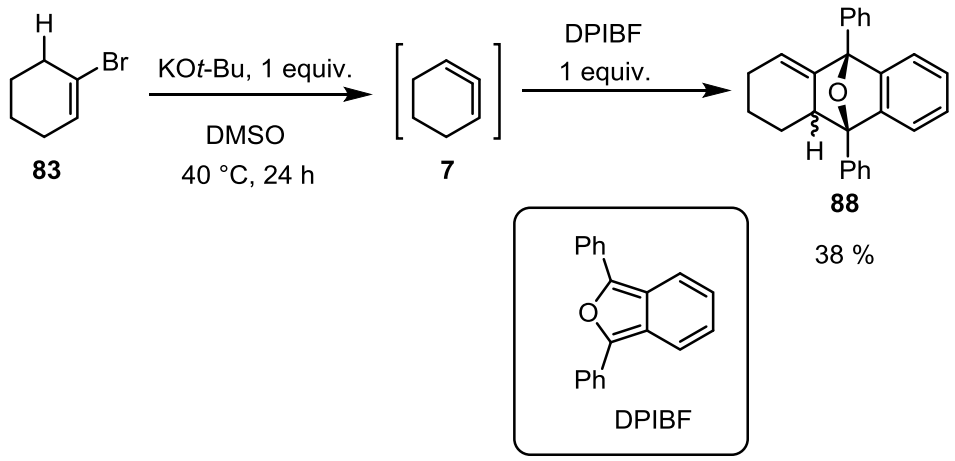

Scheme 1.12 Generation of 1,2-cyclohexadiene **7** through base elimination

A recent example of the generation of cyclic allenes through base promoted elimination used a magnesium amide (*Scheme 1.13*).[88] The starting material triflate **90** was obtained through the 1,4-addition to the commercially available enone **89** followed by triflation of the resulting enolate. It should be noted that the steric demand of the *gem*-dimethyl moiety helped favour the elimination of triflate via removal of the highlighted allylic proton on **90** to form the cyclic allene **91** in preference to the isomeric cyclic alkyne that would have resulted from elimination involving the alkenyl proton. Once **90** was generated, it was captured with DPIBF, resulting in two regioisomers, **92a** and **92b**. The main advantage of this method is the convenient accessibility of the starting material. The requirement for *gem*-dimethyl moiety might be considered a drawback, but considering how this was made, one may use the 1,4-addition in the future to install more complex substituents there.

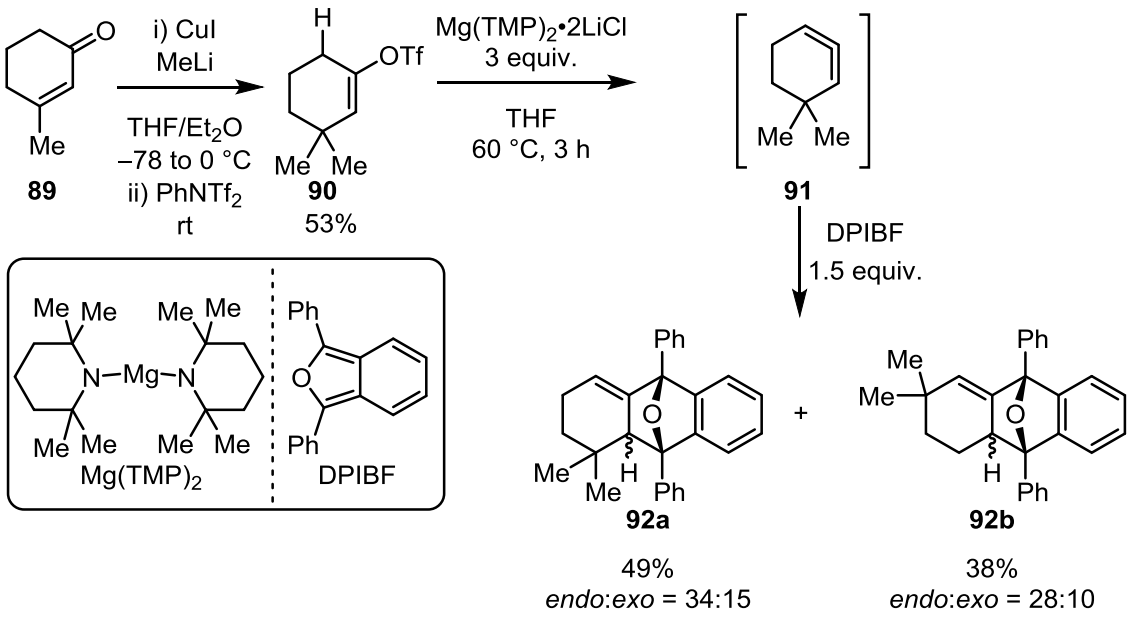

Scheme 1.13 Generation of cyclic allenes using magnesium amide base elimination

1.2.2 Doering–Moore–Skattebøl rearrangement

One of the early alternative methods developed to generate 1,2-cyclohexadiene 7 was the Doering–Moore–Skattebøl rearrangement, first investigated by Moore and Moser as a new way to generate reactive cyclic allenes (*Scheme 1.14*).[84,85] They were inspired to test this method since a similar methodology for the synthesis of acyclic allenes from *gem*-dibromocyclopropane starting materials and organolithium reagents was already in use at that time.[89–91] They were able to generate 1,2-cyclohexadiene **7** and capture it with styrene when they slowly added methyllithium to 6,6-dibromobicyclo[3.1.0]hexane **84** dissolved in styrene. The cycloadduct with styrene was obtained as a mixture of diastereomers, **93a** *exo* and **93b** *endo*, in a 2.2:1 ratio in a good yield. The starting material is obtained through the [2+1] cycloaddition of the *in situ* generated dibromocarbene to cyclopentene **94**. The advantages of this method are the short route to the starting material and the well-established use of the Doering–Moore–Skattebøl reaction. The drawbacks of this are the harsh conditions for the reaction and synthesis of starting material, which limit the variety

of possible substrates. There is also the intermediacy of carbenoid **84a** in the reaction which can undergo undesired side reactions in competition with the ring-expansion.

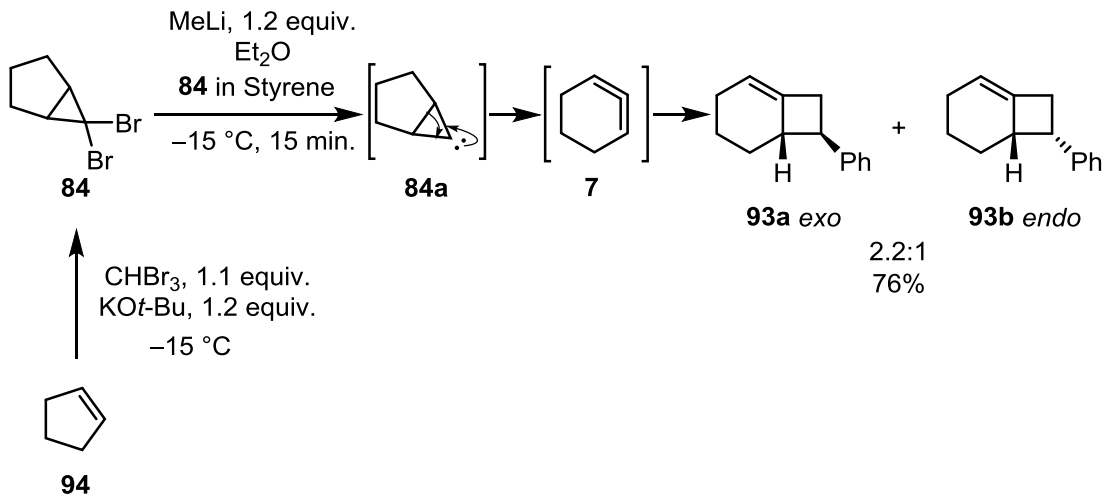

Scheme 1.14 Generation of 1,2-cyclohexadiene **7** through the DMS rearrangement

1.2.3 Fluoride promoted elimination

Shakespeare and Johnson initiated the studies in the fluoride promoted elimination method for generation of cyclic allene (*Scheme 1.15*).[86] They showed that 1,2-cyclohexadiene **7** could be easily generated from silyl bromide **85**, in the presence of cesium fluoride, and then trapped with DPIBF to provide cycloadduct **88** in similar yields with the base elimination reported by Wittig.[82,83] Although this method uses a starting material that can present certain difficulties to synthesize, there is an important advantage in the relatively mild conditions used compared to previously used methods.

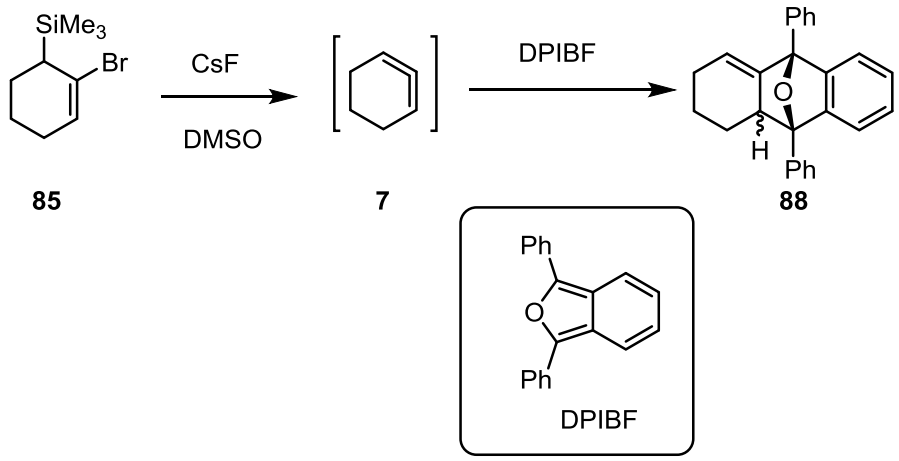

Scheme 1.15 First generation of cyclic allene through fluoride promoted elimination

After Shakespeare and Johnson's proof of concept finding in the generation of cyclic allenes through the fluoride-promoted elimination method, several groups showed interest in this method and significant developments were made over the years. The main drawback of this method was the access to the starting material. Therefore, considerable efforts were made over the years to find different strategies to access the starting material.

The Guitián group showed that the silyl triflate starting material could be accessed in 5 steps from 2-cyclohexen-1-one **95** (*Scheme1.16*).[92] This material underwent bromination fallowed by ketone protection into the acetal intermediate **96** driven by removal of water via Dean–Stark trap. Bromoacetal **96** was then employed in a lithium-halogen exchange followed by a silylation of the organolithium intermediate and then deprotection under acidic quenching conditions to furnish silyl enone **97**. Then **97** was selectively reduced with L-Selectride to obtain silyl ketone **98**, which was submitted to triflation under LDA conditions in order to obtain the starting material **99a**. The Garg group employed a similar strategy in order to access triethylsilyl **99b** starting material.[93] With those materials in hands both groups engaged in series of trapping experiments of 1,2-cyclohexadiene **7** generated through fluoride-promoted elimination from silyl triflates **99**.

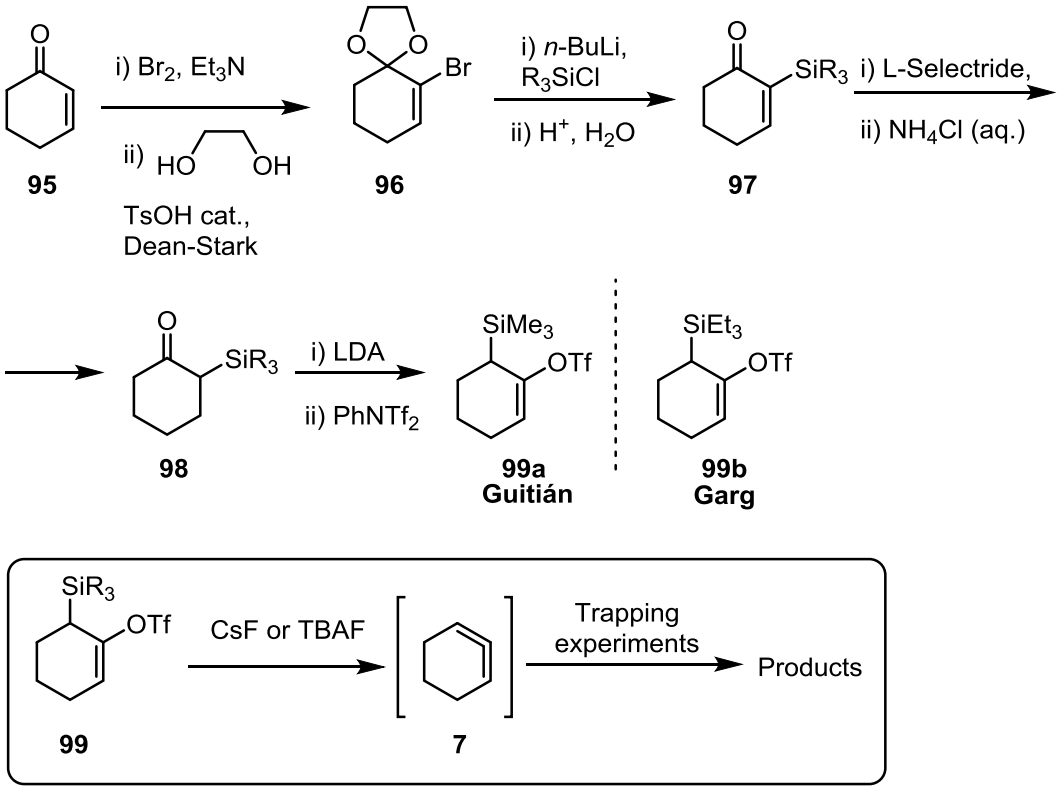

Scheme 1.16 Silyl triflates **99a** and **99b** synthesis under Guitián and Garg protocols

The West group also showed an interesting new strategy recently, where similar allene precursor **99c** for the fluoride promoted elimination to generate 1,2-cyclohexadiene **7** could be obtained in 4 steps from 1,2-cyclohexanedione **100** (*Scheme 1.17*).[94] They started the synthesis with the triflation of 1,2-cyclohexadione **100** to get triflate enone **101**. With **101** in hand, they could transform that in one step into a starting material **102** designed to generate oxygen-substituted 1-acetoxy-1,2-cyclohexadiene **103**. Also, **101** could undergo a Luche reduction followed by a tosylation to access intermediate **104**, which under Cu(I)/$PhMe_2SiLi$ conditions gave access to silyl triflate **99c**. As expected, **99c** had similar behaviour with **99a,** and **99b** described earlier.

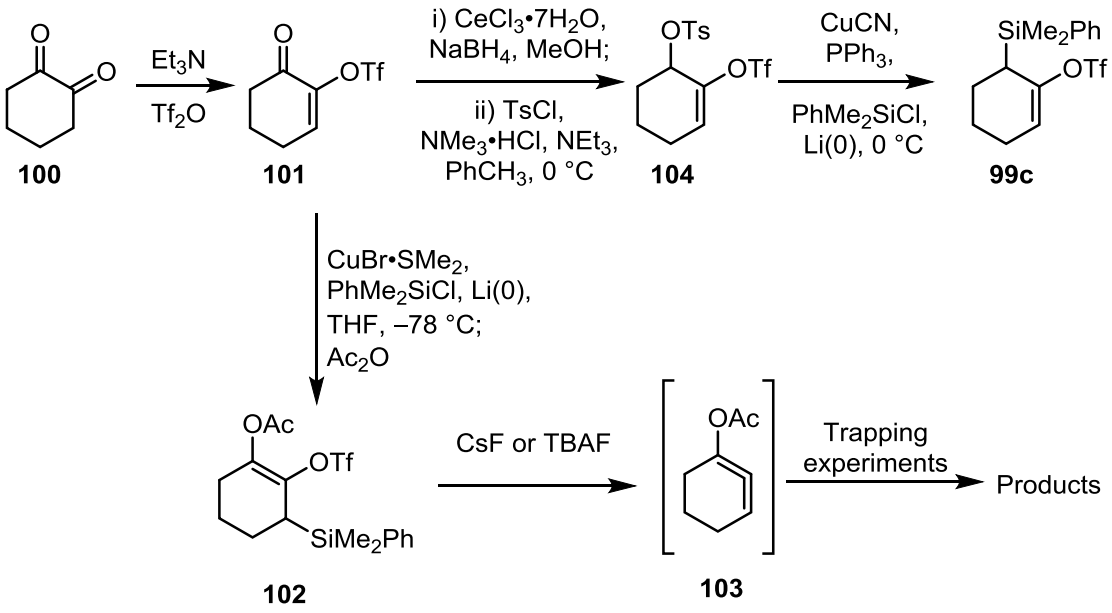

Scheme 1.17 Synthesis of silyl triflates **102** and **99c** in the West group

A more recent advance in this area was made in Mori's group (*Scheme 1.18*).[95,96] They treated a silyl enol ether **105** with LDA and potassium *tert*-butoxide in order facilitate the retro-[1,3]-Brook rearrangement of the silyl group with the deprotonation; thus enolates **106a** and **106b** in equilibrium were generated. Enolate **106a** in reaction with Comins' reagent **107** generated 5 silyl triflates **99a**, **99b**, **99d**, **99e**, and **99f**. Using another set of conditions, they could favor the other enolate **106b**, which can generate corresponding silyl triflates used in the generation of cycloalkynes.

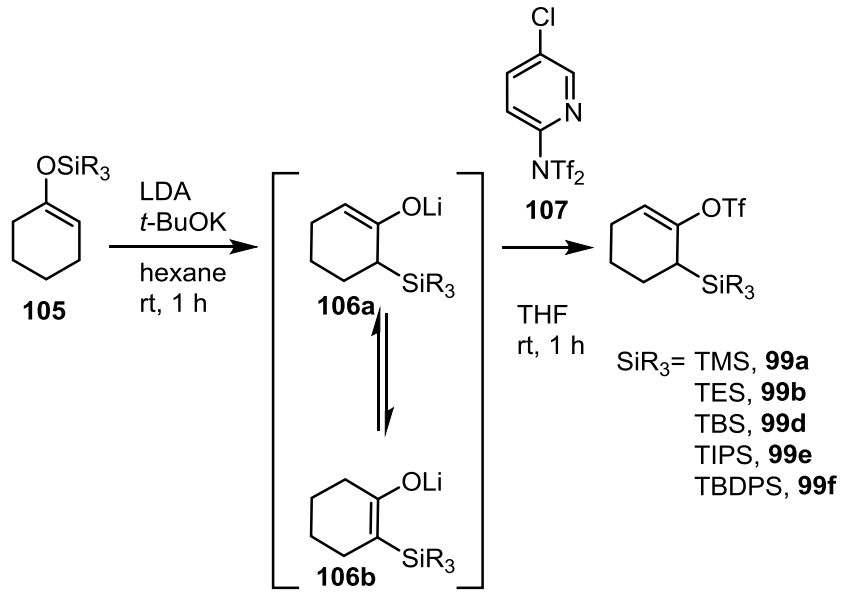

Scheme 1.18 Synthesis of silyl triflates **99a**, **99b**, **99d**, **99e**, and **99f** by Mori's group

Another recent strategy was developed by the Garg group (*Scheme 1.19*).[97,98] The synthesis starts with the silylation of bromoketone **108** to access bromo silyl enol ether **109**. Then **109** undergoes a retro-[1,3]-Brook rearrangement initiated by lithium-halogen exchange reaction to obtain silyl ketone **98a**, which will be transformed into silyl triflate **99b** as shown previously. They also showed that **98a** could be converted in the tosylate version of starting material **110**.[98]

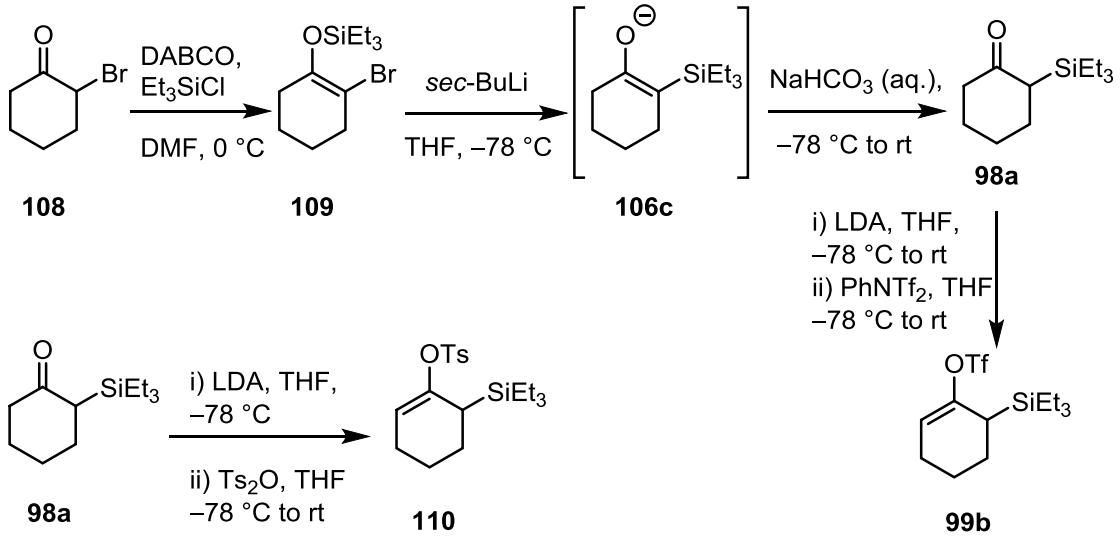

Scheme 1.19 Synthesis of silyl triflate **99b** and silyl tosylate **110**

1.2.4 Intramolecular hetero-Diels–Alder

Wills and Danheiser generated cyclic allenes through a hetero-Diels–Alder reaction (*Scheme 1.20*).[99] They used starting materials **111,** which presented conjugated ynone motif as diene and a triple bond as a dienophile. The reaction occurs at high temperatures with the generation of transient heterocyclic allenes **112**, which further underwent a rearrangement to generate the proposed intermediate carbene **113**. Once **113** was formed, a 1,2-C-H insertion took place to obtain furan **114**.

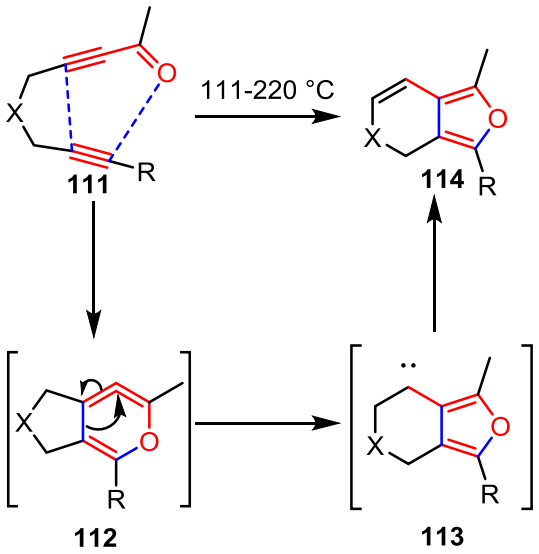

Scheme 1.20 Generation of cyclic allenes **112** through hetero-Diels–Alder cycloaddition

Wang and Hoye used a similar approach to generate heterocyclic allenes through a hetero-Diels–Alder reaction (*Scheme 1.21*).[100] They use propargyl 3-acylbutenolides **115** as starting materials, which can undergo a hetero-Diels–Alder cycloaddition in order to generate reactive intermediate heterocyclic allene **116**. Once **116** is formed, it undergoes a 6π electrocyclic ring-opening instead of the previously encountered rearrangement to generate 3-acylbutenolides **117** products. The interesting results from the hetero-Diels–Alder approaches employed by Danheiser and Hoye point to the need for more research on this strategy for cyclic allene generation, including the introduction of trapping processes to capture the transient allenes.

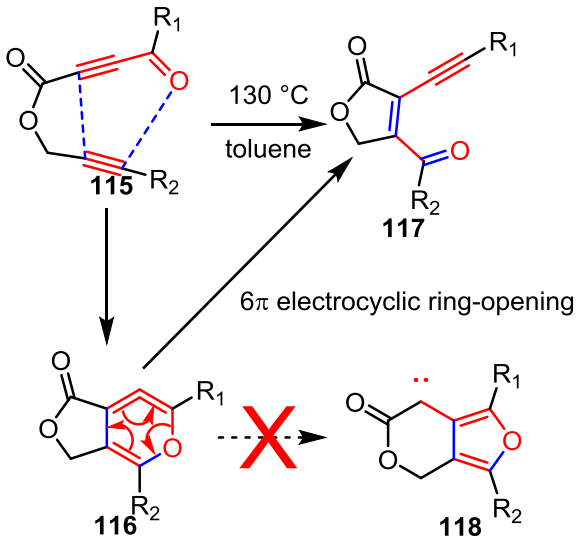

Scheme 1.21 Generation of cyclic allenes **116** through hetero-Diels–Alder

1.3 Reactions of cyclic allenes: dimerization and trapping

In this section the well-established ways of dimerization and trapping cyclic allenes will be discussed (*Scheme 1.22*). Once a transient cyclic allene species **7** is generated, there are several possible outcomes of the reaction. When no other suitable trapping reagent is present in the reaction mixture, dimerization (**119**) and oligomerization should be expected to occur. But if there is a suitable trapping reagent in the reaction system, a cycloaddition reaction can occur (**120**, **121**, and **122**) depending on the nature of the trapping reagent.

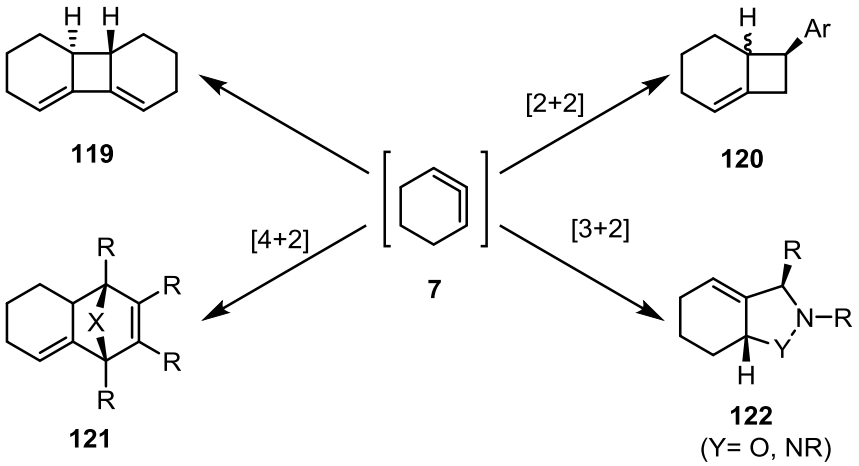

Scheme 1.22 Typical trapping reaction and dimerization of 1,2-cyclohexcadiene **7**

1.3.1 Dimerization of cyclic allenes

Although the dimer **119** of 1,2-cyclohexadiene **1** was previously isolated by Wittig[82,83], the work done by Moser and Moore was the first investigation looking more closely at the formation of dimer and oligomers once the transient cyclic allene was generated (*Scheme 1.22*).[85] In order to generate the 1,2-cyclohexadiene **7**, they used the DMS method. The authors proposed that two molecules of 1,2-cyclohexadiene **7** reacted with each other to form diradical **123**. Once diradical **123** was formed, if the reaction is at room temperature, it would quickly close to form dimer **119**. When the reaction was performed at -78 ºC the diradical intermediate **123** could react with another molecule of itself to form tetramers **124a** and **124b**. Another pathway at these low temperatures conditions was the reaction with another molecule of 1,2-cyclohexadiene **7** to form diradical **125**,which eventually closed to provide trimer **126**.

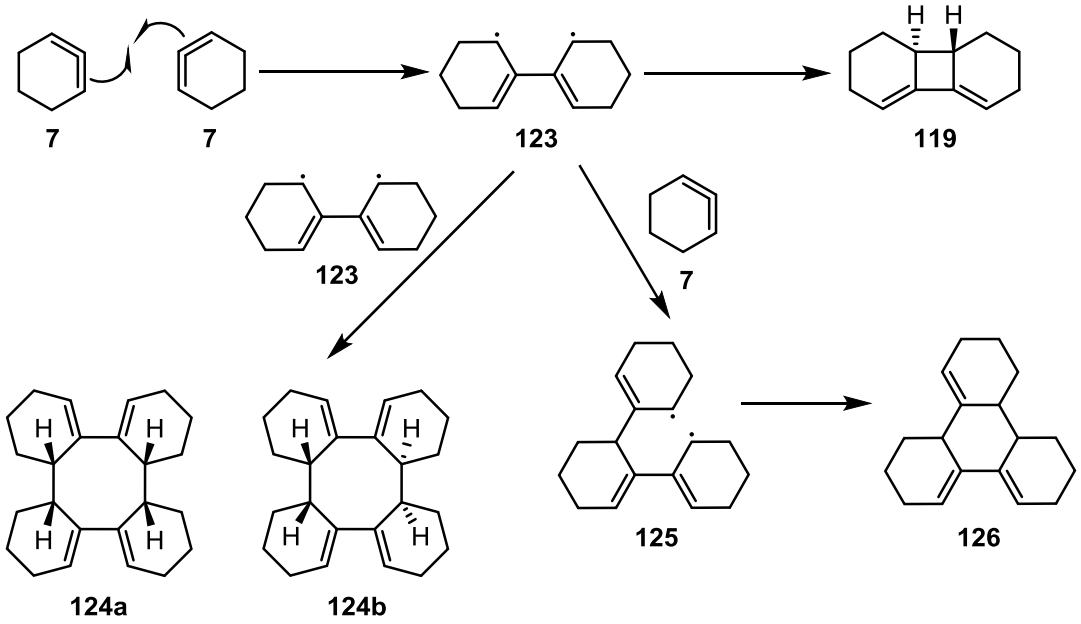

Scheme 1.23 Dimerization and oligomerization of 1,2-cyclohexadiene **7**

Christl and coworkers made some exciting discoveries related to dimerization and trimerization of 1-phenyl-1,2-cyclohexadiene **128** (*Scheme 1.23*).[101] They observed that depending on the generation method, they obtained either an unusual dimer **131** or a trimer

133. It was proposed that once 1-phenyl-1,2-cyclohexadiene **128** was generated, two molecules of itself could react to afford diradical intermediate **129**, which can undergo a reaction with one of the phenyl rings and generate dimer intermediate **130**. In the case of base promoted elimination conditions, dimer intermediate **130**, through deprotonation/protonation sequence, isomerized to give isolated dimer product **131**. In the DMS conditions, the dimer intermediate **130** reacted with a third molecule of 1-phenyl-1,2-cyclohexadiene **128** in either an ene reaction or hydrogen atom transfer followed by radical recombination to generate isolated trimer product **133**. Similar dimer products were observed in the cases of the 7- and 8-membered ring substrates.[56,102]

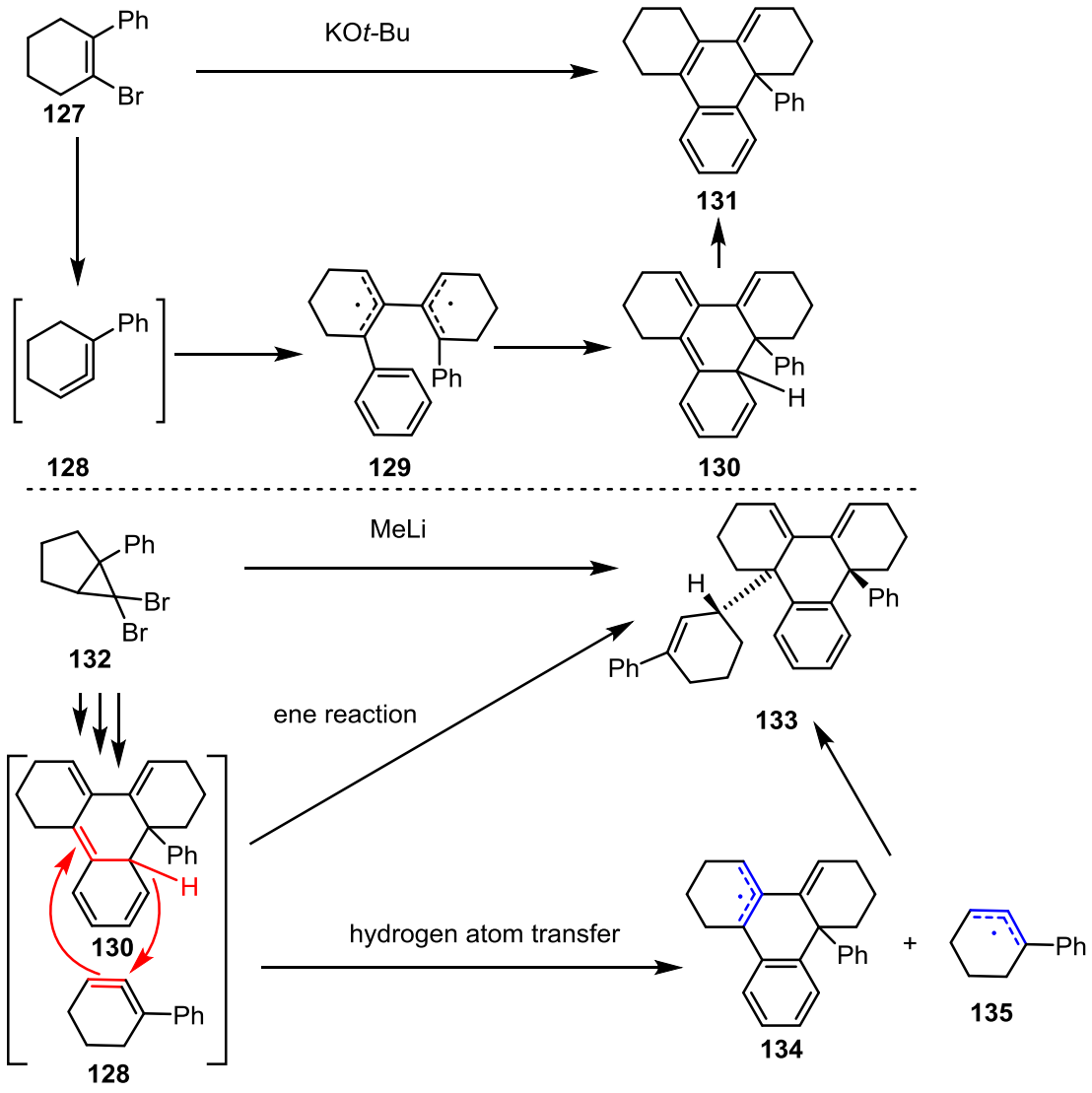

Scheme 1.24 Dimerization and trimerization of 1-phenyl-1,2-cyclohexadiene **128**

One fascinating example of tetramer formation was reported recently (*Scheme 1.24*).[103] Here, using the DMS method, the authors generated dibenzoannellated 1,2,4,6-cycloheptatetraene **137** which can react with itself first followed by a second dimerization of the diradical intermediate **137a** to get isolated tetramer **138**.

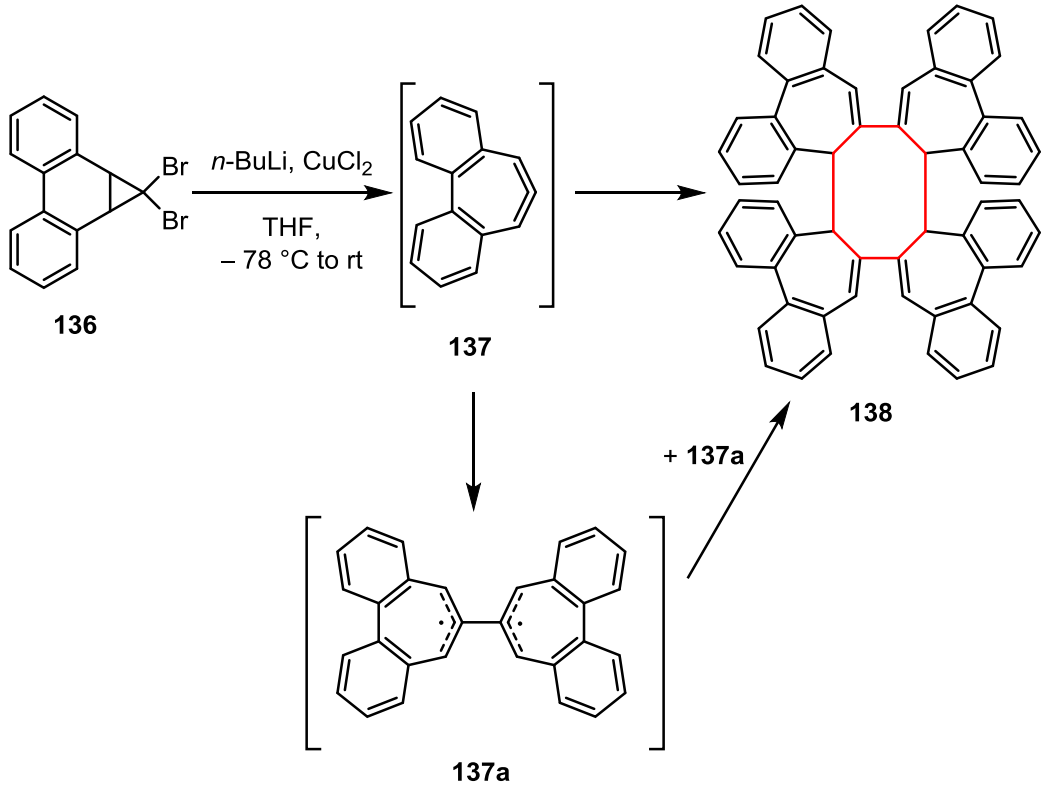

Scheme 1.25 Tetramer of dibenzoannellated 1,2,4,6-cycloheptatetraene **137**

In recent work, Zhang and Xie showed the versatility of the formal [2+2] dimerization of cyclic allenes through several examples of carborane-functionalized substrates (*Scheme 1.25*).[104] They employed a cycloaddition strategy for the generation of carborane-cyclic allene reactive intermediate. Triflate o-carborane **139** in the presence of LiHMDS underwent an elimination to obtain o-carboryne, which reacted with enyne 140 in [4+2] fashion to generate the cyclic allene **141**. Then **141** would dimerize to obtain dimers **142**.

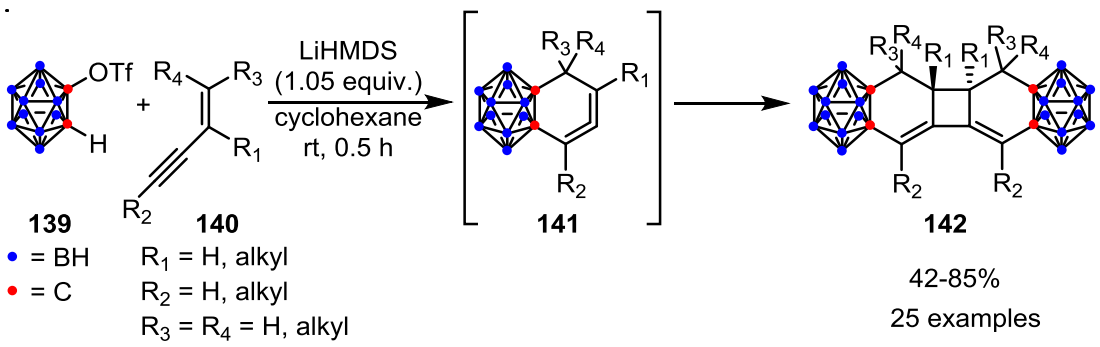

Scheme 1.26 Dimerization of carborane-functionalized cyclic allenes **141**

1.3.2 Inter- and Intramolecular [2+2] cycloaddition

Intermolecular [2+2] cycloaddition with styrenes was one of the first trapping methods used to capture transient cyclic allenes (*Scheme 1.26*). The formation of the cycloadduct was proposed to be proceed through a stepwise radical mechanism. In a first step, the central allene carbon atom of the 1,2-cyclohexadiene **7** and the distal carbon atom of the styrene **143** form a new bond with the generation of a diradical intermediate **144**. Once **144** was formed a radical ring closure would occur to obtain cyclobutanes **120a** and **120b**.

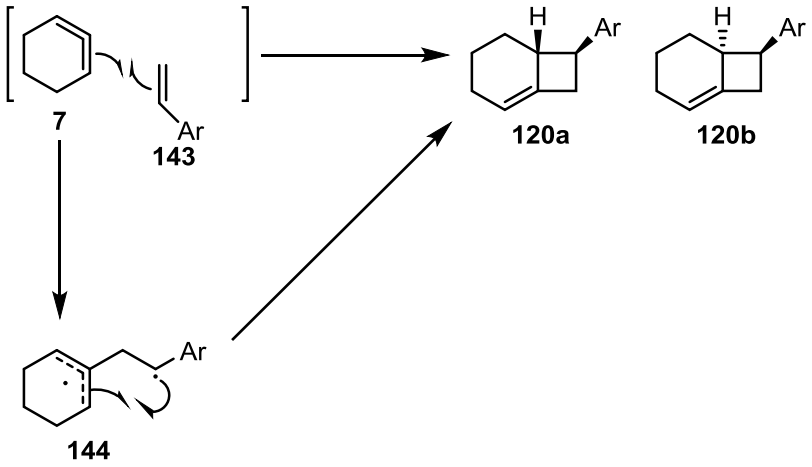

Scheme 1.27 Intermolecular [2+2] cycloaddition

Recent studies in our group showed that the [2+2] cycloaddition with styrenes could be carried out in an intramolecular fashion, where the styrene trap becomes part of the substrate through a tether (*Scheme 1.27*).[105] Well-designed starting materials **145** were used, which under the fluoride promoted elimination conditions generated the reactive intermediate cyclic allenes **146**. Once **146** were generated the [2+2] cycloaddition occurred to provide several polycyclic cycloadducts **147**. Particularly interesting products were **147f** and **147g,** where the precursor had both the furan and styrene trap tethered, and one could see that the [2+2] was favored over the Diels–Alder. The importance of this trapping strategy consists in lowering to 1 equivalent the amount of trapping reagent required for a successful cycloaddition and building of quite complex polycyclic product in one step with the formation of two new bonds and two new rings.

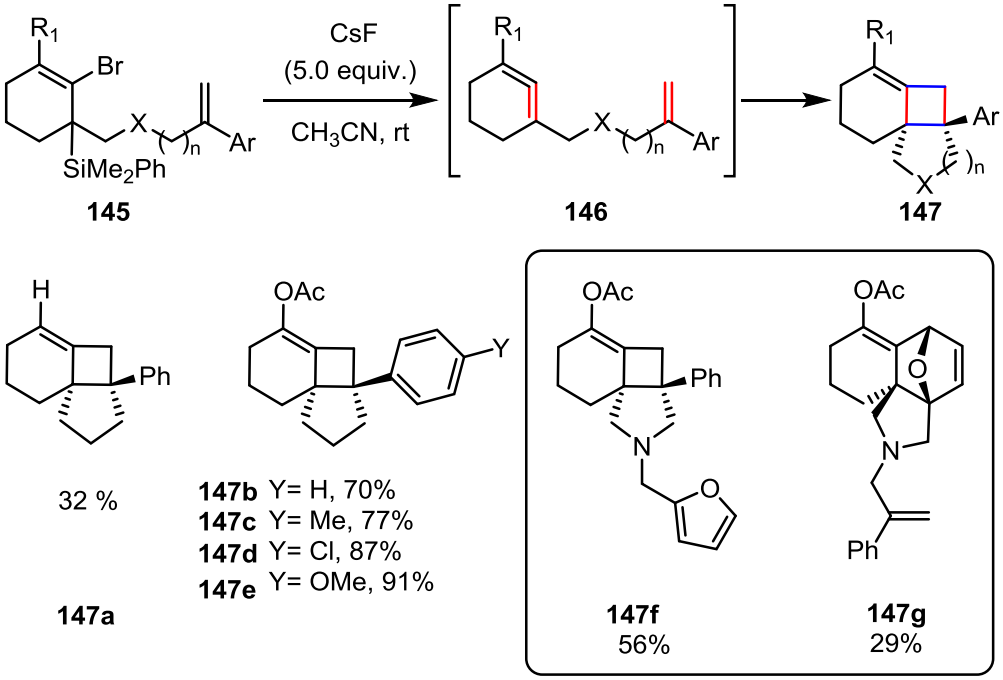

Scheme 1.28 Intramolecular [2+2] cycloaddition

1.3.3 Inter- and Intramolecular [4+2] cycloaddition

The Diels–Alder reaction is one of the typical trapping reactions for 1,2-cyclohexadiene **7**, which was used since the early days of the cyclic allene research to

capture and thus confirm the presence of this transient species (*Scheme 1.28*).[82,83] One can use a plethora of cyclic 1,3-dienes **148** to react with 1,2-cyclohexadiene **7** through a Diels–Alder reaction to obtain cycloadducts **121**. The diene in this Diels–Alder reaction can be furan, pyrrole, cyclopentadiene or cyclohexadiene based, thus an impressive number of cycloadducts have been made so far. Although most of the studies were done on 1,2-cyclohexadiene **7**, Diels–Alder cycloadducts are also known for 7-, and 8-membered rings, and heterocyclic allenes.[71,98,106]

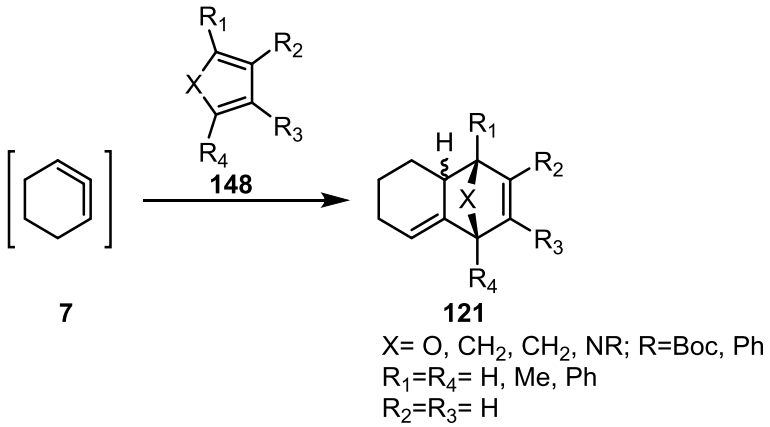

Scheme 1.29 Intermolecular [4+2] cycloaddition

In a more recent study in our group, it was found that the [4+2] Diels–Alder cycloaddition with furans can be used in an intramolecular fashion, where the furan trap is part of the allene precursor, attached via a short tether (*Scheme 1.29*).[107] A complex precursor **149** was used, which under the fluoride promoted elimination conditions generated the reactive intermediate cyclic allene **150**. Once **150** was generated, the Diels–Alder reaction occurred to obtain several polycyclic cycloadducts **151** in good yields. By increasing the tether length from 3 to 4 atoms, a significant drop in yield was observed; therefore, the use of 3-atom tethers seems to be preferred (see **151b** and **151c**). This trapping strategy's importance consists of lowering the required amount of trapping reagent to 1 equivalent for a successful cycloaddition and building a complex polycyclic product with the formation of two new bonds and two new rings in one step.

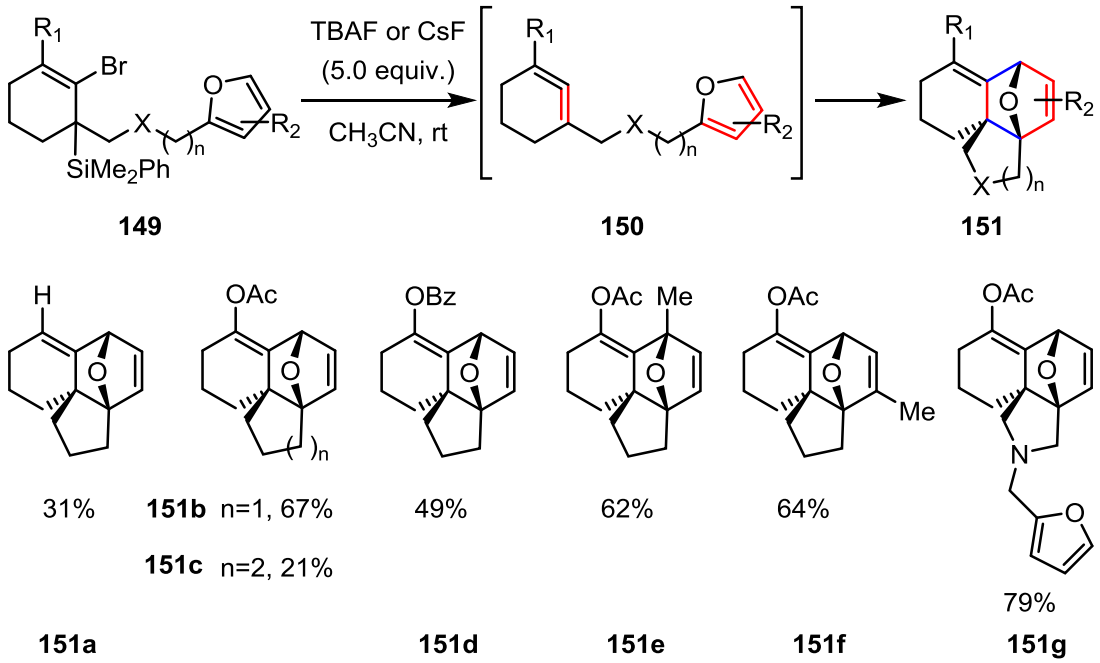

Scheme 1.30 Intramolecular [4+2] cycloaddition

The mechanism of the reaction of 1,2-cyclohexadiene **7** and furan **39** has been well studied over the years and discussed in several papers (*Scheme 1.30*).[62–65,71] The current overall consensus is that this reaction is an asynchronous concerted [4+2] cycloaddition. It was found through experiments and computationally that the formation of *endo* product is favoured. In a more recent paper, it was shown through computational studies that the bias towards the *endo* product is coming mainly from a secondary orbital interaction in between the highlighted carbon from furan and the LUMO orbital associated with the highlighted carbon of the allene in the *endo* TS.[108]

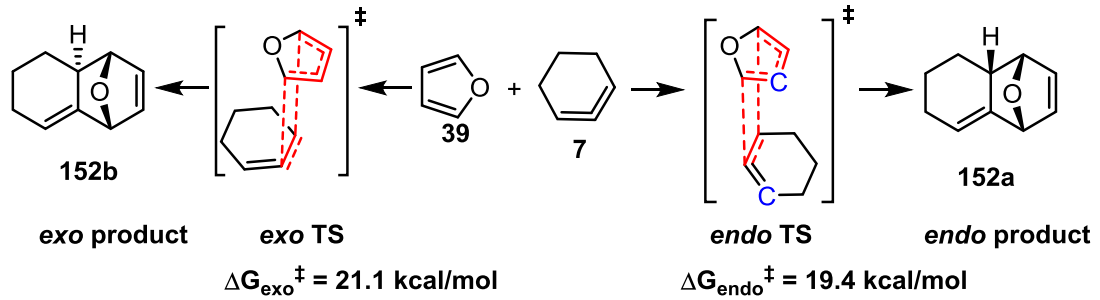

Scheme 1.31 Transition states for the Diels–Alder reaction of furan **39** with 1,2-cyclohexadiene **7**

1.3.4 The [3+2] cycloaddition of cyclic allenes

In several recent studies starting with the work of West and Garg groups, it was shown that 1,2-cyclohexadiene **7** and its derivatives could also be captured with certain 1,3-dipoles **153** resulting in cycloadducts **122** (*Scheme 1.32*).[93,94] In these reactions, 1,3-dipoles such as nitrile oxides, nitrones, and azomethine imines were able to undergo efficient cycloadditions. Later, it was shown that this type of trapping could also be used for 1,2-cycloheptadiene and heterocyclic allenes.[71,109] This newer trapping method offers access to some complex heterocyclic compounds with drug-like scaffolds that might lead to biologically active substances in future screening efforts.

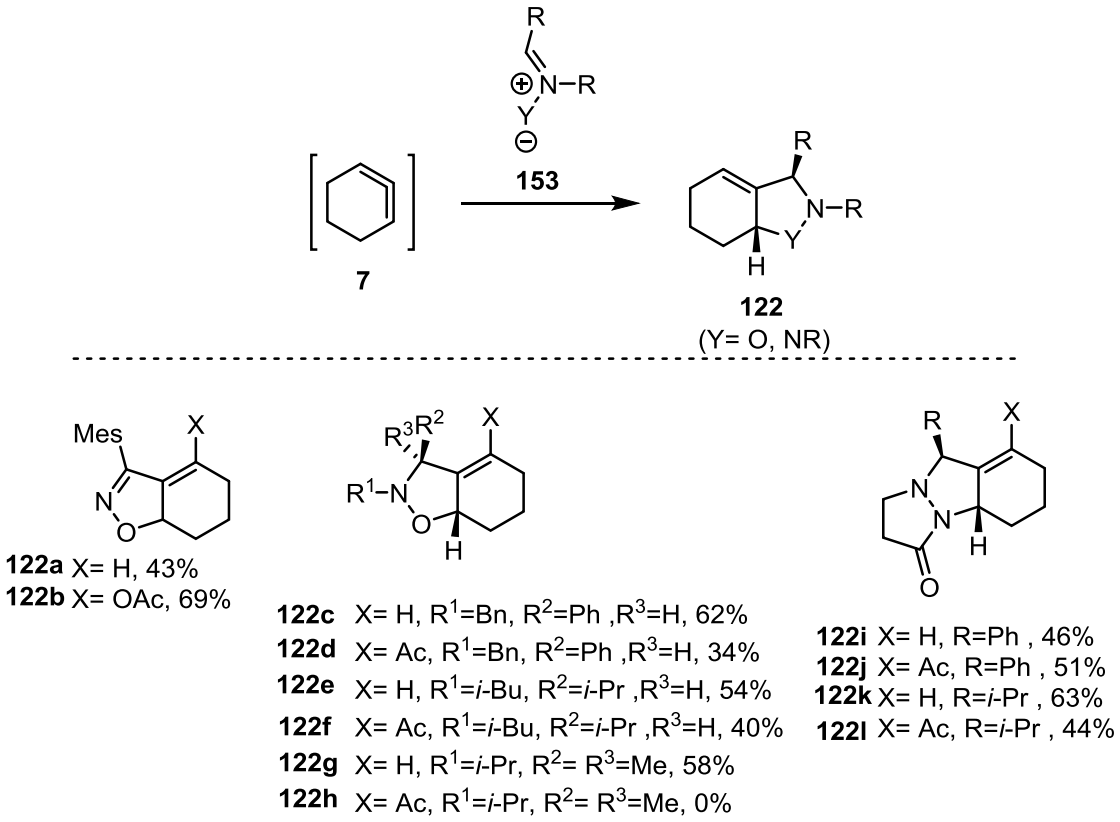

Scheme 1.32 Reaction of 1,2-cyclohexadiene **7** with 1,3-dipoles **153**

Using the ring strain of cyclic allenes to drive reactions under mild conditions could be applied in chemical biology and this is likely to be a future research direction for these

reactive intermediates. Schreiber's group recently made a DNA-encoded library using the cycloaddition of reactive cyclic allenes and carefully picked trapping partners (*Scheme 1.33*).[110] The authors described a fluoride-promoted generation of cyclic allenes from the DNA-conjugated precursors **154**, followed by typical trappings with 1,3-dipoles, 1,3-dienes and olefins to obtain cycloadducts **155**, **156**, and **157**. As an essential observation, the reaction took place in the DMSO and water solvent mixture, the latter being required in this chemical biology application. This work serves as an excellent proof of concept for further endeavours in the potential application of cyclic allenes using their ring strain.

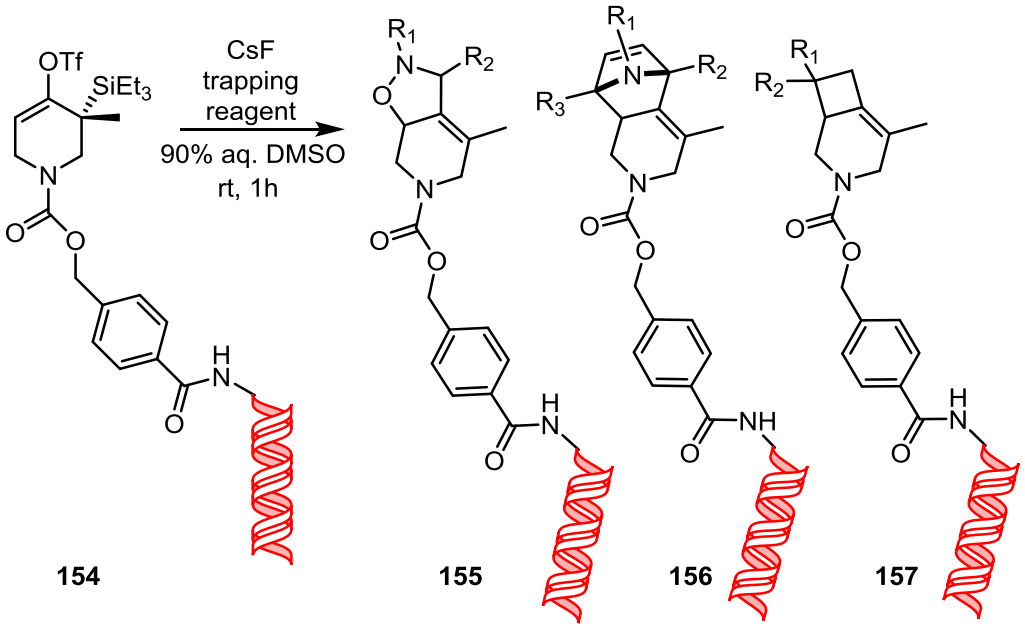

Scheme 1.33 Generation and trapping of oligonucleotide-conjugated cyclic allenes

1.4 Conclusions

A number of classes of reactive intermediates possess short lifetimes as a result of ring strain. Among these, cyclic allenes offer unique opportunities. The 6-, 7-, and 8-membered cyclic allenes are all transient and show unusual reactivity, with a strong penchant for [2+2]-dimerization. A few examples of substituted allenes and heterocyclic allenes have been described. One important aspect of cyclic allenes that distinguishes them from other intermediates with strain-induced reactivity (e.g., arynes and cyclic alkynes) is their intrinsic chirality, which may permit novel enantioselective applications employing these species. Several complementary methods for the generation of cyclic allenes have been developed, and each has certain advantages and disadvantages related to the ease with which the precursors can be prepared, and the compatibility of the allene generation conditions with sensitive functionality. The most common methods are base-mediated elimination of an alkenyl leaving group (commonly halide or triflate), Doering–Moore–Skattebøl rearrangement, and fluoride-mediated desilylative elimination. Aside from dimerization, common reactivities for cyclic allenes include [2+2]-cycloaddition (especially with styrenes), [4+2]-cycloaddition, and [3+2]-cycloaddition with several classes of 1,3-dipoles. In the case of [2+2]- and [4+2]-cycloaddition reactions, it has recently been shown that high efficiency can be realized using tethers to allow an intramolecular trapping to occur. Although there has been considerable recent progress in the chemistry of cyclic allenes, there are many aspects of the field that have been explored in only a cursory fashion, including additional methods for their generation, and a systematic look at the effect of polar substituents on their reactivity. For this reason, I expect this field to continue to grow in the coming years.

1.5 Statement of the problems studied in the thesis

As mentioned above, there are several windows of opportunity in the field of cyclic allenes that could afford valuable results, and the main part of this thesis will focus on these aspects. In this thesis, two research results chapters on cyclic allenes will be presented, and another chapter on C-acyl imine reactive intermediates, which is not related to cyclic allenes.

In Chapter 2, the development of a new methodology to generate cyclic allenes through a metal-halogen exchange promoted elimination approach was investigated. It was found that the lithium-halogen exchange method can provide access to a series of dimers, but no effective trapping was successful. An improved method using magnesium-halogen exchange provided access to both dimers and specific trapping products. The metal-halogen exchange promoted elimination studied in this chapter is a new complementary way to generate cyclic allenes.

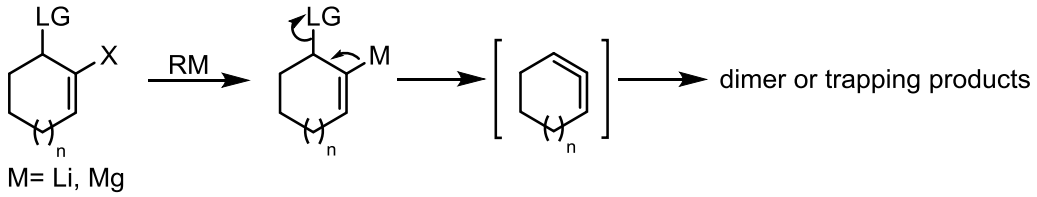

Scheme 1.34 Metal-halogen exchange promoted elimination

In Chapter 3, the discovery of an unprecedented trapping pathway of electron-deficient cyclic allenes with enamines will be discussed. In this research project, the study of electron-deficient cyclic allenes, an under-investigated research area, was undertaken. Specifically, we found that 1-acyl-1,2-cyclohexadienes can react as heterodienes in an inverse electron demand Diels–Alder reaction with electron-rich enamines to afford novel dihydropyran cycloadducts. Dr. Baolei Wang started the project, and computational analyses were performed in Prof. Rebecca Davis' group. My part in this project was the enamine trapping study.

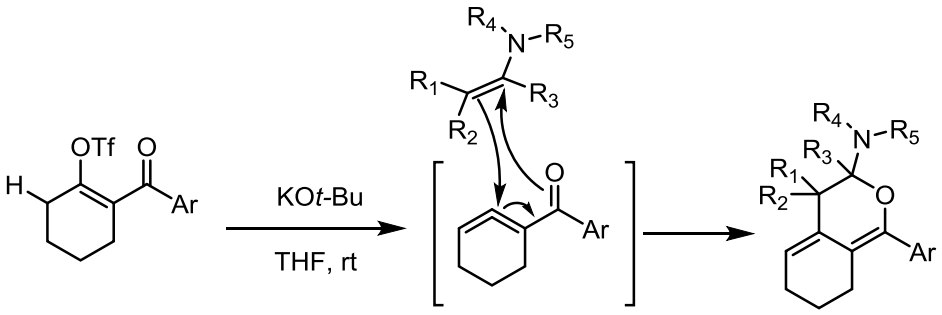

Scheme 1.35 Trapping of electron-deficient cyclic allenes with enamines

In Chapter 4, the results found in my initial research project from my doctoral studies will be disclosed. In this project the development of a new method to generate C-acyl imine reactive intermediates was attempted. Although a fascinating and unexpected product was isolated and characterized as a single diastereomer, we could not expand this method to other substrates. Later we decided to move my attention towards reactive cyclic allenes.

Chapter 5 will offer an overall conclusion for each of the projects, and discuss possible future directions that could be pursued in each of them.

1.6 References

(1) Moody, C. J.; Whitman, G. H. Introduction. In *Reactive Intermediates*; Davies, S. G., Ed.; Oxford University Press: Oxford, 1992; pp 1–4.

(2) Hopf, H. Reactive Intermediates. In *Organic Synthesis Highlights III*; Waldman, H., Ed.; Wiley-VCH Verlag GmbH: Weinheim, Germany, 1998; Vol. 5, pp 250–262.

(3) Singh, M. S. Introduction. In *Reactive Intermediates in Organic Chemistry: Structure, Mechanism, and Reactions*; Singh, M. S., Ed.; Wiley: Weinheim, Germany, 2014; pp 1–19.

(4) Dodziuk, H.; Fokin, A. A.; Schreiner, P. R. Introduction. *Strained Hydrocarbons*. March 18, 2009, pp 1–32.

(5) Carey, F. A.; Sundberg, R. J. Carbanions and Other Carbon Nucleophiles. In *Advanced Organic Chemistry. Part A: Structure and Mechanisms*; Springer US: Boston, MA, 2007; pp 579–629.

(6) Gronert, S. Carbanions. In *Reactive Intermediate Chemistry*; John Wiley & Sons, Inc.: Hoboken, NJ, USA, 2005; pp 69–119.

(7) Singh, M. S. Carbanions. In *Reactive Intermediates in Organic Chemistry Structure, Mechanism, and Reactions*; Singh, M. S., Ed.; Wiley: Weinheim, Germany, 2014; pp 65–100.

(8) Olah, G. A. *J. Org. Chem.* **2001**, *66* (18), 5943–5957.

(9) Olah, G. A. *J. Am. Chem. Soc.* **1972**, *94* (3), 808–820.

(10) McClelland, R. A. Carbocations. In *Reactive Intermediate Chemistry*; John Wiley & Sons, Inc.: Hoboken, NJ, USA, 2004; pp 1–40.

(11) Winstein, S.; Trifan, D. S. *J. Am. Chem. Soc.* **1949**, *71* (8), 2953.

(12) Winstein, S.; Trifan, D. *J. Am. Chem. Soc.* **1952**, *74* (5), 1154–1160.

(13) Olah, G. A.; Prakash, G. K. S.; Saunders, M. *Acc. Chem. Res.* **1983**, *16* (12), 440–448.

(14) Brown, H. C. *Acc. Chem. Res.* **1983**, *16* (12), 432–440.

(15) Newcomb, M. Radicals. In *Reactive Intermediate Chemistry*; Wiley Online Books; John Wiley & Sons, Inc.: Hoboken, NJ, USA, 2005; pp 121–163.

(16) Stephenson, L. M.; Cavigli, P. R.; Parlett, J. L. *J. Am. Chem. Soc.* **1971**, *93* (8), 1984–1988.

(17) Kopecky, K. R.; Soler, J. *Can. J. Chem.* **1974**, *52* (11), 2111–2118.

(18) Ventura, E.; Dallos, M.; Lischka, H. *J. Chem. Phys.* **2003**, *118* (24), 10963–10972.

(19) Singh, M. S. Carbenes. In *Reactive Intermediates in Organic Chemistry: Structure, Mechanism, and Reactions*; Singh, M. S., Ed.; Wiley: Weinheim, Germany, 2014; pp 153–196.

(20) Jones, M.; Moss, R. A. Singlet Carbenes. In *Reactive Intermediate Chemistry*; Wiley Online Books; John Wiley & Sons, Inc.: Hoboken, NJ, USA, 2004; pp 273–328.

(21) Tomioka, H. Triplet Carbenes. In *Reactive Intermediate Chemistry*; John Wiley & Sons, Inc.: Hoboken, NJ, USA, 2005; pp 375–461.

(22) Fischer, E. O.; Heinz Dötz, K. *Chem. Ber.* **1970**, *103* (4), 1273–1278.

(23) Yates, P. *J. Am. Chem. Soc.* **1952**, *74* (21), 5376–5381.

(24) Dötz, K. H. *Angew. Chem. Int. Ed. Engl.* **1984**, *23* (8), 587–608.

(25) Stoermer, R.; Kahlert, B. *Ber. Dtsch. Chem. Ges.* **1902**, *35* (2), 1633–1640.

(26) Pellissier, H.; Santelli, M. *Tetrahedron* **2003**, *59* (6), 701–730.

(27) Wenk, H. H.; Winkler, M.; Sander, W. *Angew. Chem. Int. Ed.* **2003**, *42* (5), 502–528.

(28) Gampe, C. M.; Carreira, E. M. *Angew. Chem. Int. Ed.* **2012**, *51* (16), 3766–3778.

(29) Yoshida, S.; Hosoya, T. *Chem. Lett.* **2015**, *44* (11), 1450–1460.

(30) Tadross, P. M.; Stoltz, B. M. *Chem. Rev.* **2012**, *112* (6), 3550–3577.

(31) Friedman, L.; Logullo, F. M. *J. Am. Chem. Soc.* **1963**, *85* (10), 1549–1549.

(32) Roberts, J. D.; Simmons, H. E.; Carlsmith, L. A.; Vaughan, C. W. *J. Am. Chem. Soc.* **1953**, *75* (13), 3290–3291.

(33) Roberts, J. D.; Vaughan, C. W.; Carlsmith, L. A.; Semenow, D. A. *J. Am. Chem. Soc.* **1956**, *78* (3), 611–614.

(34) Himeshima, Y.; Sonoda, T.; Kobayashi, H. *Chem. Lett.* **1983**, *12* (8), 1211–1214.

(35) Kitamura, T.; Yamane, M. *J. Chem. Soc. Chem. Commun.* **1995**, *983* (9), 983.

(36) Wittig, G.; Ludwig, R. *Angew. Chem.* **1956**, *68* (1), 40–40.

(37) Matsumoto, T.; Hosoya, T.; Katsuki, M.; Suzuki, K. *Tetrahedron Lett.* **1991**, *32*

(46), 6735–6736.

(38) Fluegel, L. L.; Hoye, T. R. *Chem. Rev.* **2021**, *121* (4), 2413–2444.

(39) Stevens, R. V.; Bisacchi, G. S. *J. Org. Chem.* **1982**, *47* (12), 2393–2396.

(40) Peña, D.; Cobas, A.; Pérez, D.; Guitián, E. *Synthesis* **2002**, 1454–1458.

(41) Wickham, P. P.; Hazen, K. H.; Guo, H.; Jones, G.; Reuter, K. H.; Scott, W. J. *J. Org. Chem.* **1991**, *56* (6), 2045–2050.

(42) Tambar, U. K.; Stoltz, B. M. *J. Am. Chem. Soc.* **2005**, *127* (15), 5340–5341.

(43) Taylor, E. C.; Sobieray, D. M. *Tetrahedron* **1991**, *47* (46), 9599–9620.

(44) Tambar, U. K.; Ebner, D. C.; Stoltz, B. M. *J. Am. Chem. Soc.* **2006**, *128* (36), 11752–11753.

(45) Hoye, T. R.; Baire, B.; Niu, D.; Willoughby, P. H.; Woods, B. P. *Nature* **2012**, *490* (7419), 208–211.

(46) Bottini, A. T.; Corson, F. P.; Fitzgerald, R.; Frost, K. A. *Tetrahedron* **1972**, *28* (19), 4883–4904.

(47) Bach, R. D. *J. Am. Chem. Soc.* **2009**, *131* (6), 5233–5243.

(48) Medina, J. M.; McMahon, T. C.; Jiménez-Osés, G.; Houk, K. N.; Garg, N. K. *J. Am. Chem. Soc.* **2014**, *136* (42), 14706–14709.

(49) Olivella, S.; Pericàs, M. A.; Riera, A.; Solé, A. *J. Org. Chem.* **1987**, *52* (19), 4160–4163.

(50) Johnson, R. P.; Daoust, K. J. *J. Am. Chem. Soc.* **1995**, *117* (1), 362–367.

(51) Hopf, H.; Grunenberg, J. Angle-Strained Cycloalkynes. In *Strained Hydrocarbons*; Wiley-VCH Verlag GmbH & Co. KGaA: Weinheim, Germany, 2009; pp 375–397.

(52) Dommerholt, J.; Rutjes, F. P. J. T.; van Delft, F. L. *Top. Curr. Chem.* **2016**, *374* (2), 1–20.

(53) Agard, N. J.; Prescher, J. A.; Bertozzi, C. R. *J. Am. Chem. Soc.* **2004**, *126* (46), 15046–15047.

(54) Huisgen, R. *Angew. Chem. Int. Ed. Engl.* **1963**, *2* (10), 565–598.

(55) Wang, Q.; Chan, T. R.; Hilgraf, R.; Fokin, V. V.; Sharpless, K. B.; Finn, M. G. *J. Am. Chem. Soc.* **2003**, *125* (11), 3192–3193.

(56) Christl, M. Cyclic Allenes Up to Seven-Membered Rings. In *Modern Allene Chemistry*; Wiley-VCH Verlag GmbH: Weinheim, Germany, 2005; pp 243–357.

(57) Kawase, T. Product Class 3: Cyclic Allenes. In *Category 6, Compounds with All-Carbon Functions*; Krause, Ed.; Georg Thieme Verlag: Stuttgart, 2008; Vol. 5, pp 395–449.

(58) Johnson, R. P. *Chem. Rev.* **1989**, *89* (5), 1111–1124.

(59) Balci, M.; Taskesenligil, Y. Recent Developments in Strained Cyclic Allenes. In *Advances in Strained and Interesting Organic Molecules*; Halton, B., Ed.; JAI Press: Stramford, Connecticut, 2000; Vol. 8, pp 43–81.

(60) Thies, R. W. *Isr. J. Chem.* **1985**, *26* (2), 191–195.

(61) Anthony, S. M.; Wonilowicz, L. G.; McVeigh, M. S.; Garg, N. K. *JACS Au* **2021**, *1* (7), 897-912.

(62) Daoust, K. J.; Hernandez, S. M.; Konrad, K. M.; Mackie, I. D.; Winstanley, J.; Johnson, R. P. *J. Org. Chem.* **2006**, *71* (15), 5708–5714.

(63) Schmidt, M. W.; Angus, R. O.; Johnson, R. P. *J. Am. Chem. Soc.* **1982**, *104* (24), 6838–6839.

(64) Dillon, P. W.; Underwood, G. R. *J. Am. Chem. Soc.* **1974**, *96* (3), 779–787.

(65) Angus, R. O.; Johnson, R. P.; Schmidt, M. W. *J. Am. Chem. Soc.* **1985**, *107* (3), 532–537.

(66) Wentrup, C.; Gross, G.; Maquestiau, A.; Flammang, R. *Angew. Chem. Int. Ed. Engl.* **1983**, *22* (7), 542–543.

(67) Engels, B.; Schöneboom, J. C.; Münster, A. F.; Groetsch, S.; Christl, M. *J. Am. Chem. Soc.* **2002**, *124* (2), 287–297.

(68) Roth, W. R.; Ruf, G.; Ford, P. W. *Chem. Ber.* **1974**, *107* (1), 48–52.

(69) Balci, M.; Jones, W. M. *J. Am. Chem. Soc.* **1980**, *102* (25), 7607–7608.

(70) Boswell, R. F.; Bass, R. G. *J. Org. Chem.* **1975**, *40* (16), 2419–2420.

(71) Barber, J. S.; Yamano, M. M.; Ramirez, M.; Darzi, E. R.; Knapp, R. R.; Liu, F.; Houk, K. N.; Garg, N. K. *Nat. Chem.* **2018**, *10* (9), 953–960.

(72) Drinkuth, S.; Groetsch, S.; Peters, E. M.; Peters, K.; Christl, M. *Eur. J. Org. Chem.* **2001**, 2665–2670.

(73) Schreck, M.; Christl, M. *Angew. Chem. Int. Ed. Engl.* **1987**, *26* (7), 690–692.

(74) Yamano, M. M.; Knapp, R. R.; Ngamnithiporn, A.; Ramirez, M.; Houk, K. N.; Stoltz, B. M.; Garg, N. K. *Angew. Chem. Int. Ed.* **2019**, *58* (17), 5653–5657.

(75) Christl, M.; Braun, M. *Chem. Ber.* **1989**, *122* (10), 1939–1946.

(76) Lloyd, D.; McNab, H. *J. Chem. Soc. Perkin Trans. 1* **1976**, *516* (16), 1784.

(77) Lee-Ruff, E.; Maleki, M.; Duperrouzel, P.; Lein, M. H.; Hopkinson, A. C. *J. Chem. Soc. Chem. Commun.* **1983**, 346-347.

(78) Elliott, R. L.; Nicholson, N. H.; Peaker, F. E.; Takle, A. K.; Richardson, C. M.; Tyler, J. W.; White, J.; Pearson, M. J.; Eggleston, D. S.; Haltiwanger, R. C. *J. Org. Chem.* **1997**, *62* (15), 4998–5016.

(79) Elliott, R. L.; Nicholson, N. H.; Peaker, F. E.; Takle, A. K.; Tyler, J. W.; White, J. *J. Org. Chem.* **1994**, *59* (7), 1606–1607.

(80) Shimizu, T.; Hojo, F.; Ando, W. *J. Am. Chem. Soc.* **1993**, *115* (8), 3111–3115.

(81) Pang, Y.; Petrich, S. A.; Young, V. G.; Gordon, M. S.; Barton, T. J. *J. Am. Chem. Soc.* **1993**, *115* (6), 2534–2536.

(82) Wittig, G.; Fritze, P. *Justus Liebigs Ann. Chem.* **1968**, *711*, 82–87.

(83) Wittig, G.; Fritze, P. *Angew. Chem.* **1966**, *78* (18–19), 905.

(84) Moore, W. R.; Moser, W. R. *J. Org. Chem.* **1970**, *35* (4), 908–912.

(85) Moore, W. R.; Moser, W. R. *J. Am. Chem. Soc.* **1970**, *92* (18), 5469–5474.

(86) Shakespeare, W. C.; Johnson, R. P. *J. Am. Chem. Soc.* **1990**, *112* (23), 8578–8579.

(87) Bottini, A. T.; Hilton, L. L.; Plott, J. *Tetrahedron* **1975**, *31* (17), 1997–2001.

(88) Hioki, Y.; Mori, A.; Okano, K. *Tetrahedron* **2020**, *76* (22), 131103.

(89) von E. Doering, W.; LaFlamme, P. M. *Tetrahedron* **1958**, *2* (1–2), 75–79.

(90) Moore, W.; Ward, H. *J. Org. Chem.* **1960**, *25* (11), 2073–2073.

(91) Skattebøl, L. *Tetrahedron Lett.* **1961**, *2* (5), 167–172.

(92) Quintana, I.; Peña, D.; Pérez, D.; Guitián, E. *Eur. J. Org. Chem.* **2009**, 5519–5524.

(93) Barber, J. S.; Styduhar, E. D.; Pham, H. V.; McMahon, T. C.; Houk, K. N.; Garg, N. K. *J. Am. Chem. Soc.* **2016**, *138* (8), 2512–2515.

(94) Lofstrand, V. A.; West, F. G. *Chem. Eur. J.* **2016**, *22* (31), 10763–10767.

(95) Nakura, R.; Inoue, K.; Okano, K.; Mori, A. *Synthesis* **2019**, *51* (7), 1561–1564.

(96) Inoue, K.; Nakura, R.; Okano, K.; Mori, A. *Eur. J. Org. Chem.* **2018**, 3343–3347.

(97) Chari, J. V.; Ippoliti, F. M.; Garg, N. K. *J. Org. Chem.* **2019**, *84* (6), 3652–3655.

(98) McVeigh, M. S.; Kelleghan, A. V.; Yamano, M. M.; Knapp, R. R.; Garg, N. K. *Org. Lett.* **2020**, *22* (11), 4500–4504.

(99) Wills, M. S. B.; Danheiser, R. L. *J. Am. Chem. Soc.* **1998**, *120* (36), 9378–9379.

(100) Wang, Y.; Hoye, T. R. *Org. Lett.* **2018**, *20* (15), 4425–4429.

(101) Christl, M.; Schreck, M.; Fischer, T.; Rudolph, M.; Moigno, D.; Fischer, H.; Deuerlein, S.; Stalke, D. *Chem. Eur. J.* **2009**, *15* (42), 11256–11265.

(102) Christl, M.; Groetsch, S.; Günther, K. *Angew. Chem. Int. Ed.* **2000**, *39* (18), 3261–3263.

(103) Mahlokozera, T.; Goods, J. B.; Childs, A. M.; Thamattoor, D. M. *Org. Lett.* **2009**, *11* (22), 5095–5097.

(104) Zhang, J.; Xie, Z. *Chem. Sci.* **2021**, *12* (15), 5616–5620.

(105) Mcintosh, K. C. Investigation of Strain-Activated Trapping Reactions of 1,2-Cyclohexadiene: Intramolecular Capture by Pendent Furans and Styrenes, University of Alberta, Edmonton, AB, 2020.

(106) Eaton, P. E.; Stubbs, C. E. *J. Am. Chem. Soc.* **1967**, *89* (22), 5722–5723.

(107) Lofstrand, V. A.; McIntosh, K. C.; Almehmadi, Y. A.; West, F. G. *Org. Lett.* **2019**, *21* (16), 6231–6234.

(108) Ramirez, M.; Svatunek, D.; Liu, F.; Garg, N. K.; Houk, K. N. *Angew. Chem. Int. Ed.* **2021**, *60*,14989–14997.

(109) Almehmadi, Y. A.; West, F. G. *Org. Lett.* **2020**, *22* (15), 6091–6095.

(110) Westphal, M. V.; Hudson, L.; Mason, J. W.; Pradeilles, J. A.; Zécri, F. J.; Briner, K.; Schreiber, S. L. *J. Am. Chem. Soc.* **2020**, *142* (17), 7776–7782.

2. Generation of cyclic allenes through metal-halogen exchange promoted elimination

2.1 Introduction

2.1.1 Research objective

Cyclic allenes offer a useful handle to get access to interesting polycyclic motifs in good regioselectivity and diastereoselectivity, which could find further utilization in synthetic organic chemistry. [1–3] Thus the interest shown in the generation and trapping of cyclic allenes increases in the organic chemistry community. The most common ways to generate cyclic allenes are Doering–Moore–Skattebøl rearrangement, base elimination, and fluoride-promoted desilylative elimination, as shown in *Scheme 2.1*.[1–3] Once generated, highly reactive cyclic allenes will undergo dimerization or cycloaddition reactions with different traps (1,3-dienes, styrene, 1,3-dipoles). Although there are several ways to generate this reactive intermediate, we think there is always room for new methods. In particular, we were interested in developing alternative routes to these intermediates that would employ readily available precursors and reaction conditions complementary to those of the existing approaches.

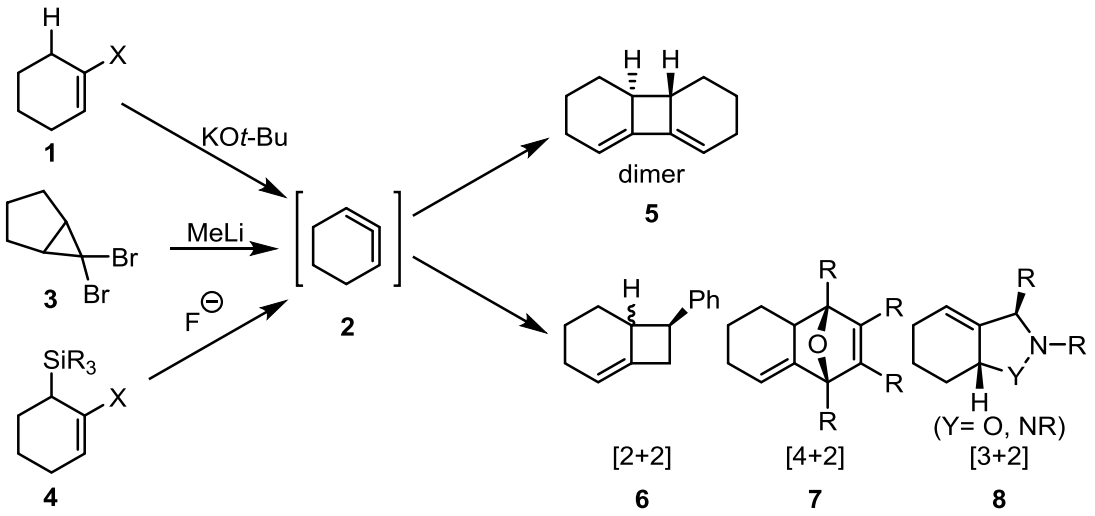

Scheme 2.1 Main methods used for generation of cyclic allenes and typical trapping

Initially, our attention focused on a new way to generate cyclic allenes in a complementary fashion with the well-established fluoride-promoted elimination.[4–6] In the latter one, the silyl group is attached to the allylic carbon, while the leaving group is placed on the neighbouring olefinic carbon as shown for substrate **9** (*Scheme 2.2.a*). Both TBAF and CsF were previously used successfully in the literature as the fluoride source. We envisioned that swapping positions of two groups in the starting material **10**, in which the leaving group would be on the allylic carbon and the silyl group on the neighbouring alkenyl carbon, would serve as a complementary way of generating 1,2-cyclohexadiene **2** (*Scheme 2.2.b*).

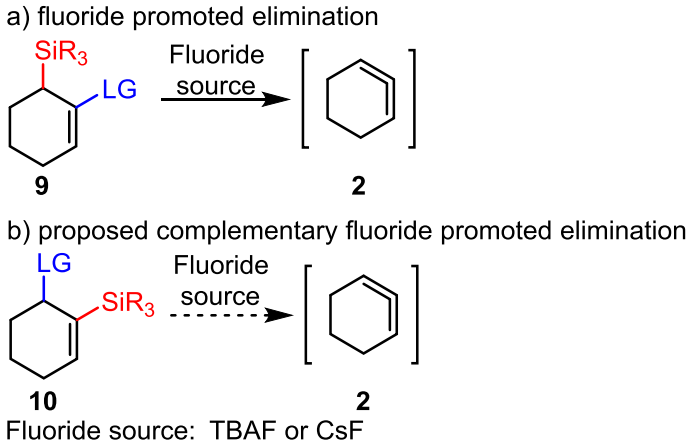

Scheme 2.2 Proposed complementary fluoride-promoted elimination

In order to explore this proposal, we tested the transformation on two starting materials **10a** and **10b** (*Scheme 2.3*). In **10a**, we used trimethylsilyl as the alkenyl anion equivalent and acetate as the leaving group. As an alternative substrate, in **10b**, we used dimethylphenylsilyl as the alkenyl anion equivalent and ethyl carbonate as the leaving group. For both starting materials, conditions with TBAF as well as CsF were used; however, formation of the anticipated cyclic allene dimer was not observed, and only starting material was recovered. It was unclear why these attempts did not work. We believed it might have been a poor orbital alignment for elimination when swapped the two groups on the starting materials.

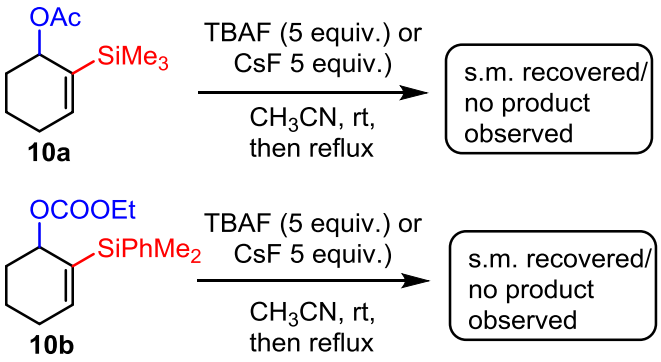

Scheme 2.3 Complementary fluoride-promoted elimination attempts

While surveying the literature, we came across a lithium-bromide exchange promoted elimination method to generate acyclic allenes **13** developed by Ichikawa's group (*Scheme 2.4*),[7] in which, in analogy to our earlier proposed method, the leaving group is on the allylic carbon. We wondered if a similar approach would be applicable in the more demanding cyclic allene series.

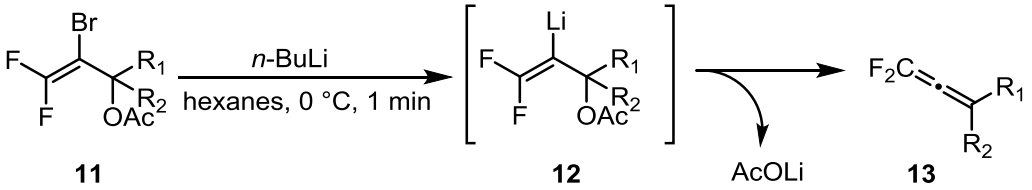

Scheme 2.4 Synthesis of 1,1-difluoroallenes **13** through lithium-halogen exchange promoted elimination

Based on our previously discussed ideas and literature precedents, we proposed a metal-halogen exchange promoted elimination to generate cyclic allenes. The use of organomagnesium or organolithium reagents and an appropriate leaving group eventually led to the successful generation of the desired cyclic allenes **16** as shown in *Scheme 2.5*, and described in detail in section 2.4.

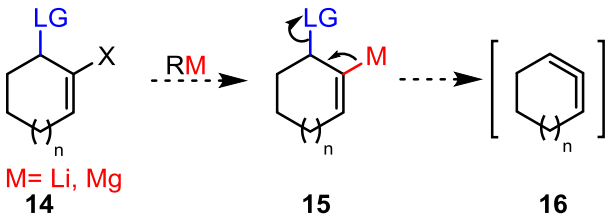

Scheme 2.5 Proposed metal-halogen exchange promoted elimination for generation of cyclic allenes

2.1.2 Lithium-halogen exchange reaction

One of the main ways to generate organolithium compounds is the lithium-halogen exchange method, in which a commonly available organolithium reagent is used to generate an organolithium compound of interest. These reactions can be viewed as equilibria in which the ratio of reactants and products depends upon the stability of the components, especially the two possible organolithium species. Therefore, certain organolithium species are favored over the others based on the relative carbanion stability scale as shown in *Scheme 2.6*. For example, in order to generate organolithium **20**, a less stable organolithium species **17** should be used. [8–11]

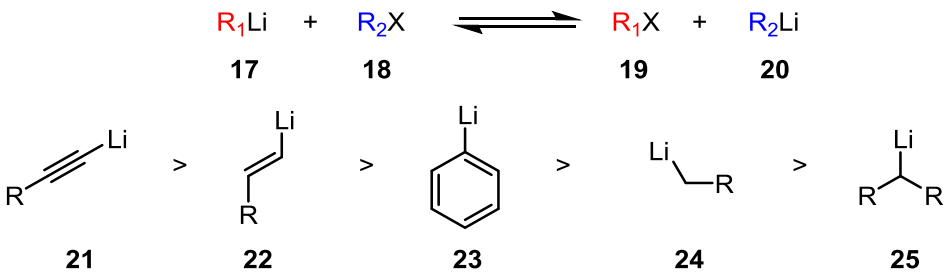

Scheme 2.6 Lithium-halogen exchange general reaction scheme and relative stability

Two possible mechanisms have been proposed for lithium-halogen exchange reactions: (1) single electron transfer and homolysis, involving a series of radical intermediates; and (2) direct nucleophilic attack at the halogen atom. The first one starts with a single electron transfer process between an organolithium reagent **17** and organic halide **18,** to generate intermediate species **17a** and **18a**, which will further break down homolytically to form radical species $\mathbf{R_1}$ and $\mathbf{R_2}$, cation $\mathbf{Li^+}$ and halide anion $\mathbf{X^-}$. Then $\mathbf{R_1}$ would recombine halide anion $\mathbf{X^-}$ to form intermediate **19a**, which upon single electron transfer with radical $\mathbf{R_2}$ would generate byproduct halide **19** and anion $\mathbf{R_2}$. Recombination of the latter one with cation $\mathbf{Li^+}$ would lead to the formation of organolithium **20** as presented in *Scheme 2.7*.[12,13]

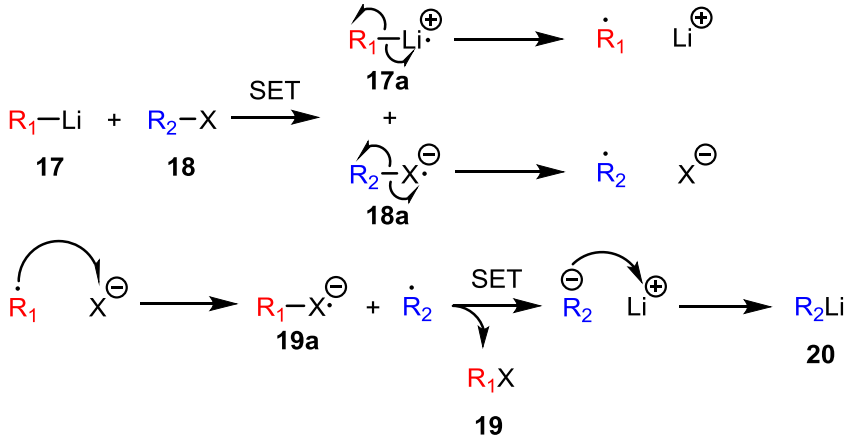

Scheme 2.7 Lithium-halogen exchange radical mechanism

Another proposed mechanism explaining the lithium-halogen exchange reaction is involving a nucleophilic substitution between organolithium **17** and organic halide **18** to form intermediate ate complex **17b**. This can further breakdown in organic halide **19** and new organolithium **20** as shown in *Scheme 2.8* .[13–15]

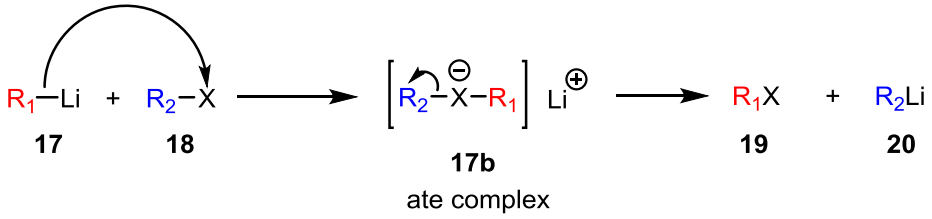

Scheme 2.8 Lithium-halogen exchange nucleophilic substitution mechanism

The utility of the lithium-halogen exchange reaction was shown in the early days in the study of this reaction by Gilman and coworkers. They performed a lithium-bromide exchange reaction on *o*-bromoanisole **26** to obtain organolithium intermediate **27** which was further treated with carbon dioxide to get access to *o*-methoxybenzoic acid **28** as presented in *Scheme 2.9*.[9]

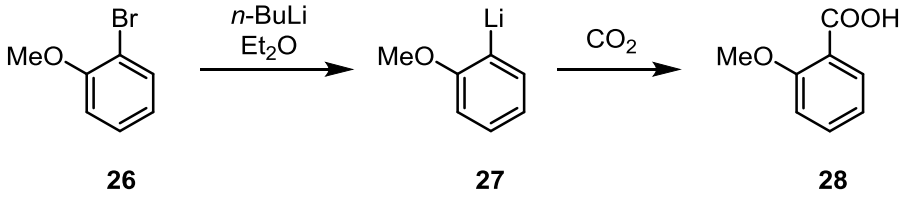

Scheme 2.9 Synthesis of *o*-methoxybenzoic acid from *o*-bromoanisole using lithium-halogen exchange

When *t*-BuLi **29** is used in the lithium-halogen exchange reaction, usually two equivalents of *t*-BuLi are necessary in the reaction to convert halide **30** to organolithium compound **32**. Once the lithium-halogen exchange reaction occurs, the *t*-butyl halide **31** formed undergoes an elimination reaction with the second equivalent of *t*-BuLi **29** which acts as the base in this reaction in order to get isobutene **33**, isobutane **34** and lithium halide **35** byproducts as illustrated in *Scheme 2.10*.[8]

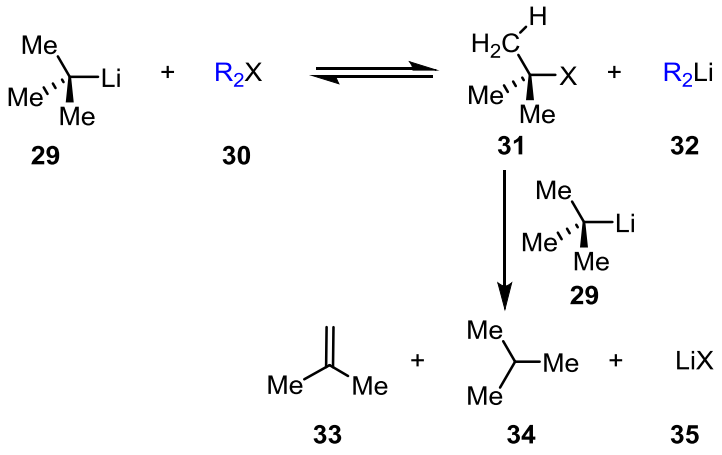

Scheme 2.10 Lithium halogen exchange with *t*-BuLi

2.1.3 Magnesium-halogen exchange

The direct oxidative addition of magnesium to organic halides is a common way to generate Grignard reagents (*Scheme 2.11)*. This reaction is usually performed in an aprotic solvent such as diethyl ether or THF. An oxide layer present on the surface of the magnesium metal can extend the induction period of the reaction. In order to address this issue, an activation agent such as 1,2-dibromoethane can be used for the magnesium surface. Although it is still debatable, a radical mechanism is accepted for this reaction.[16]

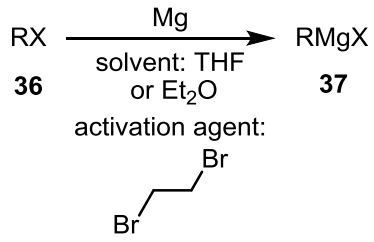

Scheme 2.11 Direct oxidative addition of magnesium to halides

Another common approach of generating organomagnesium species puts to use a common Grignard reagent **38** which through a magnesium-halogen exchange process with halide **39** will generate halide **40** and a new organomagnesium compound **41**. Similarly to lithium-halogen exchange, this is an equilibrium in which the formation of the most stable organomagnesium compound is favored, with a similar stability order as seen with organolithium reagents (*Scheme 2.12*).[16]

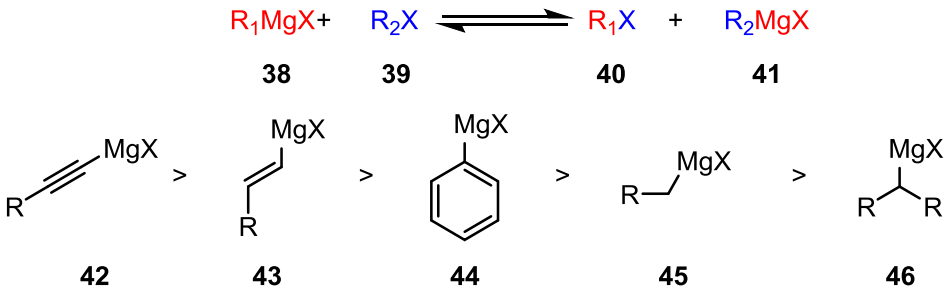

Scheme 2.12 Magnesium-halogen exchange reaction and relative stability of organomagnesium compounds

2.1.4 Metal-halogen exchange used for generation of strained reactive intermediates

Prior work showed that benzynes can be obtained in a similar fashion as we proposed for the generation of cyclic allenes. Knochel's group developed a method in which benzynes were accessed via magnesium-halogen exchange promoted elimination (*Scheme 2.13*). According to this study, the sulfonate leaving group also acts as a directing group, thus enabling magnesium-halogen exchange in just 15–30 minutes at −78 ºC, leading to organomagnesium intermediate **48** from the aryl iodide starting material **47**. Upon completion of the exchange, the addition of a trapping agent such as furan and warming up the reaction mixture to room temperature while stirring for 2 h facilitates the elimination process and generation of the reactive intermediate **49**; the latter one gets trapped in Diels–Alder reaction with furan to yield cycloadduct **50**. Through this method, they were able to obtain the desired [4+2] cycloadducts in good yields. Among various sulfonate leaving groups tested, 4-$ClC_6H_4SO_2$ was found was found to provide the best result. It was noted that EWG survived conditions in which various Grignard reagents were present.

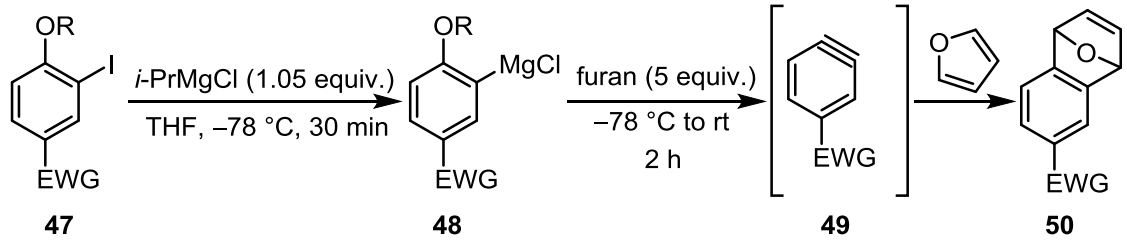

R = CH_3SO_2, 4-$MeC_6H_4SO_2$, 4-$ClC_6H_4SO_2$

EWG = CO_2Me

Scheme 2.13 Generation and trapping of arynes through magnesium-halogen exchange promoted elimination

Another approach to access strained reactive cyclic allenes taking advantage of metal-halogen exchange process is the Doering–Moore–Skattebøl rearrangement used to

generate 1,2-cyclohexadiene **2** from the starting material 6,6-dibromobicyclo[3.1.0]hexane **51**, which in the absence of suitable trapping reagent will dimerize to obtain **5** as shown in *Scheme 2.14*.[17] This method was previously discussed in section 1.2.2.

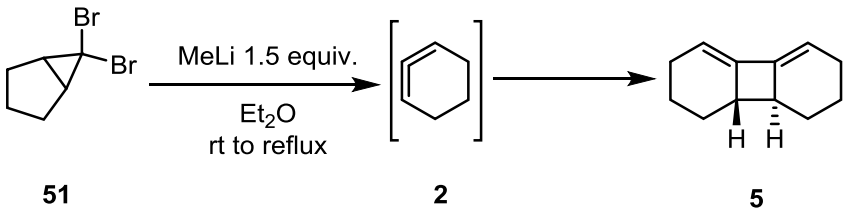

Scheme 2.14 Generation of 1,2-cyclohexadiene through Doering–Moore–Skattebøl rearrangement

Cycloheptyne **54** is a strained reactive intermediate that can be generated through a metal-sulfoxide exchange method which is a particularly interesting approach to get this reactive intermediate. In this work, the 2-sulfinylcycloheptenyl triflate **52** is treated with phenyl magnesium bromide to facilitate the magnesium-sulfoxide exchange and generate organomagnesium intermediate **53**, which will further eliminate the triflate group to get to the cycloheptyne **54**. Capturing the latter one with a suitable trap such as aryl azide gives access to triazole **55** as depicted in *Scheme 2.15*.[18]

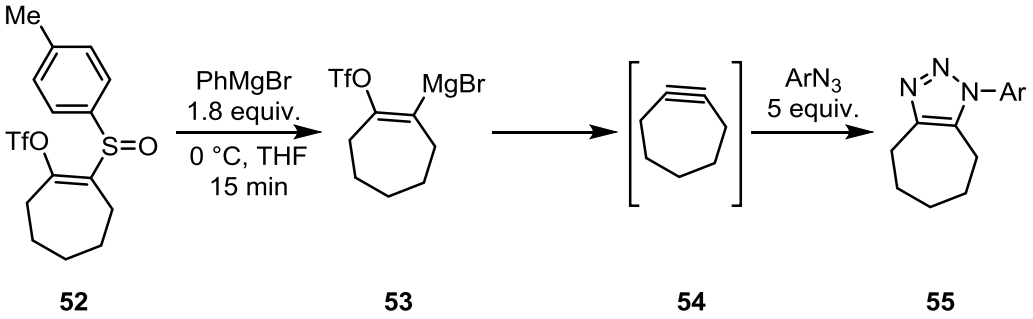

Scheme 2.15 Generation and rapping of cycloheptyne **54**

The last example of strained reactive intermediate synthesized through a lithium-halogen exchange reaction is [1.1.1]propellane.[19–21] Two recent examples have applied this reactive intermediate to generate a variety of complex products. In both works, the authors used a lithium-halogen exchange reaction to obtain [1.1.1]propellane **57** from the carefully designed starting material **56** (*Scheme 2.16*). In contrast with the other examples discussed

earlier in this subchapter, this intermediate **57** can be isolated or stored in solution for a few weeks. Baran's group used a turbo amide to open up the reactive central C-C bond in **57** to get access to different amine functionalized products **58**.[20] Knochel's group used an aryl Grignard reagent to open the same reactive bond from **57** in order to access organomagnesium intermediate **59** which can be further functionalized with ethyl chloroformate to access product **60**.[21]

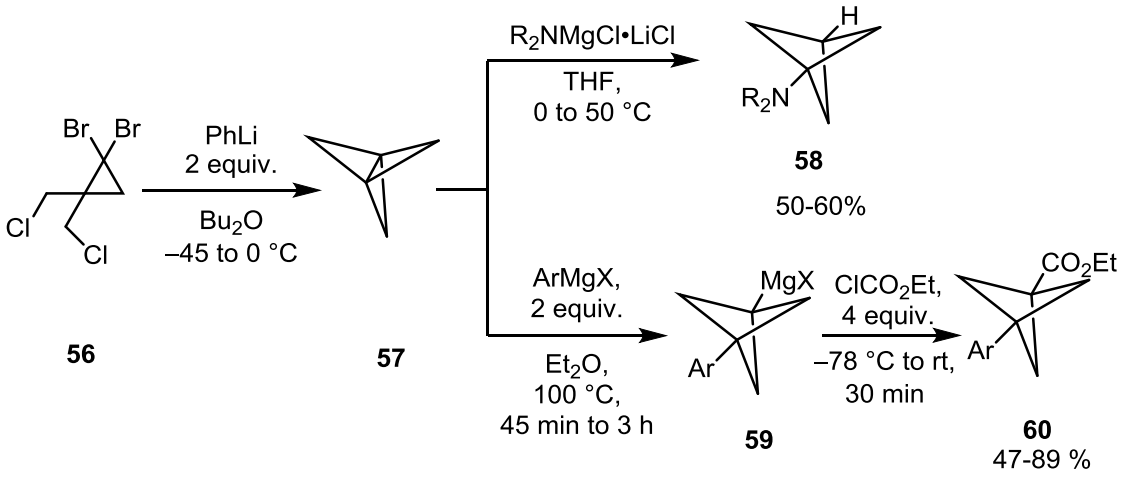

Scheme 2.16 Generation and functionalization of [1.1.1]propellane

2.1.5 Metal-halogen exchange used in generation of acyclic allenes

As described previously in section 2.1, Ichikawa's group developed a method for the synthesis of 1,1-difluoroallenes which involves a lithium-halogen promoted elimination to generate acyclic allenes.[7] They used *n*-BuLi as the optimal organolithium reagent, but they were able to observe good yields with other organolithium reagents like *t*-BuLi, *s*-BuLi and MeLi. For leaving group they surveyed several esters but in the end they opted for acetate as a suitable leaving group. The reaction was proposed to happen in two steps, starting first with the lithium-bromide exchange on starting material **11** to get access to intermediate **12**, which upon elimination will generate the acyclic allene **13** in good yields as presented in *Scheme 2.17*.

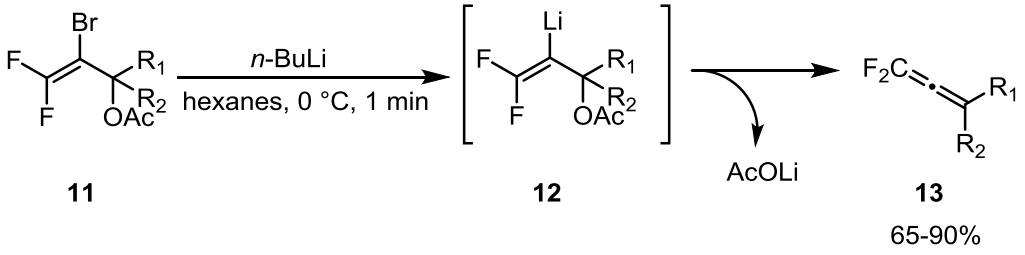

Scheme 2.17 Synthesis of 1,1-difluoroallenes through lithium-halogen exchange

A few years later the same group was able to show that the same type of 1,1-difluoro allenes **13** could be obtained in a similar manner, without the use of organolithium reagents.[22] In order to achieve this they had to change the halogen to iodine from bromine in the starting material **61** and instead of organolithium reagents they used zinc as presented in *Scheme 2.18*. Although longer reaction times were required the yields for acyclic allenes **13** were as good as in the first method.

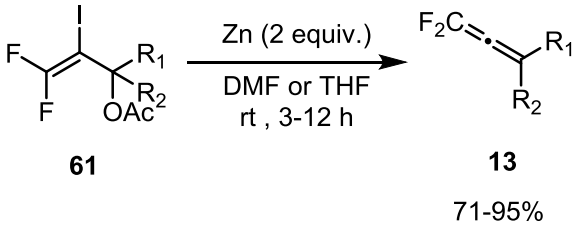

Scheme 2.18 Synthesis of acyclic allenes through zinc promoted elimination

Another synthetic method for acyclic allenes containing a similar structural motif with our proposed starting material was developed by the groups of Tanaka and Ibuka.[23] Substrate **62**, an allylic alcohol derivative containing bromine on the neighboring olefinic carbon, was used as a starting material. In order to generate the acyclic allene **63**, they used in this process a palladium(0) catalyst in combination with diethyl zinc. Mesylates as well as acetates and trichloroacetates were common leaving groups employed in these transformations. The substrates explored were monosubstituted acyclic allenes where R_2 was hydrogen, however a few disubstituted substrates with R_2 being an alkyl or aryl group were also produced.

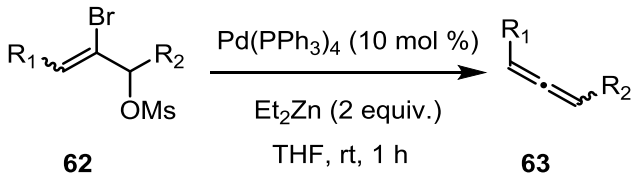

Scheme 2.19 Synthesis of acyclic allenes using a palladium(0)/diethylzinc system

2.2 Results and discussion

2.2.1 Envisioned method

Initially, we proposed a method involving the use of lithium-halogen exchange promoted elimination to generate cyclic allenes. Although the high reactivity of the stoichiometric organolithium reagents that are required represents a possible drawback of this proposed method, we were excited about the facile accessibility of starting materials as presented in *Scheme 2.20*. Another reason we were interested in testing this method was the complementary nature of the elimination reaction with the other previously known and researched elimination methods to generate cyclic allenes as previously discussed in this chapter. We envisioned this reaction to happen in two steps starting with initial lithium-halogen exchange on **64** to generate an organolithium intermediate **65**, which upon elimination would generate the reactive cyclic allene **16**. The process would terminate by either dimerization or trapping of the latter one with suitable trapping agents.

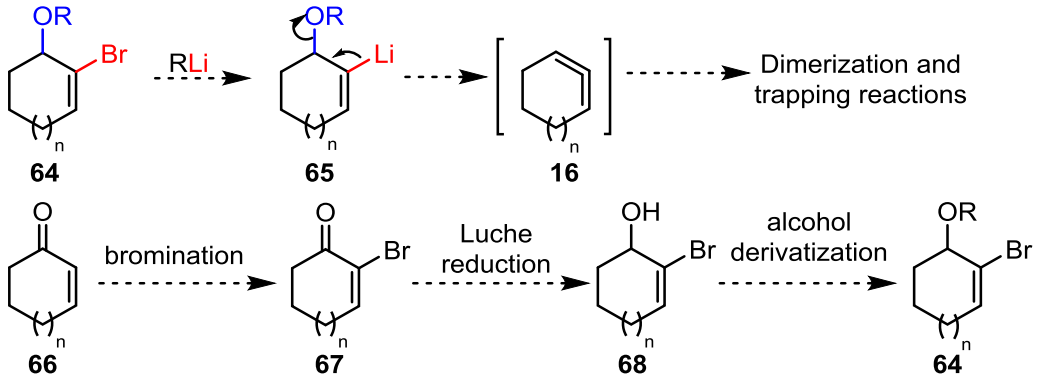

Scheme 2.20 Proposed lithium-halogen exchange promoted elimination for generation of cyclic allenes and synthesis of starting materials

Due to certain limitations of the lithium-halogen exchange based method which we consider to be related to the high reactivity of the stoichiometric organolithium reagents that are required, we decided to try to improve this protocol by proposing magnesium-halogen exchange promoted elimination method to generate cyclic allenes. Basically, in this proposal we were going to replace organolithium reagent with a Grignard analogue and the bromine precursor **64** with iodine based starting material **69** (*Scheme 2.21*). Similarly to the previous iteration, we envisioned this reaction to happen in two steps with an initial magnesium-halogen exchange to generate an organomagnesium intermediate **70**, which upon elimination would give access to the reactive cyclic allene **2**.

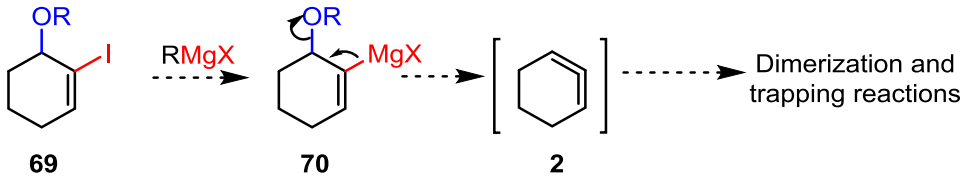

Scheme 2.21 Proposed alternative magnesium-halogen exchange promoted elimination approach to cyclic allenes

2.2.2 Substrate synthesis

Substrate synthesis proceeded from commercially available enones **66a-c**. Although 6- and 7-membered ring enones **66a-b** were easily sourced, when we looked for the 8-membered enone we were not able to find a similar option. Therefore enone **66c** for the 8-membered ring substrate was synthesized in two steps from cyclooctanone **71** according to the literature protocols.[24] In the first step, cyclooctanone **71** was transformed in the corresponding enol silane **72**, which upon modified Saegusa–Ito oxidation with O_2 in the presence of Pd(0) catalyst in DMSO yielded the desired enone **66c** as shown in *Scheme 2.22*.

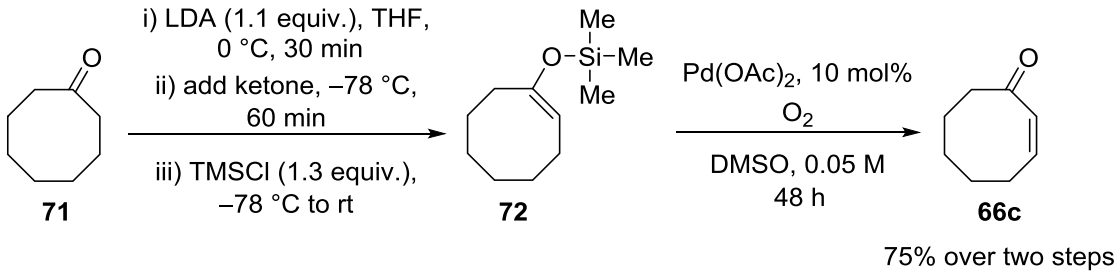

Scheme 2.22 Synthesis of cyclooctenone **66c**

All the enones were brominated by well-established literature protocols using bromine and triethylamine in DCM.[25–27] All the brominations to convert enones **66a-c** to bromoenones **67a-c** occurred in very good yields as presented in *Scheme 2.23*.

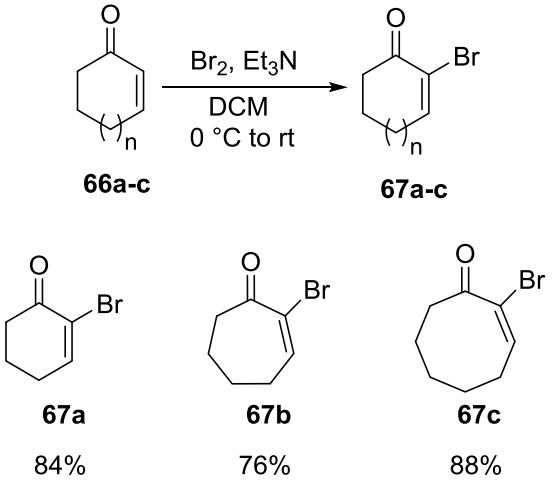

Scheme 2.23 Bromination of enones

The 6- and 7-membered ring enones **66a-b** were iodinated using a well-known literature procedure using iodine, DMAP and potassium carbonate in DCM in order to obtain the iodoenones **73a-b** in good yields as presented in Scheme 2.24.[28] The same protocol failed to provide 8-membered cyclic iodoenone substrate.

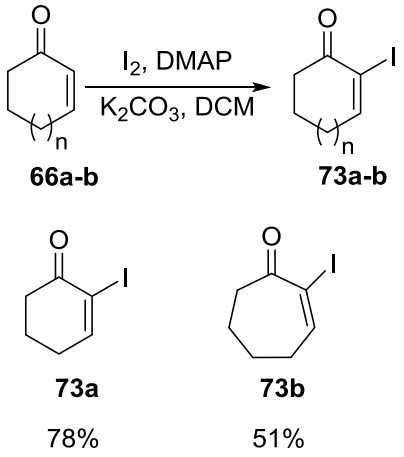

Scheme 2.24 Iodination of enones

Unsuccessful iodination attempts using cyclooctenone **66c** turned out to be intriguing for us. While iodoenones **73a** and **73b** were previously reported in several papers, there were no literature precedents for the 8-membered cyclic iodoenones such as **73c**. Absence of the protocols for the synthesis of this material was concerning; however, this could be related to the limited accessibility of the precursor cyclooctenone **66c** in comparison with its smaller ring analogues **66a** and **66b**. According to the literature, the proposed mechanism for the iodination starts with conjugate addition of DMAP to the enone system generating enolate intermediate **74** which can further capture the iodine to give intermediate **75**; the latter in the presence of a base undergoes DMAP elimination and yields the desired enone **73** as shown in *Scheme 2.25*. The reactivity differences observed may derive from the unique conformational challenges presented by the medium sized ring of **66c**. It is possible that transannular CH_2 groups may impede attack by DMAP sufficiently that the reversible equilibrium lies mainly on the side of reactants.

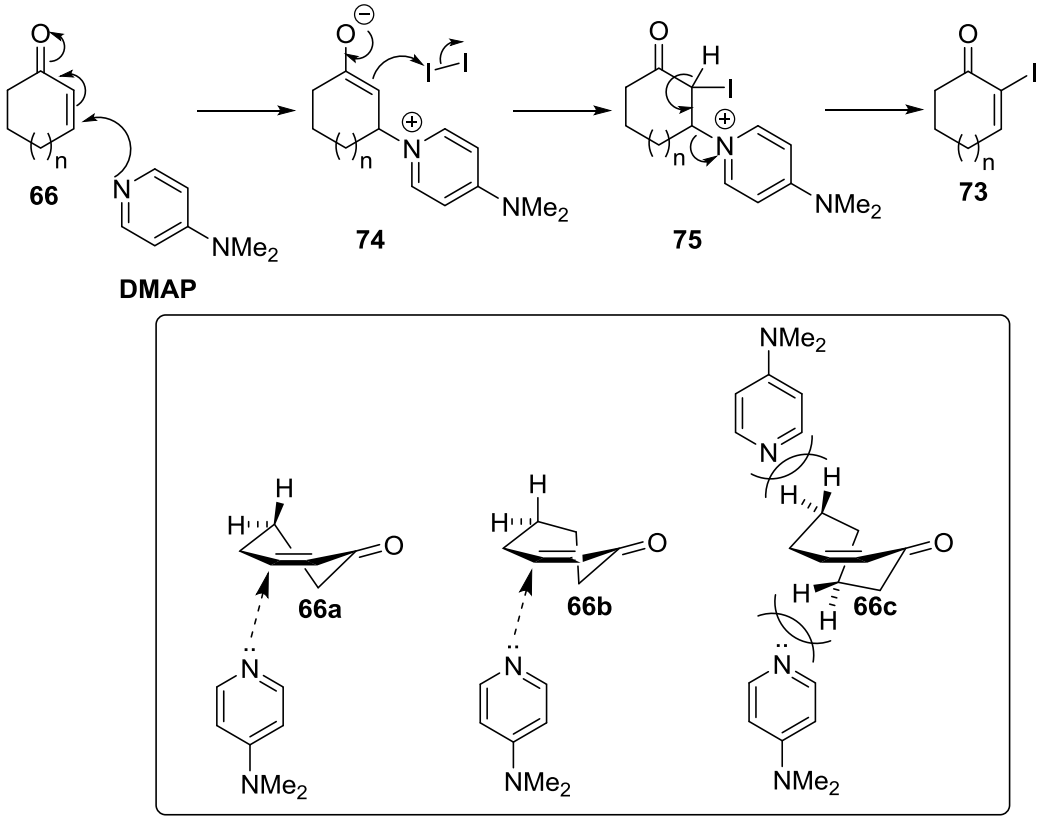

Scheme 2.25 Proposed mechanism for iodination and unfavorable DMAP attack for **66c**

With the haloenones **67a-c** and **73a-b** in hand, we continued our synthesis with the next two steps. First, following the literature protocols we performed a Luche reduction to get access to allylic alcohols **68a-c** and **76a-b** in very good yields.[29,30] Then the alcohols were derivatized to the corresponding halo carbonates **77a-c** and **78a-b** using known methods in very good yields as presented in *Scheme 2.26*.[31,32]

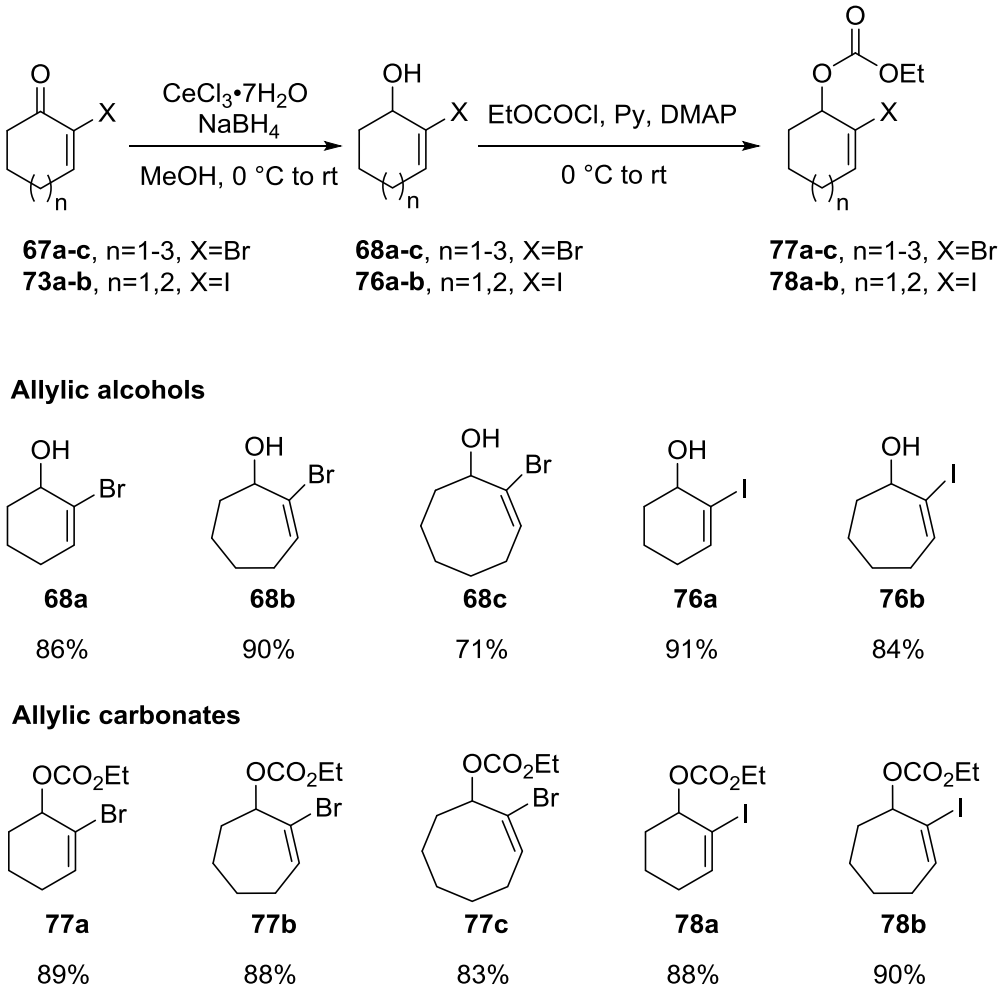

Scheme 2.26 Synthesis of the precursor allylic alcohols and allylic carbonates

As a proof of concept for the versatility of our method we also made a starting material for a substituted cyclic allene (*Scheme 2.27*). Bromoenone **67a** was methylated using methyllithium to get access to tertiary allylic alcohol **79** in good yield. This was based on an adapted similar literature procedure used to methylate other bromoenones.[33] The derivatization of the tertiary allylic alcohol **79** was a challenging step. Using the conditions shown earlier in the formations of carbonates **77** and **78** from the secondary alcohols **68** and **76**, did not convert alcohol **78** to the corresponding carbonate **80**. Also any attempt to force that conversion through changes in those conditions, for instance increasing the DMAP amount, did not provide any desired product. Eventually, we discovered a procedure used for similar tertiary alcohol substrates, in which LiHMDS was employed for

the initial deprotonation of alcohol **79** followed by addition of ethyl chloroformate to obtain carbonate **80** in good yields as shown in *Scheme 2.27*.[34]

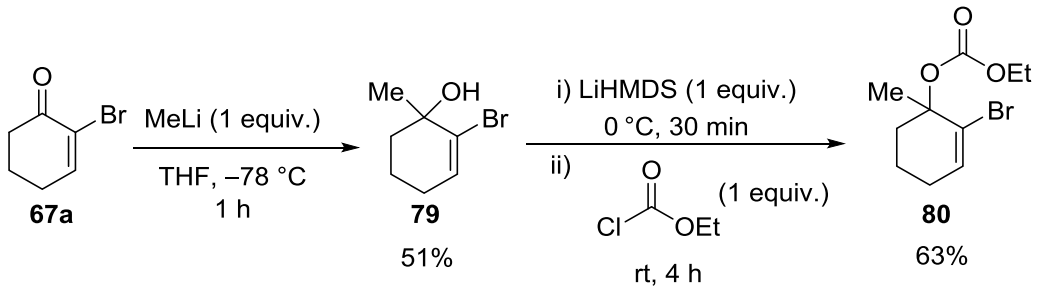

Scheme 2.27 Synthesis of methyl substituted bromocarbonate **80**

2.2.3 Lithium-halogen exchange and formation of cyclic allene dimer conditions

Since we were using an organolithium reagent, such as *t*-BuLi, we started our examination with low temperature conditions (entries 1-6 in *Table 2.1*). When a reactive cyclic allene such as 1,2-cyclohexadiene **2** is generated in the absence of a trapping reagent it will form dimer **5**. Typically one would develop conditions using one of the trapping reagents (furan, styrene) and look for the corresponding cycloadduct formation, with lithium-halogen exchange promoted elimination we observed that trapping reactions were not providing the desired cycloadducts. Therefore we attempted to generate the 6-membered cyclic allene using lithium halogen exchange and look for formation of dimer instead. In most cases, only traces of a dimer **5** were observed in a complex mixture through ^{1}H NMR and ^{13}C NMR analysis. With the use of carbonate leaving group "cleaner" complex mixture was observed in crude ^{1}H NMR and ^{13}C NMR analysis. We were able to get isolable amount of a dimer **5** when carrying the reaction in hexanes at room temperature (Entry 9, *Table 2.1*).

Table 2.1 Dimer **5** formation upon generation of 1,2-cyclohexadiene **2** using lithium-bromide exchange promoted elimination

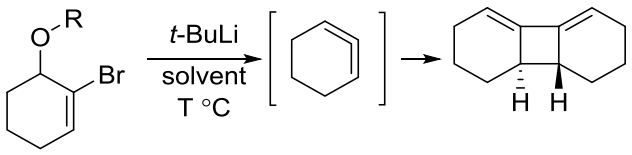

64a-c
77a

2

5

Entry	Starting material	T,°C	Solvent	Observation[b]
1	**64a**, R=Ac	−78	hexanes	Traces of dimer;
2	**64b**, R= Piv	−78	hexanes	Traces of dimer
3	**64c**, R= Bz	−78	hexanes	No dimer observed
4	**77a**, R= COOEt	−78	hexanes	Traces of dimer
5	**77a**, R= COOEt	−78	Et_2O	Traces of dimer
6	**77a**, R= COOEt	−78	THF	Traces of dimer
7	**77a**, R= COOEt	rt	Et_2O	Traces of dimer
8	**77a**, R= COOEt	rt	THF	Traces of dimer
9	**77a**, R= COOEt	rt	hexanes	23%

a) reactions were run at 0.1 mmol scale (0.03 M concentration in starting material), for 30 minutes; b) Starting materials were consumed in all experiments.

2.2.4 Magnesium-halogen exchange and cyclic allene capturing with furan conditions

We also tested a milder magnesium-halogen exchange promoted elimination process with which we were able to perform trapping reactions of the reactive cyclic allene **2**. With this early observation in hand we proceeded towards the optimization of the trapping reaction with furan. We analyzed several parameters of this reaction such as the solvent, temperature, organomagnesium reagent, and starting material concentration. Regarding the solvent, we observed similar results with THF, Et_2O, and furan and significantly lower yields with hexanes, which could be related to the low solubility of the organomagnesium reagent in this solvent (Entries 1-4, *Table 2.2*). Increasing the amount of the organomagnesium reagent and using slow addition at room temperature showed a

significant increase in the yield (Entry 7). Changing the organomagnesium reagent from *i*-PrMgCl to *t*-BuMgCl led to a noticeable decrease in the yield (Entry 8). Lowering the temperature also had a disadvantageous effect on the reaction outcome (Entry 9). Significant decreases in yield was noticed with dilution or by increasing the concentration of the starting material **78a** (Entries 10-11). Increasing the temperature along with a slow addition of 5 equivalents of *i*-PrMgCl showed the best results in terms of NMR yield (Entry 13).

Table 2.2 Optimization for the generation and trapping of 1,2-cyclohexadiene through magnesium-iodine exchange promoted elimination

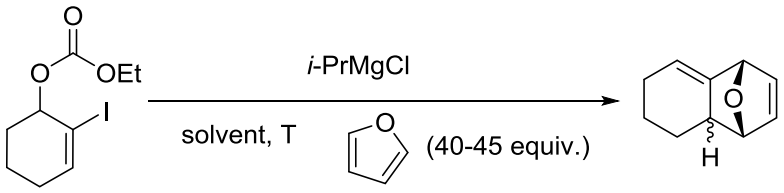

78a **81**

Entry	Solvent	Time, min	T, °C	[**78a**], M	Equiv, RMgCl	NMR Yield[c]
1	THF	30	rt	0.03	3	28%
2	Hexane	30	rt	0.03	3	3%
3	Et_2O	30	rt	0.03	3	20%
4	Furan	30	rt	0.03	3	25%
5[a]	THF	30	rt	0.03	3	24%
6[a]	Et_2O	30	rt	0.03	3	6%
7[a]	THF	30	rt	0.03	5	39%
8	THF	30	rt	0.03	5[b]	18%
9	THF	30	0 °C	0.03	5	0%
10	THF	30	rt	0.01	5	8%
11	THF	30	rt	0.1	5	26%
12	THF	30	50 °C	0.03	5	33%
13[a]	THF	30	50 °C	0.03	5	43%

a) material **78a** was used at 0.1 mmol scale and the Grignard reagent was added dropwise; b) the Grignard reagent was *t*-BuMgCl in this case; c) NMR yield was calculated as an average of two experiments for each set of conditions; mesitylene was used as an internal standard.

2.2.5 Generation and dimerization of cyclic allenes generated through metal-halogen exchange promoted elimination

The formation of dimers is a characteristic phenomenon for the reactive cyclic allene species. During the optimization for the dimerization reaction presented previously in section 2.4.3 we observed only traces of the dimer at low temperatures such as −78 ºC and isolable yields at room temperature. We propose that starting material bromocarbonate **77a** undergoes a lithium-halogen exchange process in the presence of *t*-BuLi to form organolithium intermediate **82** followed by elimination of the carbonate to form 1,2-cyclohexadiene **2**. The latter one can react with another molecule of itself in a radical fashion to form biradical intermediate **83** which upon ring closure provides dimer **5**. On the other hand, biradical **83** can trimerize into **85** via reaction with a third molecule of allene **2** followed by radical ring closing. In another reaction pathway two molecules of intermediate **83** can react with each other to form tetramers **86** as presented in *Scheme 2.30*. It seems that at lower temperature the ring closing process for **83** to form dimer **5** is slower than the reaction with another molecule of cyclic allene **2** or with itself. Our observations are consistent with the observations made by Moore and coworkers and we based our proposal on their prior observations.[17] They were generating the reactive cyclic allene **2** starting from **51** using the Doering–Moore–Skattebøl rearrangement method. In their case as well, drastic decrease in yield for dimer **5** was observed when the reaction was performed at −78 ºC and large scale synthesis allowed isolation of tetramer **86** along with trimer product **85**.

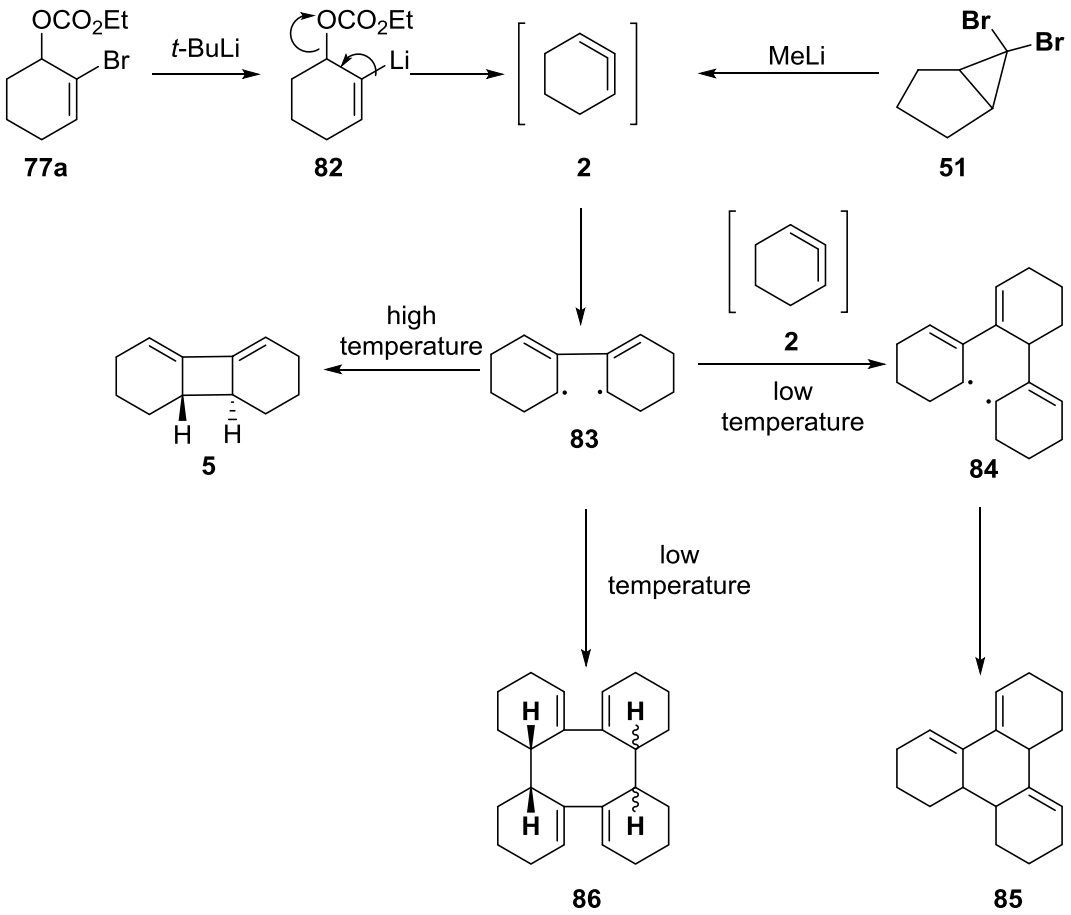

Scheme 2.28 Dimerization reaction and competing pathways to higher oligomers

Having the conditions for formation and dimerization of 1,2-cyclohexadiene in hand we turned our attention to the 7- and 8-membered ring substrates. Treatment of the bromo carbonates **77a-c** with two equivalents of *t*-BuLi in hexanes at room temperature produced known dimers **5**,[35] **87**[36] and **88**.[37] We observed moderate yields for 6- and 8-membered ring substrates and significant increase in yield for the 7-membered ring cyclic allene as shown in *Scheme 2.29*.

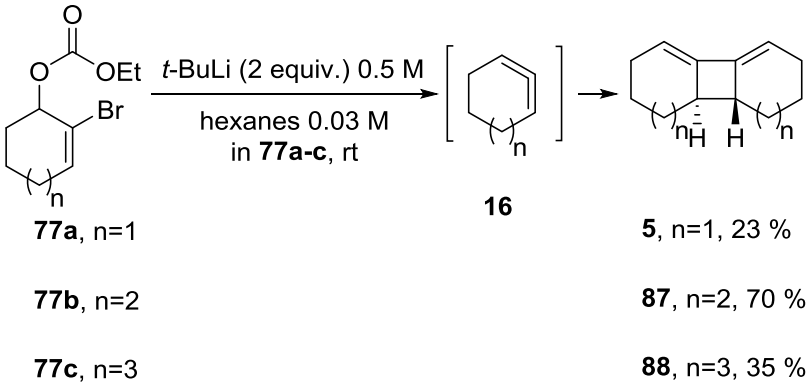

77a, n=1 — **5**, n=1, 23 %

77b, n=2 — **87**, n=2, 70 %

77c, n=3 — **88**, n=3, 35 %

Scheme 2.29 Dimerization scope for lithium-halogen exchange promoted elimination

For the dimerization of cyclic allenes through the magnesium-halogen exchange method we used four equivalents of isopropyl magnesium chloride in THF at 0 °C. Similarly with the lithium halogen series, a moderate yield was obtained for the 6-membered ring substrate and a significantly better yield was obtain for the 7-membered ring substrate.

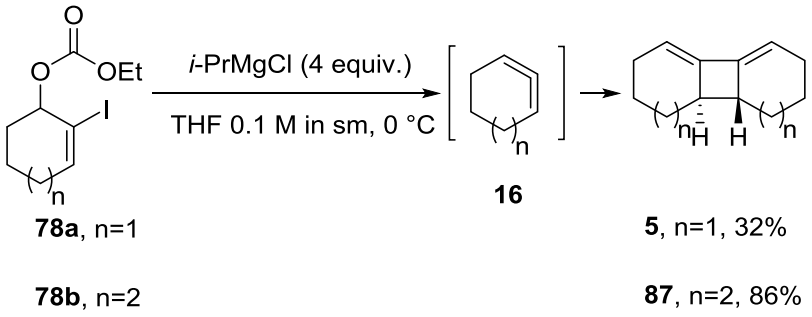

78a, n=1 — **5**, n=1, 32%

78b, n=2 — **87**, n=2, 86%

Scheme 2.30 Dimerization scope for magnesium-halogen exchange

Using similar conditions as in the experiments presented in *Scheme 2.29*, we were able to obtain a 65% yield for the known in literature methylated 6-membered ring cyclic allene dimer **89**[38] as shown in *Scheme 2.31*. This particular example shows the possibility of expanding the substrate scope by introducing additional substituents into the allene precursors via 1,2-addition to the haloenone intermediates.

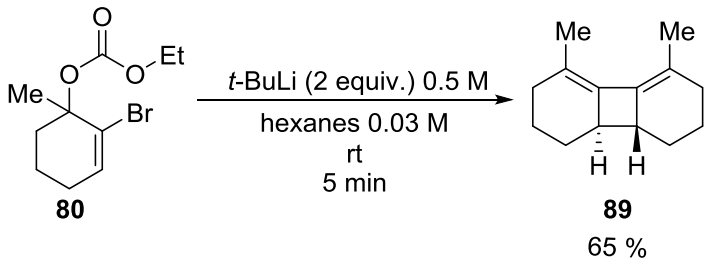

80 **89** 65 %

Scheme 2.31 Dimerization of methyl substituted substrate

In another project, Yasseen Almehmadi (former member in our group) obtained an interesting diketone dimer product **92** when he treated bromo acetal **90** with *n*-BuLi at −78 °C. We propose that when acetal **90** is treated with 1.2 equivalents of *n*-BuLi at −78 °C a lithium-halogen exchange step occurs followed by the opening of the acetal ring to generate intermediate **91**. This will further dimerize and undergo hydrolysis at work-up to provide diketone product **92** as presented in *Scheme 2.32*. The proposed structural assignment was confirmed via single crystal X-ray diffraction analysis.

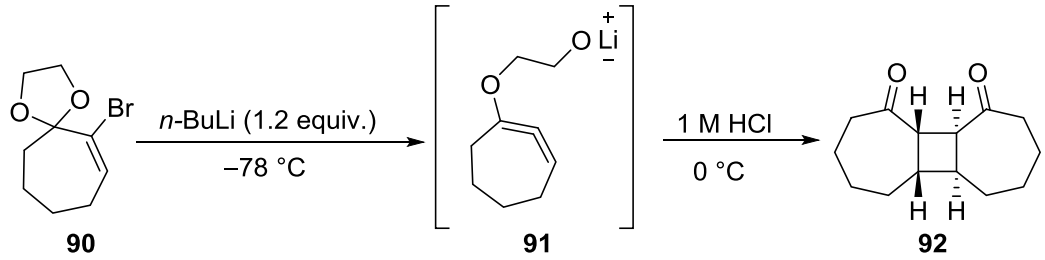

90 **91** **92**

47%

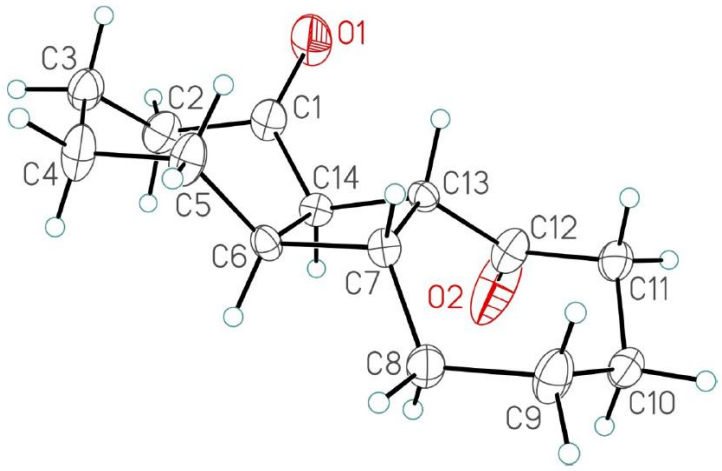

92

Scheme 2.32 Generation of diketone **92** dimer

2.2.6 Generation and trapping of 1,2-cyclohexadiene generated through metal-halogen exchange promoted elimination

In order to show the usefulness of the method described in this chapter, several cycloaddition reactions that have been applied with cyclic allenes generated by other routes were examined. While generation of cyclic allenes through the lithium-halogen exchange promoted elimination was depicted in the previous subchapter where the dimer products corresponding to several reactive cyclic allenes were isolated, the trapping of these reactive species through typical cycloaddition was not achieved. We performed several test reactions with the common traps used before in the literature such as furan, styrene and diphenylisobenzofuran (DPIBF) (*Scheme 2.33*). When furan and styrene were used as traps, the reactions resulted in a complex mixture containing dimer products and no traces of the desired cycloadducts according to the ^{1}H NMR and ^{13}C NMR analysis of the crude reaction product. Similar results were obtained with DPIBF, but in this case a trace amount of desired cycloadduct was observed in the crude NMR spectra of the resulting complex mixture.

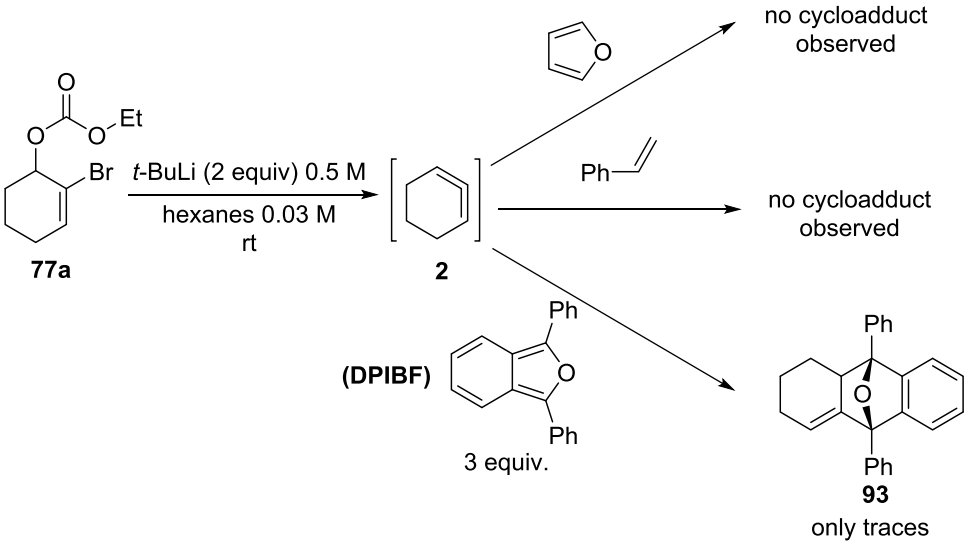

Scheme 2.33 Trapping reactions with 1,2-cyclohexadiene generated through lithium-halogen exchange promoted elimination

In contrast with the lithium-halogen exchange promoted generation of cyclic allenes where we were not able to perform any of the typical cycloaddition reactions, magnesium-halogen exchange promoted elimination allowed us to access the expected cycloadducts. Treatment of a mixture of starting material **78a** and 40 equivalents of furan with 4 equivalents of isopropyl magnesium chloride in THF at 50 °C resulted in a 10:1 mixture of *endo*- and *exo*- diastereomeric cycloadducts **81a** and **81b** in 58% yield (*Scheme 2.34*). This result is similar to previous literature reports for the trapping of 1,2-cyclohexadiene **2** with furan.[39]

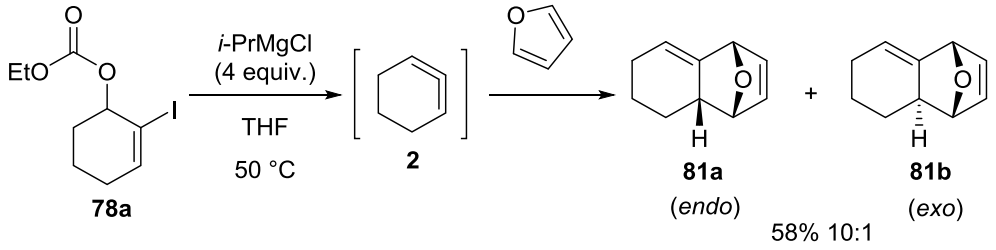

Scheme 2.34 Trapping of 1,2-cyclohexadiene **2** generated through magnesium-halogen exchange with furan

Another typical way of trapping of 1,2-cycloahexadiene **2** in a [4+2] Diels–Alder cycloaddition is the reaction with DPIBF. In this reaction we treated a mixture of starting material **78a** and 3 equivalents of DPIBF with 4 equivalents of isopropyl magnesium chloride in THF at 50 °C as in the optimized conditions. Once 1,2-cyclohexadiene **2** was generated, it was trapped by the DPIBF already present in the mixture to obtain cycloadduct **93a**. In this case, we were able to isolate only the *endo* diastereomer **93a** in 63% yield as shown in *Scheme 2.35*, in contrast with the literature reports where a mixture of the *endo* and *exo* diastereomers was observed.[39] The *endo* assignment can be done through the presence of an upfield proton at 0.47 ppm which is in the anisotropy shielding region of the benzene ring. The *exo* diastereomer would not present this kind of proton affected by anisotropy.

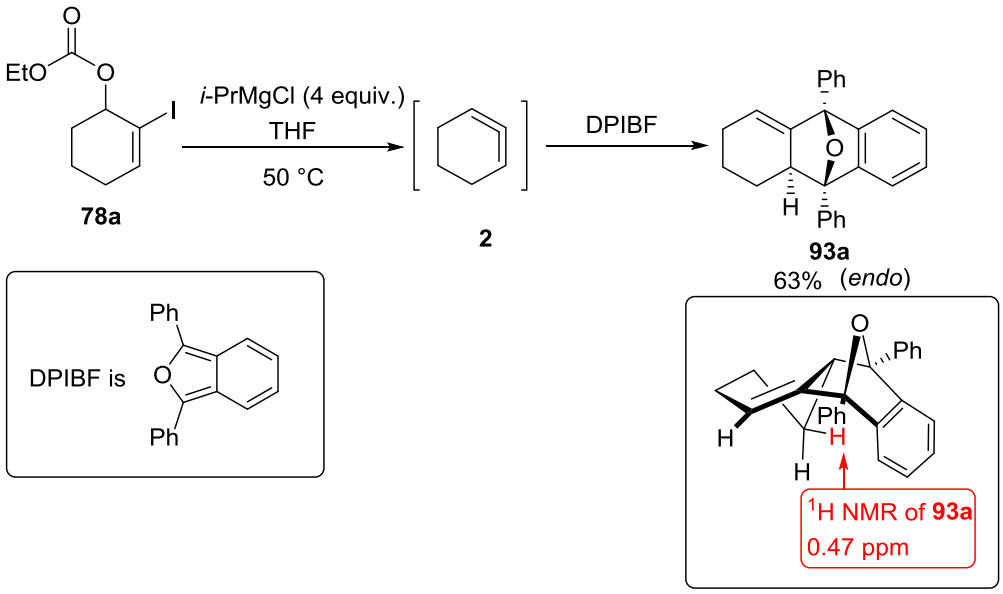

Scheme 2.35 Trapping of 1,2-cyclohexadiene **2** with DPIBF

Formal [2+2] cycloaddition with styrene is an alternative way of trapping of 1,2-cyclohexadiene **2**. In this reaction we treated a mixture of starting material **78a** and 25 equivalents of styrene with 4 equivalents of isopropyl magnesium chloride in THF at 50 °C as in the optimized conditions. Once 1,2-cyclohexadiene **2** was generated, it was trapped by the styrene already present in the mixture to obtain the 2.5:1 mixture of *exo*- and *endo*-known cycloadducts **6a** and **6b**[40] in 76% yield as shown in *Scheme 2.36*.

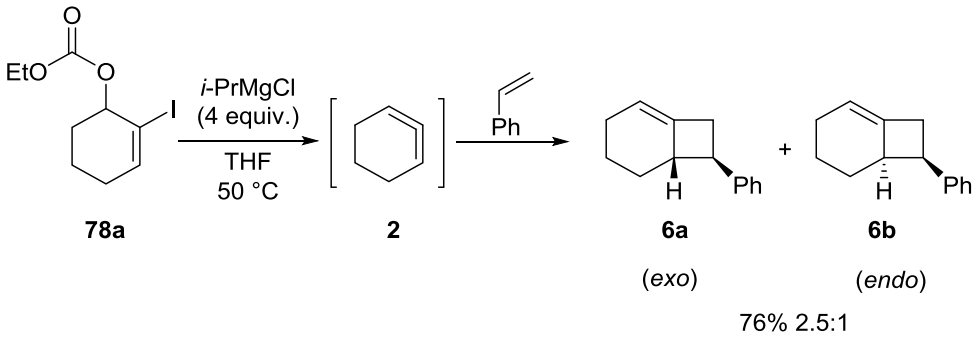

Scheme 2.36 Trapping of 1,2-cyclohexadiene **2** with styrene

A more recent development in the chemistry of cyclic allenes is their trapping in a [3+2] cycloaddition with different 1,3-dipoles.[5,6] In our attempt to perform such a reaction we were not able to obtain any desired cycloadduct (*Scheme 2.37*). From the crude NMR

spectra we were able to observe the presence of product **96**, which was obtained from the nucleophilic addition of isopropyl magnesium chloride to the 1,3-dipole system. Therefore it seems that the magnesium-halogen exchange promoted elimination conditions are not compatible with this trap, due to the reactivity at the electrophilic carbon terminus of the 1,3-dipole.

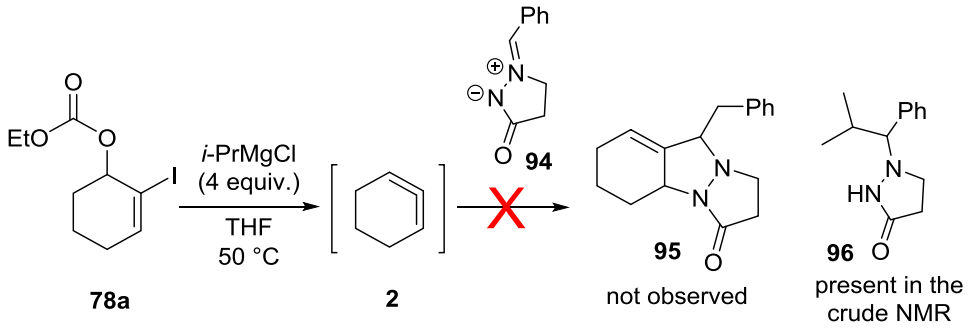

Scheme 2.37 Trapping attempt of 1,2-cyclohexadiene **2** with 1,3-dipole

2.3 Conclusions

There are several previously reported methods for the generation of reactive cyclic allenes, each employing unique substrates and reaction conditions. However, a common drawback of these methods is the effort required to prepare the precursors. Taking inspiration from the desilylative elimination, which entails carbanionic reactivity at an allylic position and elimination of a neighboring alkenyl leaving group, we sought to explore the viability of the opposite polarization, with anionic character on the sp^2-hybridized carbon and a neighbouring allylic leaving group. While alkenyl silanes proved to be unreactive, the corresponding organometallic species (either organolithium or organomagnesium) were accessible from alkenyl halide precursors. Importantly, the substrates needed for this method are easily prepared from known precursors.

In the first version of the metal-halogen exchange strategy, we examined lithium-bromine exchange promoted elimination of allylic carbonates as a method to generate reactive cyclic allenes and allowed them to undergo *in situ* dimerization. We observed significantly higher yields in dimer for 7-membered ring cyclic allene in comparison with the 6-, and 8- membered substrates. Using the 1,2-addition to bromoenones instead of simple Luche reduction we were able to generate substituted cyclic allenes. While the generality of this method was encouraging, we found that the conditions were not compatible with various trapping reagents, such as furans or styrene. The high reactivity of *t*-BuLi, used for lithium-bromine exchange, is the most likely explanation for this shortfall. However, this limitation then inspired us to look at the alternative organomagnesium intermediates, whose generation might permit a wider range of trapping reactivity.

In a second iteration of the metal-halogen exchange, we moved our attention towards magnesium-iodine exchange promoted elimination, which would use milder conditions for generating cyclic allenes than the lithium-bromide exchange method. We were able to get the dimers from two cyclic allenes with these conditions in moderate to good yields. When we performed trapping of 1,2-cyclohexadiene **2** in the [4+2] cycloaddition with furan and DPIBF and in the formal [2+2] cycloaddition with styrene we were able to obtain the corresponding cycloadducts in good yields. The magnesium-iodide

exchange conditions proved to be incompatible with the azomethine imine 1,3-dipole trap we used in our [3+2] cycloaddition attempt.

We conclude that two new methods to generate cyclic allenes were developed using easily accessible starting materials, which show potential for further substrate scope development. Although the lithium-halogen exchange version is limited to dimer products, the magnesium-halogen exchange version can provide access to [4+2] and [2+2] typical cycloadducts in the trapping of cyclic allenes.

2.4 Experimental

2.4.1 Synthesis of halocarbonates

Most of the starting materials were synthesized in 3 steps from their corresponding enones. For cyclooctenone **66c** a previously established literature protocol was used to get access to this material.[24] In the first step enones **66** were halogenated with bromine or iodine in order to obtain known haloenones **67a**,[26,41] **67c**,[42] **73a**,[28] **73b**,[28] which were matching accordingly with the literature data. Then haloenones were submitted to a Luche reduction to access allylic alcohols **68a**,[30] **68c**,[43] **76a**,[30] **76b**,[29] which were matching accordingly with the literature data. The 7-membered bromocarbonate **77b** was prepared by Almehmadi Y. A., who was working on this project in our as well.[44]

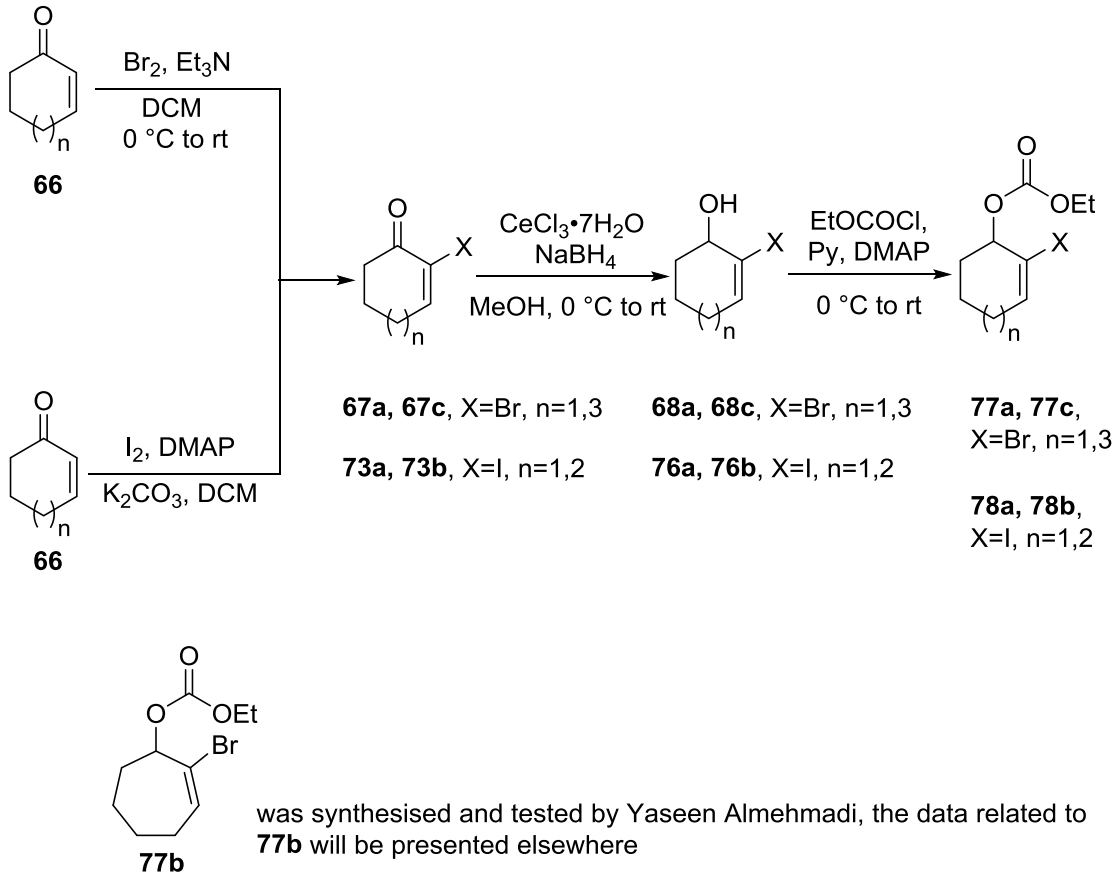

Scheme 2.38 Synthesis of halocarbonate precursors

Method for synthesis of halocarbonates from secondary alcohols

To a mixture of allylic alcohol (**68a**, **68b**, **76a**, **76b**) and 1.5 equivalents of pyridine in DCM (0.15 M in allylic alcohol) was added 1.2 equivalents of ethyl chloroformate dropwise at 0 °C. The reaction mixture was then warmed up and stirred at room temperature for one hour. By means of TLC analysis the conversion of the allylic alcohol was checked, and when required in the case of an incomplete transformation 0.1 equivalents of DMAP dissolved in DCM was added and the reaction mixture was stirred for another hour. The reaction mixture was quenched with 1 M HCl at 0 °C, and extracted with DCM three times. The combined organic layers were washed with brine, dried over $MgSO_4$, filtered, and concentrated. The crude was purified by column chromatography on silica gel with a 5% EtOAc in hexanes eluent.

2-bromocyclohex-2-en-1-yl ethyl carbonate (**77a**)

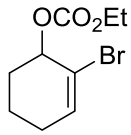

77a

Alcohol **68a** (1.02 g, 5.76 mmol) was used. Flash chromatography (95:5 hexanes:EtOAc) on silica gel gave 1.28 g of bromocarbonate **77a** in 89% yield as a colorless oil. R_f = 0.6 (9:1, hexanes:EtOAc); IR (cast film) cm^{-1} 2984, 2949, 2870, 1745, 1646, 1448, 1373, 1335, 1263, 1247, 1163;^{1}H NMR (500 MHz, $CDCl_3$) δ 6.36 (dd, J = 5.0, 3.2 Hz, 1H), 5.28 – 5.21 (m, 1H), 4.28 – 4.17 (m, 2H), 2.23 – 2.13 (m, 1H), 2.12 – 2.00 (m, 2H), 1.98 – 1.88 (m, 1H), 1.78 – 1.62 (m, 2H), 1.33 (t, J = 7.1 Hz, 3H); ^{13}C NMR (126 MHz, $CDCl_3$) δ 154.7, 135.8, 119.1, 75.0, 64.3, 30.0, 27.6, 17.0, 14.3; HRMS (ESI, $[M+Na]^+$) for $C_9H_{13}BrNaO_3$ calcd. *m/z* 270.9940, found: *m/z* 270.9936.

(*E*)-2-bromocyclooct-2-en-1-yl ethyl carbonate (**77c**)

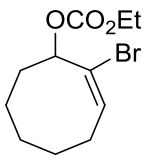

77c

Alcohol **68c** (600 mg, 2.93 mmol) was used. Flash chromatography (95:5 hexanes:EtOAc) on silica gel gave 674 mg of bromocarbonate **77c** in 83% yield as a colorless oil. R_f = 0.7 (9:1, hexanes:EtOAc); IR (cast film) cm^{-1} 2983, 2933, 2859, 1746, 1639, 1452, 1374, 1264, 1018; ^1H NMR (500 MHz, $CDCl_3$) δ 6.26 (t, J = 8.8 Hz, 1H), 5.52 (dd, J = 11.4, 5.1 Hz, 1H), 4.22 (q, J = 7.1 Hz, 2H), 2.35 – 2.19 (m, 2H), 1.91 – 1.68 (m, 5H), 1.45 – 1.35 (m, 3H), 1.33 (t, J = 7.1 Hz, 3H); ^{13}C NMR (126 MHz, $CDCl_3$) δ 154.4, 134.2, 123.3, 74.3, 64.3, 32.7, 30.2, 29.1, 26.8, 23.4, 14.3; HRMS (ESI, $[M+NH_4]^+$) for $C_{11}H_{21}BrNO_3$ calcd. *m/z* 294.0699, found: *m/z* 294.0699; (ESI, $[M+Na]^+$) for $C_{11}H_{17}BrNaO_3$ calcd. *m/z* 299.0253, found: *m/z* 299.0250.

2-iodocyclohex-2-en-1-yl ethyl carbonate (**78a**)

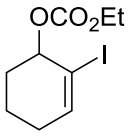

78a

Alcohol **76a** (1.167 g, 5.21 mmol) was used. Flash chromatography (95:5 hexanes:EtOAc) on silica gel gave 1.36g of iodocarbonate **78a** in 88% yield as a light yellow oil (color becomes red with decomposition; it was kept at dark in freezer). R_f = 0.65 (9:1, hexanes:EtOAc); IR (cast film) cm^{-1} 2981, 2945, 1744, 1630, 1372, 1261, 1161; ^1H NMR (500 MHz, $CDCl_3$) δ 6.74 – 6.62 (m, 1H), 5.26 (t, J = 4.4 Hz, 1H), 4.26 (m, 2H), 2.30 – 2.06 (m, 2H), 2.01 (m, 2H), 1.83 – 1.69 (m, 2H), 1.37 (t, J = 7.1 Hz, 3H); ^{13}C NMR (126 MHz, $CDCl_3$) δ 154.6, 144.1, 94.0, 77.2, 64.3, 29.9, 29.2, 17.0, 14.3; HRMS (ESI, $[M+NH_4]^+$) for $C_9H_{17}INO_3$ calcd. *m/z* 314.0248, found: *m/z* 314.0246; (ESI, $[M+Na]^+$) for $C_9H_{13}INaO_3$ calcd. *m/z* 318.9802, found: *m/z* 318.9800.

2-iodocyclohept-2-en-1-yl ethyl carbonate (**78b**)

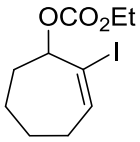

78b

Alcohol **76b** (1.737 g, 7.3 mmol) was used. Flash chromatography (95:5 hexanes:EtOAc) on silica gel gave 2.036 g carbonate **78b** in 90% yield as a light yellow oil (color becomes red with decomposition; it was kept at dark in freezer). R_f = 0.65 (9:1, hexanes:EtOAc); IR (cast film) cm^{-1} 2981, 2934, 2859, 1745, 1618, 1445, 1373, 1257; ^1H NMR (500 MHz, $CDCl_3$) δ 6.74 (t, J = 6.9 Hz, 1H), 5.33 – 5.30 (m, 1H), 4.29 – 4.19 (m, 2H), 2.28 – 2.19 (m, 1H), 2.15 – 2.06 (m, 1H), 1.97 – 1.85 (m, 3H), 1.76 – 1.68 (m, 1H), 1.66 – 1.58 (m, 2H), 1.34 (t, J = 7.1 Hz, 3H); ^{13}C NMR (126 MHz, $CDCl_3$) δ 154.4, 145.6, 99.8, 82.2, 64.3, 30.6, 30.2, 25.6, 24.5, 14.4; HRMS (ESI, $[M+Na]^+$) for $C_{10}H_{15}INaO_3$ calcd. *m/z* 332.9958, found: *m/z* 332.9965.

Method for synthesis of 2-bromo-1-methylcyclohex-2-en-1-yl ethyl carbonate (80) from bromoenone 67a

To a solution of 956 mg bromoenone **67a** (5.46 mmol) in THF (15 mL) at −78 ºC was added 7 mmol of MeLi (4.4 mL of 1.6 M in Et_2O) dropwise. After stirring the reaction mixture for 1 h, it was quenched with 10 mL of water and extraction was performed with 3 x 15 mL of Et_2O. The organic fractions were combined and dried over $MgSO_4$, filtered and concentrated. The crude product was purified by column chromatography on silica gel with a 15% EtOAc in hexanes eluent in order to obtain 523 mg of 2-bromo-1-methylcyclohex-2-en-1-ol **79** as a colorless oil in 50.1% yield. R_f = 0.3 (20% EtOAc in hexanes) ^1H NMR (500 MHz, $CDCl_3$) δ = 6.13 (t, J = 4.1 Hz, 1H), 2.16 – 2.03 (m, 2H), 2.03 – 2.00 (m, 1H), 2.00 – 1.87 (m, 2H), 1.83 – 1.74 (m, 1H), 1.71 – 1.61 (m, 1H), 1.41 (s, 3H); ^{13}C NMR (126 MHz, $CDCl_3$) δ 131.6, 131.5, 71.4, 38.5, 28.9, 28.1, 19.6.

To a solution of allylic alcohol **79** (457 mg, 2.4 mmol) in 5 mL anhydrous THF, 2.4 mmol of LiHMDS (2.4 mL of 1M solution in THF) was added dropwise at 0 ºC under a nitrogen atmosphere. After stirring the reaction mixture for 30 minutes, ethyl chloroformate (0.23 mL, 2.4 mmol) was added dropwise. Allowing a slow warm-up to room temperature the reaction mixture was stirred for another 3 h. The reaction mixture was then quenched with 5 mL of saturated ammonium chloride solution and extraction was performed with 5 x 5 mL Et_2O. The organic fractions were combined and dried over $MgSO_4$, filtered and concentrated. The crude product was purified by column

chromatography on silica gel with a 5% EtOAc in hexanes eluent in order to obtain 401 mg of 2-bromo-1-methylcyclohex-2-en-1-yl ethyl carbonate **80** as a colorless oil in 63% yield. R_f = 0.7 (9:1, hexanes:EtOAc); IR (cast film) cm^{-1} 2985, 2940, 2871, 1747, 1446, 1370, 1262, 1089; ^{1}H NMR (500 MHz, $CDCl_3$) δ 6.23 (ddd, J = 5.1, 3.3, 0.6 Hz, 1H), 4.23 – 4.10 (m, 2H), 2.71 – 2.61 (m, 1H), 2.21 (dddd, J = 18.0, 9.0, 5.5, 3.3 Hz, 1H), 2.06 (dtdd, J = 17.8, 5.3, 4.0, 1.2 Hz, 1H), 1.98 (dddd, J = 12.9, 6.2, 3.2, 1.2 Hz, 1H), 1.89 – 1.80 (m, 1H), 1.76 – 1.65 (m, 1H), 1.59 (d, J = 0.6 Hz, 3H), 1.31 (t, J = 7.1 Hz, 3H); ^{13}C NMR (126 MHz, $CDCl_3$) δ 152.8, 133.2, 126.1, 82.2, 63.6, 34.0, 27.5, 26.3, 20.2, 14.3; HRMS (ESI, $[M+Na]^+$) for $C_{10}H_{15}BrNaO_3$ calcd. *m/z* 285.0097, found: *m/z* 285.0095.

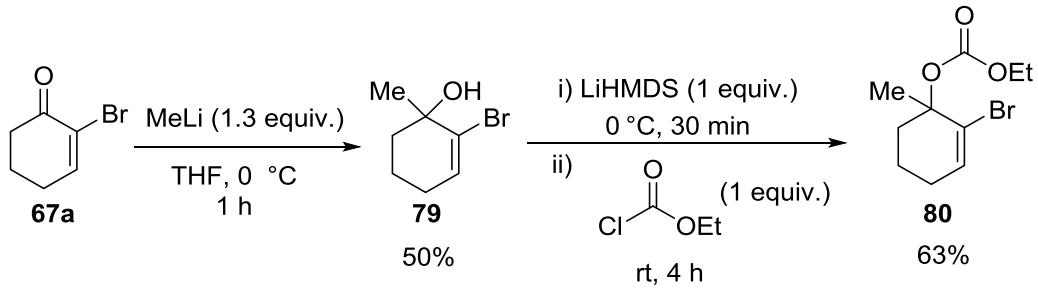

Scheme 2.39 Synthesis of bromocarbonate precursor **80**

2.4.2 Allene dimerization reactions

General method for generation of cyclic allenes via lithium-halogen exchange promoted elimination and dimerization

To a 0.03 M solution of 1 equivalent of bromocarbonate starting material (**77a**, **77c**, **80**) in dry hexanes at room temperature, 2 equivalents of 0.5 M *t*-Buli in hexanes was added dropwise. The reaction mixture was stirred for 30 minutes at room temperature and then quenched with water. The reaction mixture was then extracted 3 times with diethyl ether. The organic layers were combined, washed with brine, dried over $MgSO_4$, filtered and concentrated. The crude product was purified by careful column chromatography on silica gel. (Note: all products are nonpolar hydrocarbons with high R_f values). The ^{1}H NMR and ^{13}C NMR data for known dimers **5**,[35] **87**,[36] **88**,[37] and **89**[38] is matching with the data reported in literature.

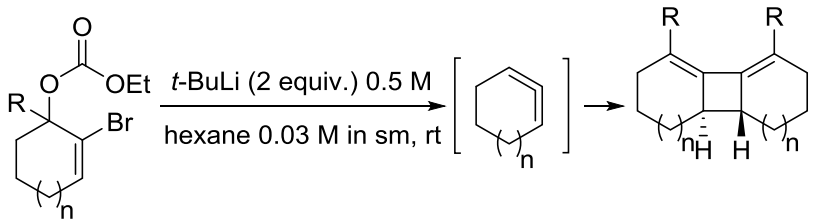

77a, n=1, R=H — **5**, n=1, R=H, 23 %

77b*, n=2, R=H — **87***, n=2, R=H, 70 %

77c, n=3, R=H — **88**, n=3, R=H, 35 %

80, n=1, R=Me — **89**, n=1, R=Me, 65 %

* **77b** to **87** was performed by Yaseen Almehmadi

Scheme 2.40 Dimers obtained through lithium-halogen exchange promoted elimination

General method for generation of cyclic allenes via magnesium-halogen exchange promoted elimination and dimerization

To a 0.1 M solution of 1 equivalent iodocarbonate starting material **78a-b** in dry THF (0.1 M) at 0 °C, 4 equivalents of isopropyl magnesium chloride (0.5 M in THF) was added slowly over 1 h using a syringe pump. The reaction mixture was stirred for 0.5 hours at 0 °C and then quenched with water. The reaction mixture was then extracted 3 times with diethyl ether (3x30mL for 1 mmol-scale reactions using **78a,b**). The organic layers were combined washed with brine, dried over $MgSO_4$, filtered and concentrated. The crude product was purified purified by careful column chromatography on silica gel. (Note: all products are nonpolar hydrocarbons with high R_f values.). The ^1H NMR and ^{13}C NMR data for known dimers **5**[35] and **87**[36] is matching with the data reported in literature.

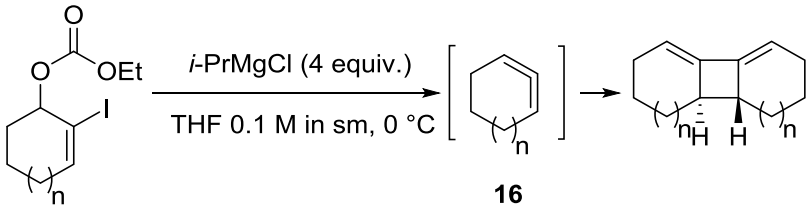

78a, n=1 — **5**, n=1, 32%

78b, n=2 — **87**, n=2, 86%

Scheme 2.41 Dimers obtained through magnesium-halogen exchange promoted elimination

trans-tricyclo[6.4.0.0^{2,7}]dodeca-2,12-diene (**5**)

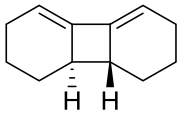

5

Bromocarbonate **77a** (260 mg, 1.04 mmol) was used to provide 19 mg of dimer **5**[35] in 23% yield for the lithium-halogen exchange method. Iodocarbonate **78a** (297 mg, 1 mmol) was used to provide 26 mg of dimer **5**[35] in 32% yield for the magnesium-halogen exchange method. Flash chromatography (hexanes) on silica gel gave product as a colorless oil. R_f = 0.75 (hexanes); IR (cast film) cm^{-1} 3017, 2928, 2884, 2854, 2832, 1444, 1431; ^{1}H NMR (500 MHz, $CDCl_3$) δ 5.42 – 5.35 (m, 2H), 2.30 – 2.23 (m, 2H), 2.16 – 2.02 (m, 4H), 1.98 – 1.92 (m, 2H), 1.82 – 1.74 (m, 2H), 1.45 – 1.34 (m, 2H), 1.19 – 1.09 (m, 2H); ^{13}C NMR (126 MHz, $CDCl_3$) δ 143.2, 111.2, 46.9, 27.6, 24.6, 21.8; HRMS (EI, M^+) for $C_{12}H_{16}$ calcd. *m/z* 160.1252, found: *m/z* 160.1252.

trans-tricyclo[7.5.0.0^{2,8}]tetradeca-7,9-diene (**87**)

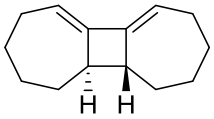

87

Iodocarbonate **78b** (158 mg, 0.51 mmol) was used for the magnesium-halogen exchange method. Flash chromatography (hexanes) on silica gel gave 41 mg of dimer **87**[36] as a colorless oil in 86% yield. R_f = 0.70 (hexanes); IR (cast film) cm^{-1} 3026, 2916, 2846, 1494, 1443; ^{1}H NMR (500 MHz, $CDCl_3$) δ 5.85 – 5.73 (m, 2H), 2.50 – 2.41 (m, 2H), 2.25 – 2.14 (m, 2H), 2.12 – 2.03 (m, 2H), 2.03 – 1.94 (m, 2H), 1.93 – 1.86 (m, 2H), 1.86 – 1.77 (m, 2H), 1.44 – 1.34 (m, 2H), 1.32 – 1.19 (m, 4H); ^{13}C NMR (126 MHz, $CDCl_3$) δ 145.9, 118.5, 48.6, 33.2, 30.9, 29.6, 28.9; HRMS (EI, M^+) for $C_{14}H_{20}$ calcd. *m/z* 188.1564, found: *m/z* 188.1563.

trans-tricyclo[8.6.0.0^{2,9}]hexadeca-16,2-diene (**88**)

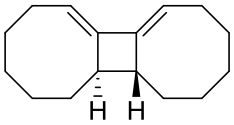

88

Bromocarbonate **77c** (200 mg, 0.72 mmol) was used. Flash chromatography (hexanes) on silica gel gave 28 mg of dimer **88**[37] as a colorless oil in 35% yield. R_f = 0.75 (hexanes); IR (cast film) cm^{-1} 3023, 2925, 2851, 1457, 1443, 1353; ^{1}H NMR (500 MHz, $CDCl_3$) δ 5.69 – 5.63 (m, 2H), 2.45 – 2.38 (m, 2H), 2.28 – 2.18 (m, 2H), 2.06 – 1.97 (m, 2H), 1.97 – 1.91 (m, 2H), 1.82 – 1.69 (m, 4H), 1.65 – 1.56 (m, 2H), 1.53 – 1.45 (m, 2H), 1.41 – 1.31 (m, 2H), 1.28 – 1.21 (m, 4H); ^{13}C NMR (126 MHz, $CDCl_3$) δ 143.5, 116.0, 48.7, 36.2, 27.1, 26.9, 26.3, 26.1; HRMS (EI, M^+) for $C_{16}H_{24}$ calcd. *m/z* 216.1878, found: *m/z* 216.1877.[

trans-3,12-dimethyltricyclo[6.4.0.0^{2,7}]dodeca-2,12-diene (**89**)

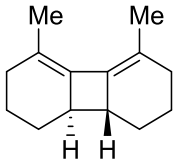

89

65 %

Bromocarbonate **80** (131 mg, 0.5 mmol) was used. Flash chromatography (hexanes) on silica gel gave 31 mg of dimer **89**[38] as a colorless oil in 65% yield; R_f = 0.70 (hexanes); IR (cast film) cm^{-1} 2966, 2926, 2878, 2857, 2824, 1444, 1374; ^{1}H NMR (500 MHz, $CDCl_3$) δ 2.24 – 2.16 (m, 2H), 2.07 (dd, J = 17.9, 6.5 Hz, 2H), 1.97 – 1.86 (m, 4H), 1.84 – 1.77 (m, 2H), 1.72 (s, 6H), 1.49 – 1.37 (m, 2H), 1.12 – 1.01 (m, 2H); ^{13}C NMR (126 MHz, $CDCl_3$) δ 136.7, 119.2, 47.3, 30.4, 27.8, 22.9, 19.5; HRMS (EI, M^+) for $C_{14}H_{20}$ calcd. *m/z* 188.1564, found: *m/z* 188.1561.

2.4.3 Synthesis of cycloadducts of 1,2-cyclohexadiene generated through magnesium-halogen exchange

General method for generation of 1,2-cyclohexadiene 2 via magnesium-halogen exchange promoted elimination and trapping with furan, DPIBF, or styrene

To a solution of 1 equivalent iodocarbonate starting material **78a** in dry THF (0.1 M) and the corresponding trapping partner (furan (40-45 equiv.), DPIBF (3 equiv.), or styrene (25 equiv.)) at 50 °C, 4 equivalents of isopropylmagnesium chloride (0.5 M in THF) was added slowly over 1 h using a syringe pump. The reaction mixture was stirred for 0.5 hours at 50 °C and then cooled down to room temperature before being quenched with water. The reaction mixture was then extracted 3 times with diethyl ether (3x30mL for 1 mmol-scale reactions using **78a**). The organic layers were combined, washed with brine, dried over $MgSO_4$, filtered and concentrated. The crude product was purified using chromatography on silica gel. The ^1H NMR and ^{13}C NMR data for known cycloadducts **81a-b**,[35] **93a**,[35] and **6a-b**[38] is matching with the data reported in literature.

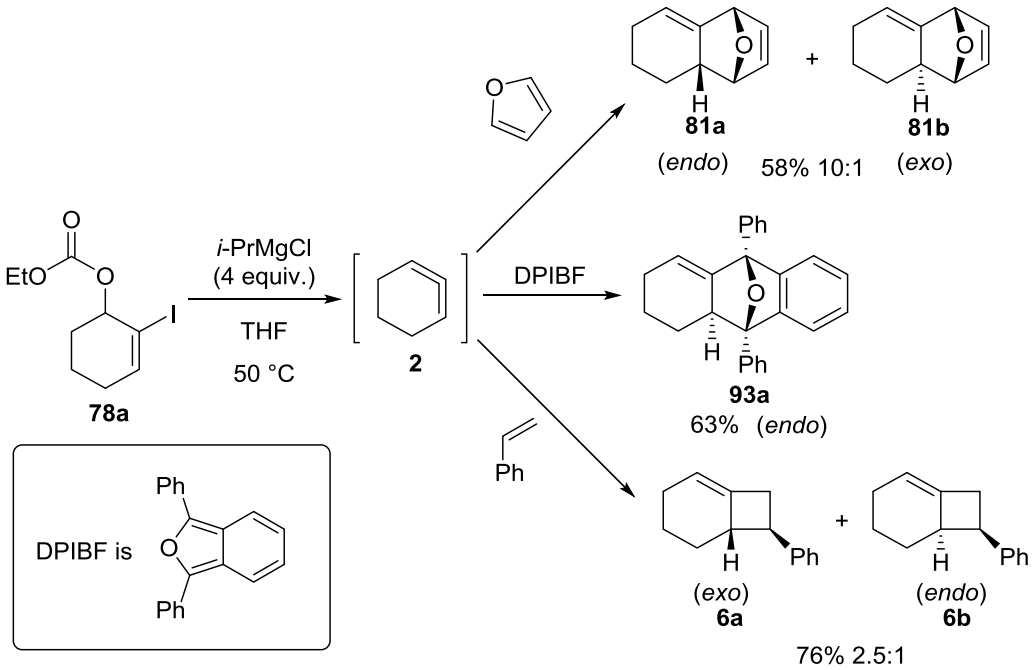

Scheme 2.42 Trapping reactions of 1,2-cyclohexadiene **2**

endo-11-oxatricyclo[6.2.1.$0^{2,7}$]undeca-2,9-diene (**81a**) and
exo-11-oxatricyclo[6.2.1.$0^{2,7}$]undeca-2,9-diene (**81b**)

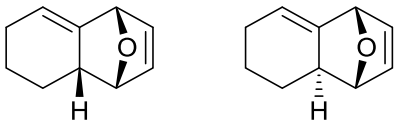

81a (*endo*) **81b** (*exo*)

58% 10:1

Iodocarbonate **78a** (290 mg, 0.98 mmol) and furan (2.8 g, 3 mL, 41 mmol) were used. Flash chromatography (5% Et_2O in hexanes) on silica gel gave 85 mg of diastereomeric mixture **88a-b**[35] *endo*/*exo* = 10 :1 as a colorless oil in 58% yield. The diastereomeric ratio was determined from ^{1}H NMR. Data for major **81a**[35] (*endo*): IR (cast film) cm^{-1} 3074, 2999, 2930, 2889, 2859, 2837, 1676, 1447, 1314, 1170, 1005; ^{1}H NMR (500 MHz, $CDCl_3$) δ 6.35 (dd, *J* = 5.7, 1.8 Hz, 1H), 6.03 (dd, *J* = 5.7, 1.6 Hz, 1H), 5.62 – 5.54 (m, 1H), 5.06 – 4.96 (m, 2H), 2.39 – 2.30 (m, 1H), 2.16 (ddd, *J* = 18.0, 6.8, 3.2 Hz, 1H), 1.98 – 1.86 (m, 2H), 1.80 (ddt, *J* = 14.5, 7.7, 3.6 Hz, 1H), 1.61 – 1.49 (m, 1H), 0.36 (dddd, *J* = 11.9, 3.3 Hz, 1H); ^{13}C NMR (126 MHz, $CDCl_3$) δ 139.7, 135.8, 129.1, 117.3, 81.7, 80.2, 40.7, 26.7, 25.1, 22.7; HRMS (EI, M^+) for $C_{10}H_{12}O$ calcd. *m/z* 148.0888, found: *m/z* 148.0884.

endo-9,10-diphenyl-1,2,3,9,9a,10-hexahydro-9,10-epoxyanthracene (**93a**)

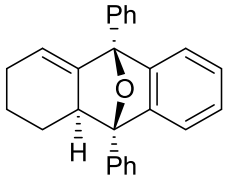

93a

63% (*endo*)

Iodocarbonate **78a** (162 mg, 0.55 mmol) and DPIBF (405 mg, 1.5 mmol) were used. Flash chromatography (5-10% DCM in hexanes) on silica gel gave 122 mg of *endo* cyloadduct **93a**[35] as a colorless oil in 63% yield. The *exo* cycloadduct was not isolated and not observed in the crude product ^{1}H NMR spectrum. IR (cast film) cm^{-1} 3056, 3026, 2950, 2933, 2873, 2848, 1618, 1601, 1490, 1446, 1265; ^{1}H NMR (500 MHz, $CDCl_3$) δ 7.92 –

7.84 (m, 2H), 7.76 – 7.68 (m, 2H), 7.53 – 7.37 (m, 6H), 7.23 – 7.20 (m, 2H), 7.17 – 7.10 (m, 2H), 5.72 – 5.67 (m, 1H), 3.11 – 3.02 (m, 1H), 2.27 – 2.16 (m, 2H), 1.91 – 1.75 (m, 2H), 1.61 (m, 1H), 0.47 (dtd, J = 13.2, 11.7, 3.2 Hz, 1H); ^{13}C NMR (126 MHz, $CDCl_3$) δ 148.5, 144.6, 144.4, 138.2, 135.0, 128.7, 128.7, 128.5, 128.4, 128.1, 127.1, 126.9, 125.9, 121.5, 120.3, 117.9, 90.4, 89.9, 48.3, 26.4, 25.1, 22.1; HRMS (EI, M^+) for $C_{26}H_{22}O$ calcd. *m/z* 350.1671, found: *m/z* 350.1670.

exo-7-phenylbicyclo[4.2.0]oct-1-en (**6a**) and *endo*-7-phenylbicyclo[4.2.0]oct-1-en (**6b**)

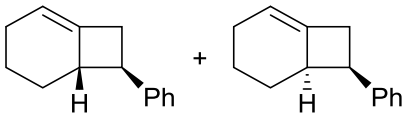

6a (*exo*) **6b** (*endo*)

76% 2.5:1

Iodocarbonate **78a** (297 mg,1 mmol) and styrene (2.727, 3 mL, 26 mmol) were used. Flash chromatography (5% Et_2O in hexanes) on silica gel gave 140 mg of diastereomeric mixture **6a-b**[38] *exo/endo* 2.5 :1 as a colorless oil in 76% yield. The diastereomeric ratio was determined from ^{1}H NMR. Data for major **6a**[38] (*exo*) IR (cast film) cm^{-1} 3084, 3060, 3027, 2933, 2868, 1665, 1495, 1452, 1058; ^{1}H NMR (500 MHz, $CDCl_3$) δ 7.33 – 7.28 (m, 2H), 7.25 – 7.23 (m, 2H), 7.22 – 7.18 (m, 1H), 5.39 – 5.35 (m, 1H), 3.10 – 3.04 (m, 1H), 3.02 – 2.96 (m, 1H), 2.94 – 2.85 (m, 2H), 2.12 – 2.00 (m, 3H), 1.85 – 1.77 (m, 1H), 1.47 – 1.38 (m, 1H), 1.29 – 1.21 (m, 1H); ^{13}C NMR (126 MHz, $CDCl_3$) δ 144.8, 138.1, 128.3, 126.6, 126.0, 113.7, 50.1, 46.2, 39.1, 28.3, 25.0, 21.5. HRMS (EI, M^+) for $C_{14}H_{16}$ calcd. *m/z* 184.1252, found: *m/z* 184.1251.

2.5 References

(1) Christl, M. Cyclic Allenes Up to Seven-Membered Rings. In *Modern Allene Chemistry*; Wiley-VCH Verlag GmbH: Weinheim, Germany, 2005; pp 243–357.

(2) Johnson, R. P. *Chem. Rev.* **1989**, *89* (5), 1111–1124.

(3) Balci, M.; Taskesenligil, Y. Recent Developments in Strained Cyclic Allenes. In *Advances in Strained and Interesting Organic Molecules*; Halton, B., Ed.; JAI Press: Stramford, Connecticut, 2000; Vol. 8, pp 43–81.

(4) Shakespeare, W. C.; Johnson, R. P. *J. Am. Chem. Soc.* **1990**, *112* (23), 8578–8579.

(5) Barber, J. S.; Styduhar, E. D.; Pham, H. V.; McMahon, T. C.; Houk, K. N.; Garg, N. K. *J. Am. Chem. Soc.* **2016**, *138* (8), 2512–2515.

(6) Lofstrand, V. A.; West, F. G. *Chem. Eur. J.* **2016**, *22* (31), 10763–10767.

(7) Yokota, M.; Fuchibe, K.; Ueda, M.; Mayumi, Y.; Ichikawa, J. *Org. Lett.* **2009**, *11* (17), 3994–3997.

(8) Clayden, J. *Organolithiums: Selectivity for Synthesis*; Manchester, UK, 2002.

(9) Gilman, H.; Langham, W.; Jacoby, A. L. *J. Am. Chem. Soc.* **1939**, *61* (1), 106–109.

(10) Jones, R. G.; Gilman, H. The Halogen-Metal Interconversion Reaction with Organolithium Compounds. In *Organic Reactions*; John Wiley & Sons, Inc.: Hoboken, NJ, USA, 2011; pp 339–366.

(11) Marvel, C. S.; Hager, F. D.; Coffman, D. D. *J. Am. Chem. Soc.* **1927**, *49* (9), 2323–2328.

(12) Bryce-Smith, D. *J. Chem. Soc.* **1956**, *53* (9), 1603.

(13) Clayden, J. Regioselective Synthesis of Organolithiums by X-Li Exchange. In *Tetrahedron Organic Chemistry Series, Volume 23, Organolithiums: Selectivity for Synthesis*; Manchester, UK, 2002; pp 111–149.

(14) Bailey, W. F.; Patricia, J. J. *J. Organomet. Chem.* **1988**, *352* (1–2), 1–46.

(15) Zefirov, N. S.; Makhon'kov, D. I. *Chem. Rev.* **1982**, *82* (6), 615–624.

(16) Wakefield, B. J. Organomagnesium Methods in Organic Synthesis; Elsevier, 1995; pp 21–71.

(17) Moore, W. R.; Moser, W. R. *J. Am. Chem. Soc.* **1970**, *92* (18), 5469–5474.

(18) Yoshida, S.; Karaki, F.; Uchida, K.; Hosoya, T. *Chem. Commun.* **2015**, *51* (42), 8745–8748.

(19) Della, E. W.; Taylor, D. K.; Tsanaktsidis, J. *Tetrahedron Lett.* **1990**, *31* (36), 5219–5220.

(20) Lopchuk, J. M.; Fjelbye, K.; Kawamata, Y.; Malins, L. R.; Pan, C. M.; Gianatassio, R.; Wang, J.; Prieto, L.; Bradow, J.; Brandt, T. A.; Collins, M. R.; Elleraas, J.; Ewanicki, J.; Farrell, W.; Fadeyi, O. O.; Gallego, G. M.; Mousseau, J. J.; Oliver, R.; Sach, N. W.; Smith, J. K.; Spangler, J. E.; Zhu, H.; Zhu, J.; Baran, P. S. *J. Am. Chem. Soc.* **2017**, *139* (8), 3209–3226.

(21) Makarov, I. S.; Brocklehurst, C. E.; Karaghiosoff, K.; Koch, G.; Knochel, P. *Angew. Chem. Int. Ed.* **2017**, *56* (41), 12774–12777.

(22) Oh, K.; Fuchibe, K.; Ichikawa, J. *Synthesis* **2011**, 881–886.

(23) Ohno, H.; Miyamura, K.; Tanaka, T.; Oishi, S.; Toda, A.; Takemoto, Y.; Fujii, N.; Ibuka, T. *J. Org. Chem.* **2002**, *67* (4), 1359–1367.

(24) Larock, R. C.; Hightower, T. R.; Kraus, G. A.; Hahn, P.; Zheng, D. *Tetrahedron Lett.* **1995**, *36* (14), 2423–2426.

(25) Nicolaou, K. C.; Ding, H.; Richard, J.-A.; Chen, D. Y.-K. *J. Am. Chem. Soc.* **2010**, *132* (11), 3815–3818.

(26) Li, K.; Alexakis, A. *Angew. Chem. Int. Ed.* **2006**, *45* (45), 7600–7603.

(27) Sadak, A. E.; Arslan, T.; Celebioglu, N.; Saracoglu, N. *Tetrahedron* **2010**, *66* (17), 3214–3221.

(28) Krafft, M. E.; Cran, J. W. *Synlett* **2005**, 1263–1266.

(29) Mayasundari, A.; Young, D. G. J. *Tetrahedron Lett.* **2001**, *42* (2), 203–206.

(30) Calvin, S. J.; Mangan, D.; Miskelly, I.; Moody, T. S.; Stevenson, P. J. *Org.*

Process Res. Dev. **2012**, *16* (1), 82–86.

(31) Bäuerlein, P. S.; Fairlamb, I. J. S.; Jarvis, A. G.; Lee, A. F.; Müller, C.; Slattery, J. M.; Thatcher, R. J.; Vogt, D.; Whitwood, A. C. *Chem. Commun.* **2009**, 5734–5736.

(32) Nwokogu, G. C. *J. Org. Chem.* **1985**, *50* (20), 3900–3908.

(33) Harmata, M.; Barnes, C. L.; Brackley, J.; Bohnert, G.; Kirchhoefer, P.; Kürti, L.; Rashatasakhon, P. *J. Org. Chem.* **2001**, *66* (15), 5232–5236.

(34) Evans, P. A.; Oliver, S.; Chae, J. *J. Am. Chem. Soc.* **2012**, *134* (47), 19314–19317.

(35) Quintana, I.; Peña, D.; Pérez, D.; Guitián, E. *Eur. J. Org. Chem.* **2009**, *2009* (32), 5519–5524.

(36) Bottini, A. T.; Frost, K. A.; Anderson, B. R.; Dev, V. *Tetrahedron* **1973**, *29* (14), 1975–1981.

(37) Pietruszka, J.; Künig, W. A.; Maelger, H.; Kopf, J. *Chem. Ber.* **1993**, *126* (1), 159–166.

(38) Christl, M.; Schreck, M. *Chem. Ber.* **1987**, *120* (6), 915–920.

(39) Quintana, I.; Peña, D.; Pérez, D.; Guitián, E. *Eur. J. Org. Chem.* **2009**, *2009* (32), 5519–5524.

(40) Moore, W. R.; Moser, W. R. *J. Org. Chem.* **1970**, *35* (4), 908–912.

(41) Singh, K.; Trinh, W.; Weaver, J. D. *Org. Biomol. Chem.* **2019**, *17* (7), 1854–1861.

(42) Ogasawara, M.; Okada, A.; Nakajima, K.; Takahashi, T. *Org. Lett.* **2009**, *11* (1), 177–180.

(43) Hagendorn, T.; Bräse, S. *Eur. J. Org. Chem.* **2014**, *2014* (6), 1280–1286.

(44) Almehmadi, Y. A. Investigation of New Mild Routes to Substituted and Unsubstituted 1,2- Cycloheptadienes and Their Trapping Reactions, University of Alberta, Edmonton, AB, 2019.

3. Trapping of electron deficient cyclic allenes generated through base elimination[11]

3.1 Polarized cyclic allenes

Once several ways to generate and trap reactive cyclic allenes chemistry were known, the question of how the reactivity of a transient species such as 1,2-cyclohexadiene **1** would be perturbed in the presence of electron-donating or electron-withdrawing groups arose (*Figure 3.1*). For electron rich examples of cyclic allenes, in which an electron-donating group is attached to the allene π system, two possible generic structures can be envisioned. In the case of allene **2**, an electron-donating heteroatom is incorporated into the allene ring adjacent to the allene unit, while allene **3** includes an electron-donating group as an exocyclic substituent on one of the allenic termini. On the other hand, examples of electron-poor cyclic allenes are limited to the structure **4** in which an exocyclic electron-withdrawing group is attached to one end of the allenic system.

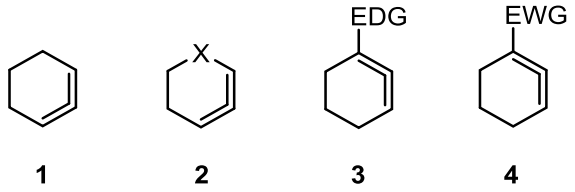

Figure 3.1 Polarized cyclic allenes

In this chapter our results regarding the generation and trapping of four electron deficient cyclic allenes will be presented. A short summary of the literature with the work previosuly done will be showcased first.

[1] The work presented in this chapter was published. (1) Wang, B.; Constantin, M. G.; Singh, S.; Zhou, Y.; Davis, R. L.; West, F. G. *Org. Biomol. Chem.* **2021**, *19* (2), 399–405.

3.1.1 Electron rich cyclic allenes

Christl and Braun generated and trapped cyclic conjugated oxaallene **7** through Doering–Moore–Skattebøl rearrangement of bromofluoro starting material **5**.[2] Depending on the trapping reagent used they observed different regioselectivity. When the reactive intermediate **7** was intercepted in a [4+2] fashion using furan or dimethylfuran, the most remote double bond from the oxygen was involved in the reaction generating cycloadducts **8**. In contrast when the trapping of **7** was done with styrene or α-methylstyrene in a [2+2] fashion, preferential reactivity via the C=C bond proximal to the ring oxygen was seen in order to generate cycloadducts **9**.[2] Ruzziconi et al. observed similar regioselectivity when they trapped oxaallene **7** generated through base promoted elimination method using **6**.[3]

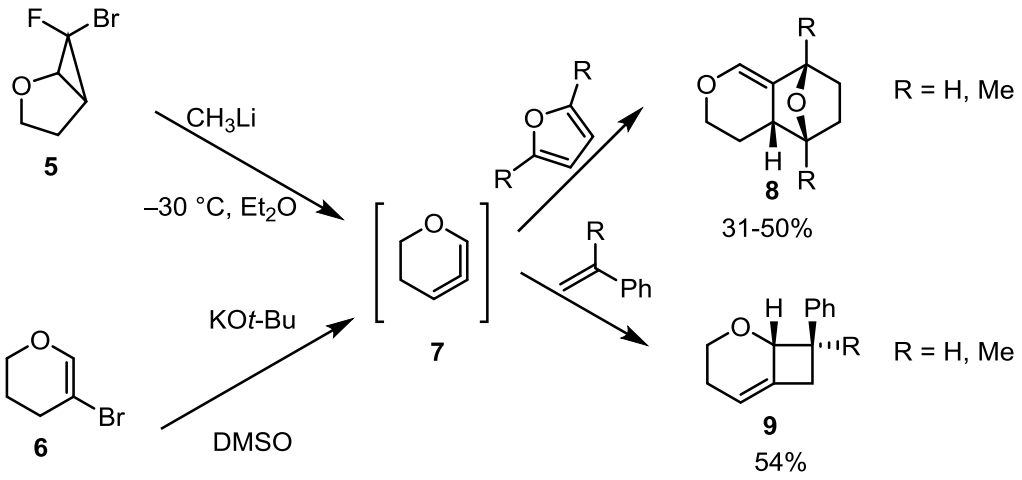

Scheme 3.1 Generation and trapping of 1-oxa-2,3-cyclohexadiene with furans and styrenes

Lofstrand and West generated 1-acetoxy-1,2-cyclohexadiene **11** through the fluoride promoted elimination of starting material **10**, which was trapped in a [4+2] fashion with furan and in a [3+2] fashion with 1,3-dipoles such as nitrile oxide, nitrone and azomethine imine obtaining cycloadducts **12-15**. Regarding the regioselectivity, this cyclic allene **11** behaves similarly to the cyclic oxaallene **7**, in which the distal C=C bond react with the diene or 1,3-dipole (Scheme 3.2). However, it should be noted that the electron-donating character of an acetoxy group may be limited.[4]

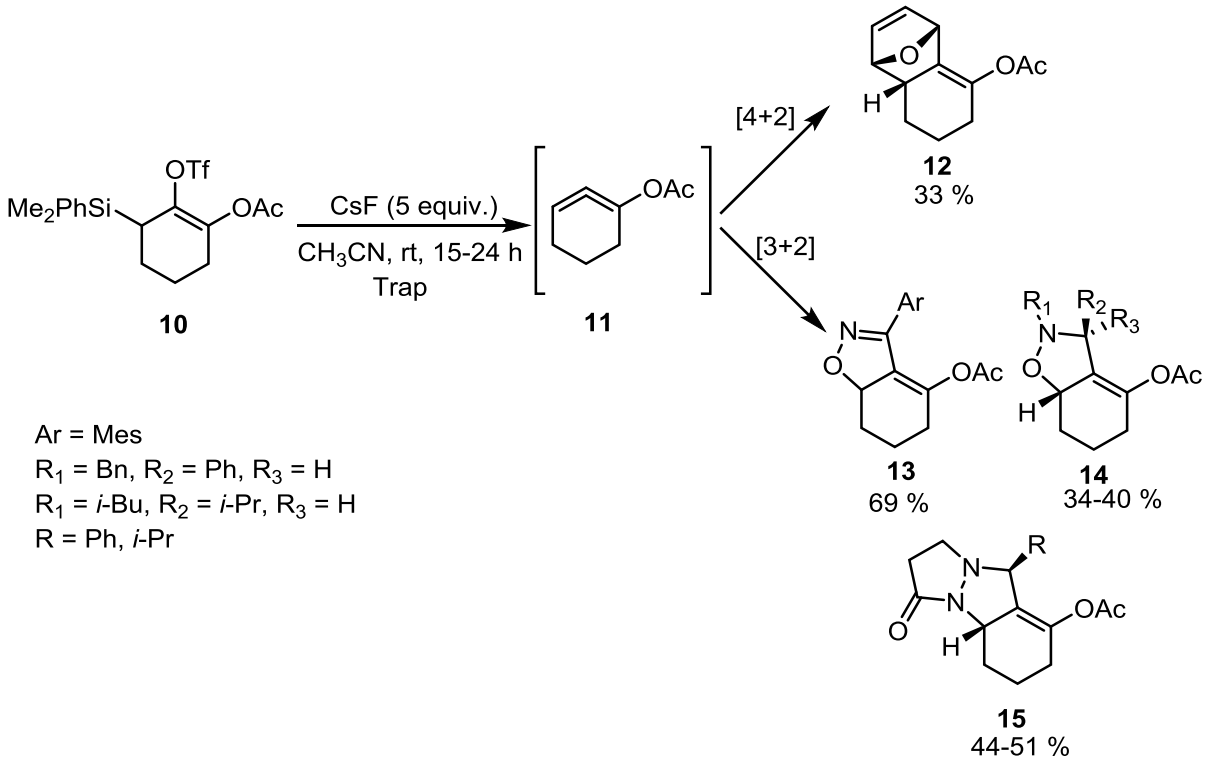

Scheme 3.2 Generation and trapping of 1-acetoxy-1,2-cylohexadiene with furan and 1,3-dipoles

3.1.2 Electron deficient cyclic allenes

Nendel et al. generated alkyl 1,2-cyclohexadienexarboxylates **18** through the base promoted elimination method, using a mixture of regioisomers **16** and **17** as starting materials (*Scheme 3.3*). When they performed trapping of the electron deficient cyclic allene **18** with furan they obtained a mixture of regioisomeric cycloadducts **19** and **20**, with predominant formation of product **19**, resulting from cycloaddition involving the allene C=C bond conjugated to the electron-withdrawing ester functionality.[5]

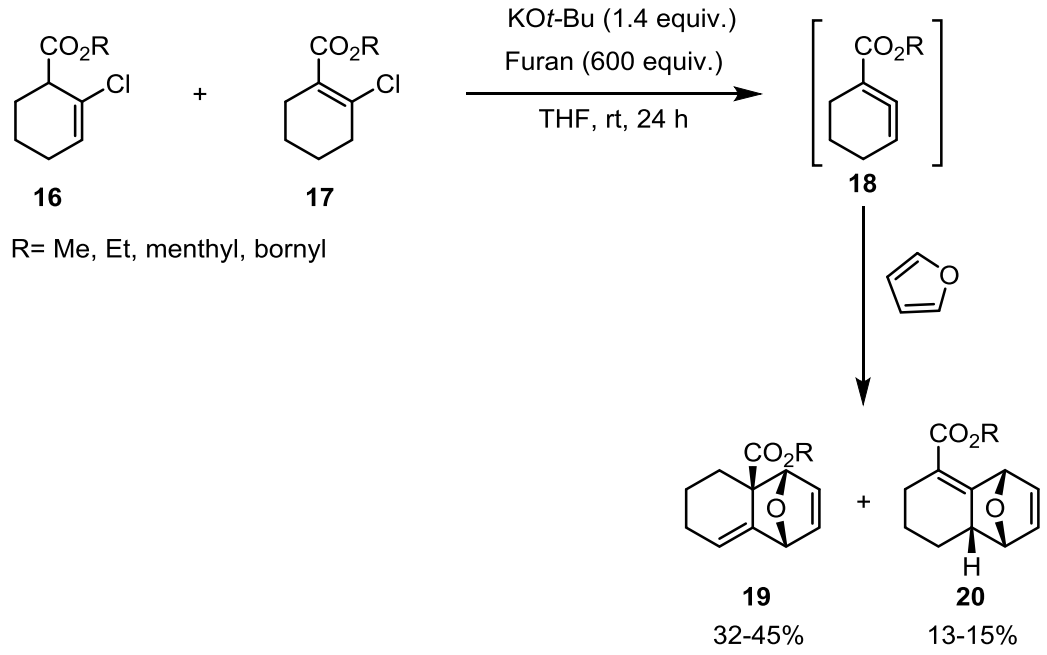

Scheme 3.3 Generation and trapping of alkyl 1,2-cyclohexadiene carboxylates with furan

Another study involving the generation and trapping of alkyl 1,2-cyclohexadiene carboxylates was performed by Zhou and West.[6] Here, using KO*t*-Bu as a base, starting material **21** is deprotonated while the triflate group is eliminated in order to generate the desired electron deficient cyclic allene **22** *(Scheme 3.4)*. Then the ethyl 1,2-cylohexadiene carboxylate **22**, was trapped with several aryl acetylenes in a [2 +2] fashion to generate cyclobutene products **23**. In these cycloadditions, the acetylene partners reacted only with the C=C bond distal to the ester, and with bond formation between the unsubstituted terminus of the alkyne and the central allene carbon, leading exclusively to regioisomers **23**.

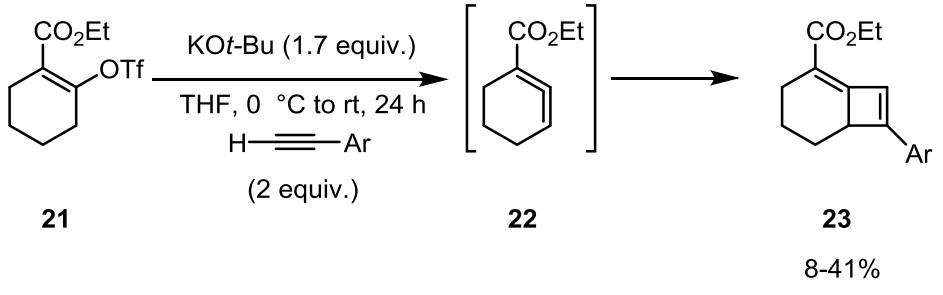

Scheme 3.4 Generation and trapping of ethyl 1,2-cyclohexadiene carboxylates with aryl acetylenes

In a more recent study published by the Garg group involving azacyclic allenes, the reactions of methyl azacyclic allene carboxylates **25** with cyclic 1,3-diene traps such as furans or pyrroles was probed (*Scheme 3.5*).[7] Using fluoride promoted elimination conditions, silyl triflates **24** were cleanly converted to azacyclic allenes **25**. Prior examples of Diels–Alder trapping of electron-deficient cyclic allenes by Nendel et al. had reported preferential reaction on the ester-substituted alkene. In the Garg examples, exclusive reaction with that C=C bond was observed, affording adducts **26** in good to excellent yields.

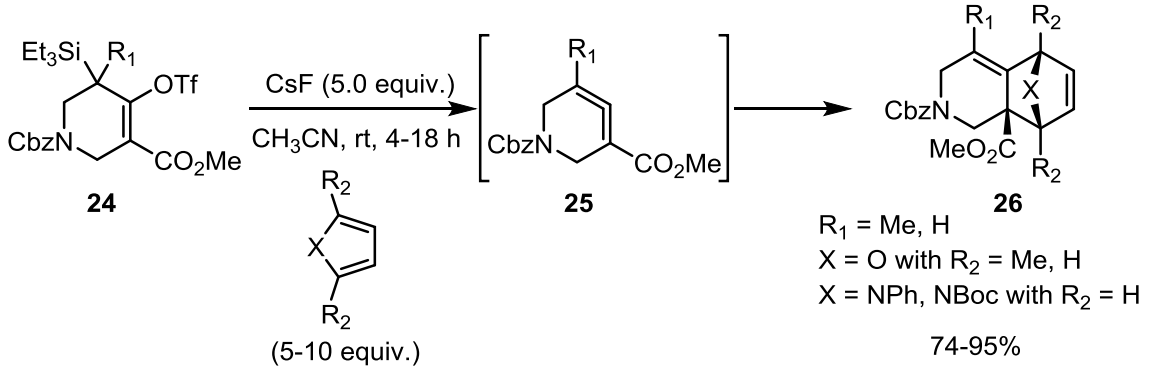

Scheme 3.5 Generation and trapping of methyl azacyclic allene carboxylates with furans and pyrroles

3.2 Envisioned generation and trapping of electron deficient cyclic allenes

Given the limited body of work that had been reported in the literature on the subject of electron-deficient cyclic allenes,[5,7] there were still many important aspects that remained to be explored.

For example, the electron-withdrawing substituent had so far been limited to ester functionality. The question of how keto- or cyano-substituted 1,2-cycloahexadienes would behave with respect to both reactivity and regioselectivity was of interest. We envisioned a base-mediated elimination strategy, employing 2-aroyl enol triflates or 2-cyano enol triflates **27** (*Scheme 3.6*).Treatment with KO*t*-Bu was expected to effect ready elimination of triflate to generate the desired allenyl ketones or nitrile. It was unclear whether the pervasive background [2+2] dimerization reaction seen with unpolarized cyclic allenes

would operate with these examples (e.g., to form cyclobutene **29**), or if alternative reactivity might arise. Regardless of the propensity for dimerization, we were interested in developing Diels–Alder trapping processes, and examining the regioselectivity of the cycloaddition reaction with these novel substituents. A priori, we expected a strong preference for the formation of isomer **30** over **31**, since that would entail participation of the activated C=C bond in the pericyclic reaction. Results of studies carried out by Dr. Baolei Wang to optimize allene generation and Diels–Alder trapping are described here, along with an unprecedented and general alternative trapping reaction with enamines via a hetero-Diels–Alder reaction that was discovered by me.

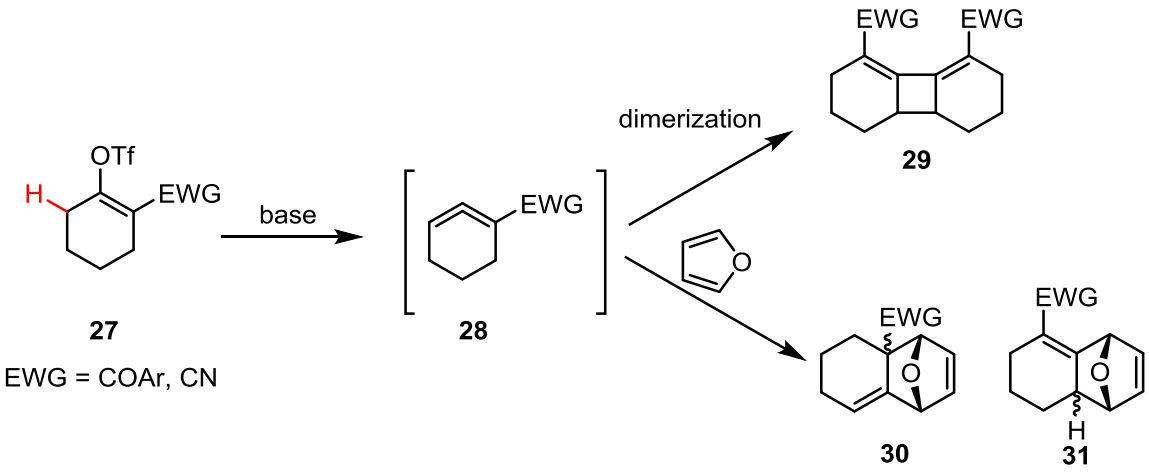

Scheme 3.6 Envisioned generation and trapping of electron deficient cyclic allenes

3.3 Results and discussion

3.3.1 Synthesis of starting materials

Four enol triflates were identified as suitable substrates for the planned allene generation approach (*Scheme 3.7*). The synthesis of the 2-aroyl enol triflates **27a-c** was achieved in two steps starting from morpholinocyclohexene **32**. In the first step, a Stork acylation was performed in order to access the desired β-diketone **33**, which upon triflation furnished the desired enol triflate substrates **27a-c**.[8,9]

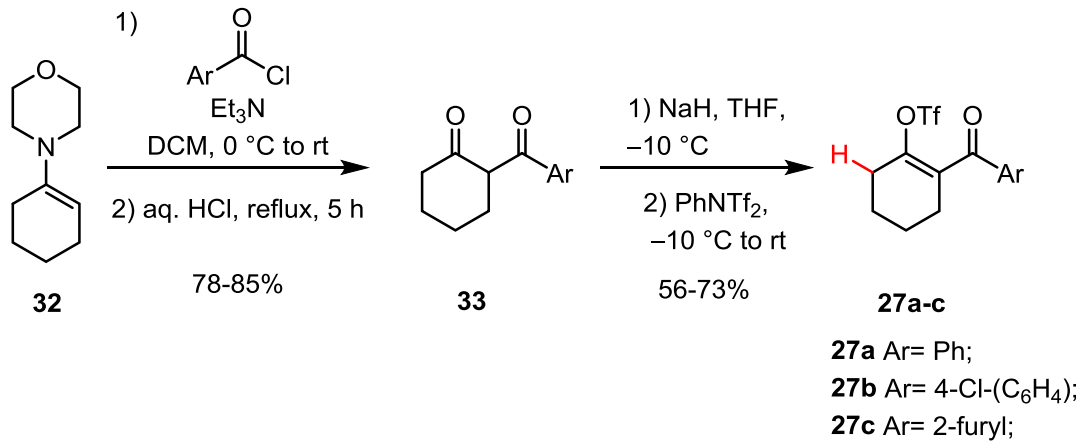

Scheme 3.7 Synthesis of 2-aroyl enol triflate starting materials

The synthesis of 2-cyano enol triflate **27d** was performed in two steps starting from pimelonitrile **34** following the literature precedent as presented in *Scheme 3.8*.[10,11] As an important observation in our synthesis of starting material we obtain only the fully substituted regioisomer of the olefin. In contrast, in Nendel's paper, they got a mixture chlorocyclohexene of regioisomers.[5]

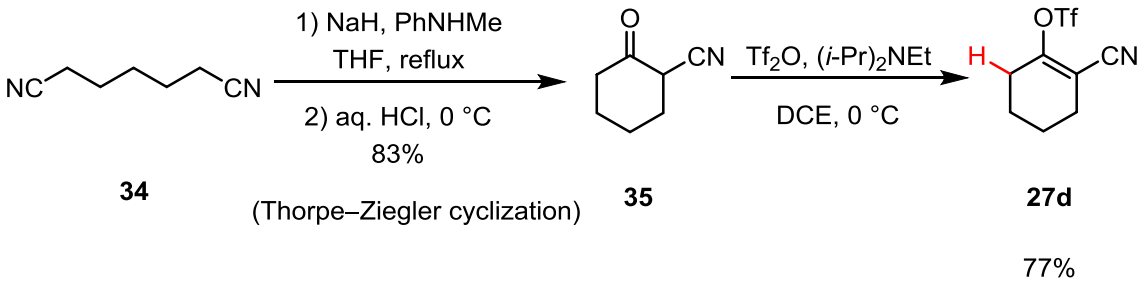

Scheme 3.8 Synthesis 2-cyano enol triflate starting materials

The initial starting material synthesis was performed by Dr. Baolei Wang, following the same protocol. Subsequently, I also repeated and scaled up the syntheses of **27a** and **27b** in comparable yields.

3.3.2 Generation of electron deficient cyclic allenes and trapping reactions with dienes

The first test reactions in the absence of a suitable trap showed an unexpected dimerization product (see section 3.3.3), which will have implication in the development of new trapping method for electron deficient cyclic allenes (see section 3.3.4). As one of the typical trapping reactions of transient cyclic allenes, the Diels–Alder cycloaddition with furan was probed in this study as well. In order to get effective cycloaddition, a large excess of furan was required so that dimerization or other unknown reactions pathways could be limited. Upon optimization it was found that 2 equivalents of KO*t*-Bu and 137 equivalents of furan were required in order to obtain the corresponding cycloadducts **30a-d** in modest to good yields (*Scheme 3.9*). Regarding the regioselectivity this is a normal demand Diels–Alder reaction. The C-C double bond of the allene conjugated with the ketone should act as the LUMO of the dienophile and it was expected to be favored in the Diels–Alder reaction over the other C-C double bond of the allene. As predicted, the conjugated double bond of the cyclic allene was favored and only the cycloadducts formed through the reaction of this C-C double bond were isolated. The ketone as a stronger electron

withdrawing group than the ester led to a better regioselectivity in comparison with the ester substrates already reported in the literature under base elimination conditions.[5]

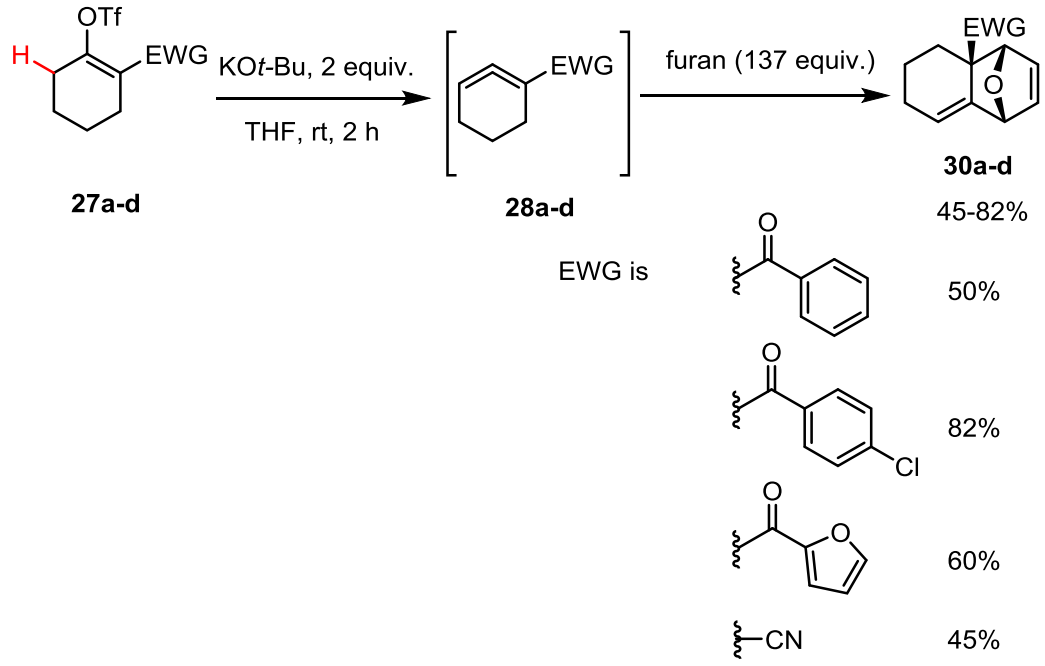

Scheme 3.9 Trapping of electron deficient cyclic allenes with furan

Regarding the diastereoselectivity, only the *endo* diastereomer **30a-d** was observed, which was characterized using TROESY correlations, along with the presence in the ^{1}H NMR spectrum of a uniquely upfield proton resonance that is specific to the *endo* stereochemistry (*Figure 3.2*). As indicated in the figure, one of the cyclohexene protons of the *endo* cycloadduct is oriented so that it lies within the shielding zone of the dihydrofuran C=C bond, causing an anomalously low chemical shift due to anisotropy.[12]

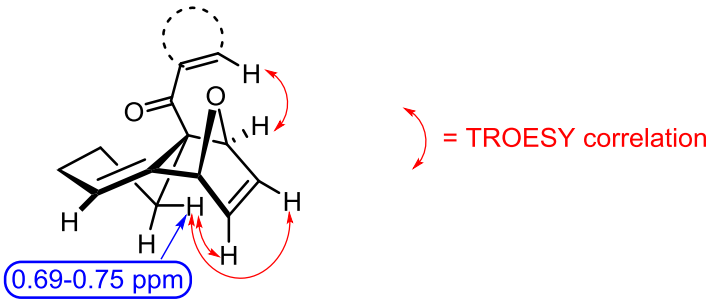

Figure 3.2 Specific upfield proton in ^{1}H NMR and TROESY correlations of *endo* cycloadduct **30a**

1,3-Diphenylisobenzofuran (DPIBF) is often used in trapping reactions of transient dienophiles such as strained cyclic allenes, and was examined in Diels–Alder reactions with **28a-d** (*Scheme 3.10*). Since DPIBF is a more reactive diene in the Diels–Alder reaction, only 2 equivalents were required. Substrates **27a-c** upon treatment with KO*t*-Bu and DPIBF furnished single regio- and diastereomers **36a-c**, showing analogous behavior to that seen with furan. In the case of cyano enol triflate substrate **27d** a mixture of *endo* and *exo* diastereomers in the ratio of 3:1 was obtained, which was confirmed through X-ray crystallographic analysis. All Diels–Alder trapping results were obtained by Dr. Baolei Wang.

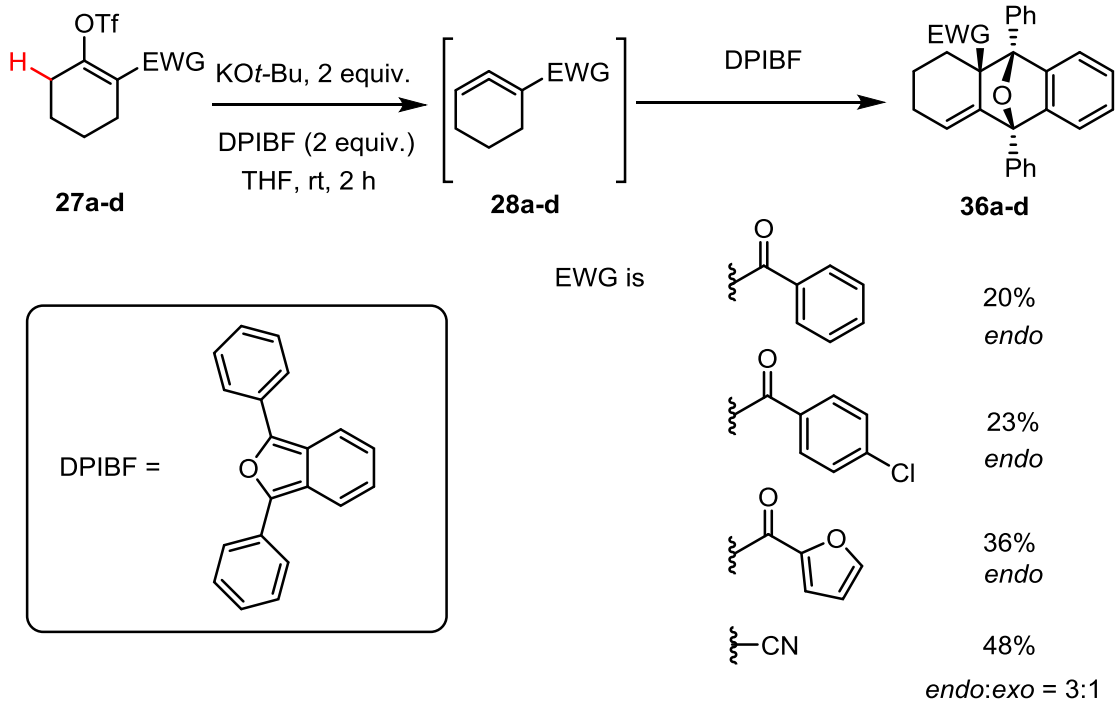

Scheme 3.10 Trapping of electron deficient cyclic allenes with DPIBF

3.3.3 Unexpected dimerization of the electron deficient cyclic allene

During the optimization process for the generation of the electron deficient cyclic allenes through base promoted elimination it was found that treatment of enol triflates with

1.2 equiv of KO*t*-Bu in THF at room temperature in the absence of any trapping agent resulted in unexpected dimer products **37a-c** (*Scheme 3.11*). Thorough spectroscopic analysis provided strong evidence for a tricyclic pyranol structure for these products, which were formed in yields ranging from 11–42%. This type of dimerization seems to be an entirely new observation for the chemistry of cyclic allenes. The usual [2+2] dimers **29a-c** were not isolated, but traces of species with the same molecular mass as the expected [2+2] dimers **29a-c** were detected in a LC-MS experiment on an impure fraction isolated from the column chromatography of crude product.

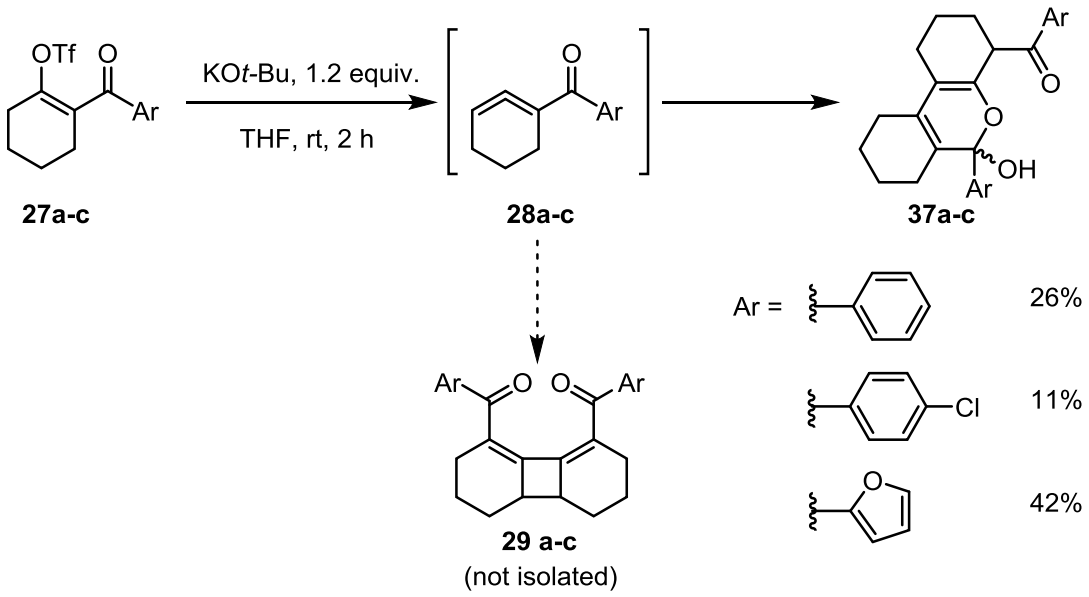

Scheme 3.11 Unexpected dimerization of the aroyl cyclic allenes **28a-c**

We hypothesized that once the cyclic allene **28** is generated, two molecules could react with each other in a hetero-Diels–Alder fashion to give intermediate **38**, which would isomerize to give intermediate **39** (*Scheme 3.12*). Then hydration of intermediate **39** would transform it into intermediate **40** which followed by tautomerization would yield the observed product **37**. One could also imagine a stepwise mechanism pathway in which the carbanion **41** formed before the elimination would act as a nucleophile and attack the ketone conjugated double bond of the allene system to provide enolate **42** which in turn would attack the remaining enone system and then eliminate triflate anion to give common intermediate **39**.

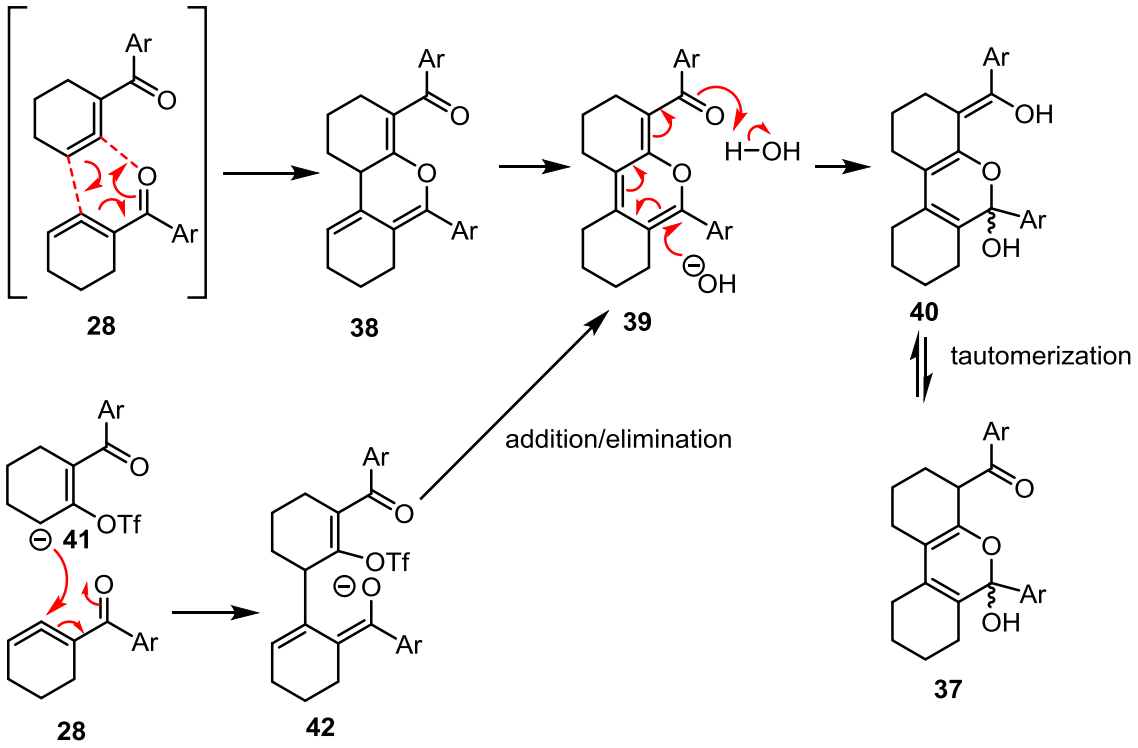

Scheme 3.12 Possible mechanisms for the unexpected dimerization of aroyl cyclic allenes **28**

3.3.4 Generation and trapping reactions of electron deficient cyclic allenes with enamines

The novel dimerization process described in the previous section raised an interesting question. If the dimerization occurred via the hetero-Diels–Alder reaction of two molecules of cyclic allene, could other hetero-Diels–Alder reactions be carried out through the addition of a suitable heterodienophile? We proposed that this [4+2]-cycloaddition would occur with inverse electron demand, in which the principal frontier molecular orbital interaction would involve the LUMO of the enone system (heterodiene) of the transient cyclic allene and the HOMO of a suitable electron-rich heterodienophile (*Scheme 3.13*).

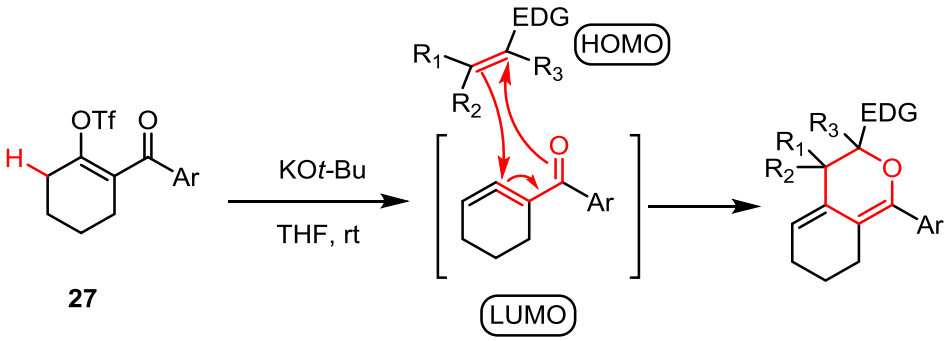

Scheme 3.13 The inverse electron-demand hetero-Diels–Alder trapping reaction proposal

Despite the frequency with which inverse electron-demand hetero-Diels–Alder reactions have been described in the organic chemistry literature, we found no reports of a reaction in which a cyclic allene or an acyclic allene conjugated with a ketone group would act as the heterodiene in the reaction with an electron rich dienophile.[13,14] The closest analogy is a report by Tsuge et al., in which a cross-conjugated 1,4-dien-3-one **43** acted as a heterodiene with enamine dienophiles **44**, in the presence of a Lewis acid catalyst such as $ZnCl_2$, in order to generate cycloadducts **45** (*Scheme 3.14*).[15]

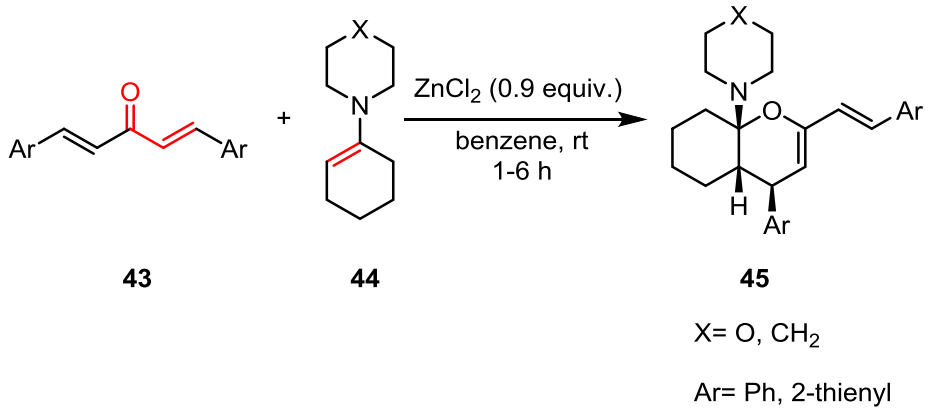

Scheme 3.14 Literature precedent for inverse electron demand hetero-Diels–Alder cycloaddition with a dienone as the heterodiene

Considering the electronic requirements of the proposed process we started our search by testing different electron rich olefins, which often act as dienophiles in inverse electron-demand Diels–Alder reactions. In preliminary experiments using substrate **27a** with the enol ethers ethyl vinyl ether **46** and 3,4-dihydro-*2H*-pyran (DHP) **47**, we observed only previously isolated dimer **37a** and no desired cycloadduct (*Scheme 3.15*). When we

tested 1-morpholino-1-cyclohexene **48a** as a dienophile trap, we were able to isolate the dihydropyran aminal cycloadduct **49a** in 30% yield. Surprisingly, this potentially acid-sensitive product was amenable to purification via normal-phase silica gel chromatography.

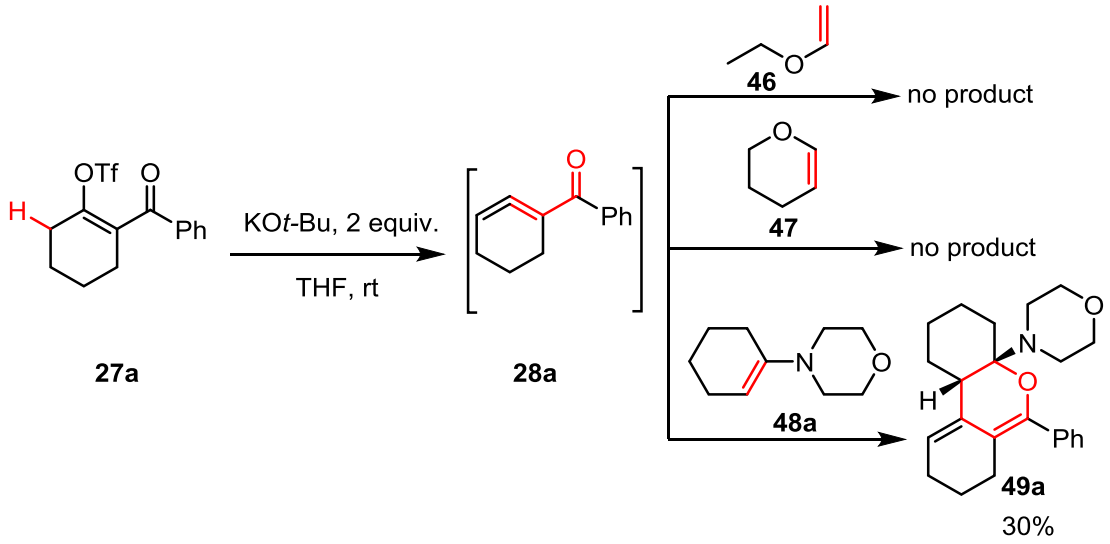

Scheme 3.15 Initial reaction discovery for trapping aroyl cyclic allenes with enamines

Having confirmed that 1-morpholino-1-cyclohexene **48a** could function as a suitable dienophile in the hetero-Diels–Alder reaction we moved forward to the optimization of the process by probing different parameters through a series of parallel reactions for each parameter. We determined NMR yields at 0.1 mmol scale of starting material as an average of two experiments with 1,3,5-trimethoxybenzene as an NMR standard. The proton reference peaks analyzed were the three equivalent aromatic protons of 1,3,5-trimethoxybenzene (singlet at 6.07 ppm) and the olefinic proton of the **49a** cycloadduct at 5.34 ppm, because these peaks were isolated from other peaks present in the ^{1}H NMR spectrum of the crude product (*Figure 3.3*).

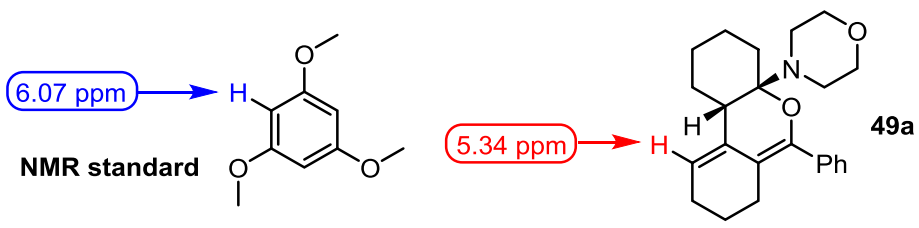

Figure 3.3 Proton peaks analyzed for NMR yield calculation

First we analyzed the stoichiometry of base, and it was found that 1.5 equivalents of KO*t*-Bu were optimal (Entry 2 in *Table 3.1*). Then we evaluated the amount of trapping agent **48a** required to favor the cycloaddition reaction over other reaction pathways, and it was found that we could lower it down to ten equivalents without significant loss in yield of cycloadduct **49a** (Entry 6). Further, we probed the concentration of the starting material **27a** in the reaction mixture before the addition of the KO*t*-Bu solution. While decreasing the concentration of the starting material to 0.05 M resulted in a lower yield, increasing it to 0.2 M did not significantly change the outcome of the process (Entries 9-11). Regarding the reaction time, it was observed that stopping the reaction after two to three hours from the addition of the base offered the best results (Entries 12-15). When we inverted the addition sequence by adding the starting material to a mixture of base and enamine, we observed a significant decrease in yield (Entry 16). In the range of temperatures from 0 °C to rt the outcome of the reaction remained unchanged. Lower and higher temperatures resulted in yield decrease (Entries 17-21). With all these data points we scaled up the reaction to 0.3 mmol of starting material **27a**, and we were able to isolate the cycloadduct **49a** in 65% yield when the 1.5 equivalents of 0.3 M KO*t*-Bu in THF were slowly added over 0.5 hours to a mixture of 10 equivalents of enamine trap **48a** with 1 equivalent of **27a** in THF (0.1 M), followed by 3 hours of stirring at room temperature (Entry 23).

With the optimized conditions in hand, we set out to explore the scope of enamine traps that could be used in this process (*Table 3.2*). First, we analyzed the reaction with cyclic enamines **48a-c**, where the trapping of six-membered cyclic enamines of morpholine **48a** and pyrrolidine **48c** with the aroyl cyclic allenes **28a-b** occurred in good yields (46-65%). In the reaction of cyclic allene **28a** with the seven-membered ring cyclic enamine **48b,** we observed a modest yield of 24%. Regarding the diastereoselectivity, we were able to isolate only one diastereomeric product **49a-d** for each case as presented in *Table 3.2*.

Then, we analyzed the reaction of aroyl cyclic allenes **28a** and **28b** with acyclic enamines **48d** and **48e**, where in modest yields (9-29%) we were able to isolate the corresponding cycloadducts (*Table 3.3*). Only one diastereomer was isolated in the reaction of enamine **48d** with each of the two transient cyclic allenes.

Table 3.1 Optimization of aroyl cyclic allenes trapping with enamine

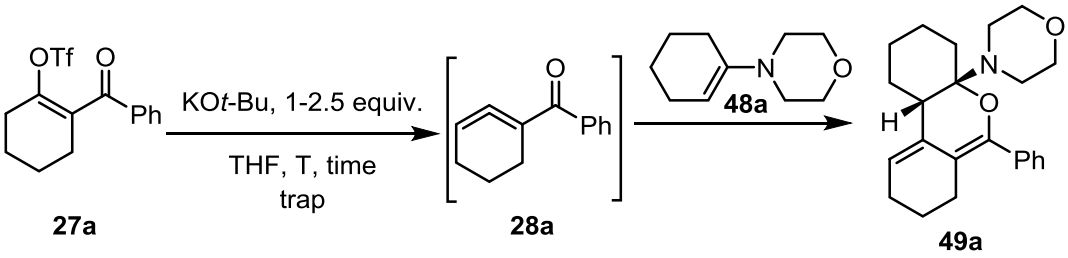

Entry	KO*t*-Bu (equiv.)	Trap **48a** (equiv.)	T (°C)	**27a** (Conc., M)	Time	Yield
1	1	60	RT	0.1	2 h	39 [a]
2	1.5	60	RT	0.1	2 h	51 [a]
3	2	60	RT	0.1	2 h	37 [a]
4	2.5	60	RT	0.1	2 h	45[a]
5	1.5	5	RT	0.1	2 h	38 [a]
6	1.5	10	RT	0.1	2 h	45[a]
7	1.5	20	RT	0.1	2 h	46[a]
8	1.5	30	RT	0.1	2 h	44[a]
9	1.5	10	RT	0.1	2 h	45[a]
10	1.5	10	RT	0.2	2 h	43[a]
11	1.5	10	RT	0.05	2 h	26[a]
12	1.5	10	RT	0.1	2 h	45[a]
13	1.5	10	RT	0.1	0.5 h	28[a]
14	1.5	10	RT	0.1	24 h	21[a]
15	1.5	10	RT	0.1	3 h	43[a]
16[c]	1.5	10	RT	0.1	2 h	18 [a]
17	1.5	10	RT	0.1	2 h	45[a]
18	1.5	10	−10	0.1	2 h	27[a]
19	1.5	10	60	0.1	2 h	38 [a]
20	1.5	10	0 to rt	0.1	3 h	45[a]
21	1.5	10	0	0.1	3 h	47[a]
22	1.5	10	0	0.1	3 h	**57** [b]
23	1.5	10	RT	0.1	3 h	**65** [b]

[a] NMR yields at 0.1 mmol scale of starting material as an average of two experiments with 1,3,5-trimethoxybenzene as NMR standard [b] isolated yields at 0.3 mmol scale of starting material [c] inversed addition

Table 3.2 Trapping reaction scope with cyclic enamines

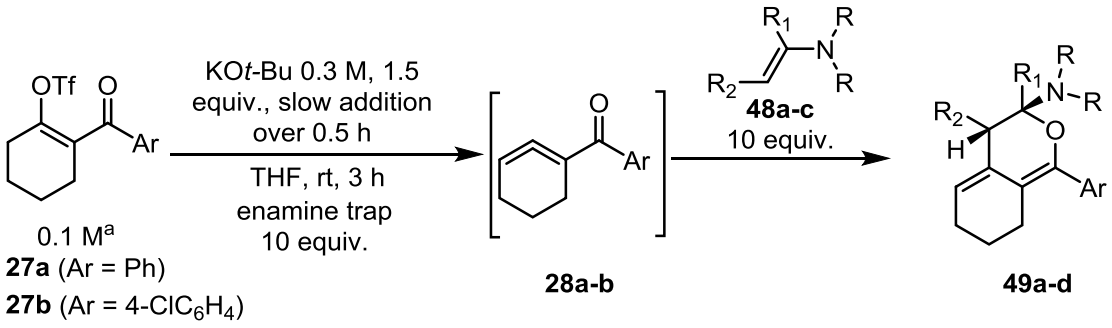

Entry	Substrate	Trap	Product	Yield[b]
1	27a	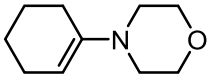 **48a**	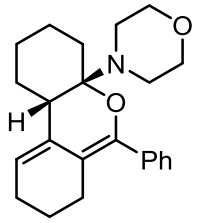 **49a**	65%
2	27a	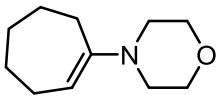 **48b**	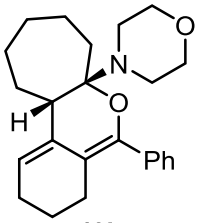 **49b**	24%
3	27b	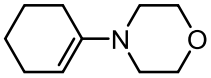 **48a**	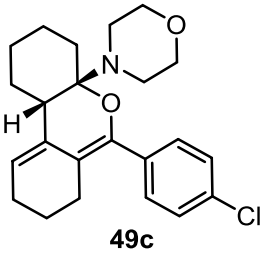 **49c**	46%
4	27a	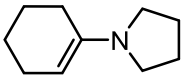 **48c**	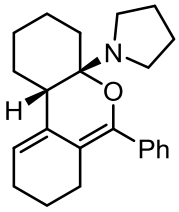 **49d**	51%

[a] 0.3 mmol of starting material **27a-b** disolved in 3 mL of THF, [b] isolated yield after column chromatography

Table 3.3 Trapping reaction scope with acyclic enamines

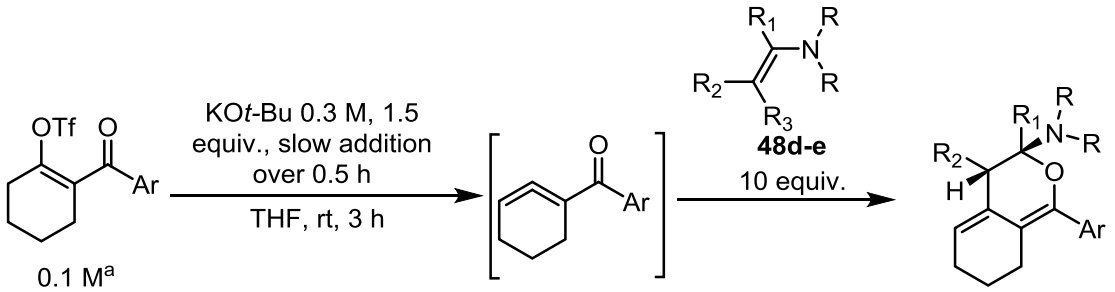

0.1 M[a]

27a (Ar = Ph)
27b (Ar = 4-ClC_6H_4)

28a-b

49e-g

Entry	Substrate	Trap	Product	Yield[b]
1	27a	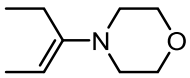 **48d**	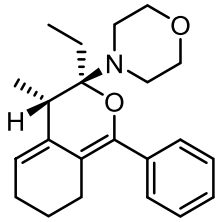 **49e**	29%
2	27b	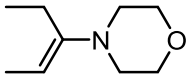 **48d**	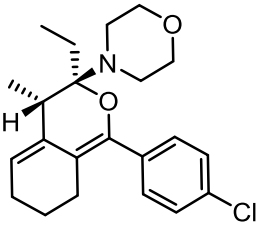 **49f**	19%
3	27a	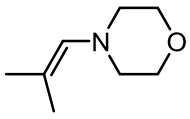 **48e**	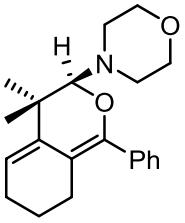 **49g**	9%

[a] 0.3 mmol of starting material **27a-b** disolved in 3 mL of THF, [b] isolated yield after column chromatography

During the study of the scope of enamine traps that could be used in this process, we were curious about introducing other functional groups in the enamine substrate. As a preliminary attempt to explore this new direction, we examined the reaction of cyclic allene **28a** with enaminone **48f** (*Scheme 3.16*). Interestingly, the expected Diels–Alder adduct **49h** was not isolated, but a small amount (6%) of dendralene **50** was obtained. The most likely explanation for the formation of this product is elimination of morpholine from the expected product **49h**, a process made more probable by the presence of an acidic proton adjacent to the leaving group. The low yield likely reflects the reduced reactivity of **48f** in the inverse electron-demand cycloaddition due to its diminished electron availability.

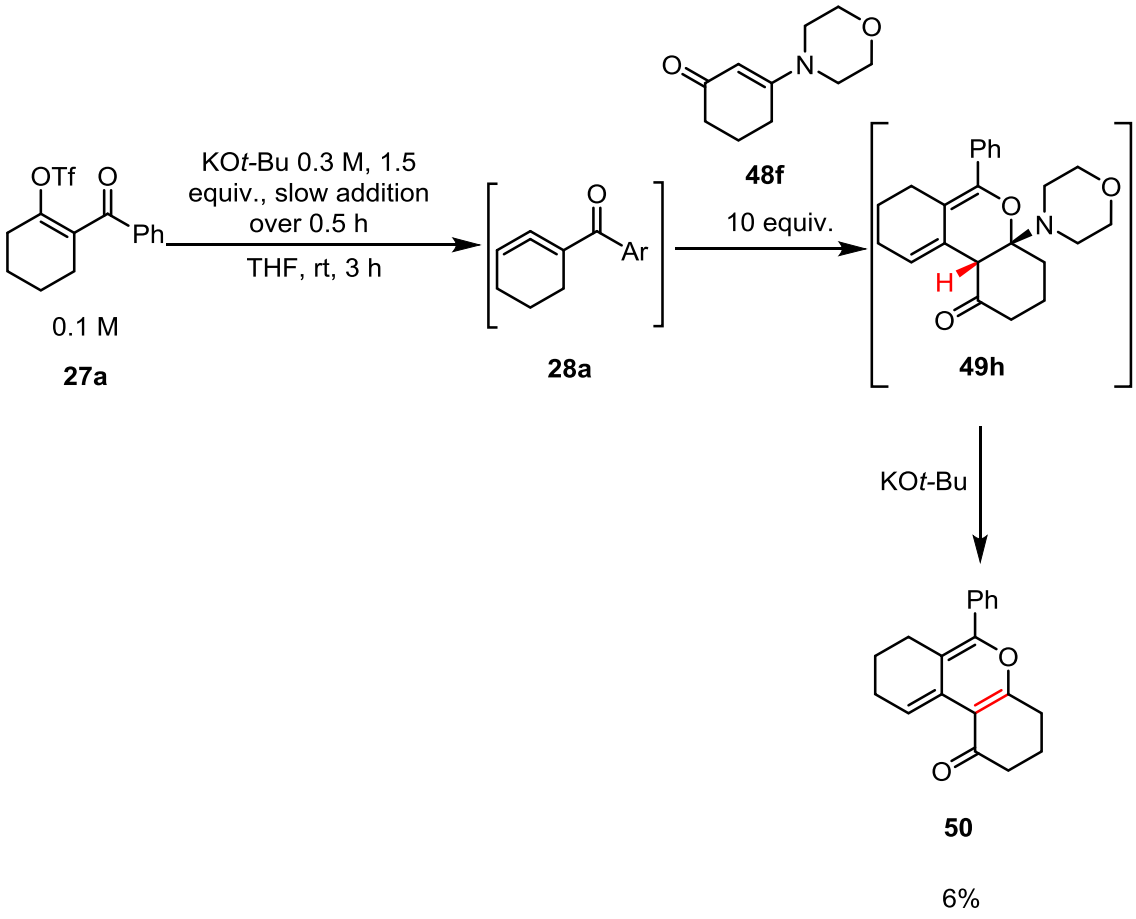

Scheme 3.16 Trapping of cyclic allene **28a** with enaminone **48f**

There were limitations in the type of enamine trap one could use. For morpholine cyclic enamines we also tested 5- and 8-membered ring enamines **48g** and **48h** respectively, which proved to be unsuitable traps for the aroyl cyclic allenes **28a** and **28b**

since these experiments did not provide the desired cycloadducts; instead, only the previously described dimeric products were observed (*Figure 3.4*). We hypothesized that the lack of reactivity of **48h** is due to steric hindrance caused by the transannular methylene protons of the enamine. The morpholine enamine of (+)-camphor **48j** also failed to react with the transient allene. In this case, we had hoped to examine the diastereofacial selectivity in the hetero-Diels–Alder cycloaddition, given the known differences in accessibility to the *endo* and *exo* faces of norbornene systems.[16] However, given the apparent sensitivity of these reactions to steric demand, we surmised that neither face was sufficiently open to permit effective trapping. Despite its close structural similarity to the successful trap **48a**, the N-methylpiperazine enamine **48i** also proved to be unreactive, for reasons that are not clear. Finally, acetophenone enamine **48k** failed to trap cyclic allenes, and in this case both steric and electronic effects may contribute to its lack of reactivity.

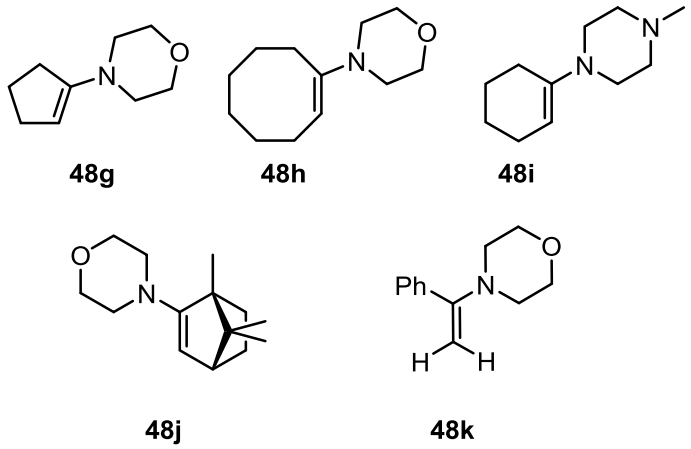

Figure 3.4 Enamines unsuitable for trapping of the aroyl cyclic allenes

3.3.5 Structural assignment discussion for the enamine cycloadducts

The structural assignment for product **49a** was initially made based on NMR and mass spectral analysis. The relative stereochemistry was determined based on TROESY correlation between the bridgehead CH on the newly formed dihydropyran ring and the N-

CH_2 of the morpholine ring, which confirmed that the morpholine and the H are on the same side of the dihydropyran ring (*Figure 3.5*).

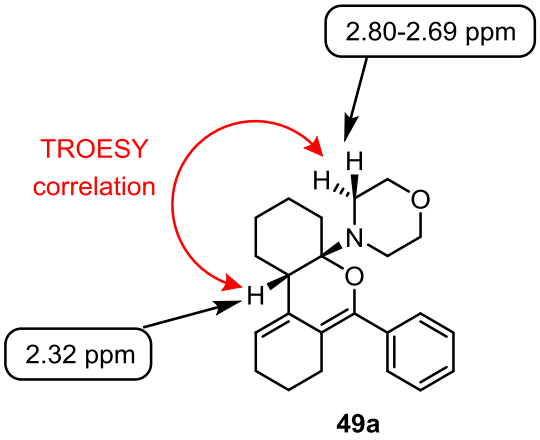

Figure 3.5 Essential TROESY correlation in cycloadduct **49a**

Later, we were able to obtain suitable crystals of cycloadduct **49a** for X-ray crystallographic analysis. The resulting crystal structure provided unambiguous proof for the *cis* ring-fusion that had been surmised from the NMR spectra. This result, along with predictable trends in NMR data, allowed for the assignment of *cis* relative configuration to other cycloadducts by analogy.

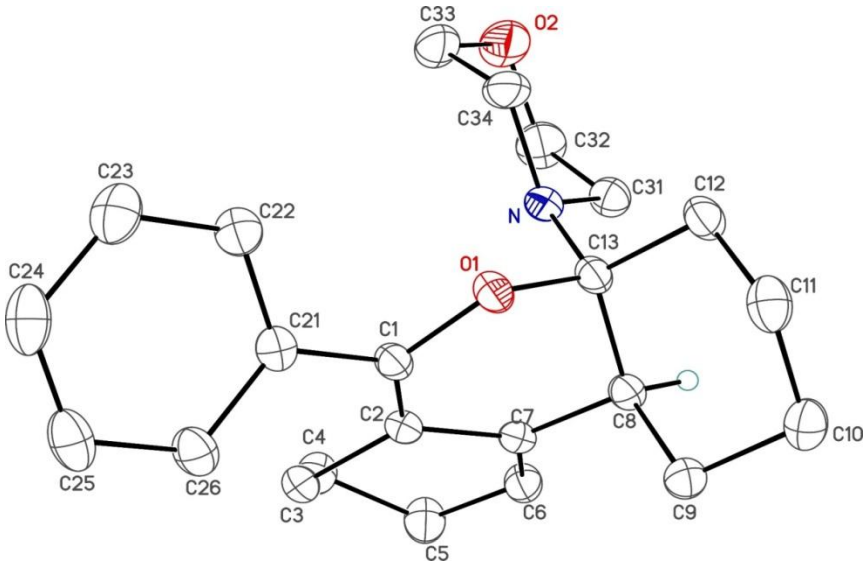

Figure 3.6 ORTEP representation for cycloadduct **49a**

The stereochemical assignments for cycloadduct **49e** were of particular interest, and could be made with confidence using the usual suite of NMR experiments, including TROESY. The formation of a single diastereomer, with retention of the stereochemical relationships found in the original enamine, has definite implications for the reaction mechanism (see section 3.3.6).

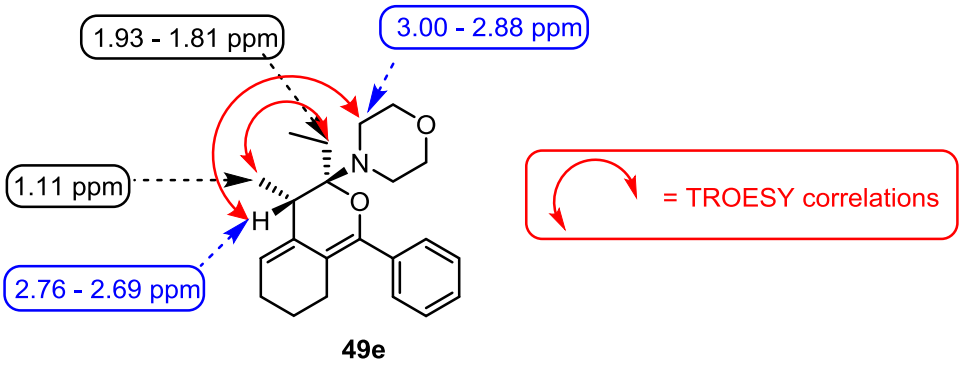

Figure 3.7 Essential TROESY correlations in cycloadduct **49e**

3.3.6 Mechanistic discussion of trapping aroyl cyclic allenes with enamines

One can imagine two possible scenarios for the reaction mechanism of trapping the aroyl cyclic allene **28a** with the enamine **48d**, a concerted or a stepwise mechanism. The stepwise mechanism would involve two steps: first a Michael addition of the nucleophilic enamine carbon of **48d** into the enone system of the cyclic allene **28a** to generate enolate intermediate **51**, followed by the nucleophilic attack of the enolate oxygen to the electrophilic carbon of the iminium (*Scheme 3.17*). If this process would occur we would expect to see a mixture of epimers **49e** and **52**, due to free rotation around the C–C single bond of the former enamine. In practice, only diasteromer **49e** was isolated from these reactions.

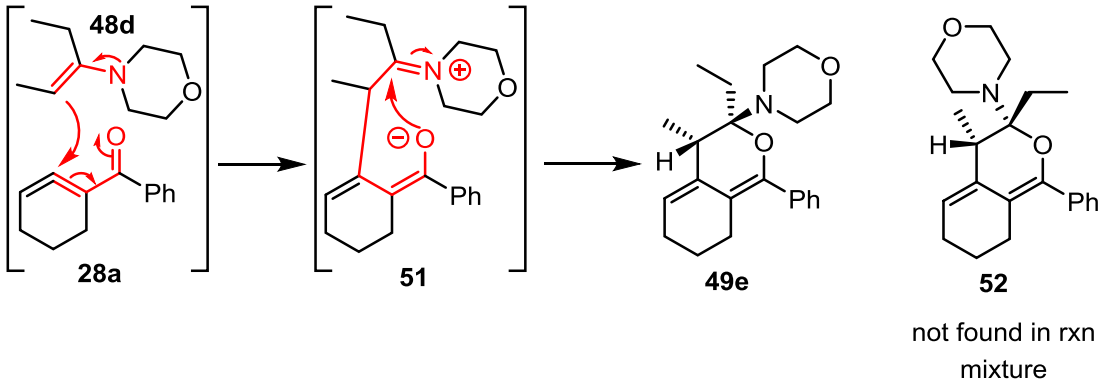

Scheme 3.17 Stepwise mechanism proposal for the reaction of aroyl cyclic allene **28a** with enamine **48d**

The second scenario involves the concerted mechanism proposal in which all the bond forming events would occur simultaneously, although likely in an asynchronous fashion (*Scheme 3.18*). In this case, the relative stereochemistry of the cycloadduct **49e** should be consistent with the alkene geometry of the enamine trapping reagent **48d**. Therefore, if the enamine trapping reagent would consist of only one stereoisomer (*E* isomer here) we should obtain only diastereomer **49e** cycloadduct as product, which was in fact the result in our experiments. In light of this stereochemical retention, we believe that there is good evidence for the concerted pathway.

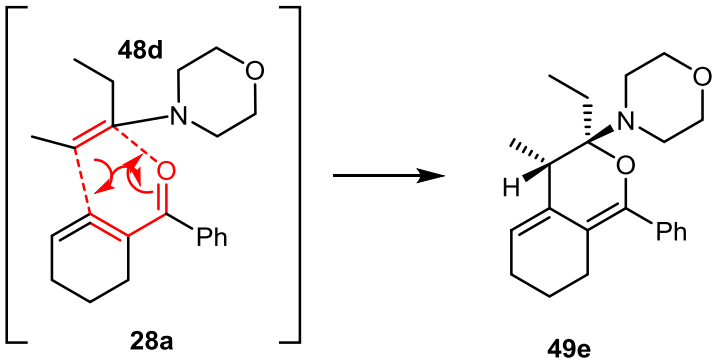

Scheme 3.18 Concerted hetero-Diels–Alder proposed mechanism

3.3.7 Mechanistic implications from computational calculations

The computational work described in this section was carried out in collaboration with Professor Rebecca Davis and her PhD student Simarpreet Singh.

In order to better understand the mechanism of trapping and dimerization processes, DFT calculations using the M062x/6-31+G(d.p) functional with IEFPCM solvent model for THF were performed.[17–19]

In the context of the trapping reaction with furan for electron deficient cyclic allene, such as **28d**, one could imagine four isomer products (two diastereomer couples of regioisomers) as possible adducts (*Scheme 3.19*).

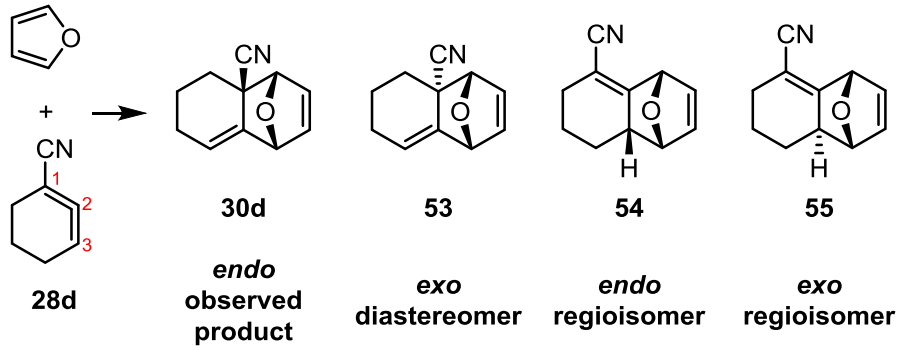

Scheme 3.19 Possible reaction products of cyclic allene **28d** with furan

When the cycloaddition reaction would occur with conjugated double bond (1,2-addition) of the cyclic allene **28d**, it would be a concerted asynchronous cycloaddition, with an energy barrier of 10.6 kcal/mol for the *endo* transition state (**TS1**) and an energy barrier of 12.7 kcal/mol for the *exo* transition state (**TS2**) according with the DFT calculations (*Figure 3.8*). The lower energy barrier for the *endo* **TS1** in comparison with the energy barrier for the *exo* **TS2** could be explained by the secondary orbital interaction between cyano group and the lone pair of the furan oxygen.

For the alternative cycloaddition with the remote double bond of the cyclic allene **28d** (2,3-addition) a stepwise mechanism where the bond between furan and C2 of the cyclic allene would form first was proposed to be favorable acording to the calculation. Both possible diastereomers for this scenario would be disfavored in comparison with the *endo* observed product **30d** with higher energy barriers of 13.7 kcal/mol for *endo* transition state (**TS3**) and 13.3 kcal/mol for *exo* transition state (**TS4**) according to the DFT calculations.

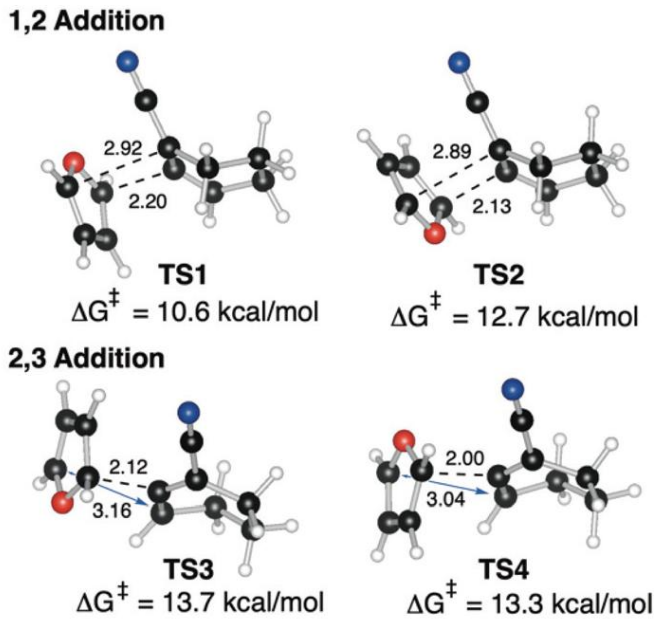

Figure 3.8 The transition states energy barriers for the four possible cycloaddition products of cyclic allene **28d** with furan

Regarding the reaction of cyclic allene **28a** with DPIBF, the *endo* transition state was favored with an energy barrier of 8.6 kcal/mol which was 1.1 kcal/mol lower than the energy barrier for the *exo* transition state (9.7 kcal/mol) according to the DFT calculations, which were consistent with experimental observations where we were able to isolate only the *endo* cycloadduct **36a** (*Table 3.4*).

Although most of the substrates obtained in the trapping of cyclic allenes with dienes showed high diastereoselectivity, there was an exception in the reaction of cyclic allene **28d** with DPIBF where a 3:1 ratio between *endo* and *exo* cycloadduct **36d** and **56** was observed. The DFT calculations showed a 0.1 kcal/mol diference in energy barriers for the *endo* (5.9 kcal/mol) and *exo* (6.0 kcal/mol) transition states, which was significantly smaller than in the other cases.

Table 3.4 Calculated energies for trapping reactions with DPIBF

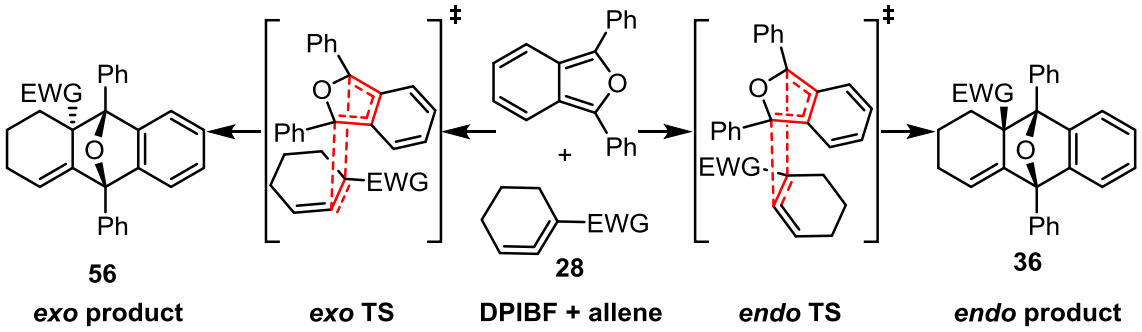

Cyclic allene	*Exo* product (kcal/mol)	*Exo* TS (kcal/mol)	Cyclic allene + DPIBF (kcal/mol)	*Endo* TS (kcal/mol)	*Endo* product (kcal/mol)
28a	-35.0	+9.7	0.0	+8.6	-35.7
28d	-46.6	+6.0	0.0	+5.9	-45.1

The dimerization according to the calculated model occurs through a concerted asynchronous [4+2] cycloaddition where the carbon-carbon bond starts forming earlier than the carbon-oxygen bond (2.20 Å vs 2.90 Å, in the transition state). Although this is an asynchronous transition state, it leads directly to reactants and products, according to the intrinsic reaction coordinate (IRC) calculations. The calculations also showed a 17.7 kcal/mol barrier for the reaction to occur and that the resulting cycloadduct **37a** is favoured by 90.5 kcal/mol in comparison with the cyclic allenes reactants (two molecules of **28a**) as presented in *Figure 3.9*.

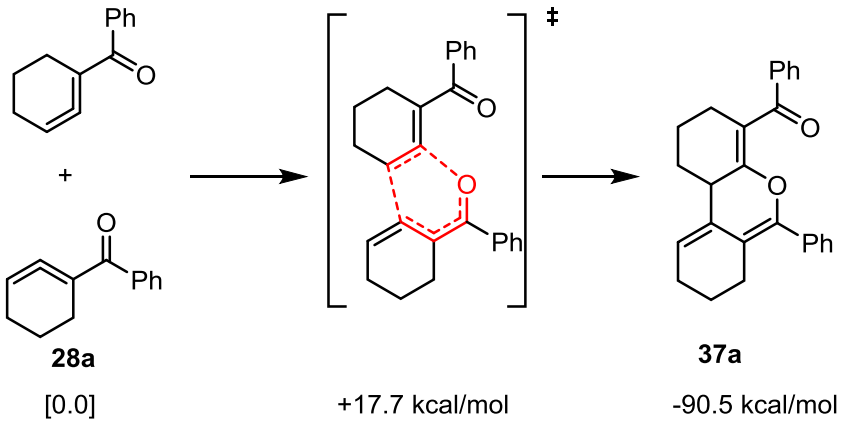

Figure 3.9 DFT calculations for the concerted dimerization pathway of the aroyl cyclic allene **28a**

As an alternative scenario one can imagine a stepwise process where a nucleophilic attack from the anionic intermediate **41** into the enone system of the cyclic allene **28a** would occur (*Figure 3.10*). In this case, the energy barrier was calculated to be 20.1 kcal/mol and the resulting intermediate **42** is favored by 34.8 kcal/mol in comparison with the reacting species, the cyclic allene **28a** and the anionic intermediate **41**. Although both reaction pathways are plausible it seems that the concerted pathway is favored.

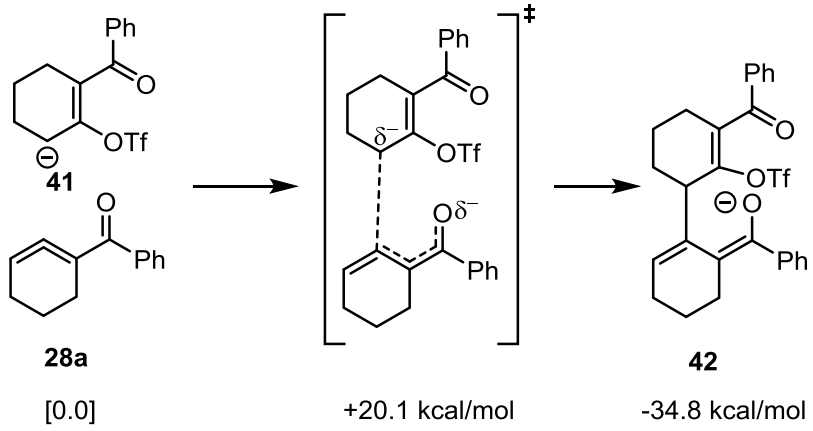

Figure 3.10 DFT calculations for the stepwise anionic pathway

Similarly with the dimerization process, in the case of enamines, two mechanistic pathways could be envisioned. In the first proposed pathway an initial nucleophilic attack of the enamine **48a** into the enone system of the cyclic allene **28a** would occur with an energy barrier of 16.2 kcal resulting in an intermediate **57** which would be favored in

comparison with the starting materials by 20.3 kcal according to the DFT calculations (*Figure 3.11*).

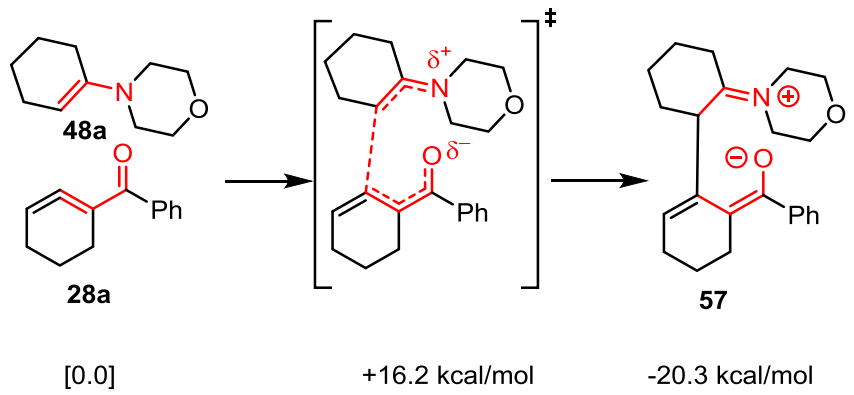

Figure 3.11 DFT calculation for the stepwise mechanism proposal of cyclic allene trapping with enamines

In the second proposed pathway, an asynchronous Diels–Alder would occur with a lower energy barrier of 12.4 kcal/mol and result in the cycloadduct **49a**, which is favored by 52.4 kcal/mol in comparison with the cyclic allene **28a** and enamine **48a** reactants according to the DFT calculations (*Figure 3.12*). Based on our experimental results and the associated DFT calculations we believe the asynchronous Diels–Alder is the more probable reaction mechanism pathway to explain our results.

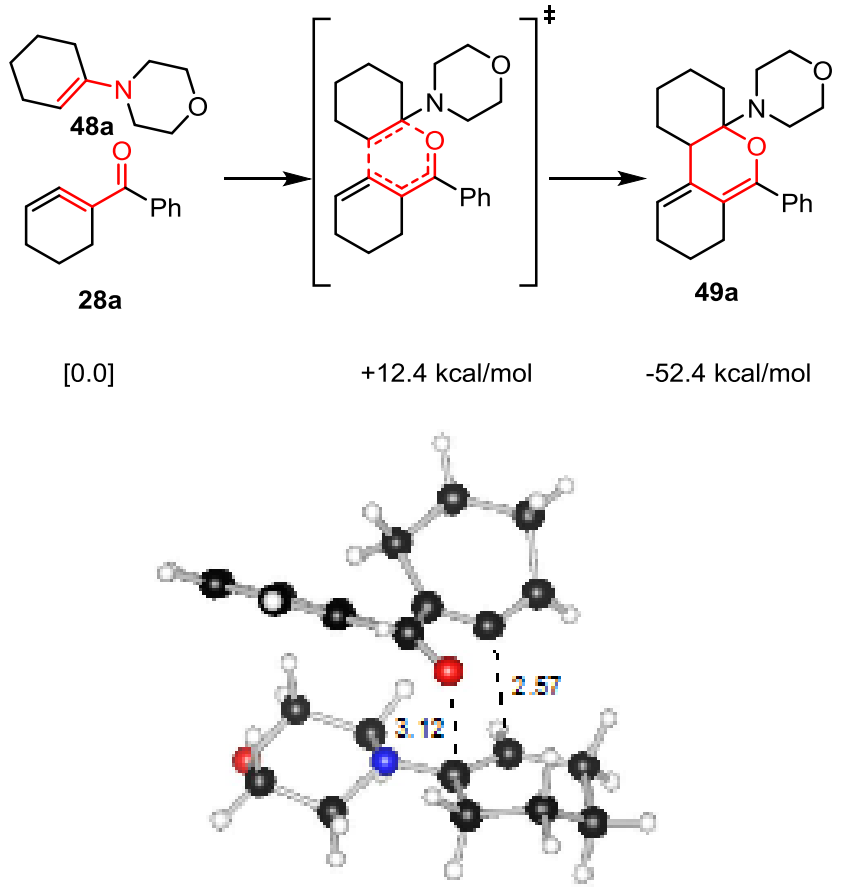

Figure 3.12 DFT calculations and transition state depiction for asynchronous Diels–Alder mechanism proposal of the reaction of cyclic allene **28a** with enamine **48a**

3.4 Conclusions

In this Chapter we presented the results of our studies concerning the reactivity of four electron deficient cyclic allenes (**28a-d**) with different trapping reagents. In the reactions with 1,3-dienes (furan and DPIBF) we observed high regioselectivity and high diastereoselectivity. It was noted that by using a stronger electron withdrawing group (aroyl and cyano) we got increased regioselectivity in comparison with the previous studies of electron deficient cyclic allenes.[5] A new way of dimerization of cyclic allenes was discovered through the [4+2] dimerization process as shown in our studies. Based on this we developed an unprecedented way of trapping cyclic allenes through a [4+2] inverse electron-demand hetero-Diels–Alder cycloaddition, which gave us access to eight complex polycyclic products in modest to good yields. Based on our experimental results and the computational calculations done by our collaborators we were able to propose with confidence an asynchronous concerted mechanism for this new type of trapping of cyclic allenes.

The results presented in this chapter have uncovered a new way of dimerization and trapping reaction for electron deficient cyclic allenes, which opens a door towards further research of these transient species. The fact that these new trapping reactions would not be possible with the much more studied typical cyclic allenes such as 1,2-cyclohexadiene **1**, confirms our initial hypothesis regarding the necessity to have more studies of polarized cyclic allenes and in particular of electron deficient cyclic allenes. One can imagine developments in generation of a more diverse set of electron deficient cyclic allenes or trapping of other electron reach olefins. Although it was not investigated at this time some of the complex polycyclic compounds isolated during this project could be biologically active. A proposal for further study directions of these reactive intermediates will be made in Chapter 5.

3.5 Experimental

3.5.1 Synthesis of enol triflates 27a and 27b

Diketones **33** were synthesized through a Stork acylation following the literature protocols and the associated data were confirmed with those in the literature.[8,9]

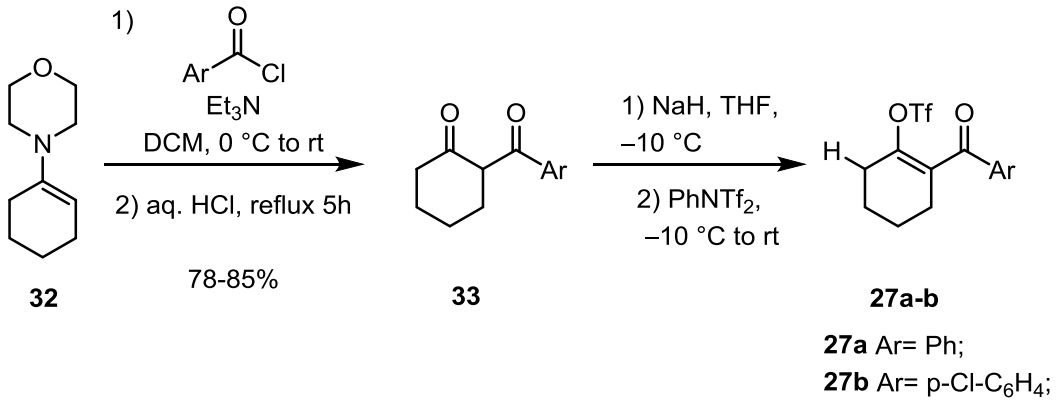

Scheme 3.20 Synthesis of enol triflate starting materials **27a** and **27b**

General procedure for the synthesis of the enol triflate starting materials 27a and 27b

A 1M solution of diketone **33** (10 mmol) in THF was added dropwise to a suspension of NaH (60% mineral oil, 12 mmol) in THF (50 mL) at -10 °C under N_2 and stirred for 45 minutes. Then a 1M solution $PhNTf_2$ (13 mmol) in THF was added and the reaction mixture was stirred and slowly warmed up to room temperature overnight. To the reaction mixture was then added 50 mL of H_2O and the solution was extracted with Et_2O (3 x 50 mL). The combined organic layers were washed with brine and dried over $MgSO_4$, filtered, and concentrated using a rotary evaporator. The crude product was further purified on column chromatography using a gradient eluent (1-5% Et_2O in hexanes) to obtain the enol triflate starting materials (**27a** and **27b**).

2-benzoylcyclohex-1-en-1-yl trifluoromethanesulfonate (**27a**)

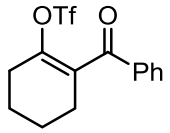

27a

Triflate **27a** was isolated as a colorless oil in 70% yield. R_f = 0.37 (hexanes/Et_2O 5:1); IR (neat) 3064, 2949, 2868, 1669, 1598, 1418, 1279, 1247, 1213, 1139, 1031 cm^{-1}; ^1H NMR (500 MHz, $CDCl_3$) δ 7.89 – 7.85 (m, 2H), 7.62 – 7.56 (m, 1H), 7.50 – 7.45 (m, 2H), 2.55 – 2.50 (m, 2H), 2.49 – 2.44 (m, 2H), 1.95 – 1.87 (m, 2H), 1.80 – 1.73 (m, 2H); ^{13}C NMR (126 MHz, $CDCl_3$) δ 194.5, 146.2, 135.4, 134.0, 130.2, 129.3, 128.8, 118.0 (q, J = 319.9 Hz, CF_3), 27.5, 27.5, 22.7, 21.1; HRMS (ESI, $[M+Na]^+$) for $C_{14}H_{13}F_3NaO_4S$ calcd. *m/z* 357.0379, found: *m/z* 357.0377; (ESI, $[M+H]^+$) for $C_{14}H_{14}F_3O_4S$ calcd. *m/z* 335.0559, found *m/z* 335.0562.

2-(4-chlorobenzoyl)cyclohex-1-en-1-yl trifluoromethanesulfonate (**27b**)

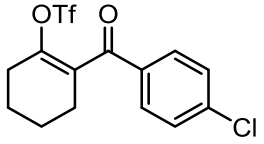

27b

Triflate **27b** was isolated as a white solid in 71% yield. R_f = 0.46 (hexanes/Et_2OAc 6:1); mp 61-63 °C; IR (cast film) 2950, 2868, 1672, 1588, 1419, 1402, 1278, 1247, 1214, 1139 1092 cm^{-1}; ^1H NMR (500 MHz, $CDCl_3$) δ 7.80 (d, J = 8.6 Hz, 2H), 7.46 (d, J = 8.6 Hz, 2H), 2.56 – 2.50 (m, 2H), 2.48 – 2.43 (m, 2H), 1.96 – 1.88 (m, 2H), 1.82 – 1.73 (m, 2H); ^{13}C NMR (126 MHz, $CDCl_3$) δ 193.3, 146.5, 140.6, 133.9, 130.7, 129.8, 129.2, 118.01 (q, J = 319.8 Hz, CF_3), 27.6, 27.4, 22.6, 21.1; HRMS (ESI, $[M+Na]^+$) for $C_{14}H_{12}ClF_3NaO_4S$ calcd. *m/z* 390.9989, found: *m/z* 390.9991; (ESI, $[M+H]^+$) for $C_{14}H_{13}ClF_3O_4S$ calcd. *m/z* 369.0170, found *m/z* 369.0171.

3.5.2 Synthesis of enamines

Enamines **48a-j** were either readily available or synthesized using adapted procedures from the literature.[20–22]

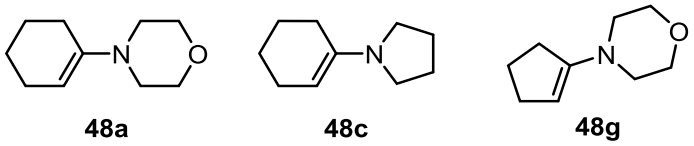

Figure 3.13 Commercially available enamines

Method A for synthesis of enamines

To a 1M ketone or aldehyde (1 equiv.) solution in toluene was added the corresponding amount of morpholine (1.2 equiv.) and *p*-toluenesulfonic acid (5 mol%) and the reaction mixture was refluxed using the Dean–Stark trap until no additional water was collected. The solvent and the excess morpholine were removed using a rotary evaporator and then the crude was distilled at low pressure in order to obtain the pure product. Product **48f** was isolated using column chromatography, being the only enamine made by us stable on silica. This procedure was adapted from the literature.[8,20]

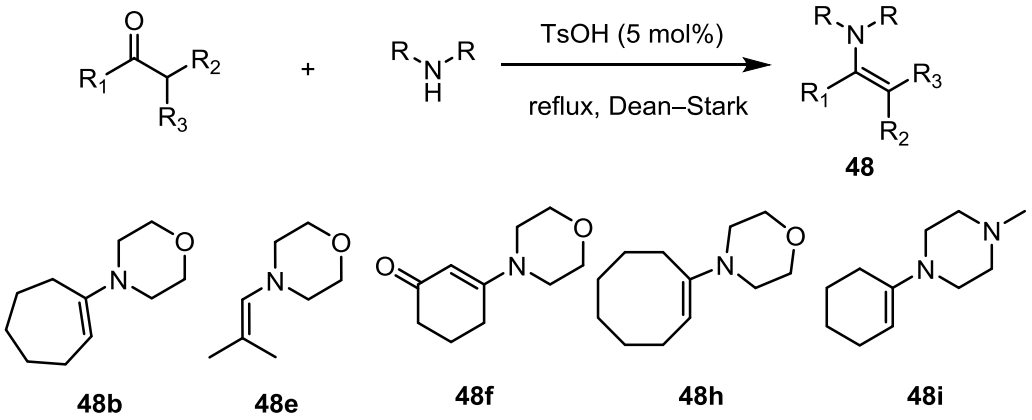

Scheme 3.21 Enamines synthesized using method A

Method B for synthesis of enamines

To the indicated amount of morpholine (it is shown for each substrate during the characterization section) solution in 50 mL hexane at 0 °C was added over 0.5 h using a

syringe pump the corresponding amount of $TiCl_4$ previously diluted in 20 mL of hexane. Then the ketone solution in 20 mL of hexane or benzene was added in one portion and the reaction mixture was stirred at room temperature for the indicated time (0.5 h for **48d**, 48 h for **48j** and 0.5 h for **48k**). The viscous mixture was cooled in an ice bath, and then it was filtered in a dry flask. The solvent and the excess of morpholine were removed using a rotary evaporator, and then the crude was distilled at low pressure. This procedure was adapted from the literature.[21,22]

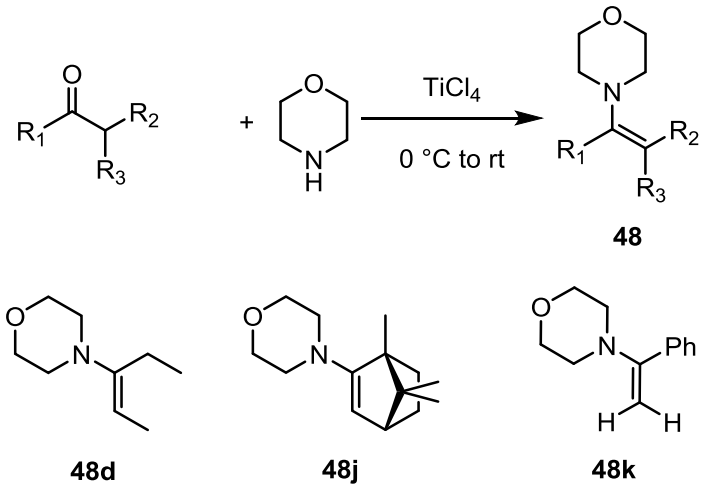

Scheme 3.22 Enamines synthesized using method B

4-(cyclohept-1-en-1-yl)morpholine (**48b**)

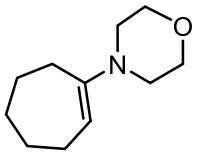

Enamine **48b** was obtained in 68% yield as a colorless oil using **Method A**. (lit.[20]) b.p. 138-140 °C, 18 mmHg); IR (neat) 3056, 2955, 2918, 2850, 1643, 1447, 1261, 1121 cm^{-1}; ^1H NMR (500 MHz, $CDCl_3$) δ 4.82 (t, J = 6.9 Hz, 1H), 3.72 – 3.63 (m, 4H), 2.69 – 2.61 (m, 4H), 2.24 – 2.14 (m, 2H), 2.09 – 1.99 (m, 2H), 1.71 – 1.64 (m, 2H), 1.46 – 1.36 (m, 4H); ^{13}C NMR (126 MHz, $CDCl_3$) δ 154.2, 107.0, 67.0, 49.9, 32.6, 31.6, 28.0, 26.7, 26.3; HRMS (EI, M^+) for $C_{11}H_{19}NO$ calcd. *m/z* 181.1467, found: *m/z* 181.1465.

(*E*)-4-(pent-2-en-3-yl)morpholine (**48d**)

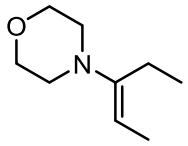

48d

Enamine **48d** was obtained in 73% yield (14.8 mmol of **48d**) as a colorless oil using **Method B** with 20.1 mmol (1 equiv.) of 3-pentanone, 114.9 mmol (5.7 equiv) of morpholine and 18.1 mmol (0.9 equiv.) of $TiCl_4$. (lit.[22] b.p. 74-75 °C, 10 mmHg); IR (neat) 2964, 2853, 1713, 1679, 1654, 1452, 1118 cm^{-1}; ^1H NMR (500 MHz, acetone-d_6) δ 4.37 (q, J = 6.7 Hz, 1H), 3.65 – 3.58 (m, 4H), 2.70 – 2.65 (m, 4H), 2.16 (q, J = 7.5 Hz, 2H), 1.58 (d, J = 6.7 Hz, 3H), 0.97 (t, J = 7.5 Hz, 4H); ^{13}C NMR (126 MHz, acetone-d_6) δ 151.6, 97.8, 67.6, 50.2, 21.3, 13.2, 12.6; HRMS (EI, M^+) for $C_9H_{17}NO$ calcd. *m/z* 155.1310, found: *m/z* 155.1310.

4-(2-methylprop-1-en-1-yl)morpholine (**48e**)

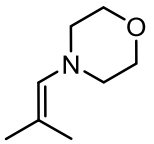

48e

Enamine **48e** was obtained in 67% yield as a colorless oil using **Method A**. (lit.[23] bp. 31 °C, 5 mmHg); IR (neat) 3344, 2964, 2854, 1680, 1451, 1432, 1271, 1116 cm^{-1}; ^1H NMR (500 MHz, $CDCl_3$) δ 5.30 – 5.27 (m, 1H), 3.71 – 3.65 (m, 4H), 2.58 – 2.52 (m, 4H), 1.67 – 1.62 (m, 3H), 1.60 – 1.55 (m, 3H); ^{13}C NMR (126 MHz, $CDCl_3$) δ 135.1, 123.3, 66.9, 53.0, 22.2, 17.3; HRMS (EI, M^+) for $C_8H_{15}NO$ calcd. *m/z* 141.1154, found: *m/z* 141.1154.

3-morpholinocyclohex-2-en-1-one (**48f**)

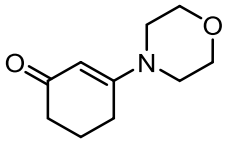

48f

Enamine **48f** was obtained in 57% yield using **Method A** and isolated as a light yellow solid from column chromatography (10-20% EtOAc in hexane); m.p. 92-94 °C; IR (cast film) 3063, 2950, 2857, 1624, 1561, 1435, 1354, 1237, 1194 cm^{-1}; ^1H NMR (500 MHz, $CDCl_3$) δ 5.27 (s, 1H), 3.77 – 3.71 (m, 4H), 3.33 – 3.27 (m, 4H), 2.41 (t, *J* = 6.2 Hz, 2H), 2.31 (dd, *J* = 7.1, 6.1 Hz, 2H), 2.01 (appquint, *J* = 6.4 Hz, 2H); ^{13}C NMR (126 MHz, $CDCl_3$) δ 197.6, 164.9, 100.9, 66.3, 46.3, 35.8, 26.8, 22.1; HRMS (EI, M^+) for $C_{10}H_{15}NO_2$ calcd. 181.11028, found: *m/z* 181.11028.

(*E*)-4-(cyclooct-1-en-1-yl)morpholine (**48h**)

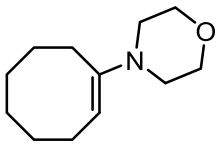

48h

Enamine **48h** was obtained in 78% yield as a colorless oil was obtained using **Method A**; (lit.[20] b.p. 156-157 °C, 19 mmHg); IR (neat) 3051, 2921, 2851, 2813, 1639, 1471, 1448, 1264, 1123 cm^{-1}; ^1H NMR (500 MHz, $CDCl_3$) δ 4.54 (t, *J* = 8.3 Hz, 1H), 3.74 – 3.67 (m, 4H), 2.81 – 2.74 (m, 4H), 2.31 – 2.24 (m, 2H), 2.13 – 2.04 (m, 2H), 1.55 – 1.40 (m, 8H); ^{13}C NMR (126 MHz, $CDCl_3$) δ 149.0, 103.5, 67.1, 49.3, 30.6, 29.8, 27.2, 26.6, 26.3, 25.9; HRMS (EI, M^+) for $C_{12}H_{21}NO$ calcd. *m/z* 195.1623, found: *m/z* 195.1623.

1-(cyclohex-1-en-1-yl)-4-methylpiperazine (**48i**)

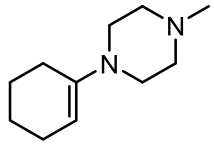

48i

Enamine **48i** was obtained in 69% yield as a colorless oil was obtained using **Method A**;IR (neat) 3057, 2966, 2931, 2856, 2793, 1646, 1452, 1383, 1290, 1207 cm^{-1}; ^1H NMR (500 MHz, $CDCl_3$) δ 4.62 (t, *J* = 3.4 Hz, 1H), 2.77 (t, *J* = 5.1 Hz, 4H), 2.40 (t, *J* = 5.0 Hz, 4H), 2.24 (s, 2H), 2.05 – 1.98 (m, 4H), 1.66 – 1.58 (m, 2H), 1.54 – 1.45 (m, 2H); ^{13}C NMR (126 MHz, $CDCl_3$) δ 145.3, 100.3, 55.3, 47.9, 46.2, 27.2, 24.5, 23.3, 22.8; HRMS (EI, M^+) for $C_{11}H_{20}N_2$ calcd. *m/z* 180.1626, found: *m/z* 180.1627.

4-((1*R*,4*R*)-1,7,7-trimethylbicyclo[2.2.1]hept-2-en-2-yl)morpholine (**48j**)

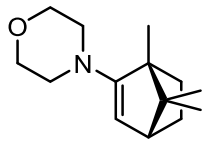

48j

Enamine **48j** was obtained in 70% yield (21.2 mmol of **48j**) as a colorless oil was obtained using **Method B** from 30 mmol (1 equiv.) of camfor, 276 mmol (9.2 equiv.) of morpholine and 39 mmol (1.3 equiv.) of $TiCl_4$; (lit.[21] b.p. 72-73 °C, 0.01 mmHg); IR (neat) 3068, 2955, 2872, 2817, 1743, 1682, 1451, 1270, 1119 cm^{-1}; ^1H NMR (500 MHz, acetone-d_6) δ 4.86 (d, *J* = 3.5 Hz, 1H), 3.63 (ddd, *J* = 5.4, 3.8, 1.4 Hz, 4H), 2.73 – 2.61 (m, 4H), 2.18 (t, *J* = 3.5 Hz, 1H), 1.84 (ddt, *J* = 11.2, 8.7, 3.6 Hz, 1H), 1.52 (ddd, *J* = 12.1, 8.8, 3.6 Hz, 1H), 1.14 (ddd, *J* = 11.6, 9.2, 3.7 Hz, 1H), 1.05 (s, 3H), 0.99 (ddd, *J* = 11.2, 9.2, 3.6 Hz, 1H), 0.82 (s, 3H), 0.73 (s, 3H); ^{13}C NMR (126 MHz, acetone-d_6) δ 159.9, 109.2, 67.2, 57.1, 54.4, 51.7, 50.6, 32.8, 27.7, 20.3, 20.2, 12.4; HRMS (EI, M^+) for $C_{14}H_{23}NO$ calcd. 221.17796, found: *m/z* 221.17784.

4-(1-phenylvinyl)morpholine (**48k**)

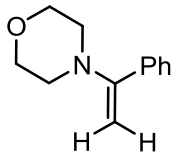

48k

Enamine **48k** was obtained in 54% yield (16.4 mmol of **48k**) as a colorless oil was obtained using **Method B** with 30 mmol (1 equiv.) of acetophenone, 138 mmol (4.6 equiv.) of morpholine and 21 mmol (0.7 equiv.) of $TiCl_4$; (lit.[21] b.p. 96-97 °C, 1 mmHg); IR (neat) 3057, 2962, 2852, 2823, 1685, 1597, 1572, 1491, 1447, 1372, 1354, 1267, 1257, 1120 cm^{-1}; ^1H NMR (500 MHz, acetone-d_6) δ 7.48 – 7.43 (m, 2H), 7.37 – 7.28 (m, 3H), 4.28 (s, 1H), 4.19 (s, 1H), 3.73 – 3.65 (m, 4H), 2.79 – 2.74 (m, 4H);^{13}C NMR (126 MHz, acetone-d_6) δ 158.2, 140.1, 129.1, 128.9, 128.5, 91.3, 67.3, 50.8;

3.5.3 General procedure for the optimization reactions of 27a with 48a

To a stirred solution of starting material **27a** (0.1 mmol, 1.0 equiv.) and enamine **48a** (5-60 equiv.) in anhydrous THF (0.5-2 mL) under nitrogen atmosphere was added a 0.3M solution of KO*t*-Bu (1-2.5 equiv.) in anhydrous THF at various temperatures. The reaction mixture was stirred for 0.5-24 h at various temperatures and then it was quenched with NH_4Cl saturated solution (3 mL) and extracted with Et_2O (5 x 5 mL). The combined organic layers were dried over $MgSO_4$, filtered, and concentrated under various temperatures reduced pressure. The crude was dissolved with a previously prepared solution of 1,3,5-trimethoxybenzene (0.3 M) in $CDCl_3$, which was then analyzed by means of ^1H NMR spectroscopy in order to determine the NMR yield.

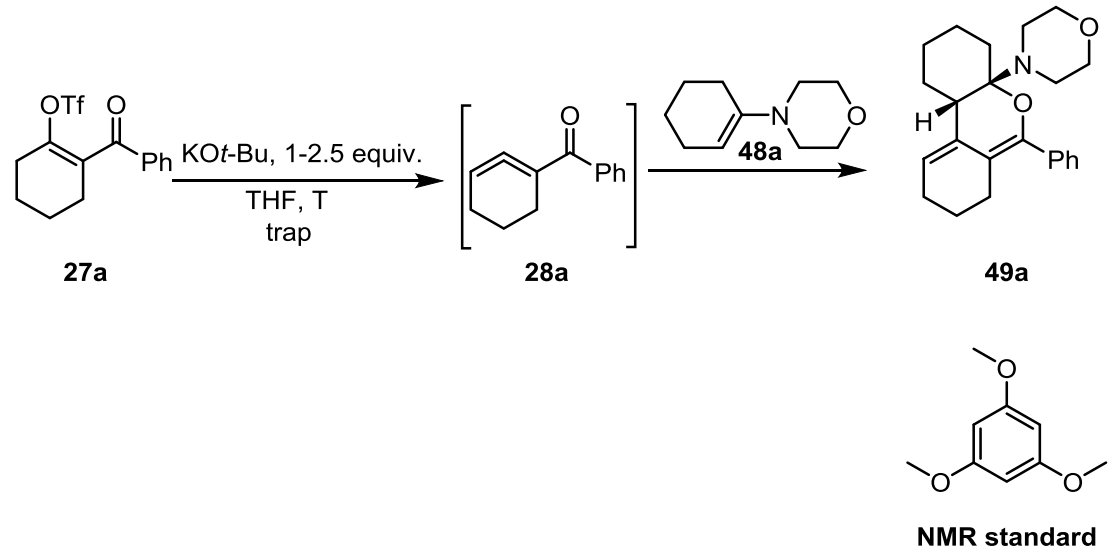

Scheme 3.23 The optimization for the trapping reaction of cyclic allene **28a** with enamine **48a**

3.5.4 General procedure for the synthesis of the cycloadducts 49a-49g and 50 through hetero-Diels–Alder trapping of cyclic allenes 28a-b with enamines 48a-f

To a stirred solution of starting material **27** (0.3 mmol, 1.0 equiv.) and enamine **48** (3 mmol, 10 equiv.) in anhydrous THF (3 mL) under nitrogen atmosphere was added dropwise a solution of KO*t*-Bu (0.45 mmol, 1.5 equiv.) in anhydrous THF (1.5 mL) at room temperature over 30 minutes. The reaction mixture was stirred for 3 h at room temperature and then it was quenched with NH_4Cl saturated solution (10 mL) and extracted with Et_2O (5 x 10 mL). The combined organic layers were dried over $MgSO_4$, filtered, and concentrated under reduced pressure. The crude was further purified by column chromatography on Al_2O_3 (neutral, Brockmann I, 40-160 μm) to afford the cycloadduct **16.** The column chromatography can be performed on silica as well, but for a slightly cleaner product we recommend the use of neutral alumina. When required, HSQC was used to aid ^{13}C NMR peak assignments.

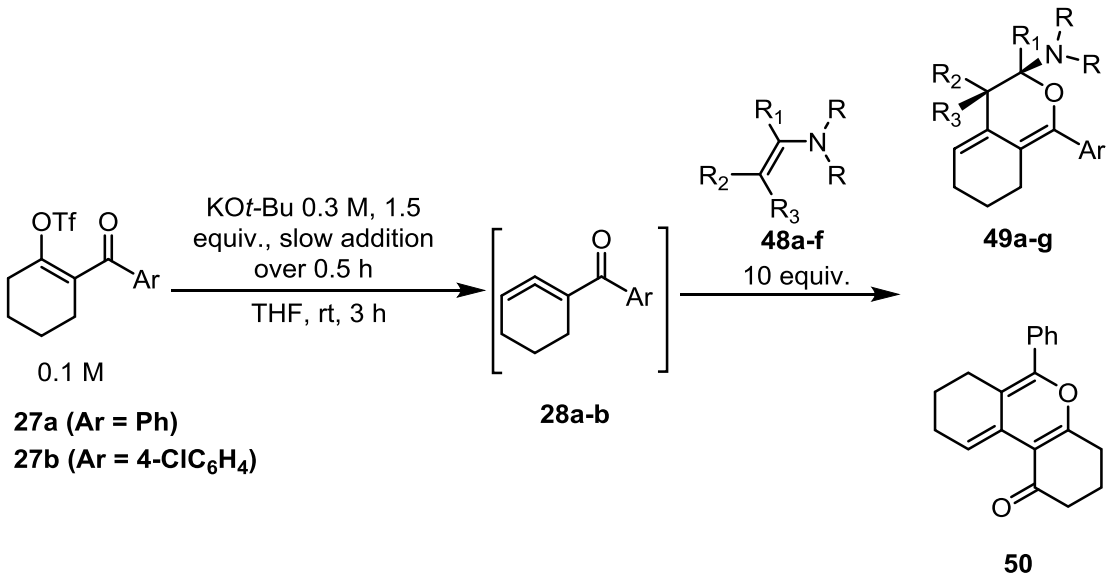

Scheme 3.24 Synthesis of cycloadducts **49a-g** and **50**

hetero-Diels–Alder cycloadduct of cyclic allene **28a** and enamine **48a** (**49a**)

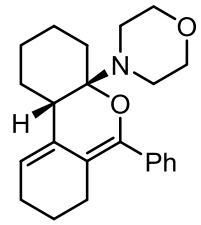

49a

Triflate **27a** (110 mg, 0.33 mmol) was used. Flash chromatography (99:1 to 20:1 hexanes : Et_2O) on neutral alumina gave **49a** (76 mg, 65%) as a light yellow solid. R_f = 0.38 (hexanes/EtOAc 9:1); mp 94-96 °C; IR (cast film) cm^{-1} 3083, 3054, 3034, 2933, 2851, 1684, 1598, 1492, 1446, 1263, 1118; ^1H NMR (500 MHz, $CDCl_3$) δ 7.42 – 7.39 (m, 2H), 7.34 (t, J = 7.5 Hz, 2H), 7.29 – 7.25 (m, 1H), 5.34 (t, J = 4.2 Hz, 1H), 3.61 (t, J = 4.6 Hz, 4H), 2.80 – 2.68 (m, 4H), 2.48 (ddd, J = 14.5, 6.0, 3.9 Hz, 1H), 2.39 (ddd, J = 14.6, 10.8, 4.0 Hz, 1H), 2.32 (dd, J = 10.1, 4.7 Hz, 1H), 2.21 – 2.09 (m, 2H), 1.99 (dtd, J = 13.5, 3.9, 1.3 Hz, 1H), 1.74 – 1.55 (m, 7H), 1.34 (ddd, J = 13.6, 11.7, 4.6 Hz, 1H), 1.25 – 1.17 (m, 1H); ^{13}C NMR (126 MHz, $CDCl_3$) δ 141.6, 136.8, 134.7, 128.8, 127.8, 127.4, 120.3, 108.8, 90.3, 67.9, 44.9, 42.0, 30.6, 27.9, 26.7, 26.0, 24.4, 24.1, 22.7; HRMS (ESI, $[M+H]^+$) for $C_{23}H_{30}NO_2$ calcd. m/z 352.2271, found: m/z 352.2275.

hetero-Diels–Alder cycloadduct of cyclic allene **28a** and enamine **48b** (**49b**)

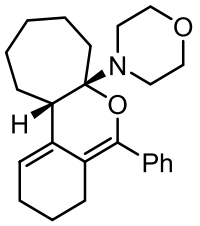

49b

Triflate **27a** (104 mg, 0.31 mmol) was used. Flash chromatography (99:1 to 20:1 hexane: Et_2O) on neutral alumina gave **49b** (28 mg, 24%) as a light yellow oil. R_f = 0.45 (hexanes/EtOAc 10:1); IR (cast film) cm^{-1} 3057, 3023, 2925, 2853, 1663, 1597, 1449, 1276, 1119; ^1H NMR (500 MHz, $CDCl_3$) δ 7.43 (dt, *J* = 6.3, 1.4 Hz, 2H), 7.33 (t, *J* = 7.6 Hz, 2H), 7.29 – 7.24 (m, 1H), 5.41 (td, *J* = 4.3, 1.2 Hz, 1H), 3.63 (t, *J* = 4.7 Hz, 4H), 2.78 (q, *J* = 4.7 Hz, 4H), 2.62 (d, *J* = 7.7 Hz, 1H), 2.52 – 2.36 (m, 2H), 2.18 (ddt, *J* = 8.1, 5.7, 3.1 Hz, 2H), 2.09 – 1.92 (m, 2H), 1.87 (ddd, *J* = 14.9, 7.2, 3.5 Hz, 1H), 1.80 – 1.39 (m, 7H), 1.36 – 1.16 (m, 2H); ^{13}C NMR (126 MHz, $CDCl_3$) δ 143.0, 136.4, 135.7, 128.8, 127.7, 127.5, 119.6, 108.7, 93.8, 67.9, 45.6, 44.1, 31.1, 28.5, 28.1, 26.8, 26.1, 26.0, 23.8, 21.7; HRMS (ESI, $[M+H]^+$) for $C_{24}H_{32}NO_2$ calcd. *m/z* 366.2428, found: *m/z* 366.2417.

hetero-Diels–Alder cycloadduct of cyclic allene **28b** and enamine **48a** (**49c**)

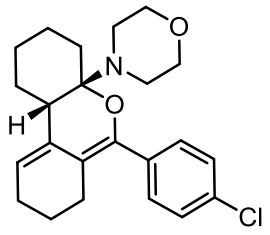

49c

Triflate **27b** (112 mg, 0.3 mmol) was used. Flash chromatography (99:1 to 20:1 hexane: Et_2O) on neutral alumina gave **49c** (54 mg, 46%) as a light yellow oil. R_f = 0.28 (hexanes/EtOAc 10:1); IR (cast film) cm^{-1} 3034, 2931, 2854, 1680, 1592, 1489, 1448, 1279, 1118, 1094; ^1H NMR (500 MHz, $CDCl_3$) δ 7.33 (d, *J* = 8.6 Hz, 2H), 7.29 (d, *J* = 8.6 Hz, 2H), 5.36 (t, *J* = 4.2 Hz, 1H), 3.59 (t, *J* = 4.6 Hz, 4H), 2.79 – 2.64 (m, 4H), 2.45 (ddd, *J* = 14.5, 6.0, 4.0 Hz, 1H), 2.38 (dd, *J* = 10.6, 4.0 Hz, 1H), 2.34 – 2.28 (m, 1H), 2.20 – 2.08

(m, 2H), 2.01 – 1.93 (m, 1H), 1.75 – 1.46 (m, 7H), 1.38 – 1.29 (m, 1H), 1.25 – 1.16 (m, 1H); ^{13}C NMR (126 MHz, $CDCl_3$) δ 140.5, 135.2, 134.5, 133.1, 130.1, 128.0, 120.9, 109.3, 90.4, 67.9, 44.9, 41.9, 30.6, 27.9, 26.7, 25.9, 24.3, 24.0, 22.7; HRMS (ESI, $[M+H]^+$) for $C_{23}H_{29}ClNO_2$ calcd. *m/z* 386.1881, found: *m/z* 386.1872.

hetero-Diels–Alder cycloadduct of cyclic allene **28a** and enamine **48c** (**49d**)

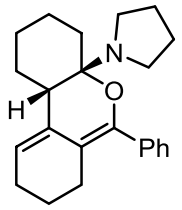

49d

Triflate **27a** (104 mg, 0.31 mmol) was used. Flash chromatography (99:1 to 20:1 hexane: Et_2O) on neutral alumina gave **49d** (53 mg, 51%) as a light yellow oil. R_f = 0.30 (hexanes/EtOAc 10:1); IR (cast film) cm^{-1} 3054, 3034, 2929, 2856, 1673, 1597, 1447, 1270, 1113; ^{1}H NMR (500 MHz, $CDCl_3$) δ 7.44 (d, *J* = 7.6 Hz, 2H), 7.34 (t, *J* = 7.5 Hz, 2H), 7.26 (t, *J* = 7.4 Hz, 1H), 5.54 (t, *J* = 4.6 Hz, 1H), 2.98 – 2.87 (m, 4H), 2.67 (s, 1H), 2.44 (t, *J* = 6.2 Hz, 2H), 2.25 – 2.14 (m, 2H), 2.10 – 2.00 (m, 1H), 1.90 – 1.52 (m, 10H), 1.35 – 1.24 (m, 3H); ^{13}C NMR (126 MHz, $CDCl_3$) δ 144.4, 137.1, 133.3, 128.9, 127.6, 127.3, 119.4, 106.8, 91.4, 44.1, 41.3, 29.7, 28.3, 26.8, 26.1, 24.6, 23.5, 23.5, 21.5; HRMS (ESI, $[M+H]^+$) for $C_{23}H_{30}NO$ calcd. *m/z* 336.2322, found: *m/z* 336.2325.

hetero-Diels–Alder cycloadduct of cyclic allene **28a** and enamine **48d** (**49e**)

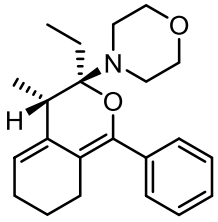

49e

Triflate **27a** (94 mg, 0.28 mmol) was used. Flash chromatography (99:1 to 20:1 hexane: Et_2O) on neutral alumina gave **49e** (28 mg, 29%) as a light yellow oil. R_f = 0.42

(hexanes/EtOAc 10:1); IR (cast film) cm^{-1} 3053, 3019, 2970, 2919, 2885, 2851, 1664, 1634, 1615, 1597, 1491, 1446, 1271, 1175, 1120, 1070; ^1H NMR (500 MHz, $CDCl_3$) δ 7.45 – 7.41 (m, 2H), 7.36 – 7.31 (m, 2H), 7.29 – 7.23 (m, 1H), 5.46 (td, *J* = 4.2, 1.3 Hz, 1H), 3.67 – 3.59 (m, 4H), 3.00 – 2.88 (m, 4H), 2.76 – 2.69 (m, 1H), 2.50 – 2.40 (m, 2H), 2.22 – 2.14 (m, 2H), 1.93 – 1.81 (m, 2H), 1.72 – 1.60 (m, 2H), 1.11 (d, *J* = 6.9 Hz, 3H), 0.94 (t, *J* = 7.6 Hz, 3H); ^{13}C NMR (126 MHz, $CDCl_3$) δ 143.9, 136.4, 136.0, 128.8, 127.7, 127.6, 119.8, 108.1, 94.3, 68.0, 45.8, 36.7, 26.7, 26.1, 25.5, 23.8, 14.4, 8.9; HRMS (ESI, $[M+H]^+$) for $C_{22}H_{30}NO_2$ calcd. *m/z* 340.2271, found: *m/z* 340.2271.

hetero-Diels–Alder cycloadduct of cyclic allene **28b** and enamine **48d** (**49f**)

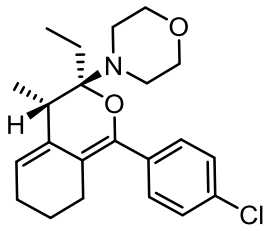

49f

Triflate **27b** (103 mg, 0.28 mmol) was used. Flash chromatography (99:1 to 20:1 hexane: Et_2O) on neutral alumina gave **49f** (20 mg, 19%) as a light yellow oil. R_f = 0.47 (hexanes/EtOAc 10:1); IR (cast film) cm^{-1} 3042, 2971, 2932, 2886, 2851, 1672, 1613, 1591, 1489, 1450, 1270, 1120; ^1H NMR (500 MHz, $CDCl_3$) δ 7.35 (d, *J* = 8.5 Hz, 2H), 7.29 (d, *J* = 8.5 Hz, 2H), 5.49 (dt, *J* = 5.2, 2.5 Hz, 1H), 3.63 (t, *J* = 4.6 Hz, 4H), 2.91 (t, *J* = 4.7 Hz, 4H), 2.76 – 2.67 (m, 1H), 2.48 – 2.34 (m, 2H), 2.25 – 2.11 (m, 2H), 1.94 – 1.78 (m, 2H), 1.75 – 1.54 (m, 2H), 1.09 (d, *J* = 6.9 Hz, 3H), 0.93 (t, *J* = 7.6 Hz, 3H); ^{13}C NMR (126 MHz, $CDCl_3$) δ 142.9, 135.7, 134.9, 133.3, 130.1, 127.9, 120.4, 108.6, 94.5, 67.9, 45.8, 36.7, 26.7, 26.0, 25.4, 23.7, 14.3, 8.9; HRMS (ESI, $[M+H]^+$) for $C_{22}H_{29}ClNO_2$ calcd. *m/z* 374.1881, found: *m/z* 374.1881.

hetero-Diels–Alder cycloadduct of cyclic allene **28a** and enamine **48e** (**49g**)

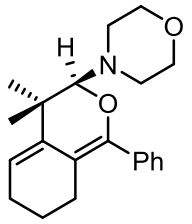

49g

Triflate **27a** (96 mg, 0.29 mmol) was used. Flash chromatography (99:1 to 20:1 hexane: Et_2O) on neutral alumina gave **49g** (9 mg, 9%) as a light yellow oil; R_f = 0.40 (hexanes/EtOAc 10:1); IR (cast film) cm^{-1} 3057, 3034, 2957, 2930, 2855, 1667, 1597, 1491, 1448, 1254, 1119, 1066; ^1H NMR (500 MHz, $CDCl_3$) δ 7.54 – 7.50 (m, 2H), 7.39 – 7.34 (m, 2H), 7.32 – 7.28 (m, 1H), 5.58 (t, *J* = 4.3 Hz, 1H), 4.26 (s, 1H), 3.72 – 3.56 (m, 4H), 3.24 – 3.17 (m, 2H), 2.75 – 2.68 (m, 2H), 2.46 – 2.32 (m, 2H), 2.22 – 2.10 (m, 2H), 1.72 – 1.63 (m, 1H), 1.52 – 1.44 (m, 1H), 1.21 (s, 3H), 1.18 (s, 3H); ^{13}C NMR (126 MHz, $CDCl_3$) δ 145.7, 139.1, 136.1, 128.8, 128.0, 127.9, 115.5, 106.7, 98.3, 67.5, 49.4, 36.5, 30.4, 26.8, 26.0, 23.2, 23.2; HRMS (ESI, $[M+H]^+$) for $C_{21}H_{28}NO_2$ calcd. *m/z* 326.2115, found: *m/z* 326.2113.

6-phenyl-2,3,4,7,8,9-hexahydro-1*H*-benzo[*c*]chromen-1-one (**50**)

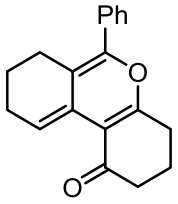

50

Triflate precursor **27a** (116 mg, 0.35 mmol) was used. Flash chromatography (99:1 to 20:1 hexane:EtOAc) on silica gave **50** (6 mg, 6%) as a light yellow oil, which in contact with the air becomes dark red. R_f = 0.30 (hexanes/EtOAc 20:1); IR (cast film) cm^{-1} 3057, 2929, 2851, 1716, 1660, 1597, 1581, 1448, 1393, 1278; ^1H NMR (500 MHz, $CDCl_3$) δ 7.47 – 7.37 (m, 5H), 6.94 (t, *J* = 4.6 Hz, 1H), 2.57 – 2.49 (m, 4H), 2.47 – 2.41 (m, 2H), 2.31 – 2.26 (m, 2H), 2.03 (p, *J* = 6.4 Hz, 2H), 1.64 (p, *J* = 6.1 Hz, 2H); ^{13}C NMR (126

MHz, $CDCl_3$) δ 197.6, 168.4, 142.3, 133.4, 128.8, 128.6, 128.2, 122.4, 117.3, 117.0, 112.4, 39.1, 28.8, 26.4, 25.5, 21.1, 20.3; HRMS (EI, M^+) for $C_{19}H_{18}O_2$ calcd. *m/z* 278.1307, found: *m/z* 278.1300.

3.6 References

(1) Wang, B.; Constantin, M. G.; Singh, S.; Zhou, Y.; Davis, R. L.; West, F. G. *Org. Biomol. Chem.* **2021**, *19* (2), 399–405.

(2) Christl, M.; Braun, M. *Chem. Ber.* **1989**, *122* (10), 1939–1946.

(3) Ruzziconi, R.; Naruse, Y.; Schlosser, M. *Tetrahedron* **1991**, *47* (26), 4603–4610.

(4) Lofstrand, V. A.; West, F. G. *Chem. Eur. J.* **2016**, *22* (31), 10763–10767.

(5) Nendel, M.; Tolbert, L. M.; Herring, L. E.; Islam, M. N.; Houk, K. N. *J. Org. Chem.* **1999**, *64* (3), 976–983.

(6) Zhou, S. Generation and Trapping of Highly Strained Reactive Intermediate: Ethyl 1,2-Cyclohexadienecarboxylate, University of Alberta, Edmonton, AB, 2015.

(7) Barber, J. S.; Yamano, M. M.; Ramirez, M.; Darzi, E. R.; Knapp, R. R.; Liu, F.; Houk, K. N.; Garg, N. K. *Nat. Chem.* **2018**, *10* (9), 953–960.

(8) Stork, G.; Brizzolara, A.; Landesman, H.; Szmuszkovicz, J.; Terrell, R. *J. Am. Chem. Soc.* **1963**, *85* (2), 207–222.

(9) Fos, E.; Borràs, L.; Gasull, M.; Mauleón, D.; Carganico, G. *J. Heterocycl. Chem.* **1992**, *29*, 203–208.

(10) Lin, H. S.; Rampersaud, A. A.; Zimmerman, K.; Steinberg, M. I.; Boyd, D. B. *J. Med. Chem.* **1992**, *35* (14), 2658–2667.

(11) Jia, Z.; Gálvez, E.; Sebastián, R. M.; Pleixats, R.; Álvarez-Larena, Á.; Martin, E.; Vallribera, A.; Shafir, A. *Angew. Chem. Int. Ed.* **2014**, *53* (42), 11298–11301.

(12) Bottini, A. T.; Hilton, L. L.; Plott, J. *Tetrahedron* **1975**, *31* (17), 1997–2001.

(13) Desimoni, G.; Faita, G.; Quadrelli, P. *Chem. Rev.* **2018**, *118* (4), 2080–2248.

(14) Pałasz, A. *Top. Curr. Chem.* **2016**, *374* (3), 30–60.

(15) Tsuge, O.; Hatta, T.; Yoshitomi, H.; Kurosaka, K.; Fujiwara, T.; Maeda, H.; Kakehi, A. *Heterocycles* **1995**, *41* (2), 225–228.

(16) Periasamy, M.; Devasagayaraj, A.; Satyanarayana, N.; Narayana, C. *Synth. Commun.* **1989**, *19* (3–4), 565–573.

(17) DFT Calculations were performed using Gaussian09.e01. DFT Calculations were performed using Gaussian09.e01. M. J.Frisch, G. W.Trucks, H. B.Schlegel, G. E.Scuseria, M. A.Robb, J. R.Cheeseman, G.Scalmani, V.Barone, G. A.Petersson, H.Nakatsuji, X.Li, M.Caric, 2016. No Title.

(18) Zhao, Y.; Truhlar, D. G. *Theor. Chem. Acc.* **2008**, *120* (1–3), 215–241.

(19) Scalmani, G.; Frisch, M. J. *J. Chem. Phys.* **2010**, *132* (11).

(20) May, G. L.; Pinhey, J. T. *Aust. J. Chem.* **1982**, *35* (9), 1859–1871.

(21) Carlson, R.; Nilsson, Å. *Acta Chem. Scand. B* **1984**, *38*, 49–53.

(22) Carlson, R.; Nilsson, Å.; Strömqvist, M. *Acta Chem. Scand. B* **1983**, *37*, 7–13.

(23) Liu, Y. P.; Wang, S. R.; Chen, T. T.; Yu, C. C.; Wang, A. E.; Huang, P. Q. *Adv. Synth. Catal.* **2019**, *361* (5), 971–975.

4. Generation and trapping of C-acylimine reactive intermediates using Mn(III) acetate

4.1 Previous work on C-acylimine reactive intermediates

Investigation of intramolecular metallocarbene/azide coupling reactions represents one of the research interests in our group. West and coworkers showed that carefully designed azide-diazocarbonyls **1** in the presence of a copper catalyst could generate reactive C-acylimines **2**, which can be captured with appropriate nucleophilic trapping reagents **3a-d** to yield 3-indolinone products **4** (*Scheme 4.1*).[1] Later, Atienza et al. synthesized a library of 2-indolylindolin-3-ones **4a**, which showed antiviral activity against respiratory syncytial virus and Zika virus.[2]

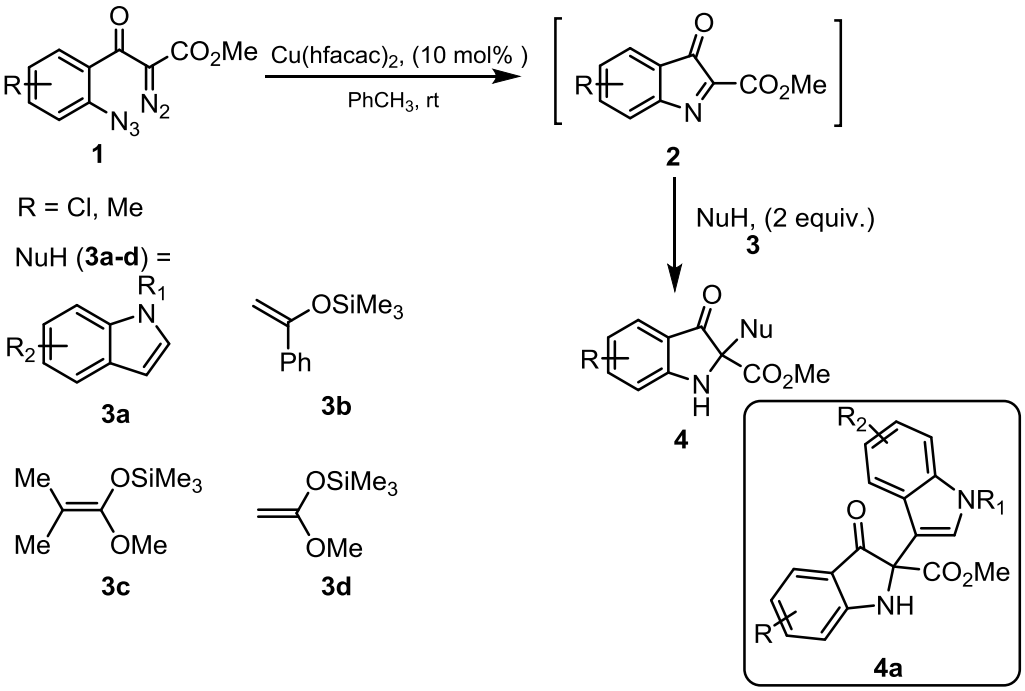

Scheme 4.1 Generation and trapping of C-acylimines

4.2 Envisioned method

When working with organic azides, diazocarbonyl compounds, or organic compounds with high nitrogen content in general, one should always have concerns regarding the safe handling of such compounds considering their possible explosive hazards. An empirical rule is that if the ratio of the combined number of carbon and oxygen atoms divided by the number of nitrogen atoms ([C+O]/N) in a compound is less than 3, explosive decomposition of the substance becomes a distinct possibility.[3] Although some of the starting materials **1**, previously tested in our group, have a ratio lower than 3, no explosive incidents have been encountered during their study by former group members (Figure 4.1) However, being aware of the possible hazards, they always used a reaction scale under 1 g in their experiments.[1] We then thought that a potentially safer starting material would be azide β-keto ester **5**, which poses lower hazard than **1** due to its reduced nitrogen content. Moreover, **5** is more readily accessible, and indeed, serves as a precursor to **1**. However, new methodology would need to be developed in order to activate the methylene group for intramolecular coupling with the neighboring azide moiety.

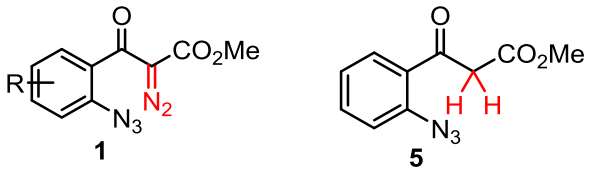

Figure 4.1 Alternative starting material with lower nitrogen content

We envisioned using $Mn(OAc)_3$ as a single electron oxidant in reaction with **5** to generate reactive intermediate **9** eventually (*Scheme 4.2*). We assumed that starting material **5** would transform into radical intermediate **6** through a single electron transfer, and that the resulting radical would cyclize onto the ortho azido group, with preferential attack on the proximal nitrogen atom to form nitrogen-centered radical intermediate **7**. Then intermediate **7** would release a N_2 molecule to generate radical intermediate **8**, which could undergo another single electron oxidation to generate C-acylimine reactive intermediate **9**. On the other hand, radical intermediate **8** could undergo a hydrogen atom shift to generate radical intermediate **10**, which through single electron oxidation could

form initially cation intermediate **11**. Then **11** could be deprotonated to form the desired C-acylimine reactive intermediate **9**, which could be captured by a suitable nucleophilic trapping reagent to generate product **12**.

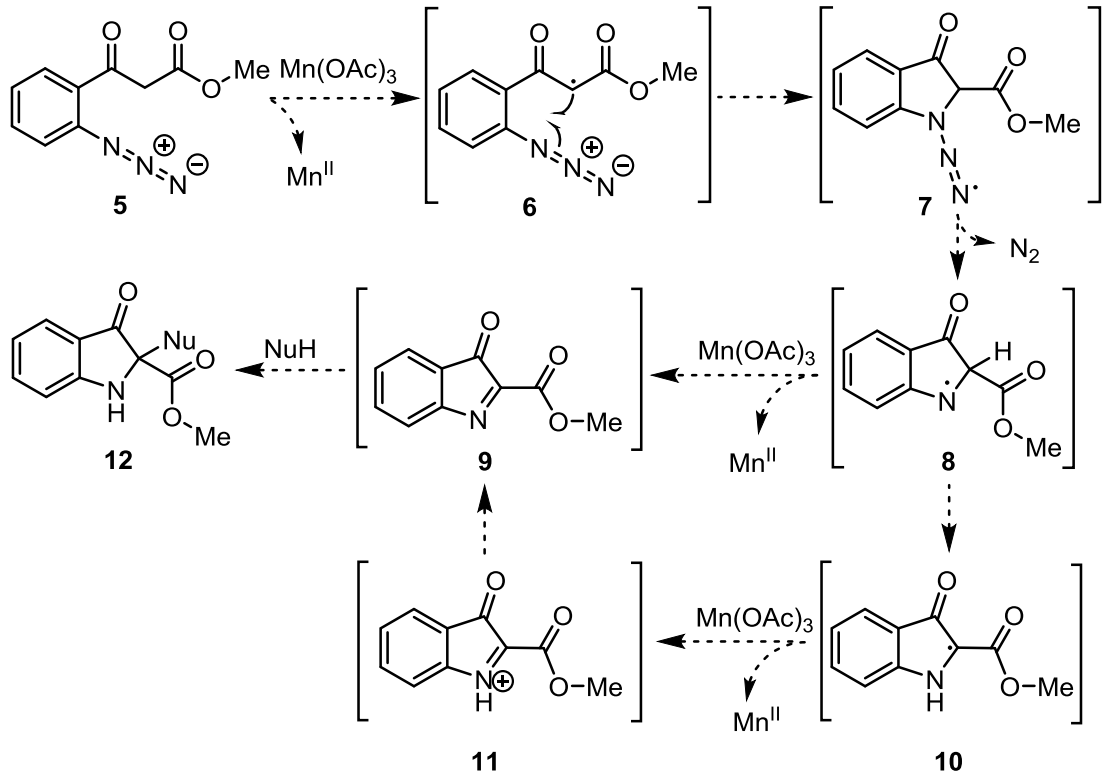

Scheme 4.2 Proposal for generation of C-acylimine **9** using $Mn(OAc)_3$

4.3 Mn(III) acetate in organic synthesis

The first examples of the oxidative radical cyclization reaction with $Mn(OAc)_3$ were done with the oxidative radical addition of acetic acid **12** to olefins **14** *(Scheme 4.3)*. The reaction starts with the single electron oxidation of acetic acid **12** in the presence of $Mn(OAc)_3$ at reflux generating radical intermediate **13**, which can easily add to olefins **14** to form radical intermediates **15**. Then a second equivalent of $Mn(OAc)_3$ will facilitate another single electron oxidation of radical intermediate**15** in order to eventually obtain γ-lactones **16**.[4–6]

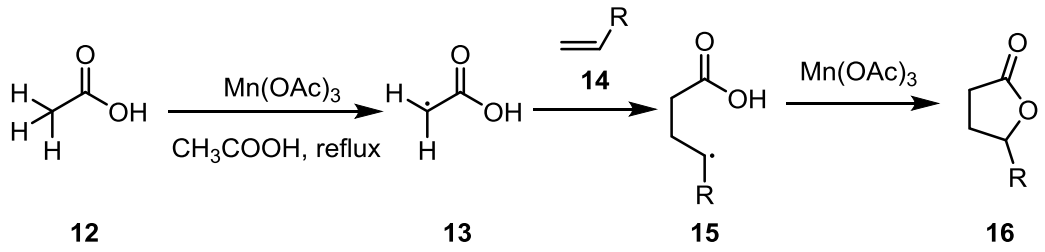

Scheme 4.3 The oxidative radical addition of **12** to olefins **14**

Regarding the structural features of $Mn(OAc)_3 \bullet H_2O$, it was found that it is an oxo-centered trimer of Mn(III) with bridging acetates **17** (*Scheme 4.4*).[7] The slow step in this proposed mechanism is the deprotonation of one of the complexed acetates giving access to intermediate **18**, which can undergo a fast single electron transfer forming radical intermediate **19**. Then radical **19** can easily undergo addition to the double bond of the olefins **14** to obtain radical intermediates **20**.[6] In the case of α-alkyl β-ketoesters **17a** it was found to behave similarly, the rate determining step being the slow enolization process. That was proposed to be followed by a fast SET to generate radical **19a**, which undergoes fast addition to olefin **14** to provide radical **20a**. In contrast, a fast and reversible enolization occurred for unsubstituted β-ketoesters **17b**. The rate determining step is the addition to olefin since the reaction rate depends on the concentration of olefin **14**. The reason for the slow enolization in the case of **17a** is the methyl substituent, which, through the electron donating effect, lowers the proton's acidity. The methyl group is also stabilizing radical **19a**, thus favouring its fast formation.[8]

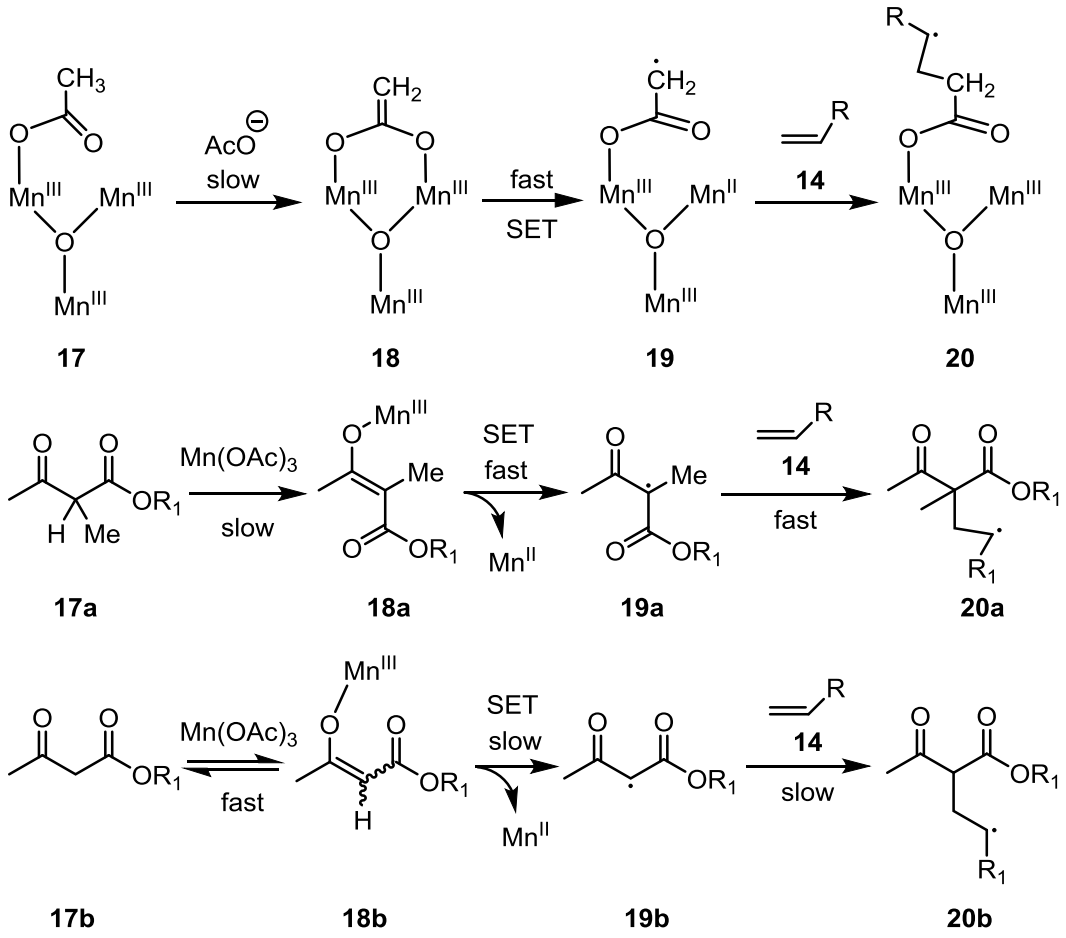

Scheme 4.4 Proposed mechanism of the oxidative radical addition of acetic acid and acetoacetate to olefins

Wang and coworkers have recently shown a pyrrole synthesis involving the use of $Mn(OAc)_3$ as a catalyst. They were able to use several substituted vinyl azides **21** in reaction with 1,3-dicarbonyl compounds **22** as β-keto esters or 1,3-diketones in the presence of a $Mn(OAc)_3$ catalyst. Using this method, they managed to obtain over 30 trisubstituted pyrroles **23** in good to excellent yields as presented in *Scheme 4.5*.[9]

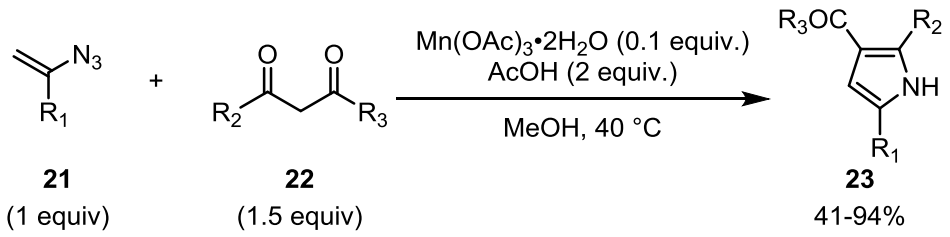

Scheme 4.5 Pyrrole synthesis using $Mn(OAc)_3$

4.4 Oxidative cyclization reactions using Mn(III) acetate

Using a carefully designed unsaturated β-keto ester **24,** Snider and coworkers could access tricyclic product **25** (*Scheme 4.6*). The reaction involves an oxidative radical cyclization which starts with single electron oxidation of the starting material **24** in the presence of $Mn(OAc)_3$, followed by the cascade of cyclization events and then a second equivalent of $Mn(OAc)_3$ will oxidize a late radical intermediate into carbocation.[10] Product **25** formed in this reaction is also a late intermediate in podocarpic acid **26** synthesis performed earlier by Welch and coworkers[11], which is a diterpene resin acid natural product.[12]

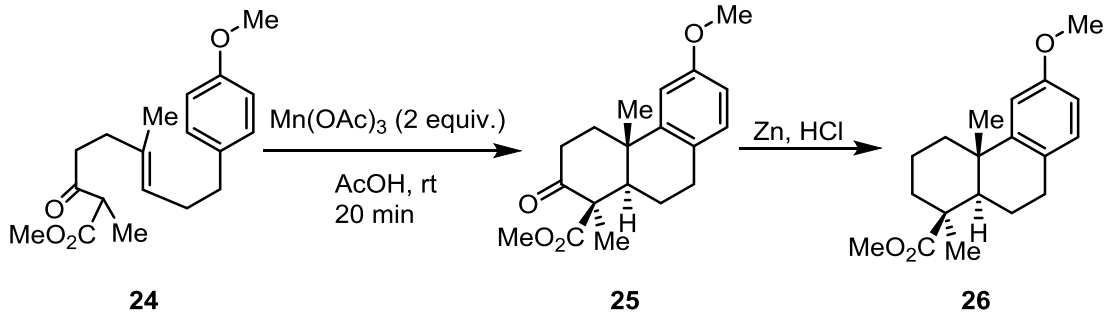

Scheme 4.6 Oxidative radical cyclization with $Mn(OAc)_3$

In another work, Snider and coworkers showed an azide interrupted oxidative cyclization.[13] In this work, an unsaturated β-keto ester **27** was used as a starting material, which in the presence of $Mn(OAc)_3$ and sodium azide underwent an oxidative radical cyclization event then was trapped with the azide to form the mixture of diastereomeric products **28a** and **28b** as shown in *Scheme 4.7*.

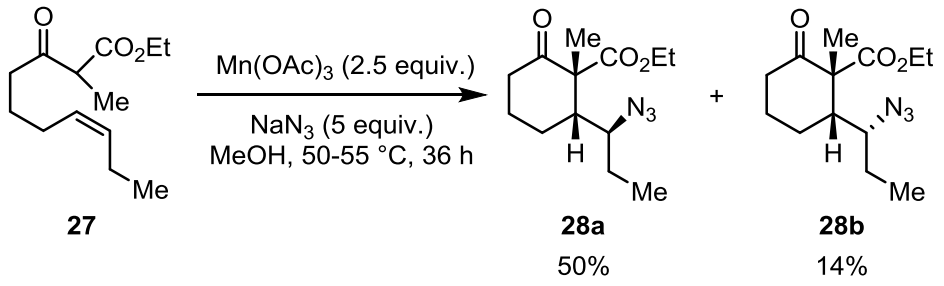

Scheme 4.7 Azide interrupted oxidative cyclization with $Mn(OAc)_3$

To sum up, β-ketoesters can engage in enolization and SET oxidation processes with $Mn(OAc)_3$ generating radical species. The literature shows a range of cyclization reactions with $Mn(OAc)_3$, including a pyrrole synthesis in which the azide starting material is losing an N_2 molecule. Based on our proposal and our literature research regarding the chemistry of $Mn(OAc)_3$, we were confident in moving forward and testing this reaction.

4.5 Results and discussion

4.5.1 Synthesis of starting materials

The desired substrate to test our proposal, *o*-azido-β-ketoester **5**, could be synthesized in two steps from anthanilic acid **29** (*Scheme 4.8*). First, the aniline moiety was converted to the corresponding azide **30** via a diazonium salt intermediate. Then a titanium(IV)-mediated crossed-Claisen condensation under the conditions of Tanabe,[14] was used to convert **30** to the necessary substrate **5**. The protocol of the starting material synthesis was initially used in the work of the previous group members who had a research interest in this area.[1,2]

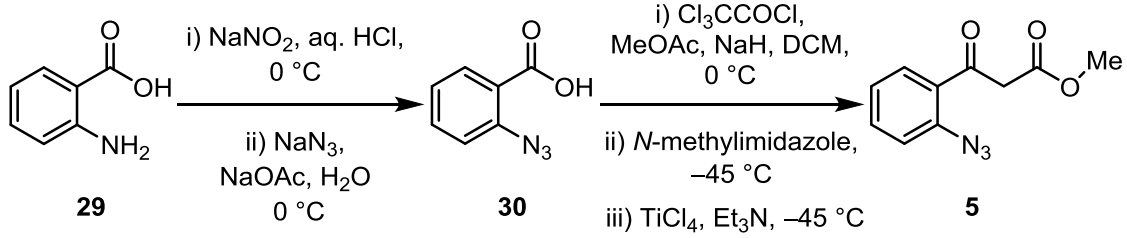

Scheme 4.8 Synthesis of substrate **5**

4.5.2 Reaction of *o*-azido-β-ketoester 5 with $Mn(OAc)_3$

In order to find the conditions for the generation of C-acylamine reactive intermediate from **5** in the presence of $Mn(OAc)_3$, various solvents and reaction temperatures were screened (*Table 4.1*). Based on our earlier proposal and literature

precedent of oxidative radical cyclizations, we decided to perform initial test reactions with two equivalents of $Mn(OAc)_3$.[6] As a general observation, no conversion of the starting material was observed in the different solvents tested at room temperature, which could be attributed to the low solubility of the $Mn(OAc)_3$ reagent in organic solvents. When the test reactions were performed in various solvents at elevated temperatures, conversion of the starting material into complex mixtures was observed. When the reaction was done in acetic acid at 70 ºC, we were able to isolate compound **31** (*Entry 11, Table 4.1*). No plausible rationale for the formation of **31** could be proposed. For the reaction in methanol at reflux in the presence of air, the formation of products **32a** and **32b** was observed, which seems to be the result of oxidative degradation at the ketoester methylene site (*Entry 16*). The reaction performed in acetonitrile at reflux provided unexpected product **33** (*Entry 18*). The formation of this product will be explained in the next section.

Table 4.1 Reaction optimization

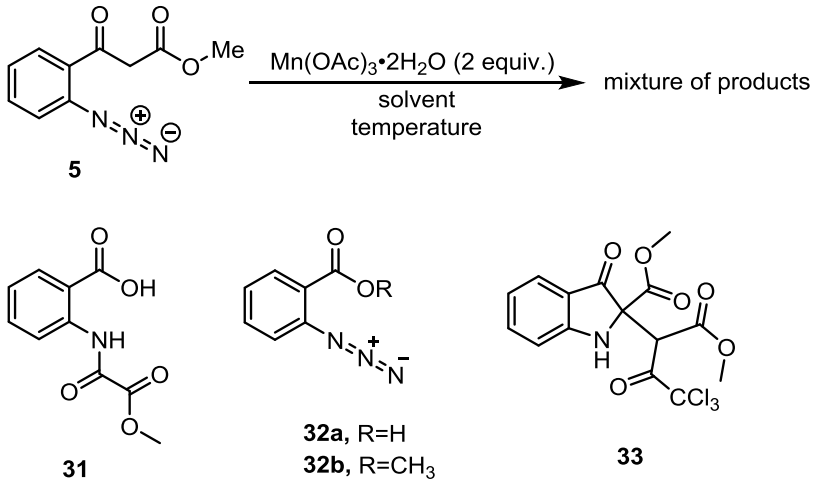

Entry	Solvent	T, °C	Result
1	DCM	r.t.	no conversion of s.m.
2		reflux	
3	DMF	r.t.	no conversion of s.m.
4		reflux	complex mixture
5	pyridine	r.t.	no conversion of s.m.
6		reflux	no conversion of s.m.
7	1,4-dioxane	r.t.	no conversion of s.m.
8		reflux	no conversion of s.m.
9	acetic acid	r.t.	no conversion of s.m.
10		reflux	complex mixture

11		70 °C	complex mixture[a]
12	ethanol	r.t.	no conversion of s.m.
13		reflux	complex mixture
14	methanol	r.t.	no conversion of s.m.
15		reflux	complex mixture
16	methanol [b]	reflux	complex mixture[c]
17	CH_3CN	r.t.	no conversion of s.m.
18		reflux	complex mixture[d]

a) compound **31** was isolated in 17%; b) in the presence of air; c) compound **32a** (7%) and **32b** (12%) were isolated; d) compound **33** was isolated 5%;

4.5.3 Serendipitous formation of compound 33

During the reaction optimization, we observed the unexpected formation of product **33**, which structurally resembles our proposed trapping products. Clearly, in order to obtain **33**, a suitable trapping partner would be required, which we proposed to be β-keto ester **34** (*Scheme 4.9*). During a careful examination of starting material **5** used in this reaction, we found that it was contaminated with β-keto ester **34**. The presence of compound **34** in the starting material could be explained as a side-product in the synthesis of starting material **5** from 2-azido-benzoic acid **30** through the Tanabe cross-Claisen condensation. Later, we performed the synthesis of known trichloroacetylacetate **34**[15] from trichloroacetyl chloride **35** and methyl acetate **36,** employing the adapted conditions of the previously used condensation reaction.

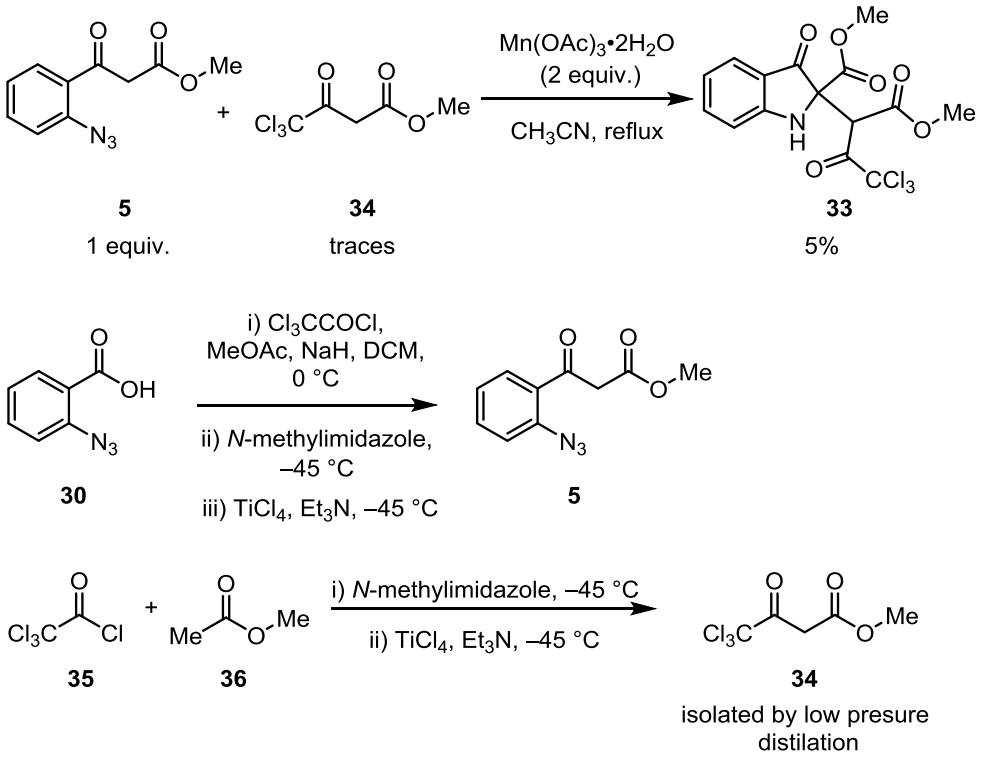

Scheme 4.9 Serendipitous formation of **33**

4.5.4 Trapping product

Once we better understood what was happening in the reaction and carried out a cursory optimization effort, we were able to obtain and isolate the compound as a single diastereomer **33** in 45% yield when we used one equivalent of each β-keto esters **5** and **34** as starting materials with two equivalents of $Mn(OAc)_3$ in acetonitrile at reflux. The structural assignment with the relative stereochemistry for **33** was determined employing X-ray crystallography analysis. To be noted, we were not able to isolate or detect the other diastereomer when we analyzed our crude mixture.

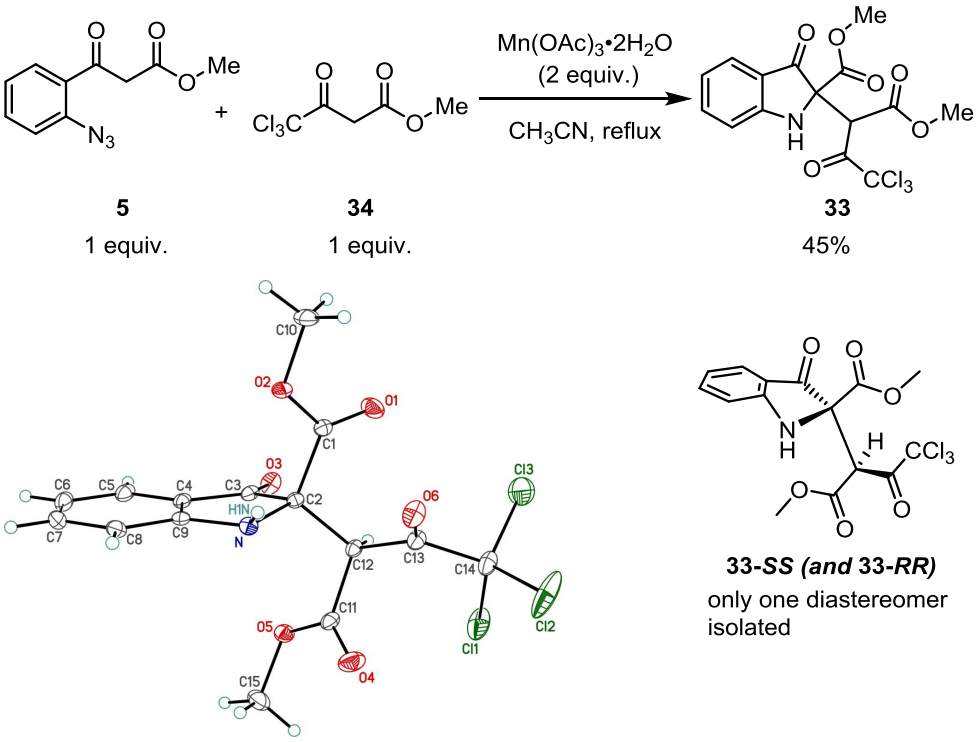

Scheme 4.10 Synthesis of product **33**

Then we moved our attention towards the possible reaction scope development by examining a series of different trapping partners **35-38** in the reaction under development. All the trapping attempts eventually proved unsuccessful, although some of the alternative trapping partners were structurally similar with **34**, which was the only trapping partner that provided the desired adduct. Considering these results, we wondered about the validity of the initial reaction pathway we proposed earlier in this chapter (see section 4.2).

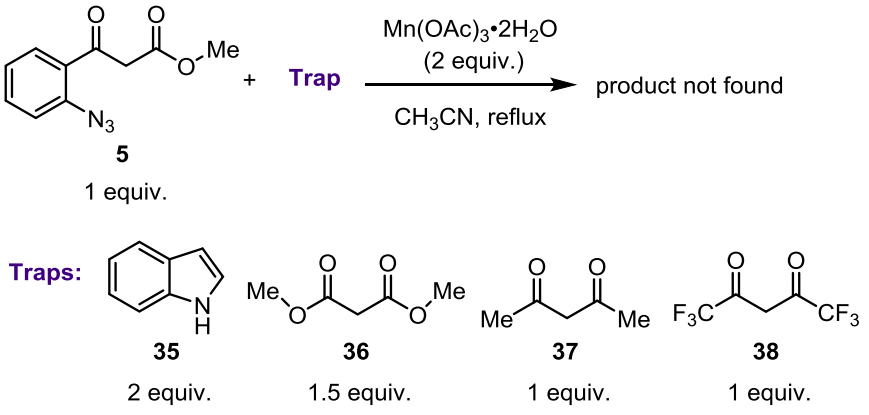

Scheme 4.11 Attempted trapping experiments

4.5.5 Possible reaction mechanism pathways towards the formation of product 33

In this section, five possible mechanistic pathways will be presented, and an explanation for the formation of only one of the two possible diastereomers (as a pair of enantiomers) will be proposed

In the first possible mechanistic pathway we will turn our attention on the step in which the two parts of the product molecule get connected. At the beginning of this project, our intention was to find a new way to generate C-acylimine reactive intermediates such as **9** (*Scheme 4.2*). In the first two pathways, it was proposed that C-acylimine **9** was generated following our initial proposal and that it would either combine with enol **34a** or with radical **34b** to form the product **33** (*Scheme 4.12*). It was assumed that the trapping reagent could be present in the reaction mixture either as an enol **34a** or a radical **34b**, which in turn could be generated by the $Mn(OAc)_3$ reagent. Since we observed no desired product with the other trapping partners tested, which were known to capture C-acylimine reactive intermediates from previous work in our group, there are doubts related to the actual generation of **9** using this new method. Then, we thought that another reactive intermediate could be involved, such as radical **10** or iminium **11**, which were actually intermediates in our initial proposal for the generation of C-acylimine **9** (*Scheme 4.2*). In the next two scenarios, radical **10** reacts with either enol **34a** or with radical **34b** towards the generation of product **33.** In the last pathway, enol **34a** nucleophilically attacks iminium salt **11** to obtain product **33**.

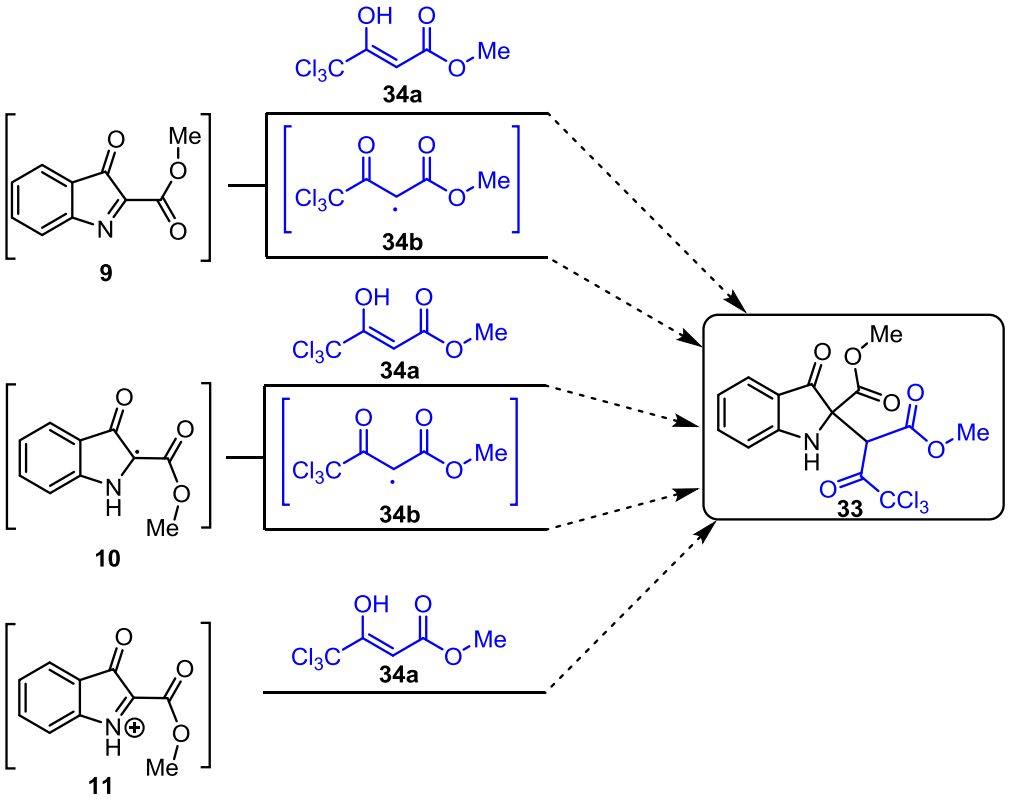

Scheme 4.12 Alternative reaction mechanism pathways towards the formation of **33**

Considering the unclear mechanism pathway for this reaction, explaining the stereochemical outcome is a challenging task. Based on our NMR spectroscopic and X-ray crystallographic analyses, we found that the reaction is diastereoselective since we obtained only one of the two possible sets of diastereomers (*Figure 4.2*).

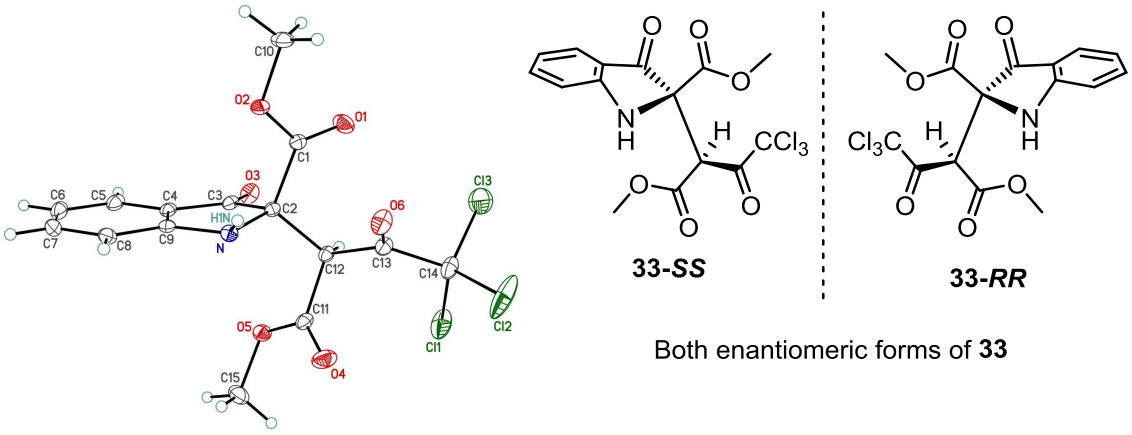

Figure 4.2 Stereochemistry of product **33**

In order to explain the stereochemical outcome, the Newman projections of the observed diastereomer **33-*SS*** (it could be replaced by **33-*RR***) and unobserved diastereomer **33-*SR*** (it could be replaced by **33-*RS***) were generated and analyzed (*Figure 4.3*). For both diastereomers, it was assumed that probably the most stable conformer would be the staggered conformer with the hydrogen over the indolinone part of the molecule. From the two Newman projections alone, it could be hard to tell the formation of which diastereomer would be favoured on thermodynamic grounds. It should also be noted that in these conformations there could be a potentially stabilizing interaction through hydrogen bonding in between the NH group and either the oxygen of an ester in the case of **33-*SS*** and the oxygen of the carbonyl group in the case of **33-*SR***. From the literature studies, it seems that, in general, esters give slightly stronger hydrogen bonding than ketones which would favour the formation of **33-*SS*** (or **33-*RR***) over **33-*SR*** (or **33-*RS***).[16] Another literature study shows that chloroacetone is a lesser hydrogen bond acceptor than acetone due to the presence of chlorine in the molecule, which increases the steric hindrance and has a significant electronic effect reducing the basicity of the carbonyl and thus its capacity to accept a hydrogen bond.[17] Based on these literature studies we proposed that potential hydrogen bond in between the carbonyl and NH (**33-*SR***) should be significantly weaker than the possible hydrogen bond in between the ester and NH (**33-*SS***); thus **33-*SS*** should be more stable than **33-*SR*** and easier to form respectively.

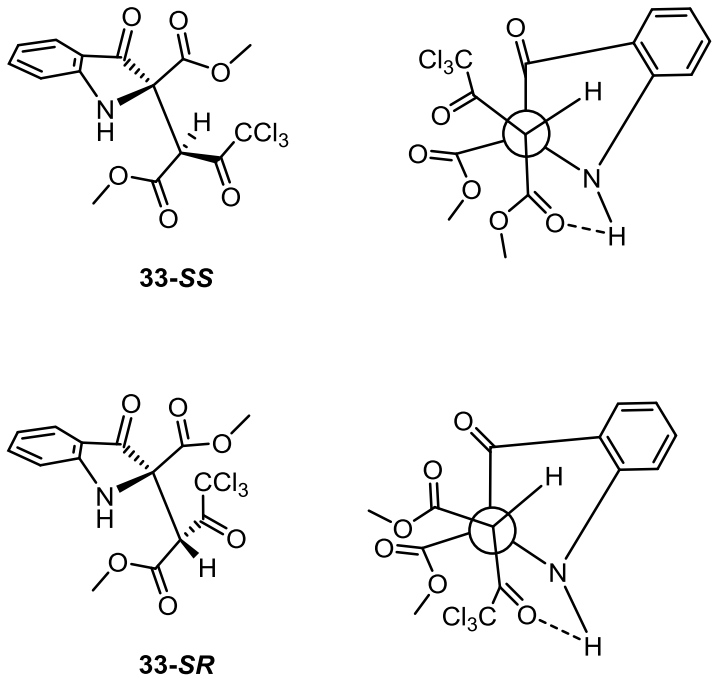

Figure 4.3 Newman projections for diastereomers **33-*SS*** and **33-*SR***

Considering the reaction conditions and unknown mechanism one should expect to obtain both diastereomers (**33-*SS***, **33-*SR***) in this reaction, but in our experiments we only observed diastereoselectivity towards **33-*SS*** (*Scheme 4.13*). Until a clearer picture of the reaction mechanism is developed, it would be hard to explain the origin of the diastereoselectivity. However, one can imagine different scenarios for the observed diastereoselectivity, such as the initial formation of a mixture of diastereomers, followed by a subsequent epimerization to the energetically favourable SS/RR diastereomer exclusively. Assuming that initially in the reaction all four diastereomers were formed and considering the reaction conditions, one could propose that an epimerization takes place at the chiral center that has a hydrogen atom between two C=O groups.

Thus, the unobserved diastereomer **33-*SR*** could potentially tautomerize into enol **39**, which upon subsequent tautomerization could convert into diastereomer **33-*SS***. If this is the origin of diastereoselectivity, then **33-*SS*** should be thermodynamically favoured over **33-*SR***. Further computational studies should be pursued in order to test this proposal.

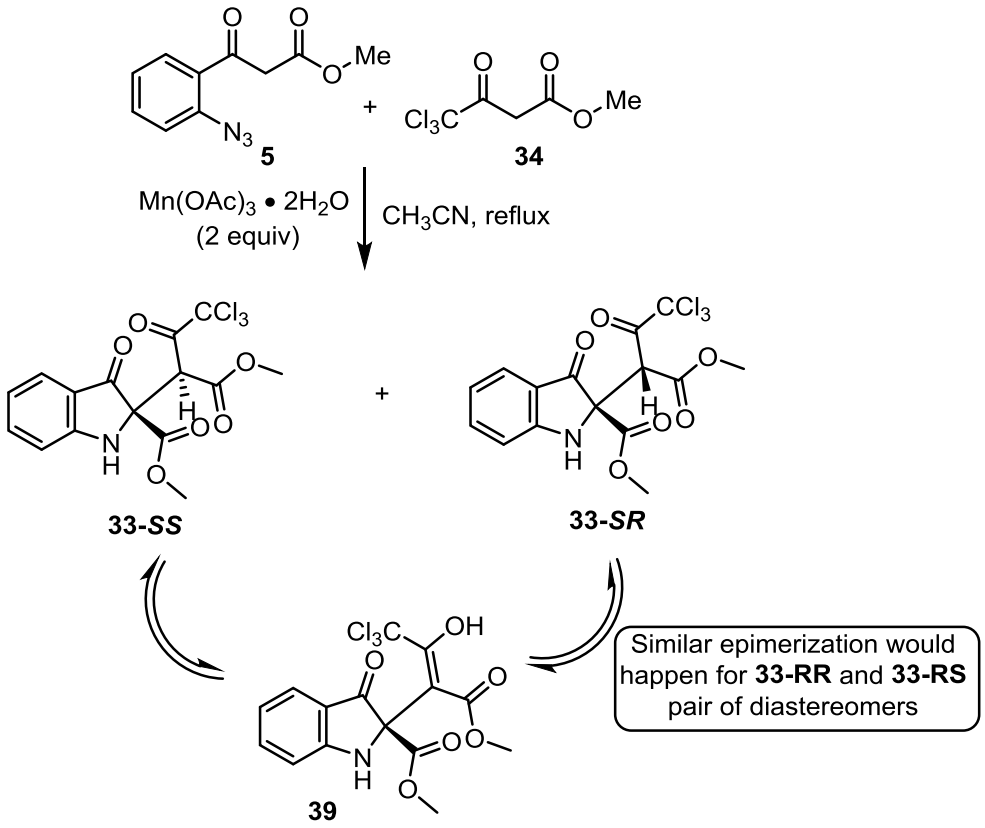

Scheme 4.13 The proposed epimerization pathway

4.6 Conclusions

In this chapter, the results related to the development of a new method to generate C-acylimine **9** were presented. Although limited to a single product, adduct **33** could be obtained in 45% yield, and was fully characterized (including relative configuration by X-ray crystallography). Our inability to generate comparable adducts with other similar traps known to intercept C-acylimines such as **9** raise questions as to whether it is in fact an intermediate in the formation of **33**. Several alternative scenarios were proposed and briefly discussed.

Although described in Chapter 4, this work was carried out early in my doctoral studies. Our inability to generalize the trapping reaction beyond the initial observation with methyl trichloroacetoacetate raised serious concerns in our minds about the viability of this chemistry as the basis for a PhD thesis. These doubts coincided with an opportunity to join a different project focusing on the generation and trapping of strained cyclic allenes, and we opted to wrap up this work for the time being. Nonetheless, there are clear opportunities to further study these interesting results, especially in understanding the mechanism by which adduct **33** is formed. That knowledge could inform future efforts to broaden the scope of this potentially valuable transformation. Some suggested areas for exploration are discussed in Chapter 5.

4.8 Experimental

Substrate **5**, which was used in all efforts to carry out $Mn(OAc)_3$-mediated coupling reactions, was prepared via the previously described route.[1,2] The product was obtained in comparable yield, and all spectral data were in agreement with those previously reported.

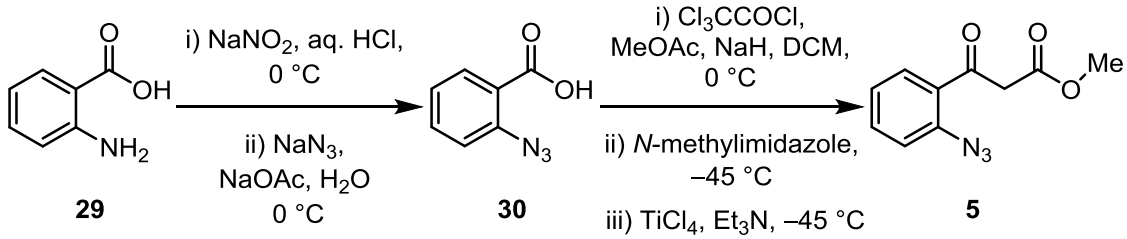

Scheme 4.14 Synthesis of starting material **5**

Procedure for synthesis of 33

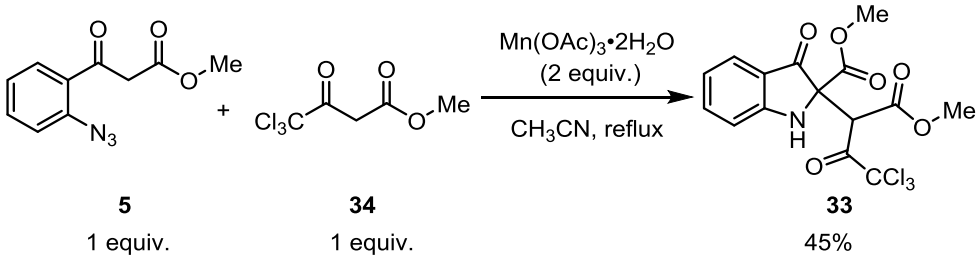

Scheme 4.15 Synthesis of product **33**

A mixture of 110 mg (0.5 mmol) starting material **5**, 111 mg (0.5 mmol) of trapping agent **34** and 268 mg (1 mmol) of $Mn(OAc)_3•2H_2O$ in 20 mL of acetonitrile under nitrogen was brought to reflux in an oil bath and stirred for 2 hours. The reaction mixture was left to cool to room temperature, and then 10 mL of water was added to the reaction mixture. The aqueous layer was separated and extracted with EtOAc (5 x 15 mL). Then the combined organic extracts were dried over $MgSO_4$, filtered, and concentrated under reduced pressure. The crude was purified by a normal phase flash column chromatography using 10-20% EtOAc in hexanes to isolate 93 mg of product **33** as a yellow powder in 45% yield. Product **33** forms yellow crystals suitable for X-Ray analysis from DCM under slow evaporation at room temperature.

methyl *rel*-(*S*)-3-oxo-2-((*S*)-4,4,4-trichloro-1-methoxy-1,3-dioxobutan-2-yl)indoline-2-carboxylate (**33**)

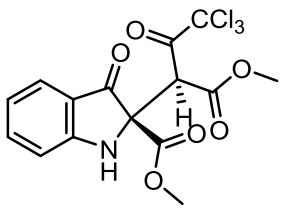

33

IR (cast film) cm^{-1} 3372, 3008, 2956, 2917, 2849, 1742, 1618, 1486, 1469, 1436, 1324, 1293, 1244, 1200, 1086, 1044; ^1H NMR (700 MHz, $CDCl_3$) δ 7.67 (m, 1H), 7.53 (ddd, *J* = 8.4, 7.1, 1.4 Hz, 1H), 7.03 (dt, *J* = 8.2, 0.8 Hz, 1H), 6.96 (ddd, *J* = 7.8, 7.1, 0.8 Hz, 1H), 5.62 (s, 1H), 5.52 (s, 1H), 3.71 (s, 3H), 3.50 (s, 3H); ^{13}C NMR (126 MHz, $CDCl_3$) δ 191.8, 188.6, 166.1, 164.8, 161.9, 138.1, 125.5, 121.0, 119.6, 113.4, 94.1, 73.7, 57.9, 54.0, 53.1; HRMS (ESI, $[M+Na]^+$) for $C_{15}H_{12}Cl_3NNaO_6$ calcd. *m/z* 429.9622, found: *m/z* 429.9621.

4.9 References

(1) Bott, T. M.; Atienza, B. J.; West, F. G. *RSC Adv.* **2014**, *4* (60), 31955–31959.

(2) Atienza, B. J. P.; Jensen, L. D.; Noton, S. L.; Ansalem, A. K. V.; Hobman, T.; Fearns, R.; Marchant, D. J.; West, F. G. *J. Org. Chem.* **2018**, *83* (13), 6829–6842.

(3) Keicher, T.; Löobbecke, S. Lab-Scale Synthesis of Azido Compounds: Safety Measures and Analysis. In *Organic Azides: Syntheses and Applications*; Bräse, S., Banert, K., Eds.; Wiley: Chichester, 2010; pp 3–27.

(4) Heiba, E. I.; Dessau, R. M.; Koehl, W. J. *J. Am. Chem. Soc.* **1968**, *90* (21), 5905–5906.

(5) Bush, J. B.; Finkbeiner, H. *J. Am. Chem. Soc.* **1968**, *90* (21), 5903–5905.

(6) Snider, B. B. *Chem. Rev.* **1996**, *96* (1), 339–364.

(7) Hessel, L. W.; Romers, C. *Recl. des Trav. Chim. des Pays-Bas* **1969**, *88* (5), 545–552.

(8) Snider, B. B.; Patricia, J. J.; Kates, S. A. *J. Org. Chem.* **1988**, *53* (10), 2137–2143.

(9) Wang, Y. F.; Ton, K. K.; Chiba, S.; Narasaka, K. *Org. Lett.* **2008**, *10* (21), 5019–5022.

(10) Snider, B. B.; Mohan, R.; Kates, S. A. *J. Org. Chem.* **1985**, *50* (19), 3659–3661.

(11) Welch, S. C.; Hagan, C. P.; Kim, J. H.; Chu, P. S. *J. Org. Chem.* **1977**, *42* (17), 2879–2887.

(12) Wenkert, E.; Afonso, A.; Bredenberg, J. B.; Kaneko, C.; Tahara, A. *J. Am. Chem. Soc.* **1964**, *86* (10), 2038–2043.

(13) Snider, B. B.; Duvall, J. R. *Org. Lett.* **2004**, *6* (8), 1265–1268.

(14) Misaki, T.; Nagase, R.; Matsumoto, K.; Tanabe, Y. *J. Am. Chem. Soc.* **2005**, *127*

(9), 2854–2855.

(15) Martins, M. A. P.; Pereira, C. M. P.; Zimmermann, N. E. K.; Moura, S.; Sinhorin, A. P.; Cunico, W.; Zanatta, N.; Bonacorso, H. G.; Flores, A. C. F. *Synthesis* **2003**, 2353–2357.

(16) Lommerse, J. P. M.; Price, S. L.; Taylor, R. *J. Comput. Chem.* **1997**, *18* (6), 757–774.

(17) Tan, N. Y.; Li, R.; Bräuer, P.; D'Agostino, C.; Gladden, L. F.; Zeitler, J. A. *Phys. Chem. Chem. Phys.* **2015**, *17* (8), 5999–6008.

5. Thesis conclusions and future plans

5.1 Thesis conclusions

In this chapter, a set of global conclusions and possible future research plans for the projects presented will be discussed. In Chapter 1, a short review of the literature in the research area of reactive intermediates in general and the chemistry of cyclic allenes, in particular, was done. The focus was on the research area of cyclic allenes, with some selected recent examples showcased. For a more comprehensive review of the literature, we recommend inspecting several book chapters and review papers in this area.[1–4] Although this research area started over half a century ago,[5,6] the chemistry of reactive cyclic allenes chemistry remains an area of ongoing research today with numerous potentially fruitful research directions. Some of these directions are directed towards the generation and trapping of functionalized cyclic allenes such as heterocyclic allenes, polarized allenes, and substituted cyclic allenes, potentially uncovering new trapping reactions and obtaining more complex products. Another area that should be investigated in more detail is the generation of chiral cyclic allenes. Finding applications in chemical biology or other areas should also be one of the future research directions in the chemistry of cyclic allenes.

In Chapter 2, the project results in which we developed a method to generate cyclic allenes through metal-halogen exchange promoted elimination were presented. In our view, finding new complementary ways to generate cyclic allenes represents an important ongoing research direction in the chemistry of cyclic allenes. These new methods can provide easier access to a more diverse range of cyclic allenes and potentially uncover new reactions involving these intermediates.

In Chapter 3, a project involving the generation of electron-deficient cyclic allenes was presented. A new dimerization pathway and a new trapping reaction of hetero-Diels–Alder nature specific for these electron-deficient cyclic allenes were discovered. Those results would not be possible in an unfunctionalized cyclic allene since aroyl substituent is an essential part of the molecule involved in those reactions. Although this research

direction is in its incipient phase with only a few papers published in the literature, some interesting findings are already known from our work and others. [7–9]

In Chapter 4, the results presented were from a project involving the generation of C-acylimine intermediates. We were interested in finding a method to generate C-acylimine intermediates using a precursor with a lower content of nitrogen having possible explosion hazards when working with such materials. We proposed using an oxidative cyclization approach with $Mn(OAc)_3$ and *o*-azito-β-ketoester precursor. In that project, a new single diastereomer product was isolated in 45% yield and characterized. All the efforts towards the development of a substrate scope however, were unsuccessful.

5.2 Future plans for the generation of cyclic allenes through metal-halogen exchange promoted elimination

As previously discussed in Chapter 2, we found a metal-halogen exchange promoted elimination method to generate cyclic allenes (*Scheme 5.1*). This is a complementary approach to the well-known ways to generate cyclic allenes, such as base elimination and fluoride-promoted elimination. There were two iterations of this reaction studied. First, we developed a lithium-bromine exchange promoted elimination method to generate reactive cyclic allenes. The facile access to starting material and the potential for substrate scope development made this method attractive. Using the lithium-bromine exchange promoted elimination, we were able to isolate 5 dimeric products in moderate to good yields. Our attempts to trap these cyclic allenes were unsuccessful, which represented the limitations of this new method. Although unclear, we believe that the highly reactive *t*-BuLi conditions used in this reaction are the reason for the unsuccessful trapping experiments. Considering our initial results with lithium-bromine exchange promoted elimination, we decided to move to a magnesium-iodine exchange promoted elimination in which the reaction conditions should be milder than in the one studied first. We observed that changing from organolithium to organomagnesium reagent allowed us to extend the reaction from dimerization (**4**) to some of the typical trapping reaction for 1,2-cyclohexadiene **3**, such as Diels–Alder cycloaddition with furan (**5**) and DPIBF (**6**) and formal [2+2] cycloaddition with styrene (**7**). Therefore we developed two versions of a metal-halogen exchange promoted elimination which is complementary to previously

known methods such as the base elimination, and fluoride-promoted elimination. Although the lithium-halogen exchange version is limited to dimer products, the magnesium-halogen exchange version can provide access to [4+2] and [2+2] typical cycloadducts in the trapping of cyclic allenes.

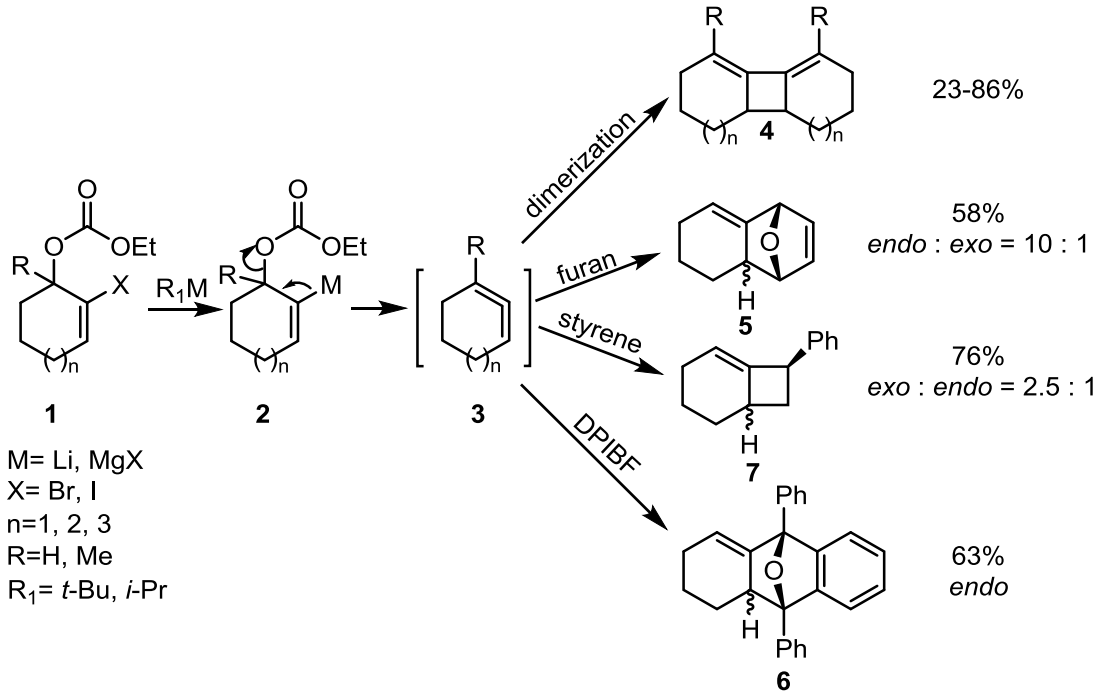

Scheme 5.1 The metal-halogen exchange promoted elimination generation and trapping of cyclic allenes

One can envision several directions for further research investigations related to this method. The first that comes to mind is to find milder conditions through the replacement of the metal. A zinc and palladium approach was attempted based on known literature precedent for acyclic allenes,[10] but it was unsuccessful for similar precursors of cyclic allenes. Further studies with other organometallic systems can be done.

The most immediate research investigation can be in the extension of the substrate scope through substituted cyclic allenes and the generation of chiral cyclic allenes by using an enantioenriched starting material. One way to access an enantioenriched starting material is to use enantioenriched allylic alcohol with the iodide already in place. In fact, the synthesis of such allylic alcohols is already known. Thus the literature procedures can be followed (*Scheme 5.2*). For example, the *R* enantiomer of the unsubstituted alcohol **10**

can be obtained through an enantioselective reduction of the corresponding ketone **8** as described in the literature.[11] Then, alcohol **10** should be transformed in carbonate **11** using the conditions described in Chapter 2. Synthesis of the (*S*) enantiomer **15** is also known,[12] and its carbonate could be obtained similarly as well. Through the enantioselective allylation of iodoketone **8** in the presence of *R*-Br_2Binol catalyst, one can get enantioenriched tertiary alcohol **12** as shown by Taber and Berry.[13] Then it should be possible to transform tertiary alcohol **12** to the corresponding carbonate **13** using the conditions described in Chapter 2. There is also literature precedent for the tertiary alcohol **16**,[14], which is the corresponding enantiomer of **13**.

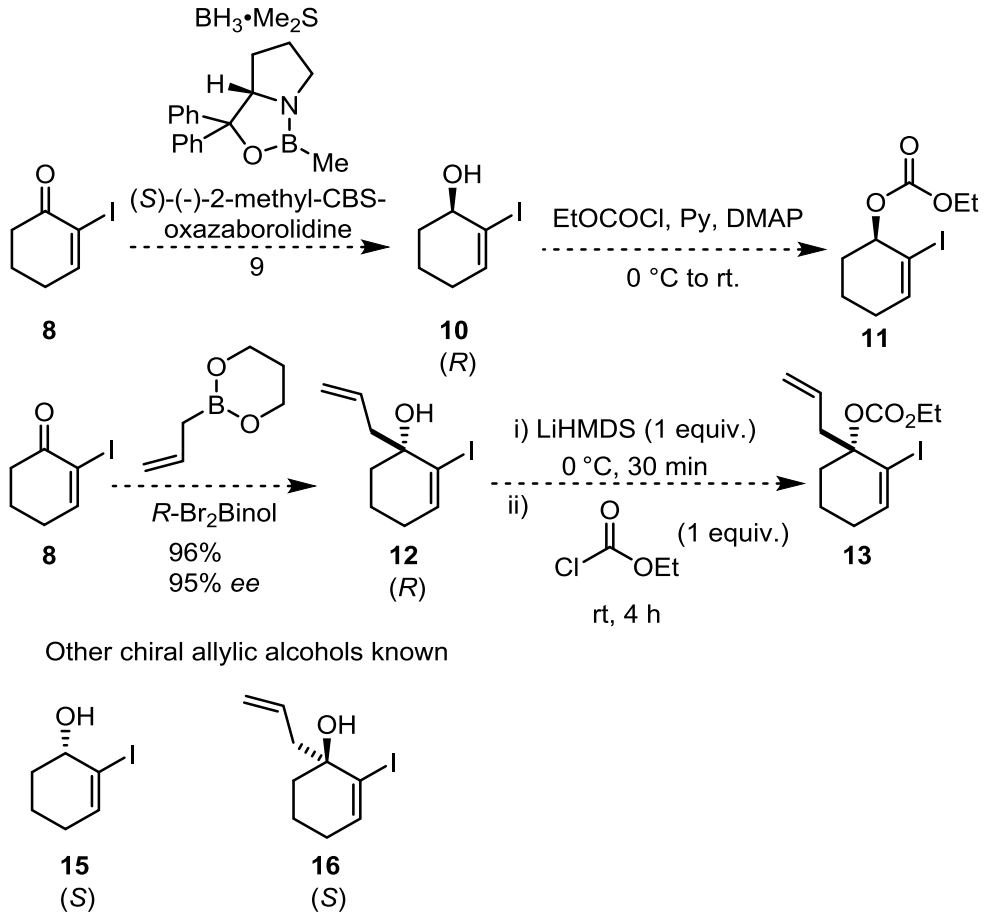

Scheme 5.2 Synthesis of enantiomerically enriched and substituted precursors **11** and **13**

With these precursors in hand, one can perform the reaction using the magnesium-iodide exchange to promote elimination and then analyze if the stereochemical information is preserved or lost during the reaction (*Scheme 5.3*). Using a standard trapping reagent

such as furan in reaction with 1,2-cyclohexadiene **3**, one would get enantioenriched cycloadducts **5a** and **5b** if the chirality would be transferred. Overall there is great potential to extend this chemistry by making enantioenriched starting materials with or without substitution.

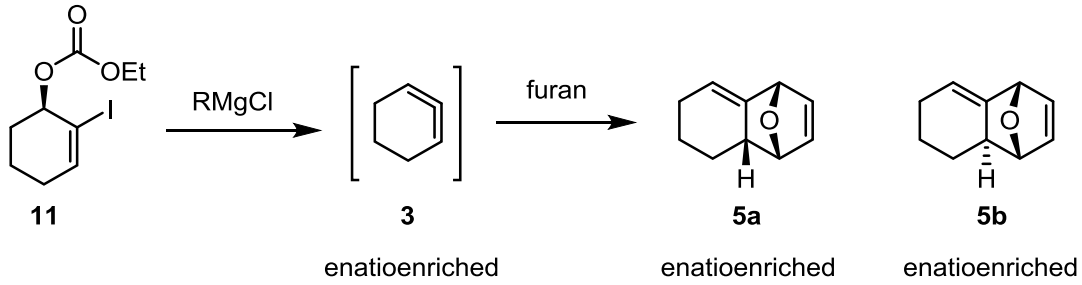

Scheme 5.3 The proposed generation and trapping of enantioenriched cyclic allenes

5.3 Future plans for electron-deficient cyclic allenes

In Chapter 3, work was presented related to the reactivity of electron-deficient cyclic allenes with the discovery of a new dimerization pathway and new trapping with enamines. High regioselectivity and diastereoselectivity was observed in the typical Diels–Alder cycloadditions with furan and DPIBF. To explain the dimerization process, we proposed a hetero-Diels–Alder pathway. Then inspired by this dimerization process, we developed a way of trapping cyclic allenes through an [4+2] inverse electron-demand hetero-Diels–Alder cycloaddition (*Scheme 5.4*) between enamine **18** and cyclic allene **19,** which gave us access to eight complex polycyclic products **20** in modest to good yields. To confirm with confidence the obtaining of such structurally complex compounds, we also used X-ray analysis. We proposed an asynchronous concerted inversed electron-demand Diels–Alder reaction mechanism for this new type of trapping of cyclic allenes, based on our experimental results and the computational calculations performed by our collaborators.

These reactions would not be possible on a typical unsubstituted cyclic allene, which which confirms the value of further studies involving new classes of electron-deficient cyclic allenes. More studies of polarized, substituted or heterocyclic allenes are required to unveil potentially unknown reactivity of these species. Getting access to complex products, as described in Chapter 3, is one of the ongoing research activities for

cyclic allenes since these compounds could potentially have a biological activity or other interesting properties.

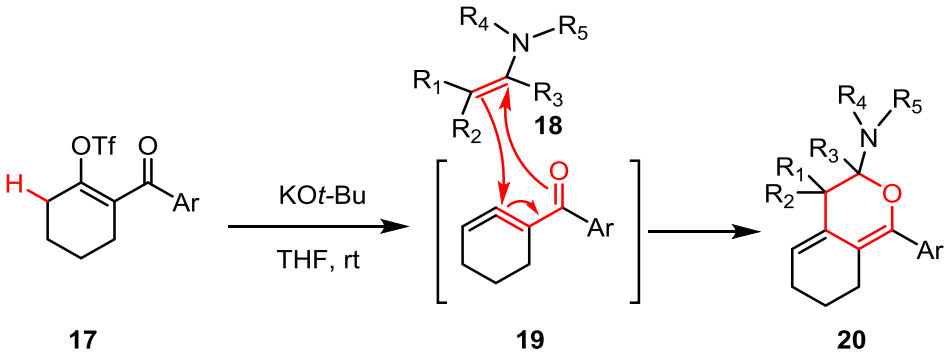

Scheme 5.4 Work presented in Chapter 3

To extend the substrate scope of this reaction described in Chapter 3, one can take several approaches. One obvious direction is expanding the scope of the transformation with other electron-rich dienophiles beyond the enamine used already. For example, some test reactions could be made with electron-rich acetylenes **21,** such as ethoxy acetylene, whose reaction with cyclic allene **19** would afford cycloadduct **22** if this dienophile follows similar reactivity patterns as enamines. A second approach would be to vary the nature of the carbonyl EWG from the aryl ketones examined so far, shown generically for substrate **23**, with alkyl ketone or ester functionality, which in the presence of base should generate cyclic allene **24**. Then this transient species would further react with the enamine **18** to give cycloadduct **25**. There are several ketone and ester examples of triflate **23** reported in the literature.[15] These two approaches have the potential to increase the scope of this hetero-Diels–Alder reaction.

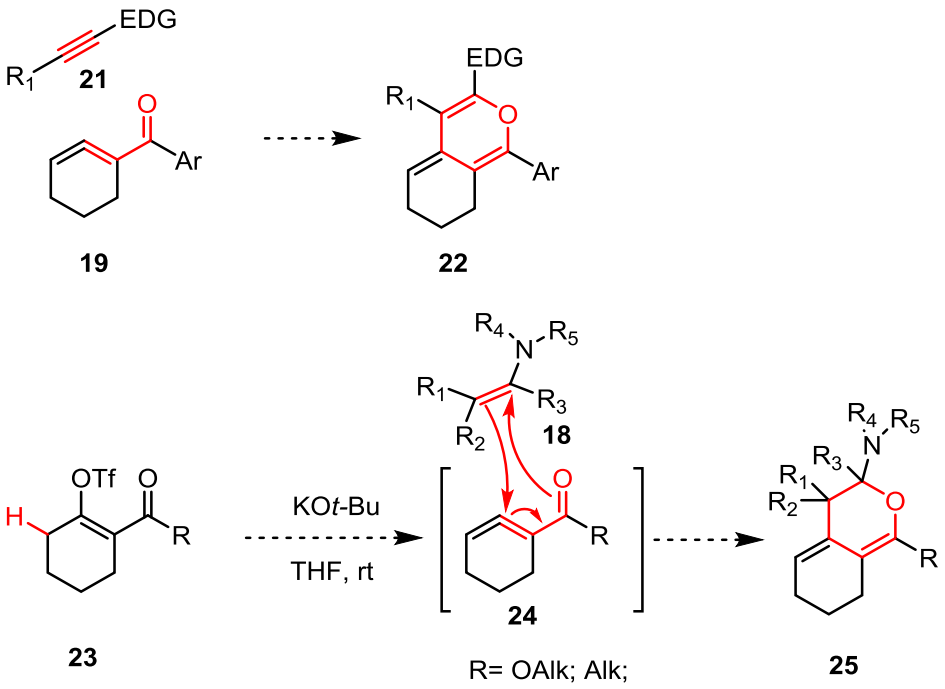

Scheme 5.5 Electron-deficient cyclic allenes proposal

Another direction for the research into electron-deficient cyclic allenes would be to try to make a starting material for the fluoride-promoted elimination method. A brief proposal on how to access the precursor is shown in the following *Scheme 5.6*. Silyl enol ethers **26** are materials known in literature[16] made through silylation of corresponding 1,3-dicarbonyls. Unsubstituted versions of these silyl enol ethers were used by Mori's group for a short synthesis of silyl triflates precursors for the fluoride-promoted method to generate cyclic allenes.[17,18] The LDA/KO*t*-Bu treatment of **26** should produce enolates **27**, which in the presence of Comins' reagent should provide silyl triflates **28**. With precursors **28** in hand, one can then test this reaction with the fluoride-promoted conditions to generate cyclic allenes **29**. Using this method, one would have a milder system that can significantly increase yields and potentially have access to a larger pool of similar starting materials.

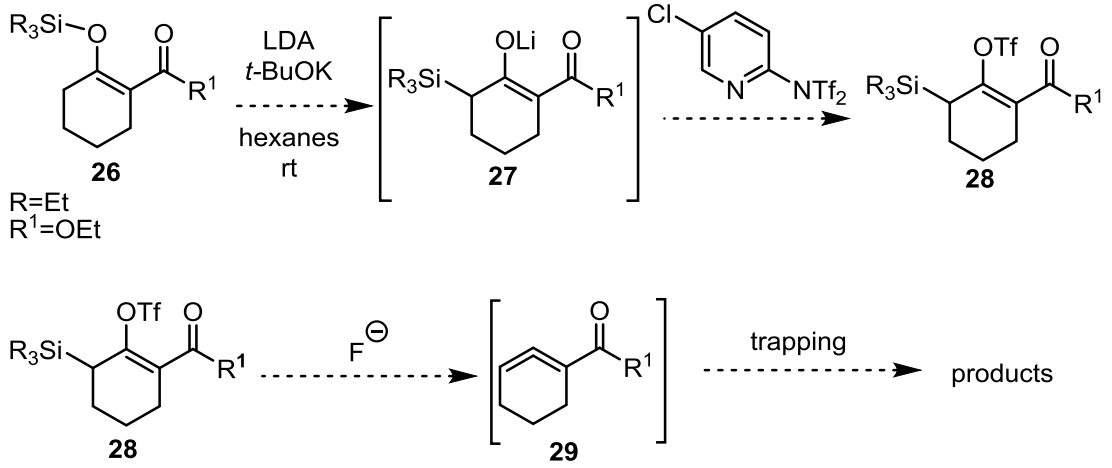

Scheme 5.6 A fluoride-promoted approach for the generation of electron-deficient cyclic allenes

5.4 Future plans for the generation of C-acylimine reactive intermediates

In Chapter 4, the work towards the generation and trapping of C-acylimine intermediate **33** was presented. In this project, we observed a reaction between o-azido-β-ketoester **30** and β-ketoester **31** in the presence of $Mn(OAc)_3$ which resulted in product **32** isolated in 45% yield as a single diastereomer (*Scheme 5.7*). Our inability to generate comparable adducts with other similar traps known to intercept C-acylimines such as **33** raised questions as to whether it is, in fact, an intermediate in the formation of **32**. Several possible pathways to **32** were previously described in Chapter 4. Several combinations of reactive intermediates **33**, **34**, and **35** originating from precursor **30** with enol **36**, and radical **37** were put forward as possible reasoning for obtaining **32**. Therefore, an immediate future plan would be to try to understand the reaction mechanism better. A test for radical presence with TEMPO **38** would be the first step in that direction. If we would observe **39** and **40** as part of the resulting product mixture in that experiment, we would confirm the intermediacy of their corresponding radical species **34** and **37**.

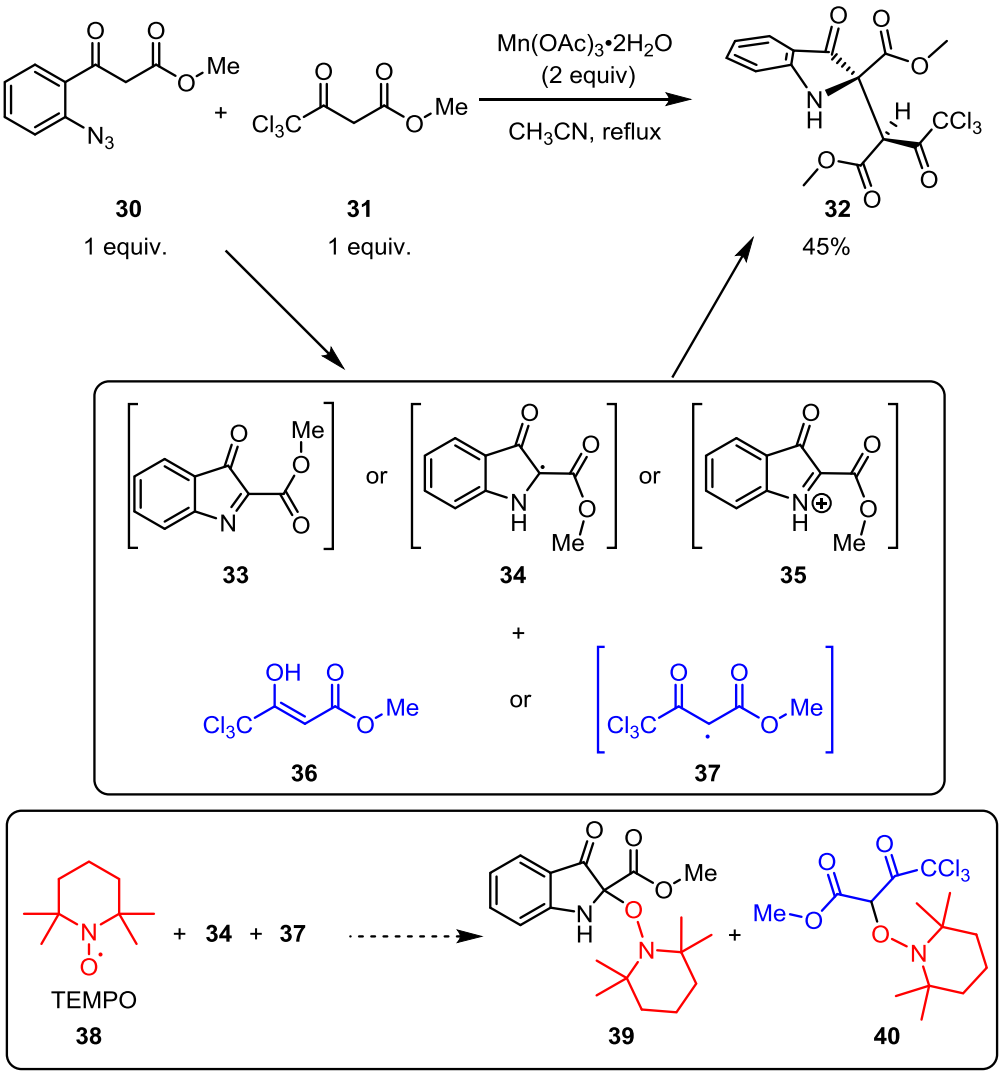

Scheme 5.7 Test reaction with TEMPO

Jung's group recently reported the synthesis of vicinal tricarbonyl compounds using NBS (*Scheme 5.8*).[19] They used as starting material β-ketoester **41,** which was brominated to generate intermediate **42**. The latter, in reaction with piperidine transformed in iminium ion **43**. Upon quenching with water, tricarbonyl **44** was obtained. Based on this known chemistry, one could envision a similar approach for ortho azido substrate **45** to get **46**. Applying the Staudinger reaction conditions on tricarbonyl **46** should provide ylide **47**, which can undergo hydrolysis to obtain **48,** or it could cyclize and generate C-acylimine **49**. If tricarbonyl **48** is generated, it could provide C-acylimine **49** through a condesation reaction.

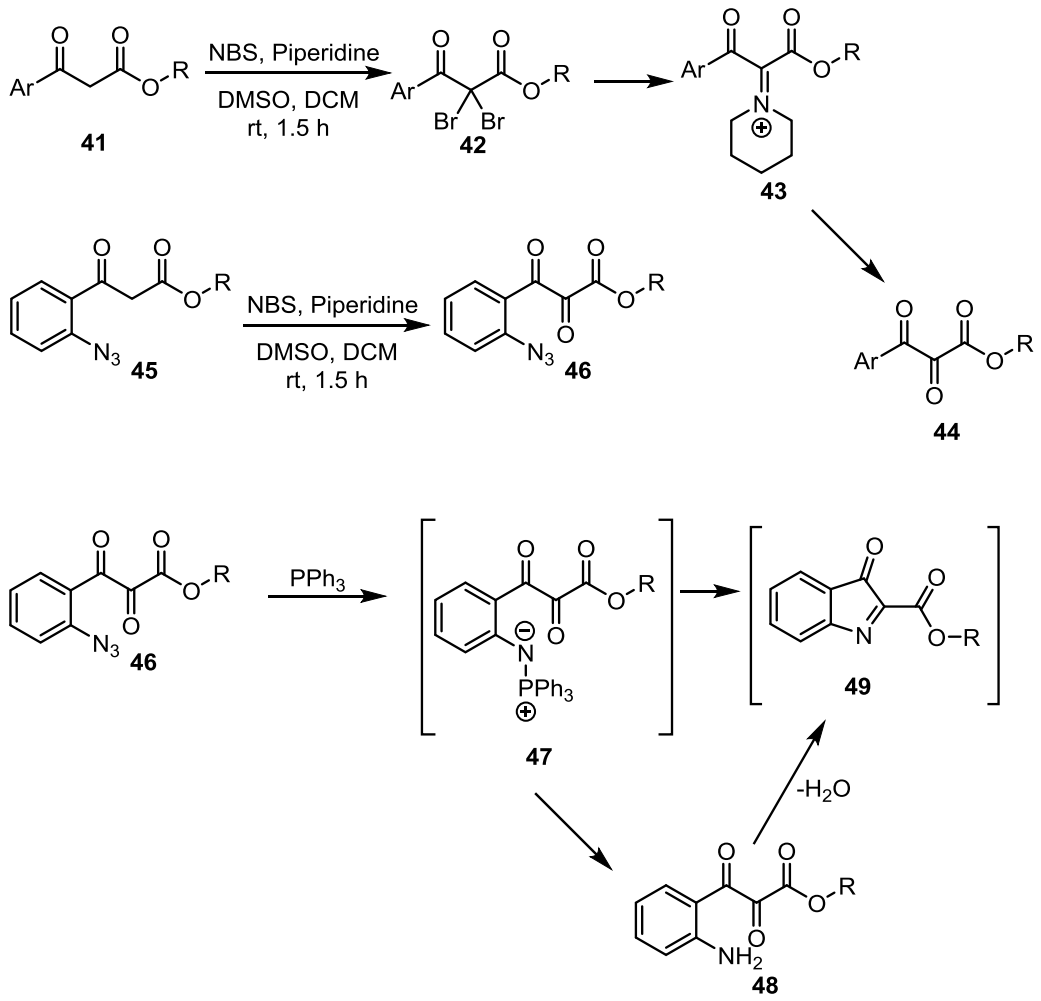

Scheme 5.8 Future plans for C-acylimine **49** generation

5.5 References

(1) Balci, M.; Taskesenligil, Y. Recent Developments in Strained Cyclic Allenes. In *Advances in Strained and Interesting Organic Molecules*; Halton, B., Ed.; JAI Press: Stramford, Connecticut, 2000; Vol. 8, pp 43–81.

(2) Kawase, T. Product Class 3: Cyclic Allenes. In *Category 6, Compounds with All-Carbon Functions*; Krause, Ed.; Georg Thieme Verlag: Stuttgart, 2008; Vol. 5, pp 395–449.

(3) Johnson, R. P. *Chem. Rev.* **1989**, *89* (5), 1111–1124.

(4) Thies, R. W. *Isr. J. Chem.* **1985**, *26* (2), 191–195.

(5) Wittig, G.; Fritze, P. *Angew. Chem.* **1966**, *78* (18–19), 905.

(6) Wittig, G.; Fritze, P. *Justus Liebigs Ann. Chem.* **1968**, *711*, 82–87.

(7) Nendel, M.; Tolbert, L. M.; Herring, L. E.; Islam, M. N.; Houk, K. N. *J. Org. Chem.* **1999**, *64* (3), 976–983.

(8) Barber, J. S.; Yamano, M. M.; Ramirez, M.; Darzi, E. R.; Knapp, R. R.; Liu, F.; Houk, K. N.; Garg, N. K. *Nat. Chem.* **2018**, *10* (9), 953–960.

(9) Wang, B.; Constantin, M. G.; Singh, S.; Zhou, Y.; Davis, R. L.; West, F. G. *Org. Biomol. Chem.* **2021**, *19* (2), 399–405.

(10) Ohno, H.; Miyamura, K.; Tanaka, T.; Oishi, S.; Toda, A.; Takemoto, Y.; Fujii, N.; Ibuka, T. *J. Org. Chem.* **2002**, *67* (4), 1359–1367.

(11) Xu, G.; Wu, J.; Li, L.; Lu, Y.; Li, C. *J. Am. Chem. Soc.* **2020**, *142* (36), 15240–15245.

(12) Skotnitzki, J.; Spessert, L.; Knochel, P. *Angew. Chem. - Int. Ed.* **2019**, *58* (5), 1509–1514.

(13) Taber, D. F.; Berry, J. F. *J. Org. Chem.* **2013**, *78* (17), 8437–8441.

(14) Taber, D. F.; Gerstenhaber, D. A.; Berry, J. F. *J. Org. Chem.* **2011**, *76* (18), 7614–7617.

(15) Zhou, S. Generation and Trapping of Highly Strained Reactive Intermediate: Ethyl 1,2-Cyclohexadienecarboxylate, University of Alberta, Edmonton, AB, 2015.

(16) Langer, P.; Schneider, T. *Synlett* **2000**, *2000* (04), 497–500.

(17) Inoue, K.; Nakura, R.; Okano, K.; Mori, A. *Eur. J. Org. Chem.* **2018**, *2018* (25), 3343–3347.

(18) Nakura, R.; Inoue, K.; Okano, K.; Mori, A. *Synthesis* **2019**, *51* (07), 1561–1564.

(19) Sim, J.; Jo, H.; Viji, M.; Choi, M.; Jung, J. A.; Lee, H.; Jung, J. K. *Adv. Synth. Catal.* **2018**, *360* (5), 852–858.

Bibliography

Chapter 1

(1) Moody, C. J.; Whitman, G. H. Introduction. In *Reactive Intermediates*; Davies, S. G., Ed.; Oxford University Press: Oxford, 1992; pp 1–4.

(2) Hopf, H. Reactive Intermediates. In *Organic Synthesis Highlights III*; Waldman, H., Ed.; Wiley-VCH Verlag GmbH: Weinheim, Germany, 1998; Vol. 5, pp 250–262.

(3) Singh, M. S. Introduction. In *Reactive Intermediates in Organic Chemistry: Structure, Mechanism, and Reactions*; Singh, M. S., Ed.; Wiley: Weinheim, Germany, 2014; pp 1–19.

(4) Dodziuk, H.; Fokin, A. A.; Schreiner, P. R. Introduction. *Strained Hydrocarbons*. March 18, 2009, pp 1–32.

(5) Carey, F. A.; Sundberg, R. J. Carbanions and Other Carbon Nucleophiles. In *Advanced Organic Chemistry. Part A: Structure and Mechanisms*; Springer US: Boston, MA, 2007; pp 579–629.

(6) Gronert, S. Carbanions. In *Reactive Intermediate Chemistry*; John Wiley & Sons, Inc.: Hoboken, NJ, USA, 2005; pp 69–119.

(7) Singh, M. S. Carbanions. In *Reactive Intermediates in Organic Chemistry Structure, Mechanism, and Reactions*; Singh, M. S., Ed.; Wiley: Weinheim, Germany, 2014; pp 65–100.

(8) Olah, G. A. *J. Org. Chem.* **2001**, *66* (18), 5943–5957.

(9) Olah, G. A. *J. Am. Chem. Soc.* **1972**, *94* (3), 808–820.

(10) McClelland, R. A. Carbocations. In *Reactive Intermediate Chemistry*; John Wiley & Sons, Inc.: Hoboken, NJ, USA, 2004; pp 1–40.

(11) Winstein, S.; Trifan, D. S. *J. Am. Chem. Soc.* **1949**, *71* (8), 2953.

(12) Winstein, S.; Trifan, D. *J. Am. Chem. Soc.* **1952**, *74* (5), 1154–1160.

(13) Olah, G. A.; Prakash, G. K. S.; Saunders, M. *Acc. Chem. Res.* **1983**, *16* (12), 440–448.

(14) Brown, H. C. *Acc. Chem. Res.* **1983**, *16* (12), 432–440.

(15) Newcomb, M. Radicals. In *Reactive Intermediate Chemistry*; Wiley Online Books; John Wiley & Sons, Inc.: Hoboken, NJ, USA, 2005; pp 121–163.
(16) Stephenson, L. M.; Cavigli, P. R.; Parlett, J. L. *J. Am. Chem. Soc.* **1971**, *93* (8), 1984–1988.
(17) Kopecky, K. R.; Soler, J. *Can. J. Chem.* **1974**, *52* (11), 2111–2118.
(18) Ventura, E.; Dallos, M.; Lischka, H. *J. Chem. Phys.* **2003**, *118* (24), 10963–10972.
(19) Singh, M. S. Carbenes. In *Reactive Intermediates in Organic Chemistry: Structure, Mechanism, and Reactions*; Singh, M. S., Ed.; Wiley: Weinheim, Germany, 2014; pp 153–196.
(20) Jones, M.; Moss, R. A. Singlet Carbenes. In *Reactive Intermediate Chemistry*; Wiley Online Books; John Wiley & Sons, Inc.: Hoboken, NJ, USA, 2004; pp 273–328.
(21) Tomioka, H. Triplet Carbenes. In *Reactive Intermediate Chemistry*; John Wiley & Sons, Inc.: Hoboken, NJ, USA, 2005; pp 375–461.
(22) Fischer, E. O.; Heinz Dötz, K. *Chem. Ber.* **1970**, *103* (4), 1273–1278.
(23) Yates, P. *J. Am. Chem. Soc.* **1952**, *74* (21), 5376–5381.
(24) Dötz, K. H. *Angew. Chem. Int. Ed. Engl.* **1984**, *23* (8), 587–608.
(25) Stoermer, R.; Kahlert, B. *Ber. Dtsch. Chem. Ges.* **1902**, *35* (2), 1633–1640.
(26) Pellissier, H.; Santelli, M. *Tetrahedron* **2003**, *59* (6), 701–730.
(27) Wenk, H. H.; Winkler, M.; Sander, W. *Angew. Chem. Int. Ed.* **2003**, *42* (5), 502–528.
(28) Gampe, C. M.; Carreira, E. M. *Angew. Chem. Int. Ed.* **2012**, *51* (16), 3766–3778.
(29) Yoshida, S.; Hosoya, T. *Chem. Lett.* **2015**, *44* (11), 1450–1460.
(30) Tadross, P. M.; Stoltz, B. M. *Chem. Rev.* **2012**, *112* (6), 3550–3577.
(31) Friedman, L.; Logullo, F. M. *J. Am. Chem. Soc.* **1963**, *85* (10), 1549–1549.
(32) Roberts, J. D.; Simmons, H. E.; Carlsmith, L. A.; Vaughan, C. W. *J. Am. Chem. Soc.* **1953**, *75* (13), 3290–3291.
(33) Roberts, J. D.; Vaughan, C. W.; Carlsmith, L. A.; Semenow, D. A. *J. Am. Chem. Soc.* **1956**, *78* (3), 611–614.
(34) Himeshima, Y.; Sonoda, T.; Kobayashi, H. *Chem. Lett.* **1983**, *12* (8), 1211–1214.
(35) Kitamura, T.; Yamane, M. *J. Chem. Soc. Chem. Commun.* **1995**, *983* (9), 983.

(36) Wittig, G.; Ludwig, R. *Angew. Chem.* **1956**, *68* (1), 40–40.

(37) Matsumoto, T.; Hosoya, T.; Katsuki, M.; Suzuki, K. *Tetrahedron Lett.* **1991**, *32* (46), 6735–6736.

(38) Fluegel, L. L.; Hoye, T. R. *Chem. Rev.* **2021**, *121* (4), 2413–2444.

(39) Stevens, R. V.; Bisacchi, G. S. *J. Org. Chem.* **1982**, *47* (12), 2393–2396.

(40) Peña, D.; Cobas, A.; Pérez, D.; Guitián, E. *Synthesis* **2002**, 1454–1458.

(41) Wickham, P. P.; Hazen, K. H.; Guo, H.; Jones, G.; Reuter, K. H.; Scott, W. J. *J. Org. Chem.* **1991**, *56* (6), 2045–2050.

(42) Tambar, U. K.; Stoltz, B. M. *J. Am. Chem. Soc.* **2005**, *127* (15), 5340–5341.

(43) Taylor, E. C.; Sobieray, D. M. *Tetrahedron* **1991**, *47* (46), 9599–9620.

(44) Tambar, U. K.; Ebner, D. C.; Stoltz, B. M. *J. Am. Chem. Soc.* **2006**, *128* (36), 11752–11753.

(45) Hoye, T. R.; Baire, B.; Niu, D.; Willoughby, P. H.; Woods, B. P. *Nature* **2012**, *490* (7419), 208–211.

(46) Bottini, A. T.; Corson, F. P.; Fitzgerald, R.; Frost, K. A. *Tetrahedron* **1972**, *28* (19), 4883–4904.

(47) Bach, R. D. *J. Am. Chem. Soc.* **2009**, *131* (6), 5233–5243.

(48) Medina, J. M.; McMahon, T. C.; Jiménez-Osés, G.; Houk, K. N.; Garg, N. K. *J. Am. Chem. Soc.* **2014**, *136* (42), 14706–14709.

(49) Olivella, S.; Pericàs, M. A.; Riera, A.; Solé, A. *J. Org. Chem.* **1987**, *52* (19), 4160–4163.

(50) Johnson, R. P.; Daoust, K. J. *J. Am. Chem. Soc.* **1995**, *117* (1), 362–367.

(51) Hopf, H.; Grunenberg, J. Angle-Strained Cycloalkynes. In *Strained Hydrocarbons*; Wiley-VCH Verlag GmbH & Co. KGaA: Weinheim, Germany, 2009; pp 375–397.

(52) Dommerholt, J.; Rutjes, F. P. J. T.; van Delft, F. L. *Top. Curr. Chem.* **2016**, *374* (2), 1–20.

(53) Agard, N. J.; Prescher, J. A.; Bertozzi, C. R. *J. Am. Chem. Soc.* **2004**, *126* (46), 15046–15047.

(54) Huisgen, R. *Angew. Chem. Int. Ed. Engl.* **1963**, *2* (10), 565–598.

(55) Wang, Q.; Chan, T. R.; Hilgraf, R.; Fokin, V. V.; Sharpless, K. B.; Finn, M. G. *J. Am. Chem. Soc.* **2003**, *125* (11), 3192–3193.

(56) Christl, M. Cyclic Allenes Up to Seven-Membered Rings. In *Modern Allene Chemistry*; Wiley-VCH Verlag GmbH: Weinheim, Germany, 2005; pp 243–357.

(57) Kawase, T. Product Class 3: Cyclic Allenes. In *Category 6, Compounds with All-Carbon Functions*; Krause, Ed.; Georg Thieme Verlag: Stuttgart, 2008; Vol. 5, pp 395–449.

(58) Johnson, R. P. *Chem. Rev.* **1989**, *89* (5), 1111–1124.

(59) Balci, M.; Taskesenligil, Y. Recent Developments in Strained Cyclic Allenes. In *Advances in Strained and Interesting Organic Molecules*; Halton, B., Ed.; JAI Press: Stramford, Connecticut, 2000; Vol. 8, pp 43–81.

(60) Thies, R. W. *Isr. J. Chem.* **1985**, *26* (2), 191–195.

(61) Anthony, S. M.; Wonilowicz, L. G.; McVeigh, M. S.; Garg, N. K. *JACS Au* **2021**, *1* (7), 897-912.

(62) Daoust, K. J.; Hernandez, S. M.; Konrad, K. M.; Mackie, I. D.; Winstanley, J.; Johnson, R. P. *J. Org. Chem.* **2006**, *71* (15), 5708–5714.

(63) Schmidt, M. W.; Angus, R. O.; Johnson, R. P. *J. Am. Chem. Soc.* **1982**, *104* (24), 6838–6839.

(64) Dillon, P. W.; Underwood, G. R. *J. Am. Chem. Soc.* **1974**, *96* (3), 779–787.

(65) Angus, R. O.; Johnson, R. P.; Schmidt, M. W. *J. Am. Chem. Soc.* **1985**, *107* (3), 532–537.

(66) Wentrup, C.; Gross, G.; Maquestiau, A.; Flammang, R. *Angew. Chem. Int. Ed. Engl.* **1983**, *22* (7), 542–543.

(67) Engels, B.; Schöneboom, J. C.; Münster, A. F.; Groetsch, S.; Christl, M. *J. Am. Chem. Soc.* **2002**, *124* (2), 287–297.

(68) Roth, W. R.; Ruf, G.; Ford, P. W. *Chem. Ber.* **1974**, *107* (1), 48–52.

(69) Balci, M.; Jones, W. M. *J. Am. Chem. Soc.* **1980**, *102* (25), 7607–7608.

(70) Boswell, R. F.; Bass, R. G. *J. Org. Chem.* **1975**, *40* (16), 2419–2420.

(71) Barber, J. S.; Yamano, M. M.; Ramirez, M.; Darzi, E. R.; Knapp, R. R.; Liu, F.; Houk, K. N.; Garg, N. K. *Nat. Chem.* **2018**, *10* (9), 953–960.

(72) Drinkuth, S.; Groetsch, S.; Peters, E. M.; Peters, K.; Christl, M. *Eur. J. Org. Chem.* **2001**, 2665–2670.

(73) Schreck, M.; Christl, M. *Angew. Chem. Int. Ed. Engl.* **1987**, *26* (7), 690–692.

(74) Yamano, M. M.; Knapp, R. R.; Ngamnithiporn, A.; Ramirez, M.; Houk, K. N.; Stoltz, B. M.; Garg, N. K. *Angew. Chem. Int. Ed.* **2019**, *58* (17), 5653–5657.

(75) Christl, M.; Braun, M. *Chem. Ber.* **1989**, *122* (10), 1939–1946.

(76) Lloyd, D.; McNab, H. *J. Chem. Soc. Perkin Trans. 1* **1976**, *516* (16), 1784.

(77) Lee-Ruff, E.; Maleki, M.; Duperrouzel, P.; Lein, M. H.; Hopkinson, A. C. *J. Chem. Soc. Chem. Commun.* **1983**, 346-347.

(78) Elliott, R. L.; Nicholson, N. H.; Peaker, F. E.; Takle, A. K.; Richardson, C. M.; Tyler, J. W.; White, J.; Pearson, M. J.; Eggleston, D. S.; Haltiwanger, R. C. *J. Org. Chem.* **1997**, *62* (15), 4998–5016.

(79) Elliott, R. L.; Nicholson, N. H.; Peaker, F. E.; Takle, A. K.; Tyler, J. W.; White, J. *J. Org. Chem.* **1994**, *59* (7), 1606–1607.

(80) Shimizu, T.; Hojo, F.; Ando, W. *J. Am. Chem. Soc.* **1993**, *115* (8), 3111–3115.

(81) Pang, Y.; Petrich, S. A.; Young, V. G.; Gordon, M. S.; Barton, T. J. *J. Am. Chem. Soc.* **1993**, *115* (6), 2534–2536.

(82) Wittig, G.; Fritze, P. *Justus Liebigs Ann. Chem.* **1968**, *711*, 82–87.

(83) Wittig, G.; Fritze, P. *Angew. Chem.* **1966**, *78* (18–19), 905.

(84) Moore, W. R.; Moser, W. R. *J. Org. Chem.* **1970**, *35* (4), 908–912.

(85) Moore, W. R.; Moser, W. R. *J. Am. Chem. Soc.* **1970**, *92* (18), 5469–5474.

(86) Shakespeare, W. C.; Johnson, R. P. *J. Am. Chem. Soc.* **1990**, *112* (23), 8578–8579.

(87) Bottini, A. T.; Hilton, L. L.; Plott, J. *Tetrahedron* **1975**, *31* (17), 1997–2001.

(88) Hioki, Y.; Mori, A.; Okano, K. *Tetrahedron* **2020**, *76* (22), 131103.

(89) von E. Doering, W.; LaFlamme, P. M. *Tetrahedron* **1958**, *2* (1–2), 75–79.

(90) Moore, W.; Ward, H. *J. Org. Chem.* **1960**, *25* (11), 2073–2073.

(91) Skattebøl, L. *Tetrahedron Lett.* **1961**, *2* (5), 167–172.

(92) Quintana, I.; Peña, D.; Pérez, D.; Guitián, E. *Eur. J. Org. Chem.* **2009**, 5519–5524.

(93) Barber, J. S.; Styduhar, E. D.; Pham, H. V.; McMahon, T. C.; Houk, K. N.; Garg, N. K. *J. Am. Chem. Soc.* **2016**, *138* (8), 2512–2515.

(94) Lofstrand, V. A.; West, F. G. *Chem. Eur. J.* **2016**, *22* (31), 10763–10767.

(95) Nakura, R.; Inoue, K.; Okano, K.; Mori, A. *Synthesis* **2019**, *51* (7), 1561–1564.

(96) Inoue, K.; Nakura, R.; Okano, K.; Mori, A. *Eur. J. Org. Chem.* **2018**, 3343–3347.

(97) Chari, J. V.; Ippoliti, F. M.; Garg, N. K. *J. Org. Chem.* **2019**, *84* (6), 3652–3655.

(98) McVeigh, M. S.; Kelleghan, A. V.; Yamano, M. M.; Knapp, R. R.; Garg, N. K. *Org. Lett.* **2020**, *22* (11), 4500–4504.

(99) Wills, M. S. B.; Danheiser, R. L. *J. Am. Chem. Soc.* **1998**, *120* (36), 9378–9379.

(100) Wang, Y.; Hoye, T. R. *Org. Lett.* **2018**, *20* (15), 4425–4429.

(101) Christl, M.; Schreck, M.; Fischer, T.; Rudolph, M.; Moigno, D.; Fischer, H.; Deuerlein, S.; Stalke, D. *Chem. Eur. J.* **2009**, *15* (42), 11256–11265.

(102) Christl, M.; Groetsch, S.; Günther, K. *Angew. Chem. Int. Ed.* **2000**, *39* (18), 3261–3263.

(103) Mahlokozera, T.; Goods, J. B.; Childs, A. M.; Thamattoor, D. M. *Org. Lett.* **2009**, *11* (22), 5095–5097.

(104) Zhang, J.; Xie, Z. *Chem. Sci.* **2021**, *12* (15), 5616–5620.

(105) Mcintosh, K. C. Investigation of Strain-Activated Trapping Reactions of 1,2-Cyclohexadiene: Intramolecular Capture by Pendent Furans and Styrenes, University of Alberta, Edmonton, AB, 2020.

(106) Eaton, P. E.; Stubbs, C. E. *J. Am. Chem. Soc.* **1967**, *89* (22), 5722–5723.

(107) Lofstrand, V. A.; McIntosh, K. C.; Almehmadi, Y. A.; West, F. G. *Org. Lett.* **2019**, *21* (16), 6231–6234.

(108) Ramirez, M.; Svatunek, D.; Liu, F.; Garg, N. K.; Houk, K. N. *Angew. Chem. Int. Ed.* **2021**, *60*,14989–14997.

(109) Almehmadi, Y. A.; West, F. G. *Org. Lett.* **2020**, *22* (15), 6091–6095.

(110) Westphal, M. V.; Hudson, L.; Mason, J. W.; Pradeilles, J. A.; Zécri, F. J.; Briner, K.; Schreiber, S. L. *J. Am. Chem. Soc.* **2020**, *142* (17), 7776–7782.

Chapter 2

(1) Christl, M. Cyclic Allenes Up to Seven-Membered Rings. In *Modern Allene Chemistry*; Wiley-VCH Verlag GmbH: Weinheim, Germany, 2005; pp 243–357.

(2) Johnson, R. P. *Chem. Rev.* **1989**, *89* (5), 1111–1124.

(3) Balci, M.; Taskesenligil, Y. Recent Developments in Strained Cyclic Allenes. In *Advances in Strained and Interesting Organic Molecules*; Halton, B., Ed.; JAI Press: Stramford, Connecticut, 2000; Vol. 8, pp 43–81.

(4) Shakespeare, W. C.; Johnson, R. P. *J. Am. Chem. Soc.* **1990**, *112* (23), 8578–8579.

(5) Barber, J. S.; Styduhar, E. D.; Pham, H. V.; McMahon, T. C.; Houk, K. N.; Garg, N. K. *J. Am. Chem. Soc.* **2016**, *138* (8), 2512–2515.

(6) Lofstrand, V. A.; West, F. G. *Chem. Eur. J.* **2016**, *22* (31), 10763–10767.

(7) Yokota, M.; Fuchibe, K.; Ueda, M.; Mayumi, Y.; Ichikawa, J. *Org. Lett.* **2009**, *11* (17), 3994–3997.

(8) Clayden, J. *Organolithiums: Selectivity for Synthesis*; Manchester, UK, 2002.

(9) Gilman, H.; Langham, W.; Jacoby, A. L. *J. Am. Chem. Soc.* **1939**, *61* (1), 106–109.

(10) Jones, R. G.; Gilman, H. The Halogen-Metal Interconversion Reaction with Organolithium Compounds. In *Organic Reactions*; John Wiley & Sons, Inc.: Hoboken, NJ, USA, 2011; pp 339–366.

(11) Marvel, C. S.; Hager, F. D.; Coffman, D. D. *J. Am. Chem. Soc.* **1927**, *49* (9), 2323–2328.

(12) Bryce-Smith, D. *J. Chem. Soc.* **1956**, *53* (9), 1603.

(13) Clayden, J. Regioselective Synthesis of Organolithiums by X-Li Exchange. In *Tetrahedron Organic Chemistry Series, Volume 23, Organolithiums: Selectivity for Synthesis*; Manchester, UK, 2002; pp 111–149.

(14) Bailey, W. F.; Patricia, J. J. *J. Organomet. Chem.* **1988**, *352* (1–2), 1–46.

(15) Zefirov, N. S.; Makhon'kov, D. I. *Chem. Rev.* **1982**, *82* (6), 615–624.

(16) Wakefield, B. J. Organomagnesium Methods in Organic Synthesis; Elsevier, 1995; pp 21–71.

(17) Moore, W. R.; Moser, W. R. *J. Am. Chem. Soc.* **1970**, *549* (9), 5469–5474.

(18) Yoshida, S.; Karaki, F.; Uchida, K.; Hosoya, T. *Chem. Commun.* **2015**, *51* (42), 8745–8748.

(19) Della, E. W.; Taylor, D. K.; Taanakfsldls, J. **1990**, *2* (36), 5219–5220.

(20) Lopchuk, J. M.; Fjelbye, K.; Kawamata, Y.; Malins, L. R.; Pan, C. M.; Gianatassio, R.; Wang, J.; Prieto, L.; Bradow, J.; Brandt, T. A.; Collins, M. R.; Elleraas, J.; Ewanicki, J.; Farrell, W.; Fadeyi, O. O.; Gallego, G. M.; Mousseau, J.

J.; Oliver, R.; Sach, N. W.; Smith, J. K.; Spangler, J. E.; Zhu, H.; Zhu, J.; Baran, P. S. *J. Am. Chem. Soc.* **2017**, *139* (8), 3209–3226.

(21) Makarov, I. S.; Brocklehurst, C. E.; Karaghiosoff, K.; Koch, G.; Knochel, P. *Angew. Chem. Int. Ed.* **2017**, *56* (41), 12774–12777.

(22) Oh, K.; Fuchibe, K.; Ichikawa, J. *Synthesis* **2011**, 881–886.

(23) Ohno, H.; Miyamura, K.; Tanaka, T.; Oishi, S.; Toda, A.; Takemoto, Y.; Fujii, N.; Ibuka, T. *J. Org. Chem.* **2002**, *67* (4), 1359–1367.

(24) Larock, R. C.; Hightower, T. R.; Kraus, G. A.; Hahn, P.; Zheng, D. *Tetrahedron Lett.* **1995**, *36* (14), 2423–2426.

(25) Nicolaou, K. C.; Ding, H.; Richard, J.-A.; Chen, D. Y.-K. *J. Am. Chem. Soc.* **2010**, *132* (11), 3815–3818.

(26) Li, K.; Alexakis, A. *Angew. Chem. Int. Ed.* **2006**, *45* (45), 7600–7603.

(27) Sadak, A. E.; Arslan, T.; Celebioglu, N.; Saracoglu, N. *Tetrahedron* **2010**, *66* (17), 3214–3221.

(28) Krafft, M. E.; Cran, J. W. *Synlett* **2005**, 1263–1266.

(29) Mayasundari, A.; Young, D. G. J. *Tetrahedron Lett.* **2001**, *42* (2), 203–206.

(30) Calvin, S. J.; Mangan, D.; Miskelly, I.; Moody, T. S.; Stevenson, P. J. *Org. Process Res. Dev.* **2012**, *16* (1), 82–86.

(31) Bäuerlein, P. S.; Fairlamb, I. J. S.; Jarvis, A. G.; Lee, A. F.; Müller, C.; Slattery, J. M.; Thatcher, R. J.; Vogt, D.; Whitwood, A. C. *Chem. Commun.* **2009**, 5734–5736.

(32) Nwokogu, G. C. *J. Org. Chem.* **1985**, *50* (20), 3900–3908.

(33) Harmata, M.; Barnes, C. L.; Brackley, J.; Bohnert, G.; Kirchhoefer, P.; Kürti, L.; Rashatasakhon, P. *J. Org. Chem.* **2001**, *66* (15), 5232–5236.

(34) Evans, P. A.; Oliver, S.; Chae, J. *J. Am. Chem. Soc.* **2012**, *134* (47), 19314–19317.

(35) Quintana, I.; Peña, D.; Pérez, D.; Guitián, E. *Eur. J. Org. Chem.* **2009**, *2009* (32), 5519–5524.

(36) Bottini, A. T.; Frost, K. A.; Anderson, B. R.; Dev, V. *Tetrahedron* **1973**, *29* (14), 1975–1981.

(37) Pietruszka, J.; Künig, W. A.; Maelger, H.; Kopf, J. *Chem. Ber.* **1993**, *126* (1), 159–166.

(38) Christl, M.; Schreck, M. *Chem. Ber.* **1987**, *120* (6), 915–920.

(39) Quintana, I.; Peña, D.; Pérez, D.; Guitián, E. *Eur. J. Org. Chem.* **2009**, *2009* (32), 5519–5524.

(40) Moore, W. R.; Moser, W. R. *J. Org. Chem.* **1970**, *35* (4), 908–912.

(41) Singh, K.; Trinh, W.; Weaver, J. D. *Org. Biomol. Chem.* **2019**, *17* (7), 1854–1861.

(42) Ogasawara, M.; Okada, A.; Nakajima, K.; Takahashi, T. *Org. Lett.* **2009**, *11* (1), 177–180.

(43) Hagendorn, T.; Bräse, S. *Eur. J. Org. Chem.* **2014**, *2014* (6), 1280–1286.

(44) Almehmadi, Y. A. Investigation of New Mild Routes to Substituted and Unsubstituted 1,2- Cycloheptadienes and Their Trapping Reactions, University of Alberta, Edmonton, AB, 2019.

Chapter 3

(1) Wang, B.; Constantin, M. G.; Singh, S.; Zhou, Y.; Davis, R. L.; West, F. G. *Org. Biomol. Chem.* **2021**, *19* (2), 399–405.

(2) Christl, M.; Braun, M. *Chem. Ber.* **1989**, *122* (10), 1939–1946.

(3) Ruzziconi, R.; Naruse, Y.; Schlosser, M. *Tetrahedron* **1991**, *47* (26), 4603–4610.

(4) Lofstrand, V. A.; West, F. G. *Chem. Eur. J.* **2016**, *22* (31), 10763–10767.

(5) Nendel, M.; Tolbert, L. M.; Herring, L. E.; Islam, M. N.; Houk, K. N. *J. Org. Chem.* **1999**, *64* (3), 976–983.

(6) Zhou, S. Generation and Trapping of Highly Strained Reactive Intermediate: Ethyl 1,2-Cyclohexadienecarboxylate, University of Alberta, Edmonton, AB, 2015.

(7) Barber, J. S.; Yamano, M. M.; Ramirez, M.; Darzi, E. R.; Knapp, R. R.; Liu, F.; Houk, K. N.; Garg, N. K. *Nat. Chem.* **2018**, *10* (9), 953–960.

(8) Stork, G.; Brizzolara, A.; Landesman, H.; Szmuszkovicz, J.; Terrell, R. *J. Am. Chem. Soc.* **1963**, *85* (2), 207–222.

(9) Fos, E.; Borràs, L.; Gasull, M.; Mauleón, D.; Carganico, G. *J. Heterocycl. Chem.* **1992**, *29*, 203–208.

(10) Lin, H. S.; Rampersaud, A. A.; Zimmerman, K.; Steinberg, M. I.; Boyd, D. B. *J. Med. Chem.* **1992**, *35* (14), 2658–2667.

(11) Jia, Z.; Gálvez, E.; Sebastián, R. M.; Pleixats, R.; Álvarez-Larena, Á.; Martin, E.; Vallribera, A.; Shafir, A. *Angew. Chem. Int. Ed.* **2014**, *53* (42), 11298–11301.

(12) Bottini, A. T.; Hilton, L. L.; Plott, J. *Tetrahedron* **1975**, *31* (17), 1997–2001.

(13) Desimoni, G.; Faita, G.; Quadrelli, P. *Chem. Rev.* **2018**, *118* (4), 2080–2248.

(14) Pałasz, A. *Top. Curr. Chem.* **2016**, *374* (3), 30–60.

(15) Tsuge, O.; Hatta, T.; Yoshitomi, H.; Kurosaka, K.; Fujiwara, T.; Maeda, H.; Kakehi, A. *Heterocycles* **1995**, *41* (2), 225–228.

(16) Periasamy, M.; Devasagayaraj, A.; Satyanarayana, N.; Narayana, C. *Synth. Commun.* **1989**, *19* (3–4), 565–573.

(17) DFT Calculations were performed using Gaussian09.e01. DFT Calculations were performed using Gaussian09.e01. M. J.Frisch, G. W.Trucks, H. B.Schlegel, G. E.Scuseria, M. A.Robb, J. R.Cheeseman, G.Scalmani, V.Barone, G. A.Petersson, H.Nakatsuji, X.Li, M.Caric, 2016. No Title.

(18) Zhao, Y.; Truhlar, D. G. *Theor. Chem. Acc.* **2008**, *120* (1–3), 215–241.

(19) Scalmani, G.; Frisch, M. J. *J. Chem. Phys.* **2010**, *132* (11).

(20) May, G. L.; Pinhey, J. T. *Aust. J. Chem.* **1982**, *35* (9), 1859–1871.

(21) Carlson, R.; Nilsson, Å. *Acta Chem. Scand. B* **1984**, *38*, 49–53.

(22) Carlson, R.; Nilsson, Å.; Strömqvist, M. *Acta Chem. Scand. B* **1983**, *37*, 7–13.

(23) Liu, Y. P.; Wang, S. R.; Chen, T. T.; Yu, C. C.; Wang, A. E.; Huang, P. Q. *Adv. Synth. Catal.* **2019**, *361* (5), 971–975.

Chapter 4

(1) Bott, T. M.; Atienza, B. J.; West, F. G. *RSC Adv.* **2014**, *4* (60), 31955–31959.

(2) Atienza, B. J. P.; Jensen, L. D.; Noton, S. L.; Ansalem, A. K. V.; Hobman, T.; Fearns, R.; Marchant, D. J.; West, F. G. *J. Org. Chem.* **2018**, *83* (13), 6829–6842.

(3) Keicher, T.; Löobbecke, S. Lab-Scale Synthesis of Azido Compounds: Safety Measures and Analysis. In *Organic Azides: Syntheses and Applications*; Bräse, S., Banert, K., Eds.; Wiley: Chichester, 2010; pp 3–27.

(4) Heiba, E. I.; Dessau, R. M.; Koehl, W. J. *J. Am. Chem. Soc.* **1968**, *90* (21), 5905–5906.

(5) Bush, J. B.; Finkbeiner, H. *J. Am. Chem. Soc.* **1968**, *90* (21), 5903–5905.

(6) Snider, B. B. *Chem. Rev.* **1996**, *96* (1), 339–364.

(7) Hessel, L. W.; Romers, C. *Recl. des Trav. Chim. des Pays-Bas* **1969**, *88* (5), 545–552.

(8) Snider, B. B.; Patricia, J. J.; Kates, S. A. *J. Org. Chem.* **1988**, *53* (10), 2137–2143.

(9) Wang, Y. F.; Ton, K. K.; Chiba, S.; Narasaka, K. *Org. Lett.* **2008**, *10* (21), 5019–5022.

(10) Snider, B. B.; Mohan, R.; Kates, S. A. *J. Org. Chem.* **1985**, *50* (19), 3659–3661.

(11) Welch, S. C.; Hagan, C. P.; Kim, J. H.; Chu, P. S. *J. Org. Chem.* **1977**, *42* (17), 2879–2887.

(12) Wenkert, E.; Afonso, A.; Bredenberg, J. B.; Kaneko, C.; Tahara, A. *J. Am. Chem. Soc.* **1964**, *86* (10), 2038–2043.

(13) Snider, B. B.; Duvall, J. R. *Org. Lett.* **2004**, *6* (8), 1265–1268.

(14) Misaki, T.; Nagase, R.; Matsumoto, K.; Tanabe, Y. *J. Am. Chem. Soc.* **2005**, *127* (9), 2854–2855.

(15) Martins, M. A. P.; Pereira, C. M. P.; Zimmermann, N. E. K.; Moura, S.; Sinhorin, A. P.; Cunico, W.; Zanatta, N.; Bonacorso, H. G.; Flores, A. C. F. *Synthesis* **2003**, 2353–2357.

(16) Lommerse, J. P. M.; Price, S. L.; Taylor, R. *J. Comput. Chem.* **1997**, *18* (6), 757–774.

(17) Tan, N. Y.; Li, R.; Bräuer, P.; D'Agostino, C.; Gladden, L. F.; Zeitler, J. A. *Phys. Chem. Chem. Phys.* **2015**, *17* (8), 5999–6008.

Chapter 5

(1) Balci, M.; Taskesenligil, Y. Recent Developments in Strained Cyclic Allenes. In *Advances in Strained and Interesting Organic Molecules*; Halton, B., Ed.; JAI Press: Stramford, Connecticut, 2000; Vol. 8, pp 43–81.

(2) Kawase, T. Product Class 3: Cyclic Allenes. In *Category 6, Compounds with All-Carbon Functions*; Krause, Ed.; Georg Thieme Verlag: Stuttgart, 2008; Vol. 5, pp 395–449.

(3) Johnson, R. P. *Chem. Rev.* **1989**, *89* (5), 1111–1124.

(4) Thies, R. W. *Isr. J. Chem.* **1985**, *26* (2), 191–195.

(5) Wittig, G.; Fritze, P. *Angew. Chem.* **1966**, *78* (18–19), 905.

(6) Wittig, G.; Fritze, P. *Justus Liebigs Ann. Chem.* **1968**, *711*, 82–87.

(7) Nendel, M.; Tolbert, L. M.; Herring, L. E.; Islam, M. N.; Houk, K. N. *J. Org.*

Chem. **1999**, *64* (3), 976–983.

(8) Barber, J. S.; Yamano, M. M.; Ramirez, M.; Darzi, E. R.; Knapp, R. R.; Liu, F.; Houk, K. N.; Garg, N. K. *Nat. Chem.* **2018**, *10* (9), 953–960.

(9) Wang, B.; Constantin, M. G.; Singh, S.; Zhou, Y.; Davis, R. L.; West, F. G. *Org. Biomol. Chem.* **2021**, *19* (2), 399–405.

(10) Ohno, H.; Miyamura, K.; Tanaka, T.; Oishi, S.; Toda, A.; Takemoto, Y.; Fujii, N.; Ibuka, T. *J. Org. Chem.* **2002**, *67* (4), 1359–1367.

(11) Xu, G.; Wu, J.; Li, L.; Lu, Y.; Li, C. *J. Am. Chem. Soc.* **2020**, *142* (36), 15240–15245.

(12) Skotnitzki, J.; Spessert, L.; Knochel, P. *Angew. Chem. Int. Ed.* **2019**, *58* (5), 1509–1514.

(13) Taber, D. F.; Berry, J. F. *J. Org. Chem.* **2013**, *78* (17), 8437–8441.

(14) Taber, D. F.; Gerstenhaber, D. A.; Berry, J. F. *J. Org. Chem.* **2011**, *76* (18), 7614–7617.

(15) Zhou, S. Generation and Trapping of Highly Strained Reactive Intermediate: Ethyl 1,2-Cyclohexadienecarboxylate, University of Alberta, Edmonton, AB, 2015.

(16) Langer, P.; Schneider, T. *Synlett* **2000**, *2000* (04), 497–500.

(17) Inoue, K.; Nakura, R.; Okano, K.; Mori, A. *Eur. J. Org. Chem.* **2018**, *2018* (25), 3343–3347.

(18) Nakura, R.; Inoue, K.; Okano, K.; Mori, A. *Synthesis* **2019**, *51* (07), 1561–1564.

(19) Sim, J.; Jo, H.; Viji, M.; Choi, M.; Jung, J. A.; Lee, H.; Jung, J. K. *Adv. Synth. Catal.* **2018**, *360* (5), 852–858.

Apendix 1.1 Selected ^{1}H NMR and ^{13}C NMR from Chapter 2

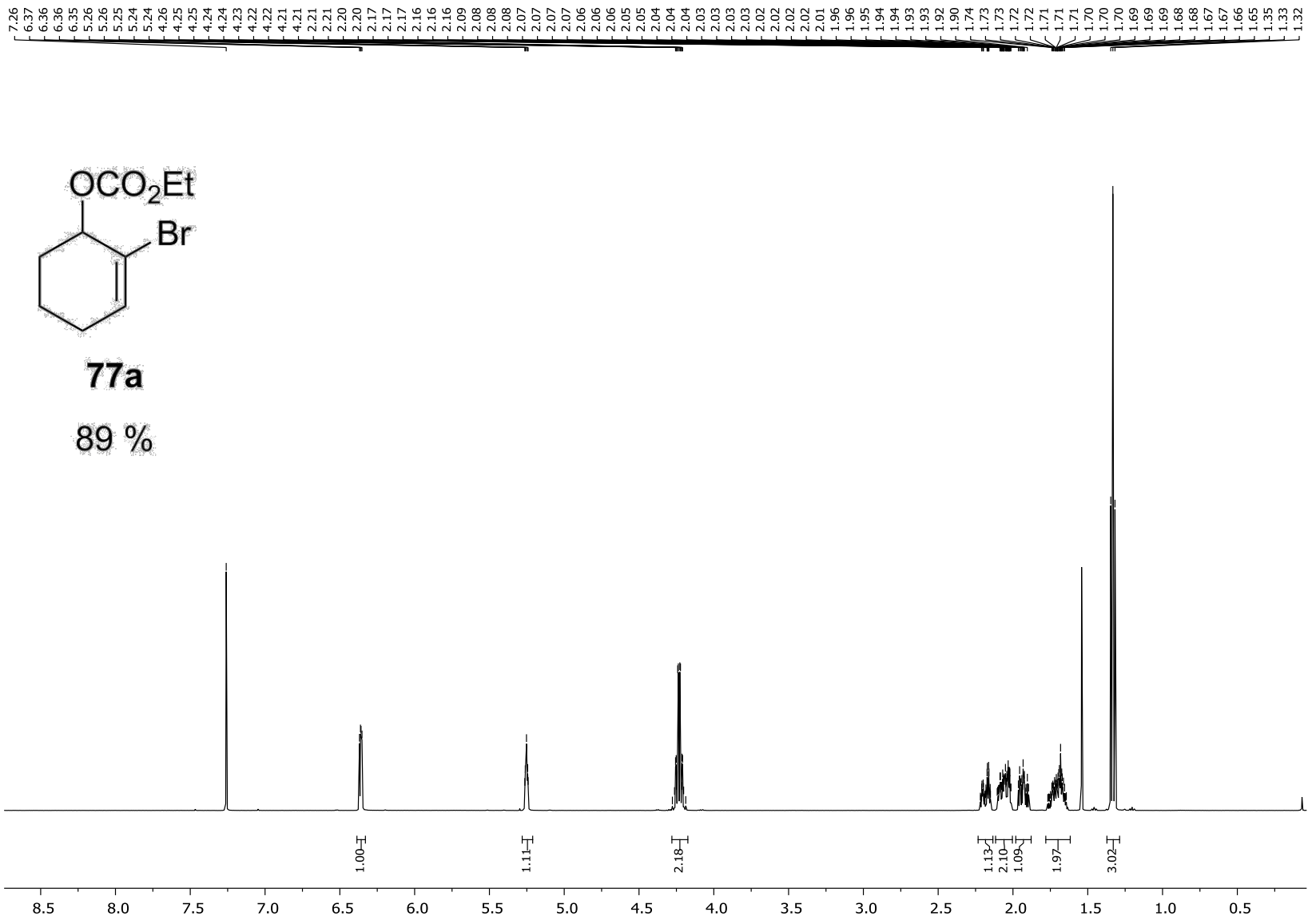
OCO2Et
Br
77a
89 %
1.00
1.11
2.18
1.13
2.10
1.09
1.97
3.02

APT for **77a** (Chapter 2)

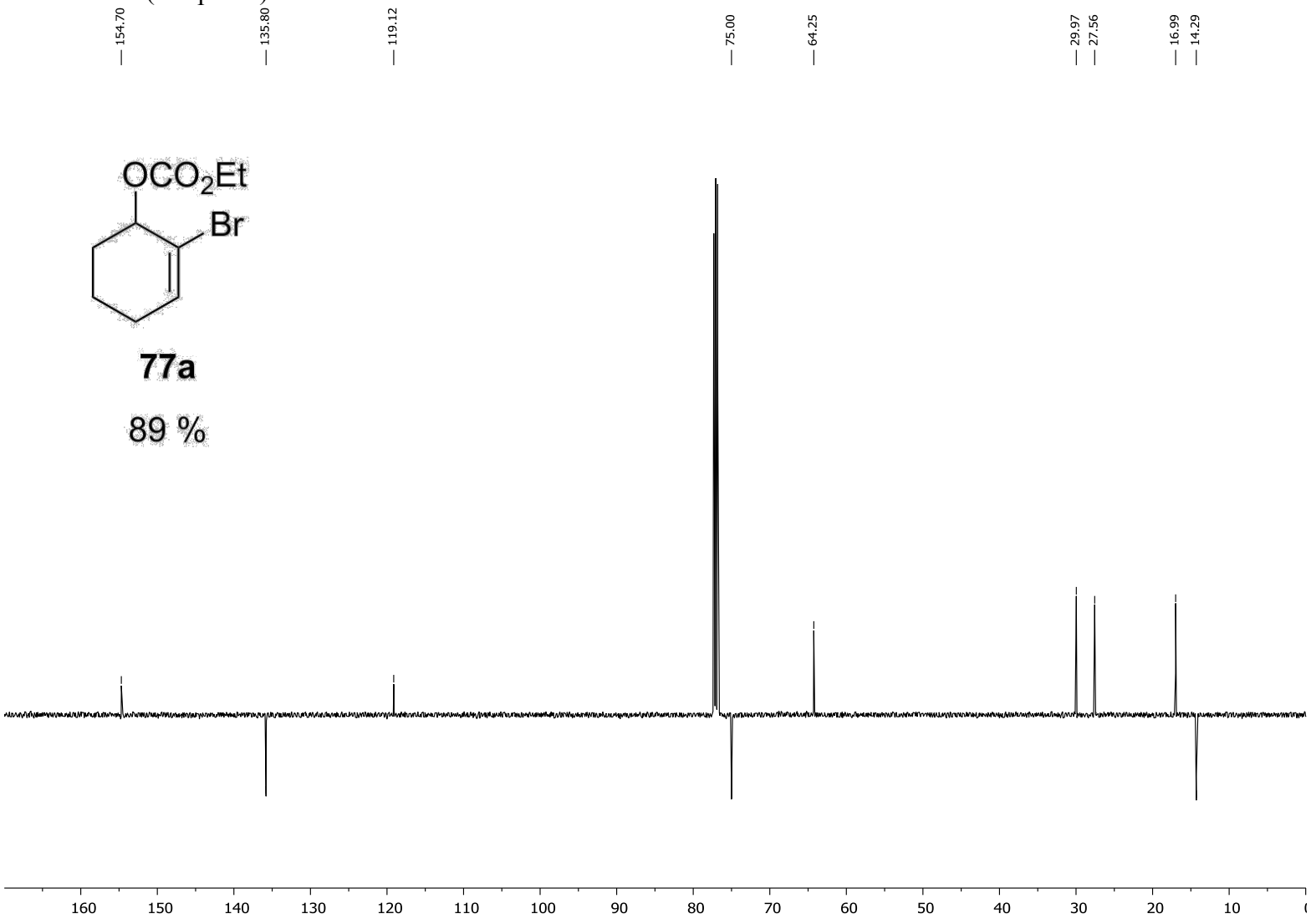

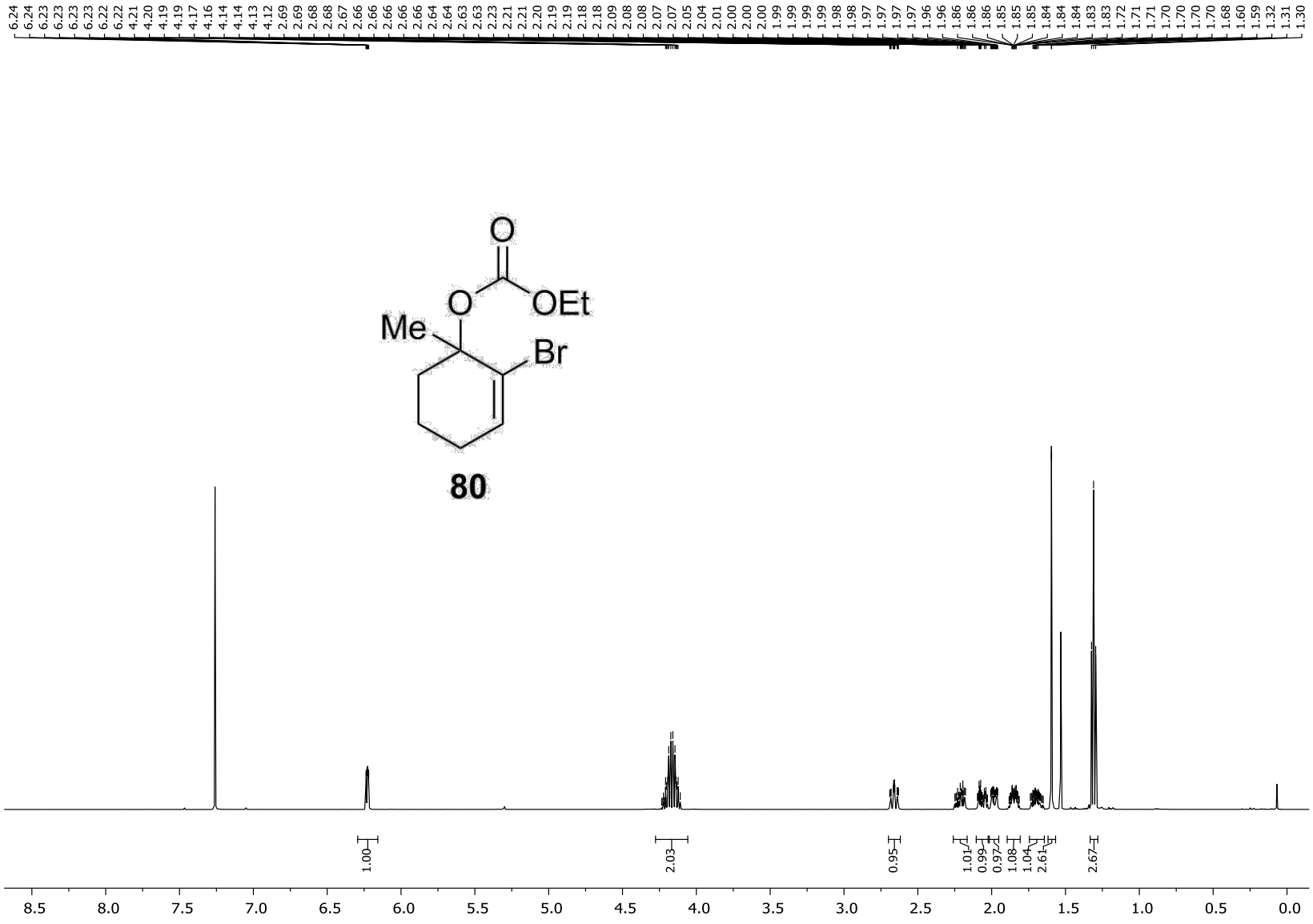
6.24 6.24 6.23 6.23 6.23 6.23 6.22 6.22 4.21 4.20 4.19 4.19 4.17 4.16 4.14 4.14 4.13 4.12 2.69 2.69 2.68 2.68 2.67 2.66 2.66 2.66 2.66 2.66 2.64 2.64 2.63 2.63 2.23 2.21 2.21 2.20 2.19 2.19 2.18 2.18 2.09 2.08 2.08 2.07 2.07 2.05 2.04 2.01 2.00 2.00 2.00 1.99 1.99 1.99 1.99 1.98 1.98 1.97 1.97 1.97 1.97 1.96 1.96 1.86 1.86 1.86 1.85 1.85 1.85 1.84 1.84 1.84 1.83 1.83 1.72 1.71 1.71 1.70 1.70 1.70 1.70 1.68 1.60 1.59 1.32 1.31 1.30
O
O
OEt
Me
Br
80
1.00
2.03
0.95
1.01
0.99
0.97
1.08
1.04
2.61
2.67
8.5 8.0 7.5 7.0 6.5 6.0 5.5 5.0 4.5 4.0 3.5 3.0 2.5 2.0 1.5 1.0 0.5 0.0

APT for **80** (Chapter 2)

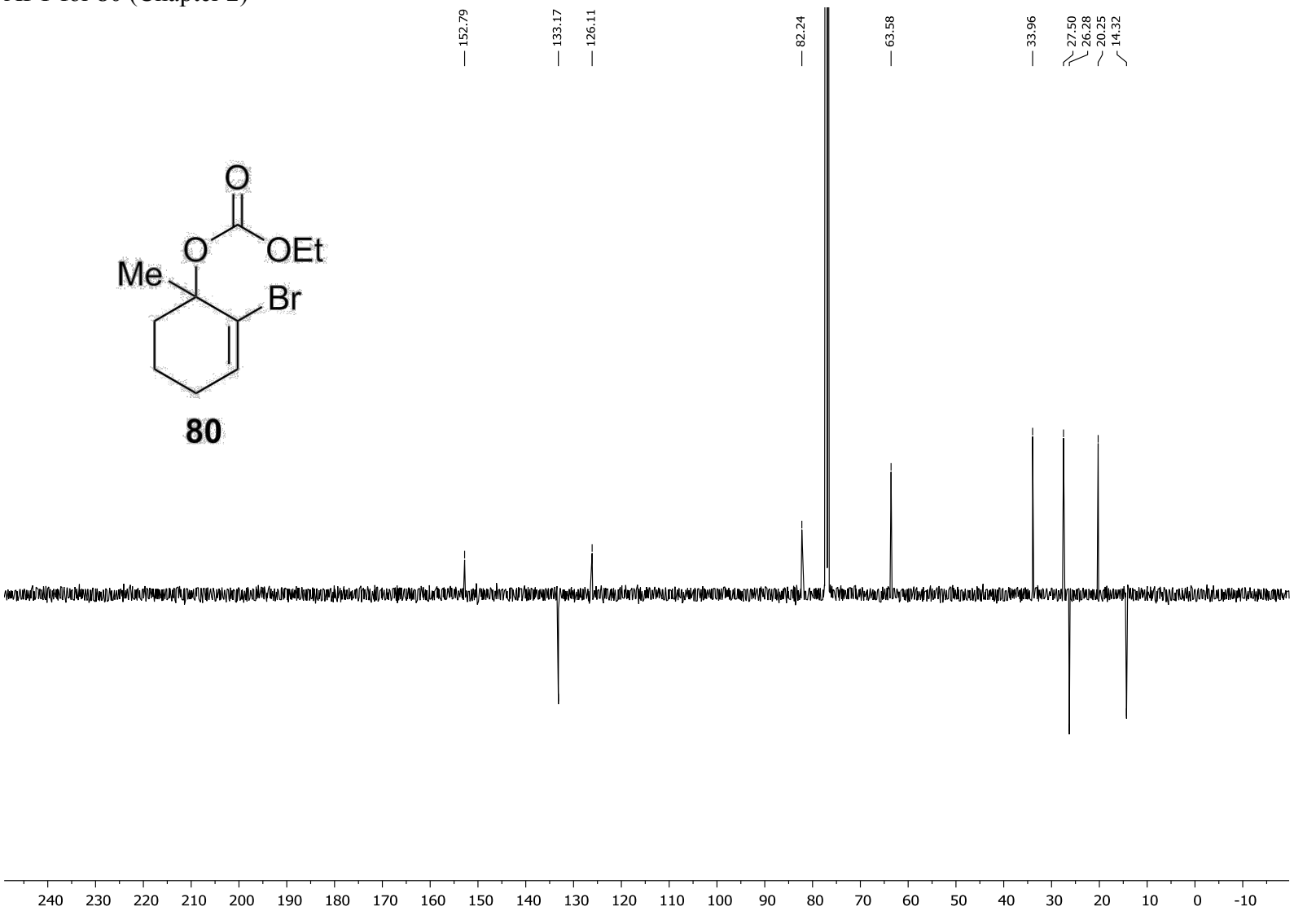

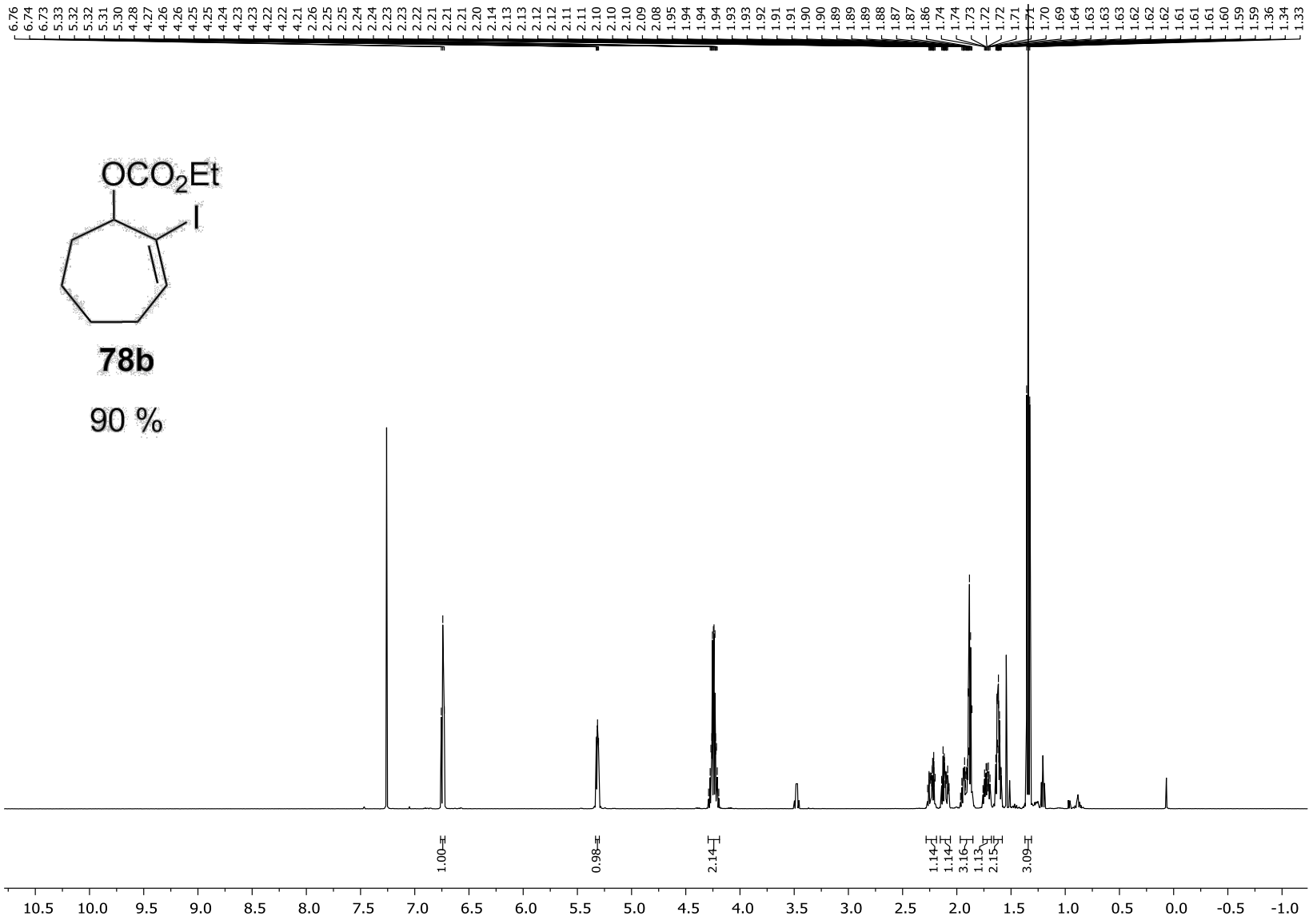
OCO2Et
I
78b
90 %

APT for **78b** (Chapter 2)

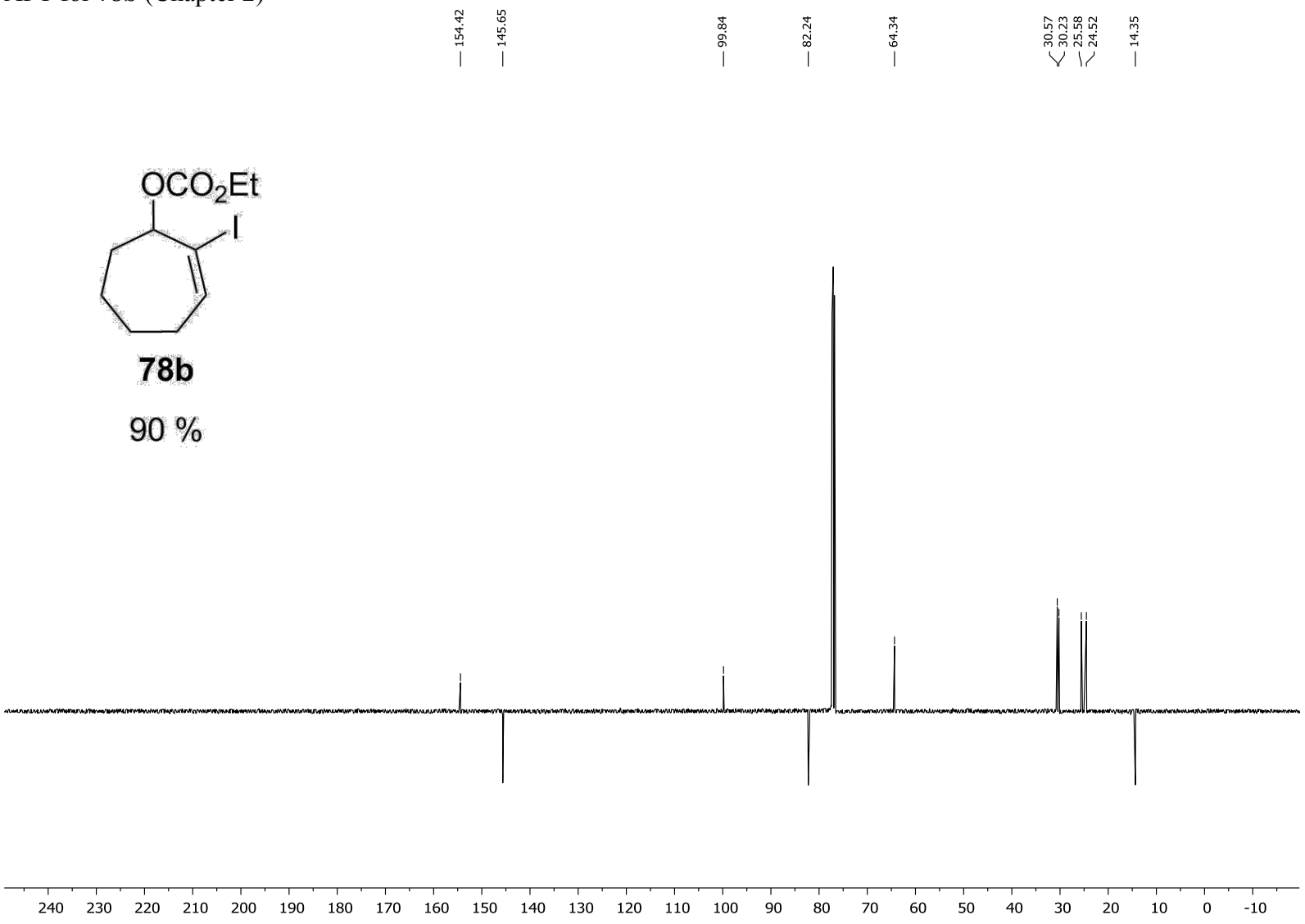

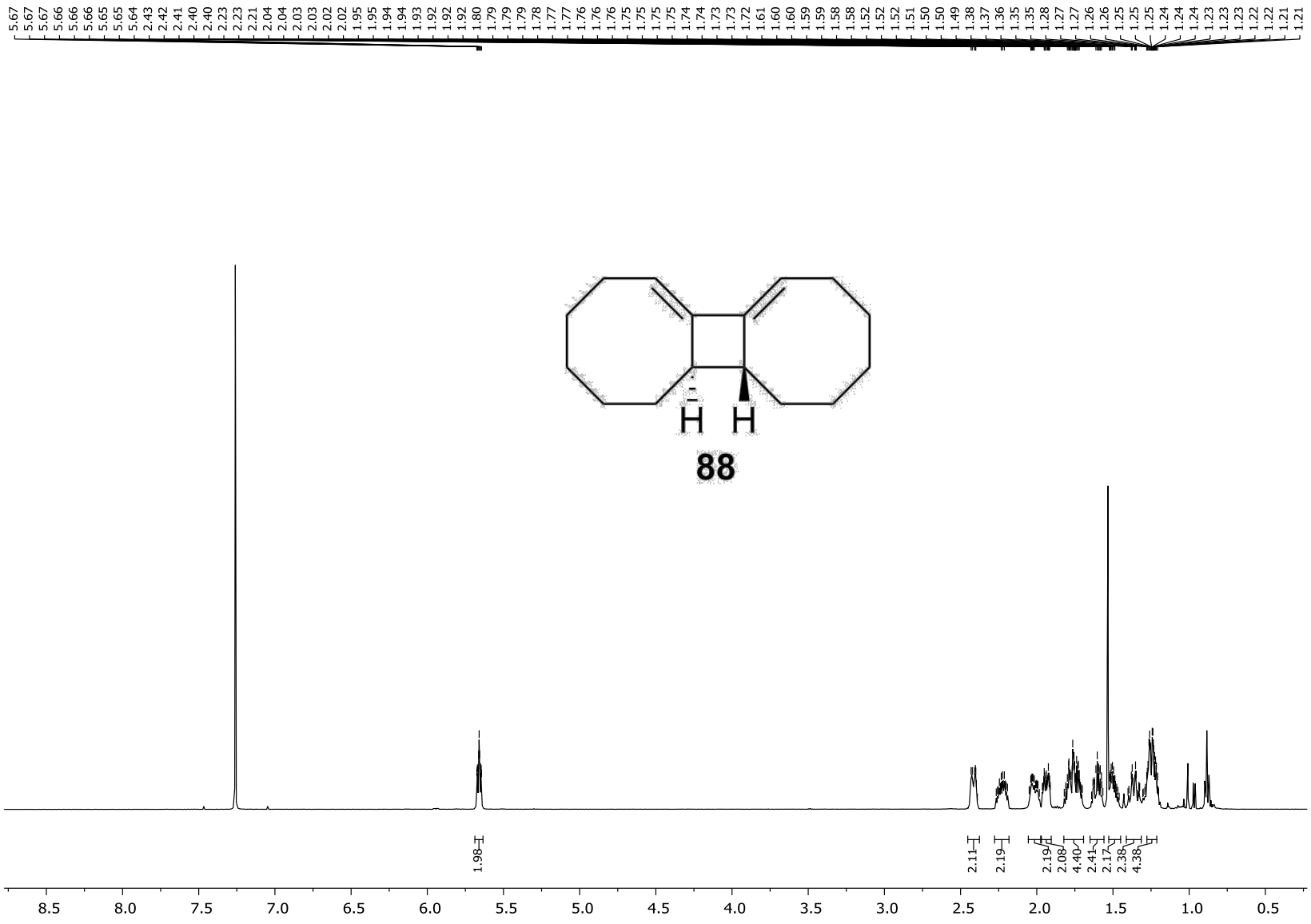
5.67 5.67 5.67 5.66 5.66 5.66 5.65 5.65 5.64 2.43 2.42 2.41 2.40 2.40 2.23 2.23 2.21 2.04 2.04 2.03 2.03 2.02 2.02 1.95 1.95 1.94 1.94 1.93 1.92 1.92 1.92 1.80 1.79 1.79 1.79 1.78 1.77 1.77 1.76 1.76 1.76 1.75 1.75 1.75 1.75 1.74 1.74 1.73 1.73 1.72 1.61 1.60 1.60 1.59 1.59 1.58 1.58 1.52 1.52 1.52 1.51 1.50 1.50 1.49 1.38 1.37 1.36 1.35 1.35 1.28 1.27 1.27 1.26 1.26 1.25 1.25 1.25 1.24 1.24 1.24 1.23 1.23 1.22 1.22 1.21 1.21
H H
88
1.98
2.11
2.19
2.19
2.08
4.40
2.41
2.17
2.38
4.38
8.5 8.0 7.5 7.0 6.5 6.0 5.5 5.0 4.5 4.0 3.5 3.0 2.5 2.0 1.5 1.0 0.5

APT for **88** (Chapter 2)

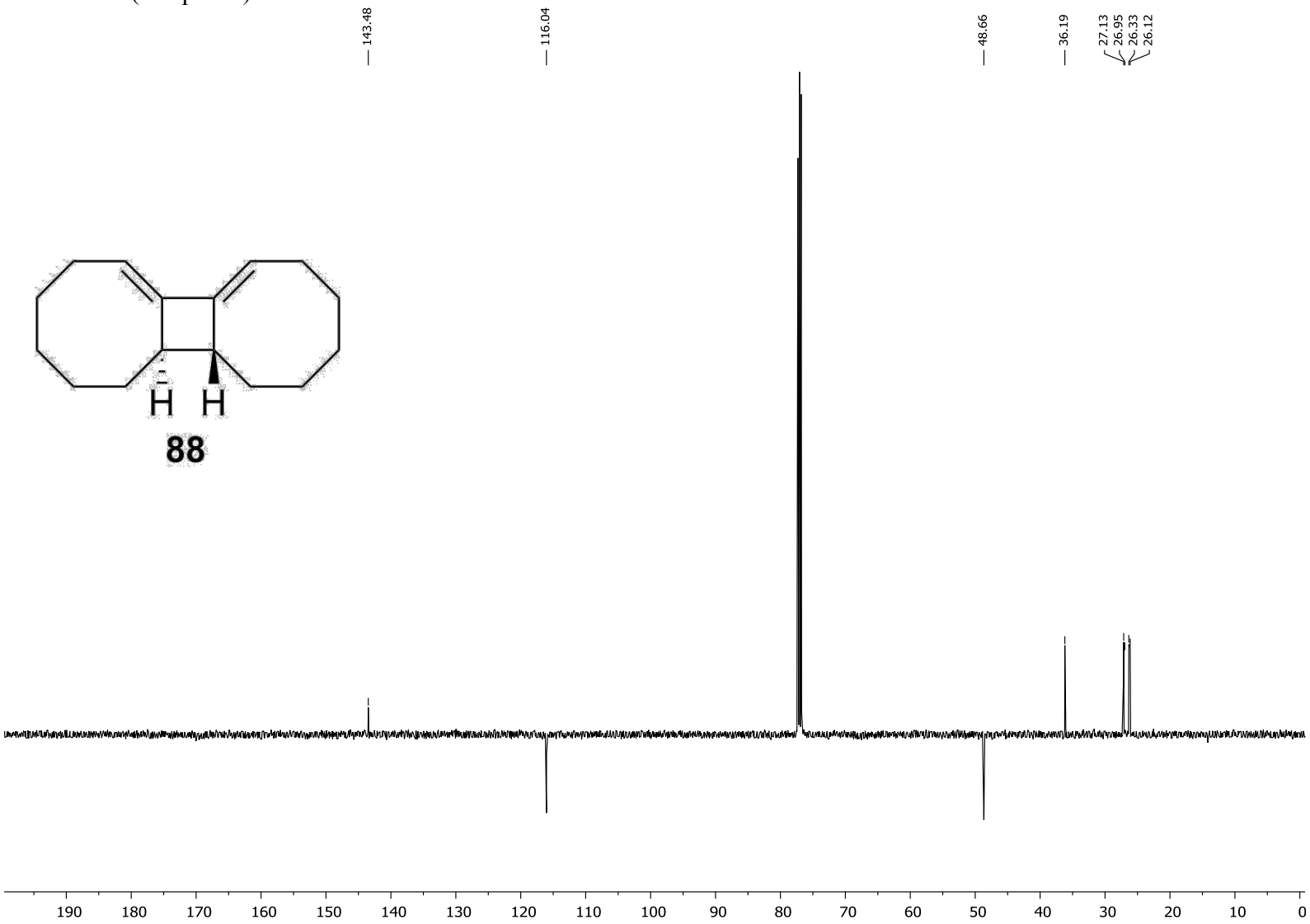

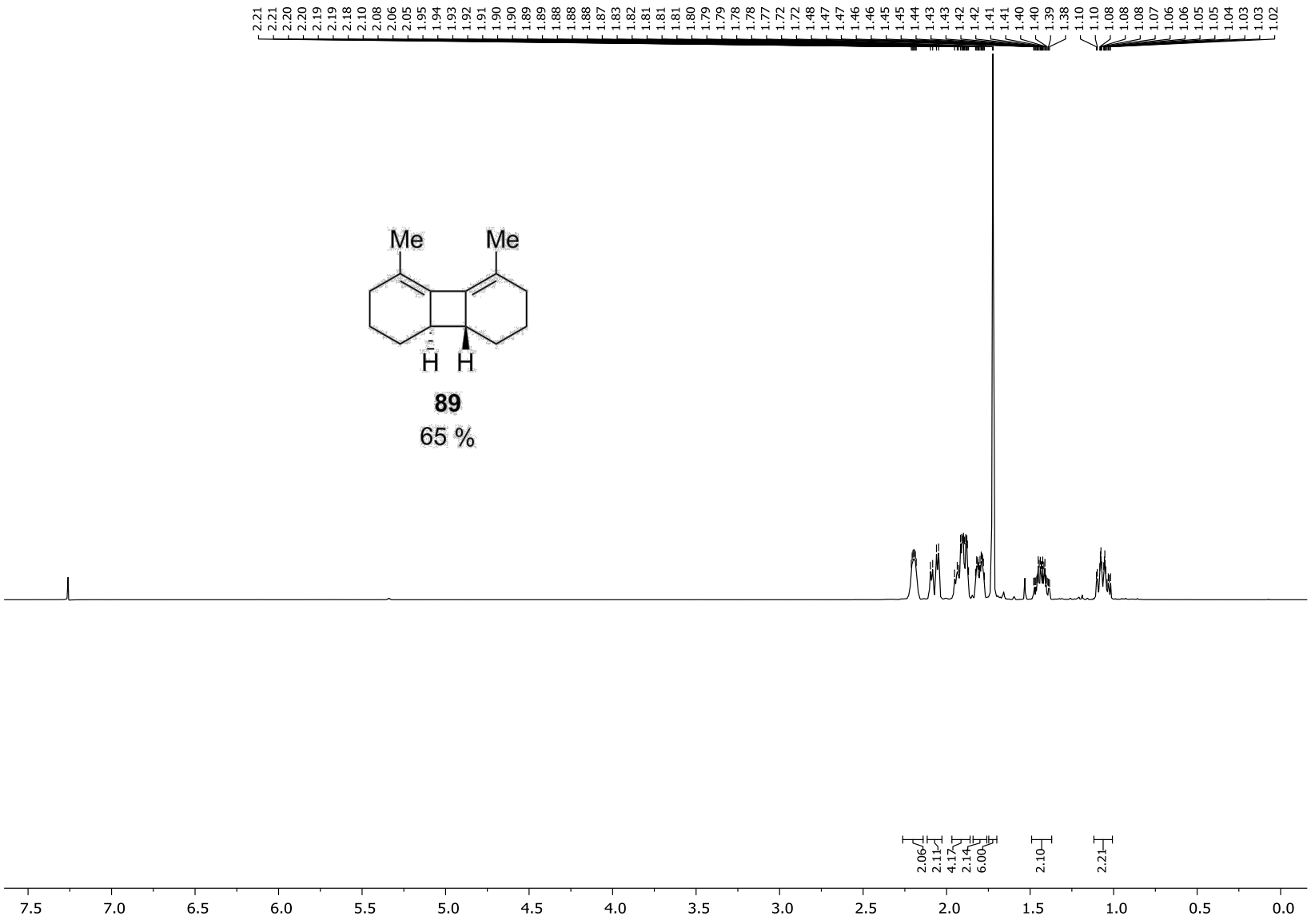
2.21 2.21 2.20 2.20 2.19 2.19 2.18 2.10 2.08 2.06 2.05 1.95 1.94 1.93 1.92 1.91 1.90 1.90 1.89 1.89 1.88 1.88 1.88 1.87 1.83 1.82 1.81 1.81 1.81 1.80 1.79 1.79 1.78 1.78 1.77 1.72 1.72 1.48 1.47 1.47 1.46 1.46 1.45 1.45 1.44 1.43 1.43 1.42 1.42 1.41 1.41 1.40 1.40 1.39 1.38 1.10 1.10 1.08 1.08 1.08 1.07 1.06 1.06 1.05 1.05 1.04 1.03 1.03 1.02
Me
Me
H
H
89
65 %
2.06
2.11
4.17
2.14
6.00
2.10
2.21
7.5
7.0
6.5
6.0
5.5
5.0
4.5
4.0
3.5
3.0
2.5
2.0
1.5
1.0
0.5
0.0

APT for **89** (Chapter 2)

Apendix 1.2 Selected ^{1}H NMR and ^{13}C NMR from Chapter 3

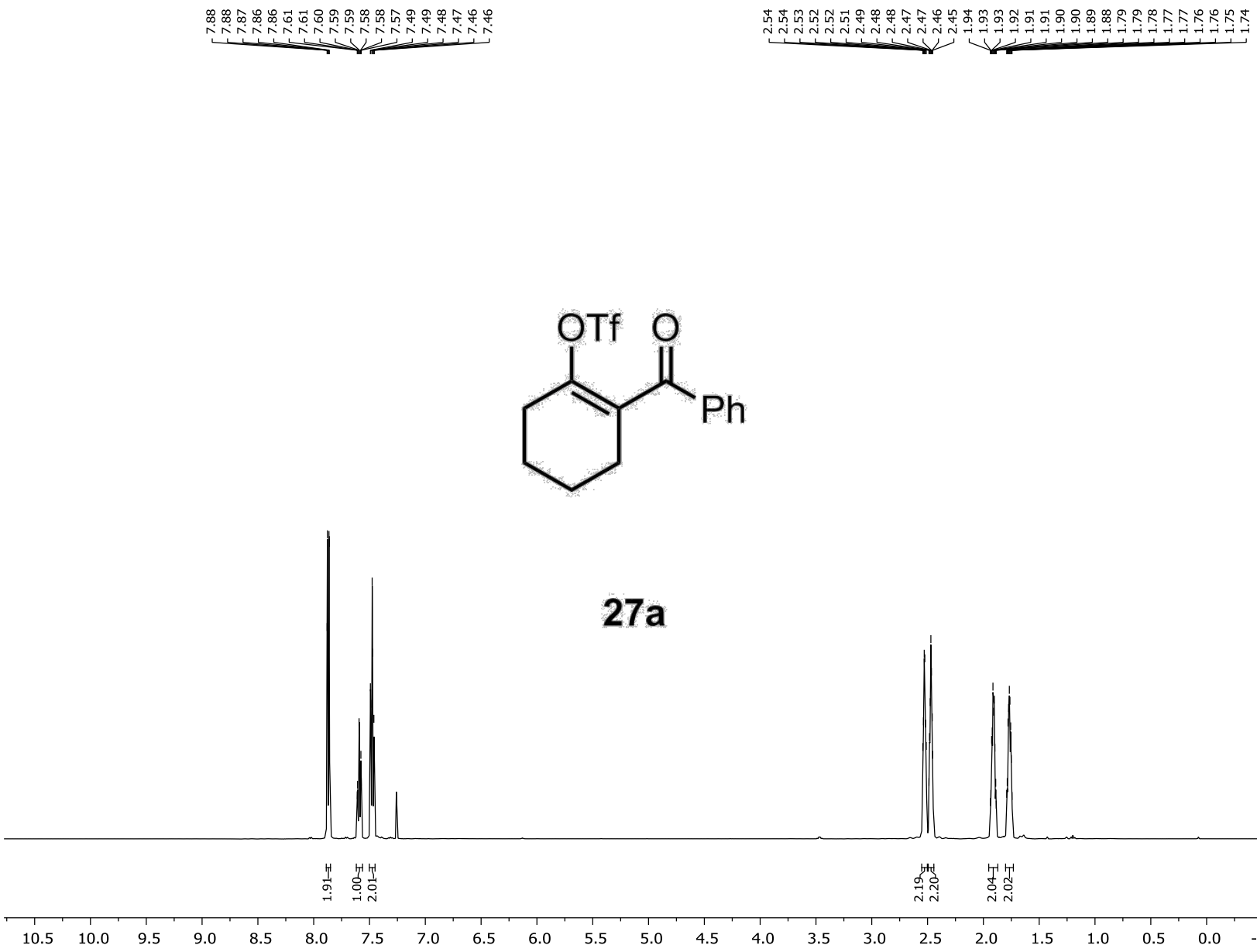
7.88
7.88
7.87
7.86
7.86
7.61
7.61
7.60
7.59
7.59
7.58
7.58
7.57
7.49
7.49
7.48
7.47
7.46
7.46
2.54
2.54
2.53
2.52
2.52
2.51
2.49
2.48
2.48
2.47
2.47
2.46
2.45
1.94
1.93
1.93
1.92
1.91
1.91
1.90
1.90
1.89
1.88
1.79
1.79
1.78
1.77
1.77
1.76
1.76
1.75
1.74
OTf
O
Ph
27a
1.91
1.00
2.01
2.19
2.20
2.04
2.02
10.5
10.0
9.5
9.0
8.5
8.0
7.5
7.0
6.5
6.0
5.5
5.0
4.5
4.0
3.5
3.0
2.5
2.0
1.5
1.0
0.5
0.0
-0.5
-1.0

APT for **27a** (Chapter 3)

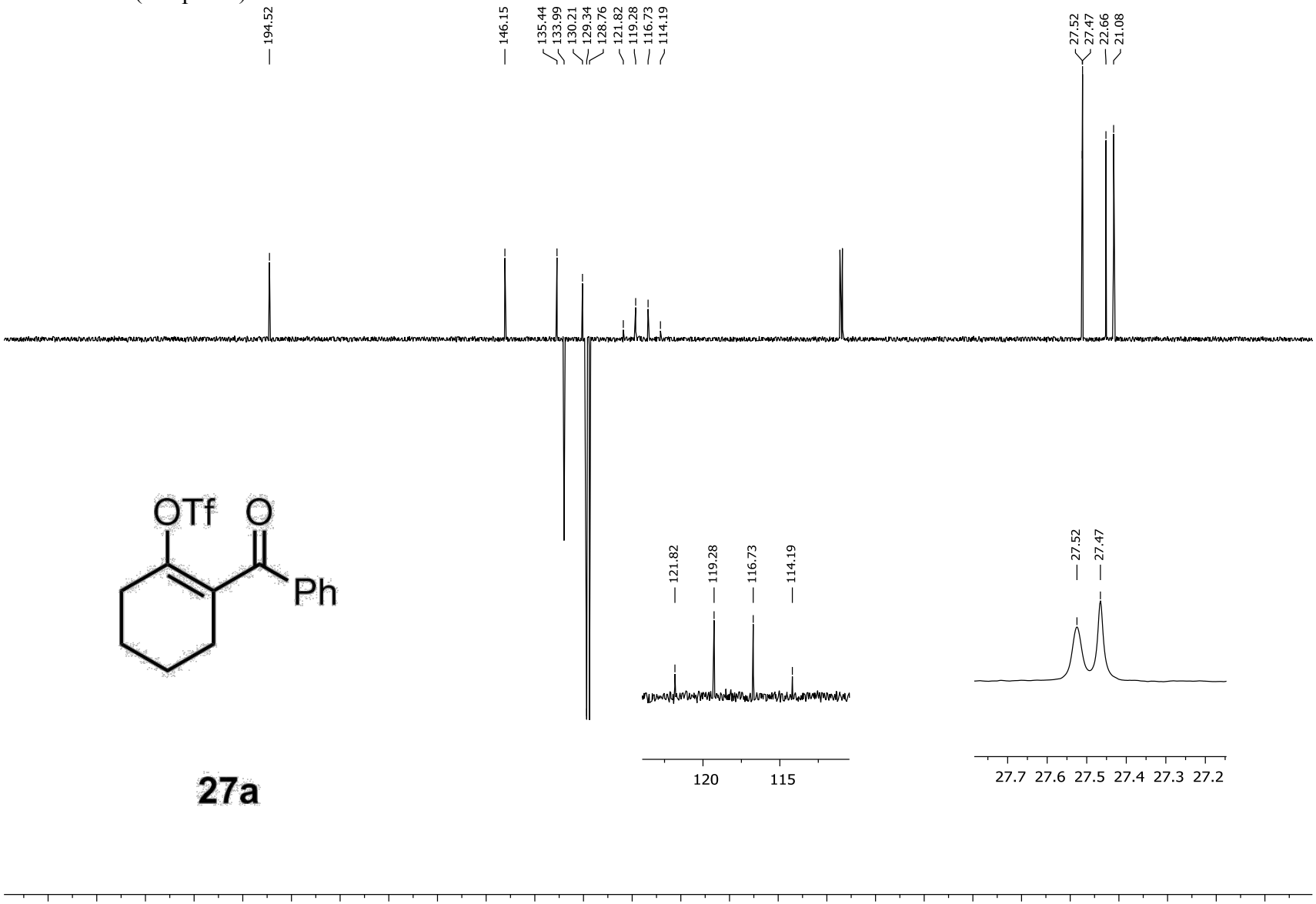

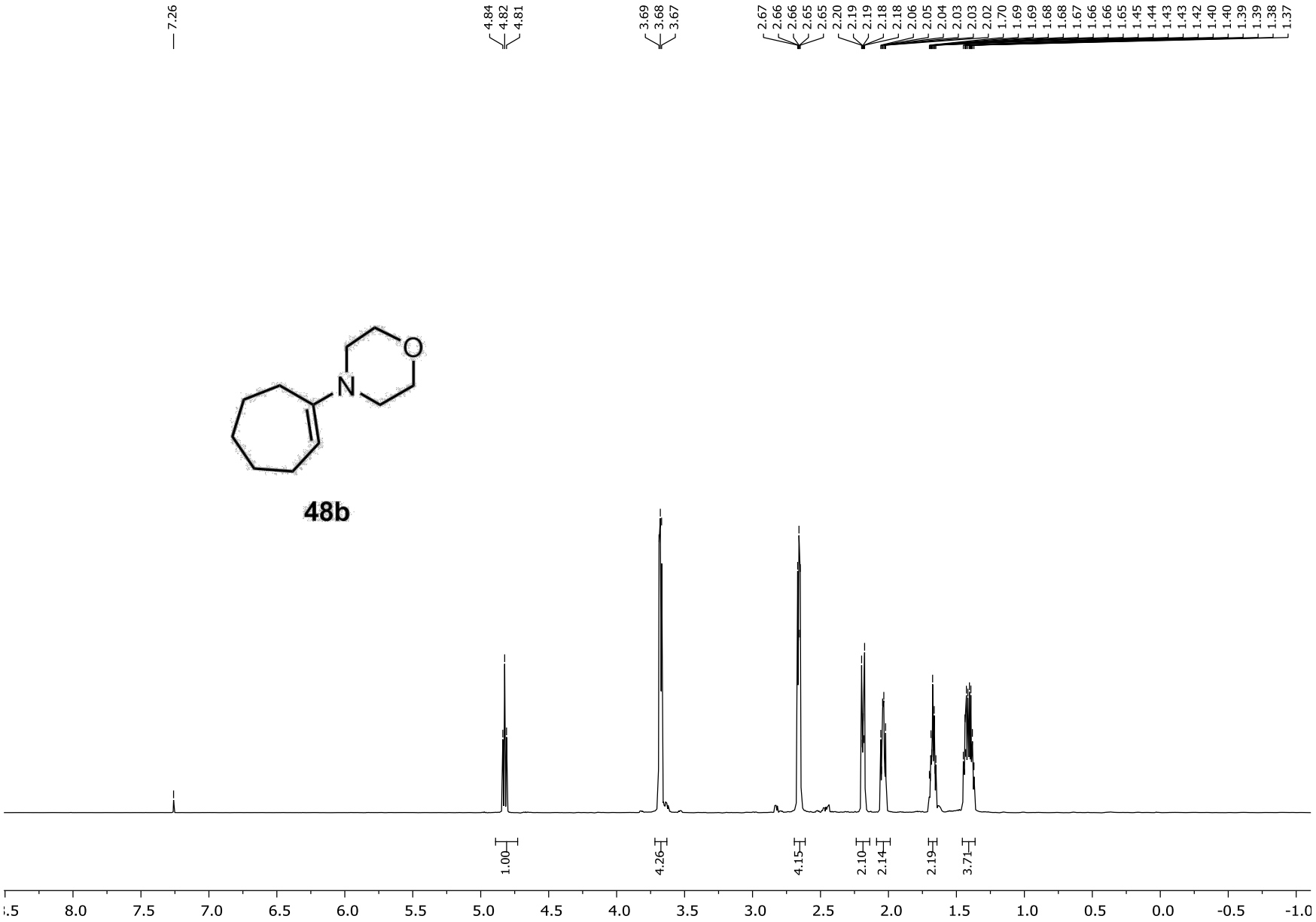
7.26
4.84
4.82
4.81
3.69
3.68
3.67
2.67
2.66
2.66
2.65
2.65
2.20
2.19
2.19
2.18
2.18
2.06
2.05
2.04
2.03
2.03
2.02
1.70
1.69
1.69
1.68
1.68
1.67
1.66
1.66
1.65
1.45
1.44
1.43
1.43
1.42
1.40
1.40
1.39
1.39
1.38
1.37
O
N
48b
1.00
4.26
4.15
2.10
2.14
2.19
3.71
8.0
7.5
7.0
6.5
6.0
5.5
5.0
4.5
4.0
3.5
3.0
2.5
2.0
1.5
1.0
0.5
0.0
-0.5
-1.0

APT for **48b** (Chapter 3)

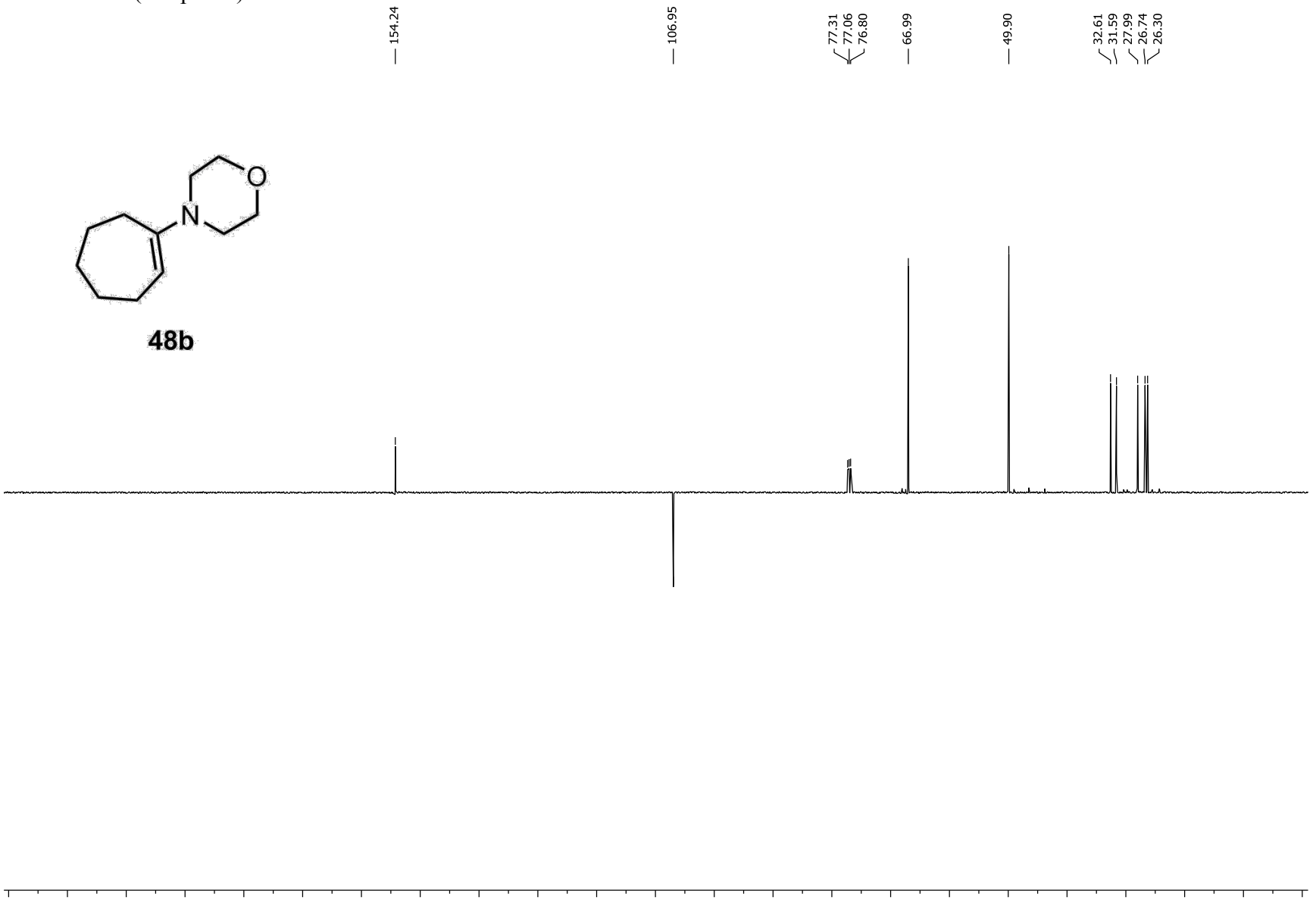

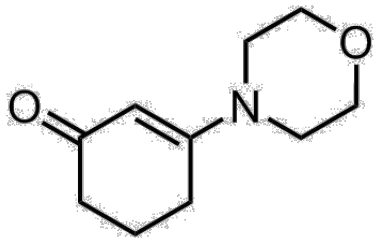
O
N
O

48f

5.27
3.75
3.74
3.74
3.74
3.73
3.73
3.73
3.31
3.30
3.30
3.30
3.29
2.42
2.41
2.40
2.32
2.31
2.30
2.29
2.03
2.02
2.01
1.99
1.98
1.12
4.11
4.11
2.09
2.12
2.09
10.5
10.0
9.5
9.0
8.5
8.0
7.5
7.0
6.5
6.0
5.5
5.0
4.5
4.0
3.5
3.0
2.5
2.0
1.5
1.0
0.5
0.0
-0.5
-1.0

APT for **48f** (Chapter 3)

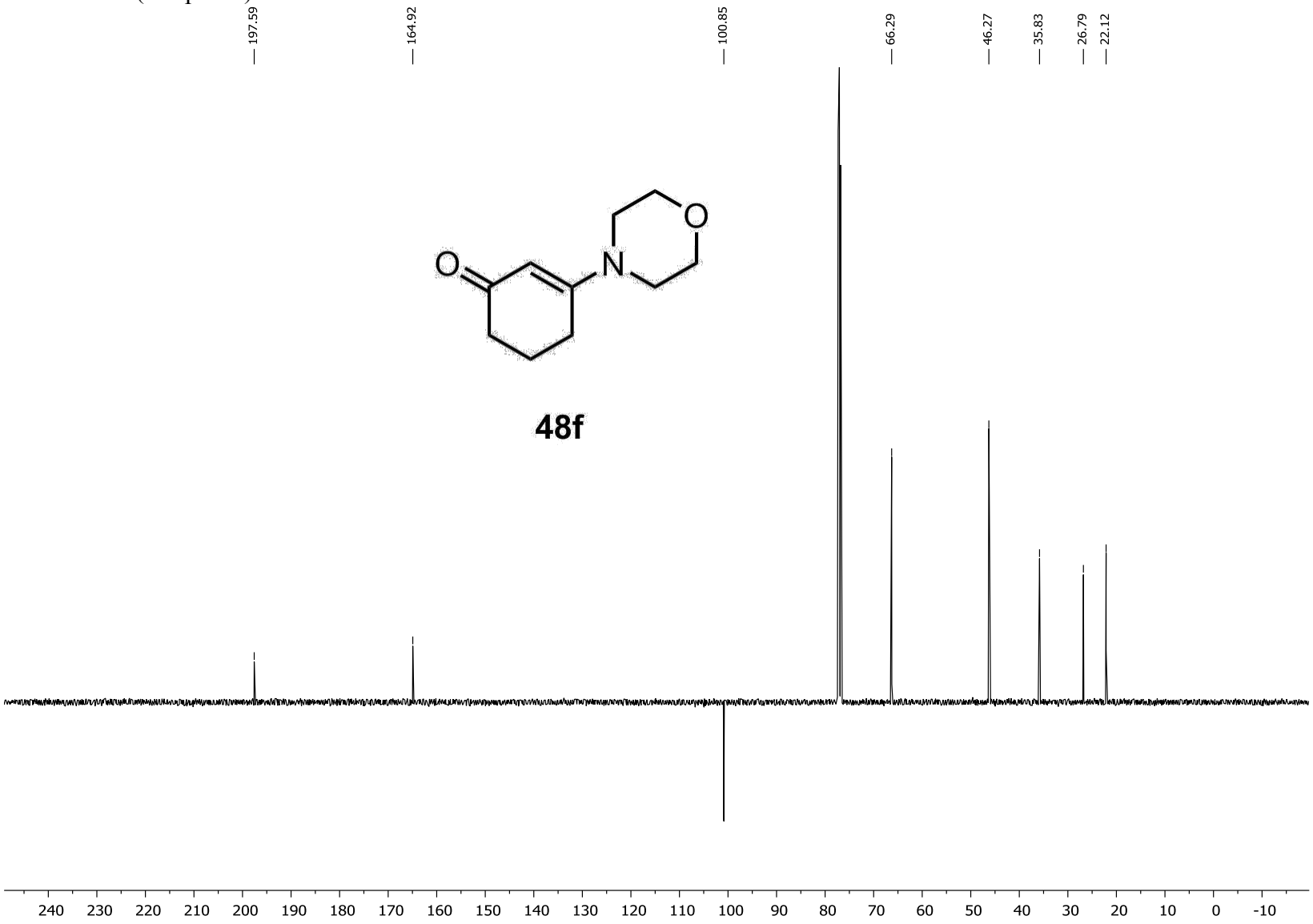

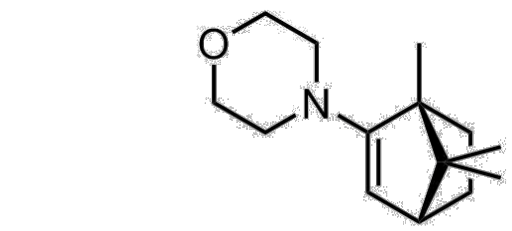
O
N

48j

0.89
3.58
4.00
0.94
1.12
1.14
1.14
2.90
1.15
2.88
2.93
10.5
10.0
9.5
9.0
8.5
8.0
7.5
7.0
6.5
6.0
5.5
5.0
4.5
4.0
3.5
3.0
2.5
2.0
1.5
1.0
0.5
0.0
-0.5
-1.0

APT for **48j** (Chapter 3)

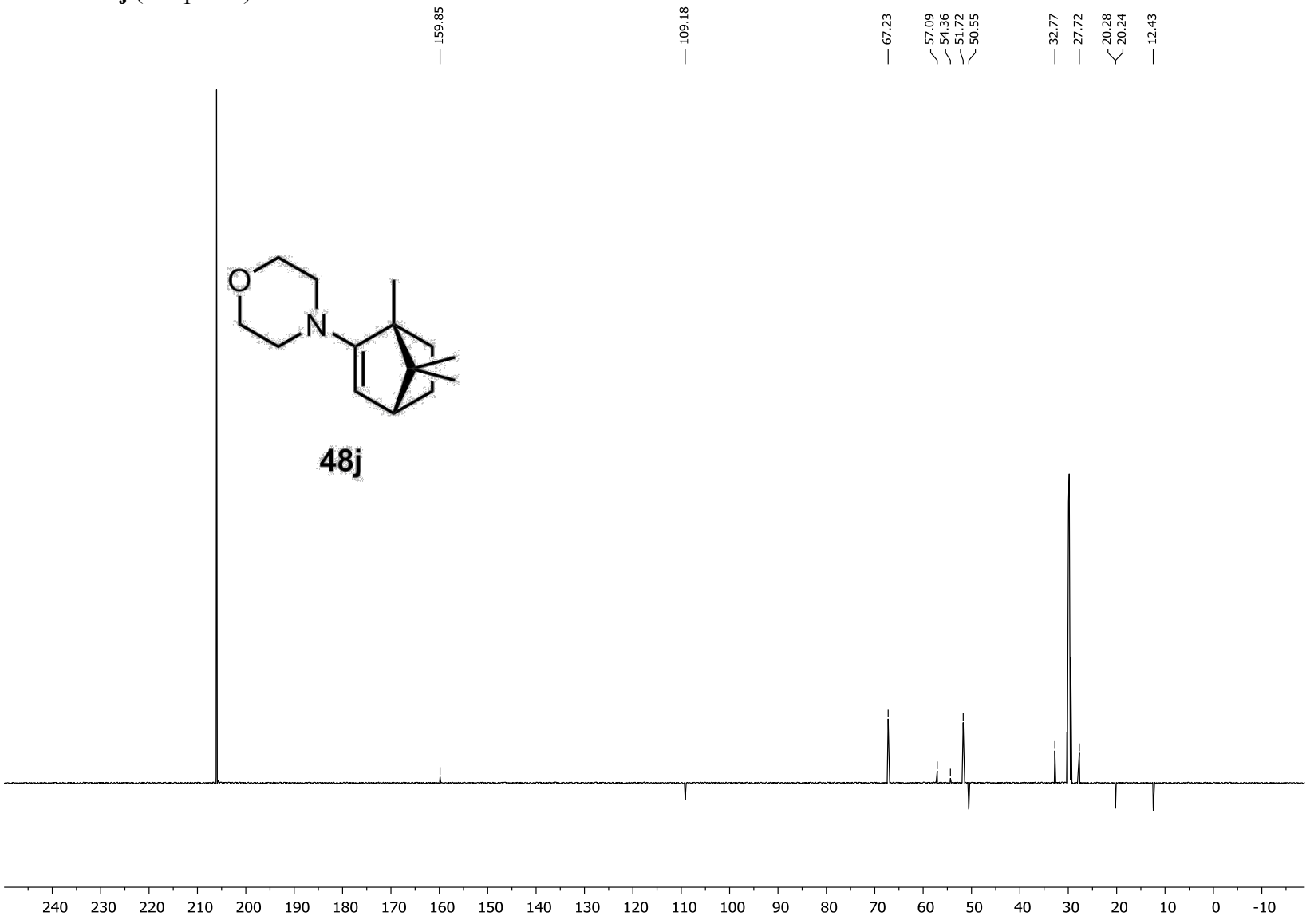

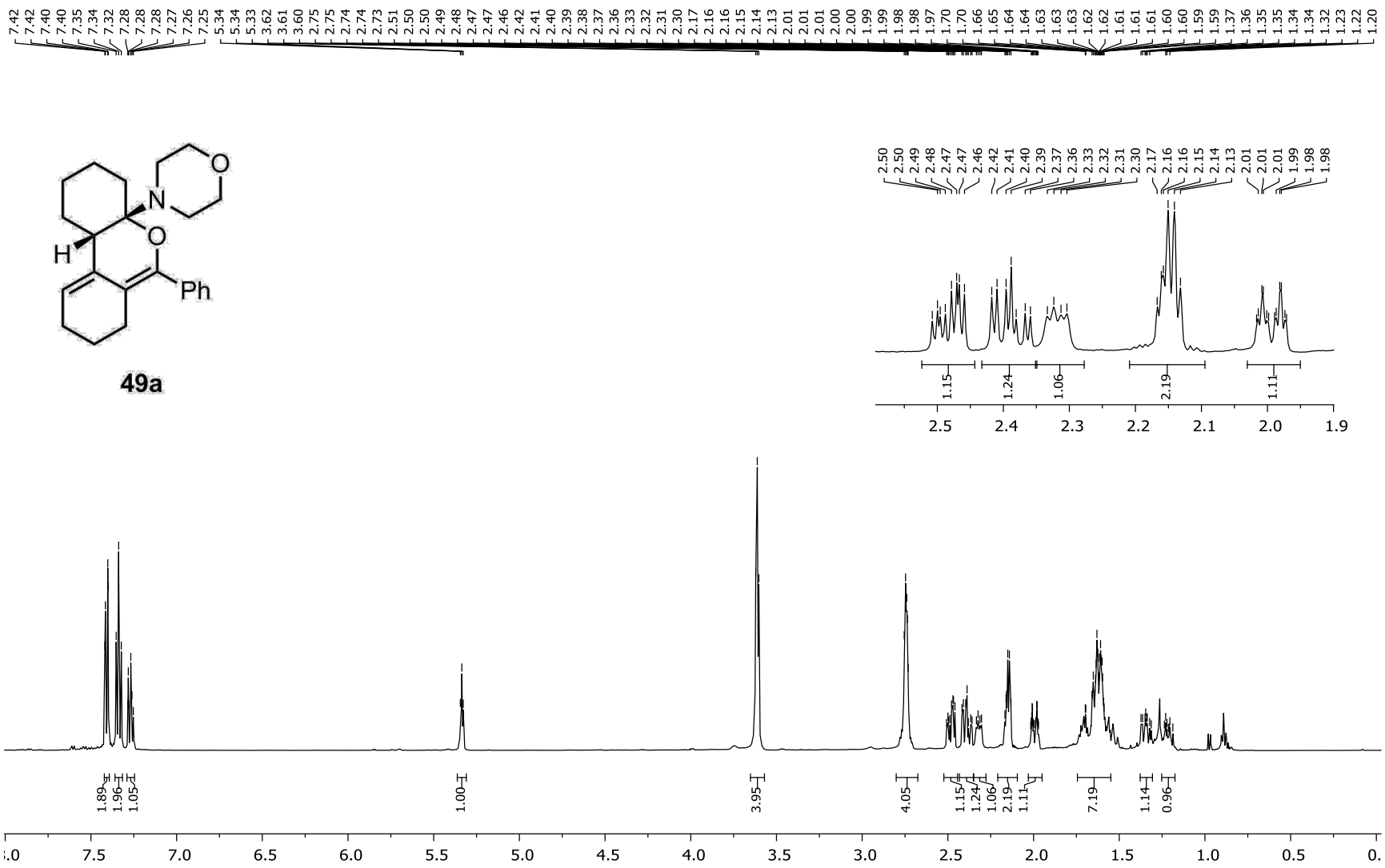
7.42 7.42 7.40 7.40 7.35 7.34 7.32 7.28 7.28 7.28 7.27 7.26 7.25
5.34 5.34 5.33 3.62 3.61 3.60 2.75 2.75 2.74 2.74 2.73 2.51 2.50 2.50 2.49 2.48 2.47 2.47 2.46 2.42 2.41 2.40 2.39 2.38 2.37 2.36 2.33 2.32 2.31 2.30 2.17 2.16 2.16 2.15 2.14 2.13 2.01 2.01 2.01 2.00 2.00 1.99 1.99 1.98 1.98 1.97 1.70 1.70 1.66 1.65 1.64 1.64 1.63 1.63 1.63 1.62 1.62 1.61 1.61 1.61 1.60 1.60 1.59 1.59 1.37 1.36 1.35 1.35 1.34 1.32 1.23 1.22 1.20
O
N
O
H
Ph
49a
2.50 2.50 2.49 2.48 2.47 2.47 2.46 2.42 2.41 2.40 2.39 2.37 2.36 2.33 2.32 2.31 2.30 2.17 2.16 2.16 2.15 2.14 2.13 2.01 2.01 2.01 1.99 1.98 1.98
1.15 1.24 1.06 2.19 1.11
2.5 2.4 2.3 2.2 2.1 2.0 1.9
1.89 1.96 1.05 1.00 3.95 4.05 1.15 1.24 1.06 2.19 1.11 7.19 1.14 0.96
7.5 7.0 6.5 6.0 5.5 5.0 4.5 4.0 3.5 3.0 2.5 2.0 1.5 1.0 0.5

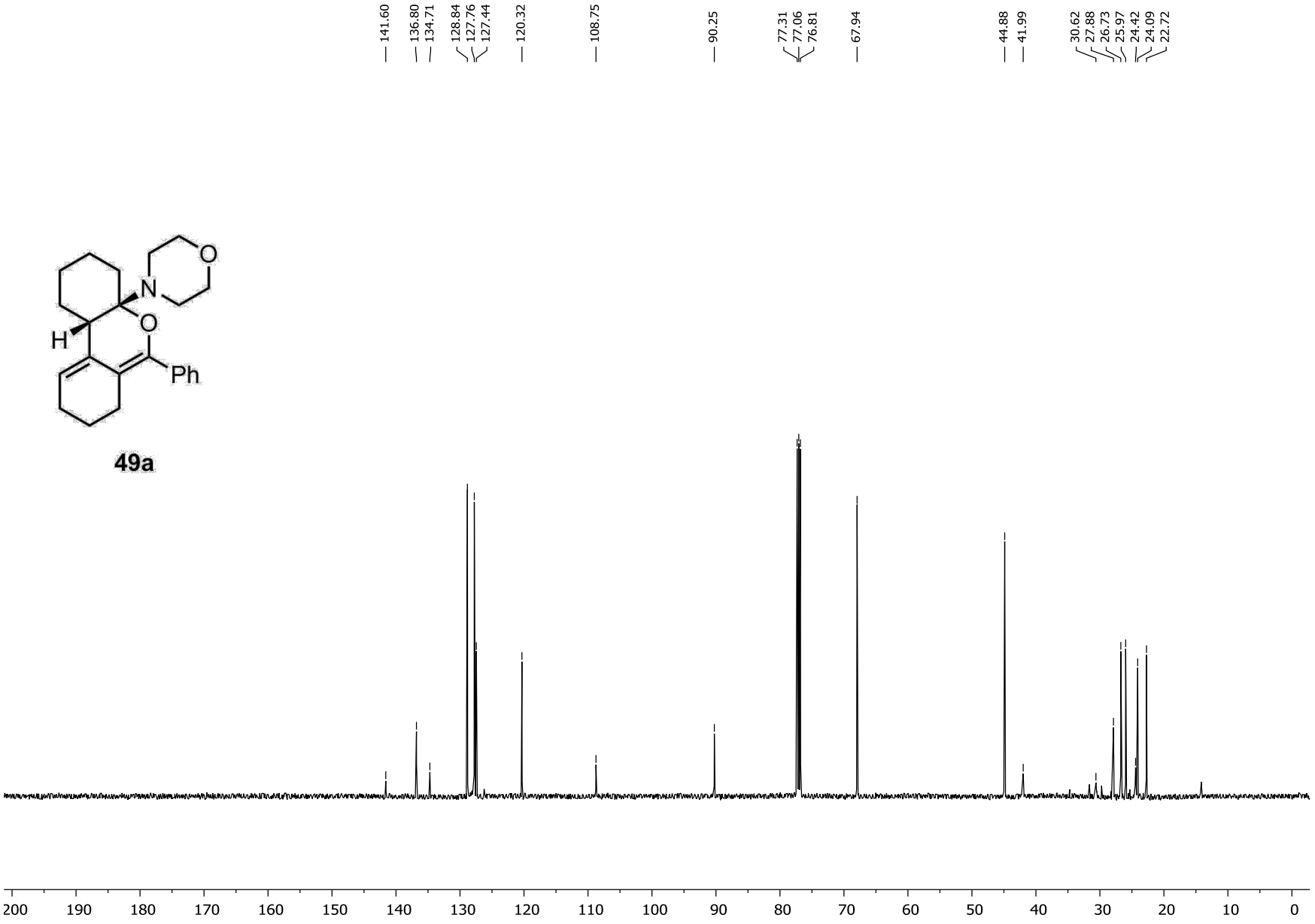
141.60
136.80
134.71
128.84
127.76
127.44
120.32
108.75
90.25
77.31
77.06
76.81
67.94
44.88
41.99
30.62
27.88
26.73
25.97
24.42
24.09
22.72
O
N
O
H
Ph
200
190
180
170
160
150
140
130
120
110
100
90
80
70
60
50
40
30
20
10
0

49a

HSQC for **49a** (Chapter 3)

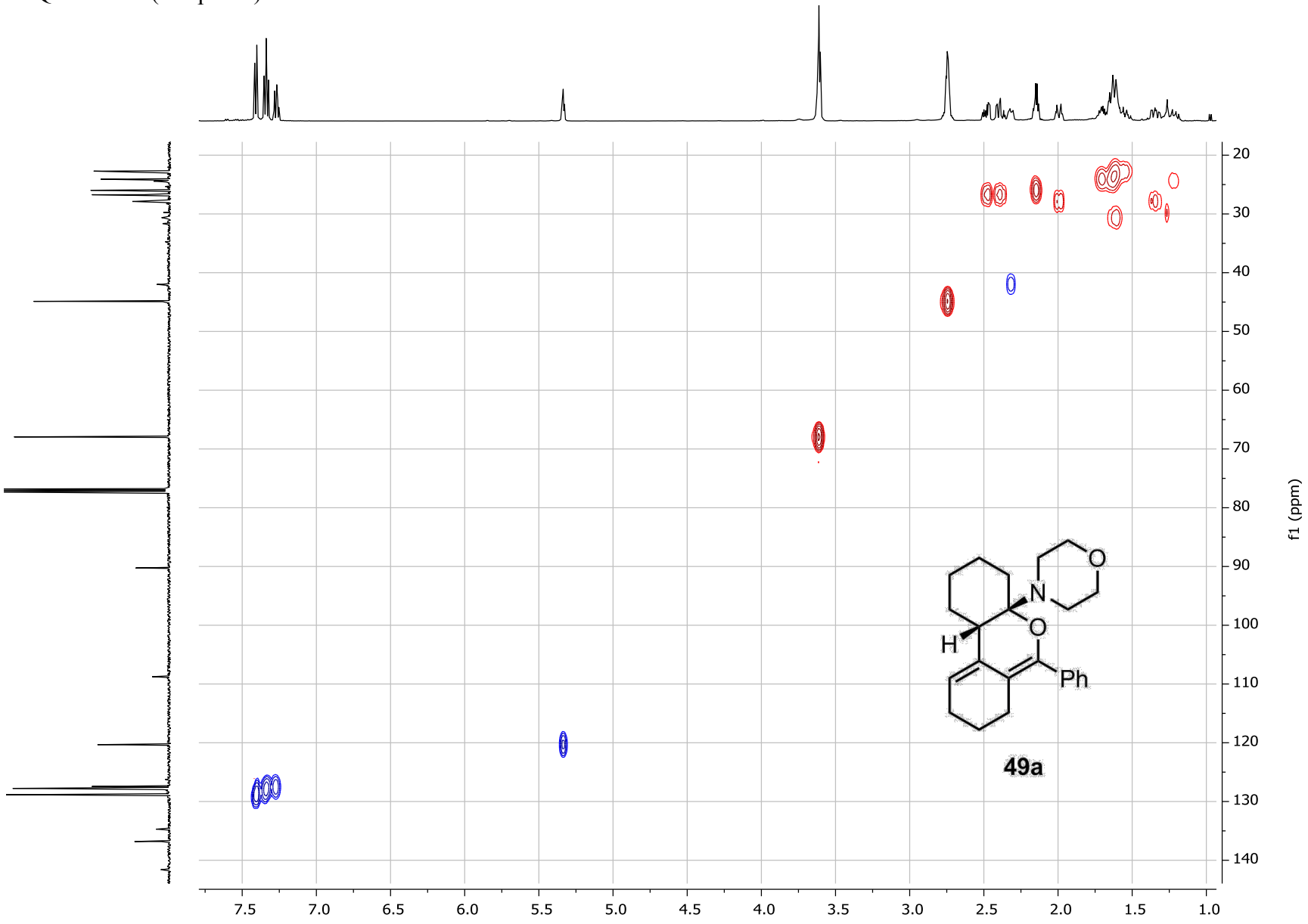

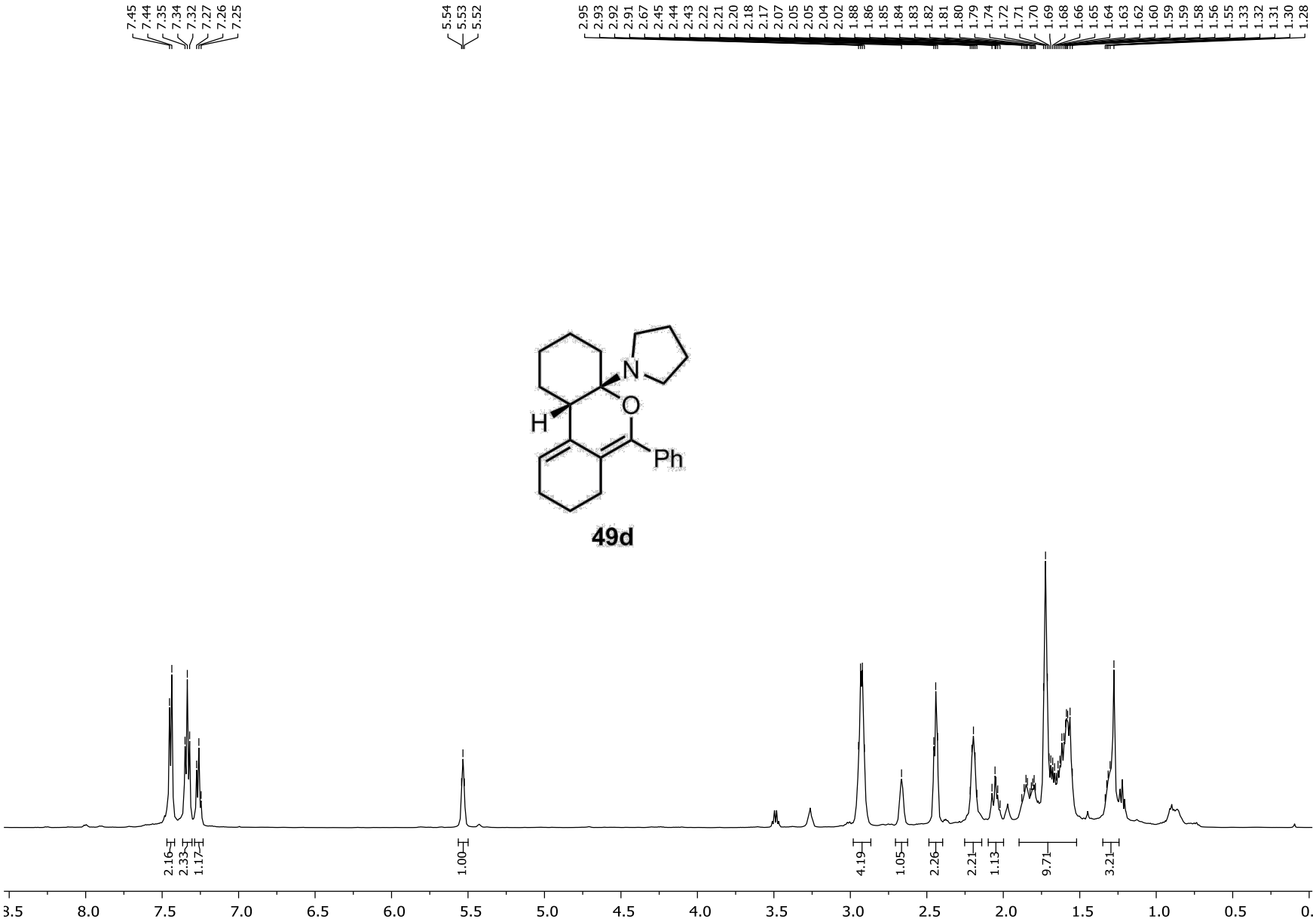
7.45
7.44
7.35
7.34
7.32
7.27
7.26
7.25
5.54
5.53
5.52
2.95
2.93
2.92
2.91
2.67
2.45
2.44
2.43
2.22
2.21
2.20
2.18
2.17
2.07
2.05
2.05
2.04
2.02
1.88
1.86
1.85
1.84
1.83
1.82
1.81
1.80
1.79
1.74
1.72
1.71
1.70
1.69
1.68
1.66
1.65
1.64
1.63
1.62
1.60
1.59
1.59
1.58
1.56
1.55
1.33
1.32
1.31
1.30
1.28
N
O
H
Ph
49d
2.16
2.33
1.17
1.00
4.19
1.05
2.26
2.21
1.13
9.71
3.21
8.0
7.5
7.0
6.5
6.0
5.5
5.0
4.5
4.0
3.5
3.0
2.5
2.0
1.5
1.0
0.5

APT for **49d** (Chapter 3)

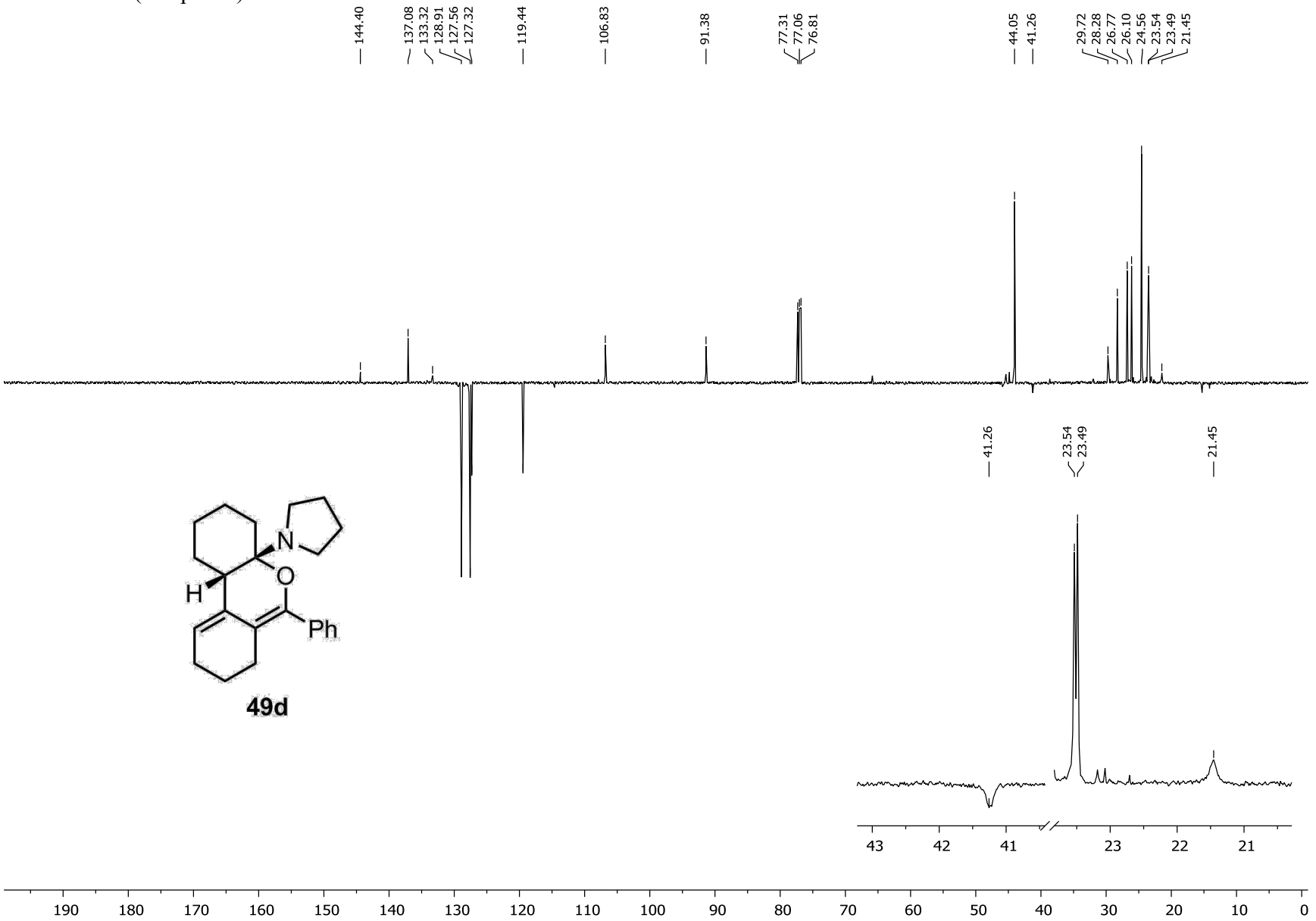

HSQC for **49d** (Chapter 3)

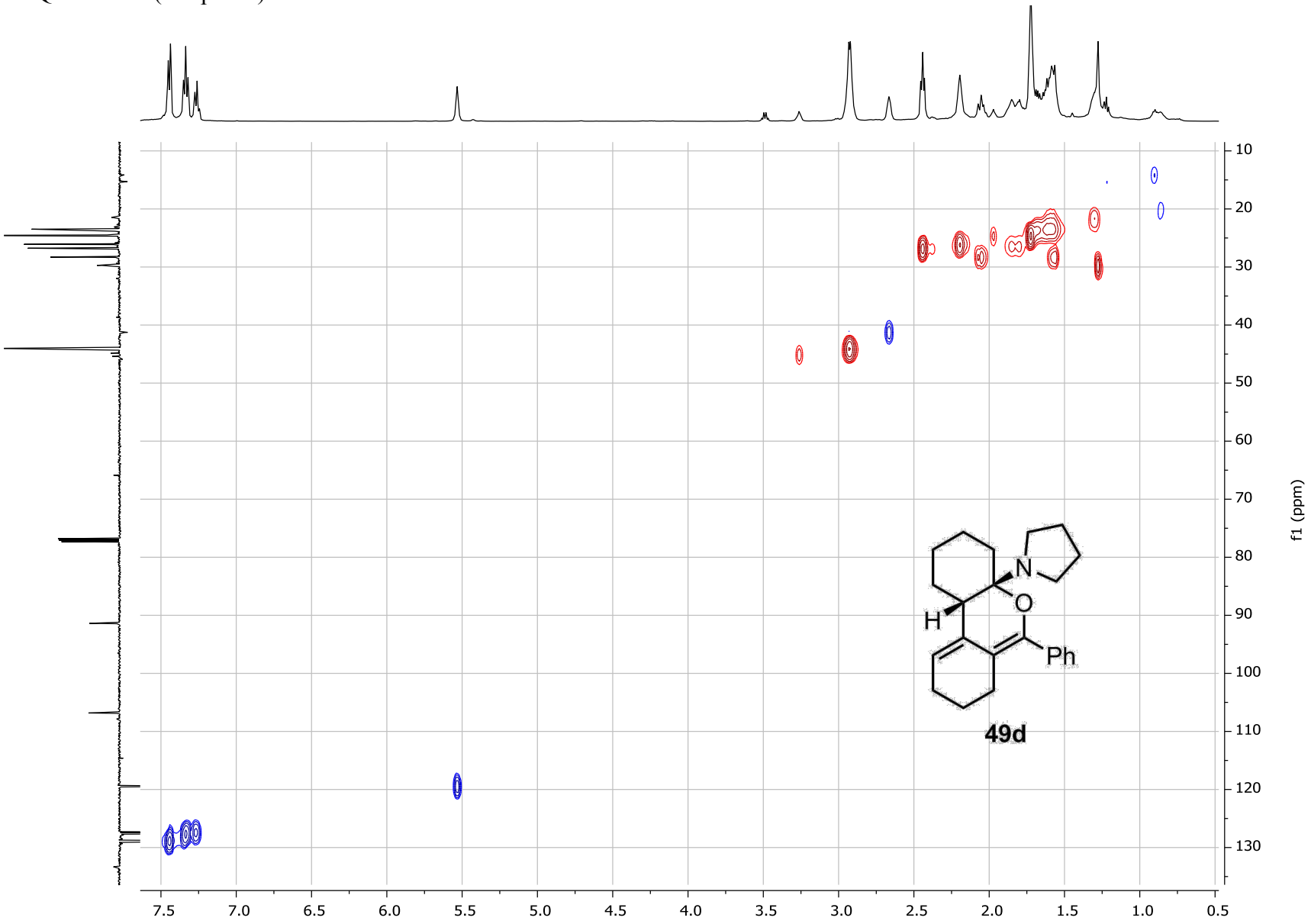

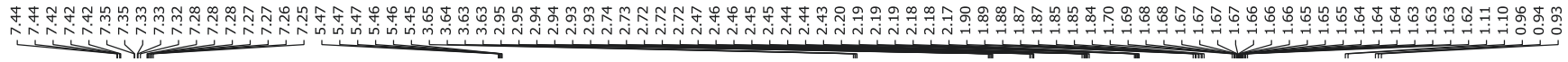
7.44 7.44 7.42 7.42 7.42 7.35 7.35 7.33 7.33 7.32 7.28 7.28 7.28 7.27 7.27 7.26 7.25
5.47 5.47 5.47 5.46 5.46 5.45 3.65 3.64 3.63 3.63 2.95 2.95 2.94 2.94 2.93 2.93 2.74 2.73 2.72 2.72 2.72 2.47 2.46 2.46 2.45 2.45 2.44 2.44 2.43 2.20 2.19 2.19 2.19 2.18 2.18 2.17 1.90 1.89 1.88 1.87 1.87 1.85 1.85 1.84 1.70 1.69 1.68 1.68 1.67 1.67 1.67 1.67 1.66 1.66 1.66 1.65 1.65 1.65 1.64 1.64 1.64 1.63 1.63 1.63 1.62 1.11 1.10 0.96 0.94 0.93

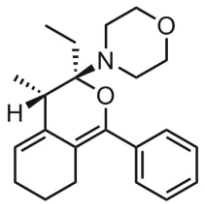
O
N
O
H

49e

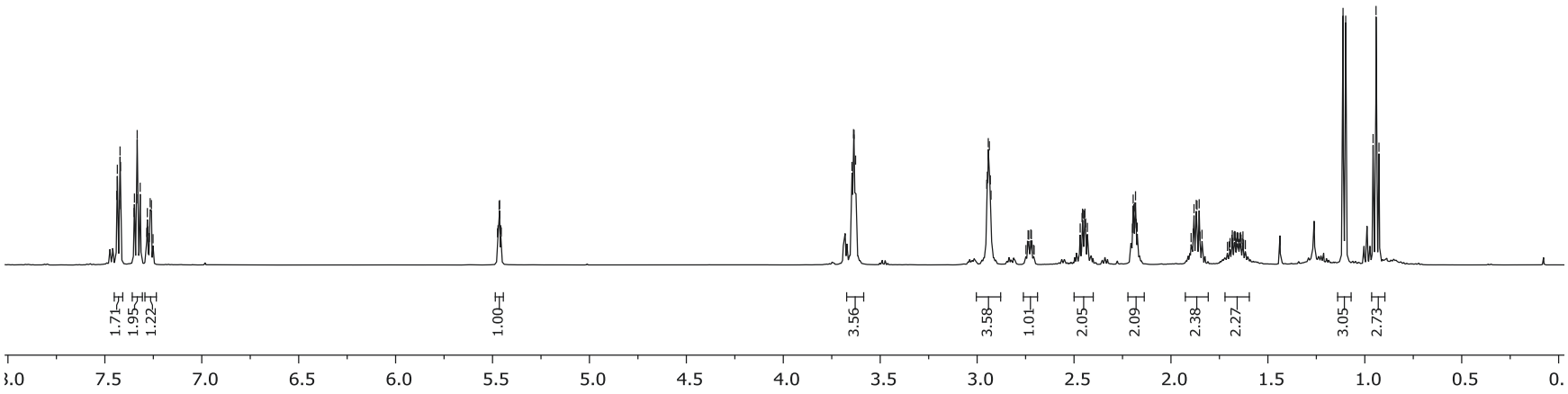
1.71
1.95
1.22
1.00
3.56
3.58
1.01
2.05
2.09
2.38
2.27
3.05
2.73
7.5
7.0
6.5
6.0
5.5
5.0
4.5
4.0
3.5
3.0
2.5
2.0
1.5
1.0
0.5

APT for **49e** (Chapter 3)

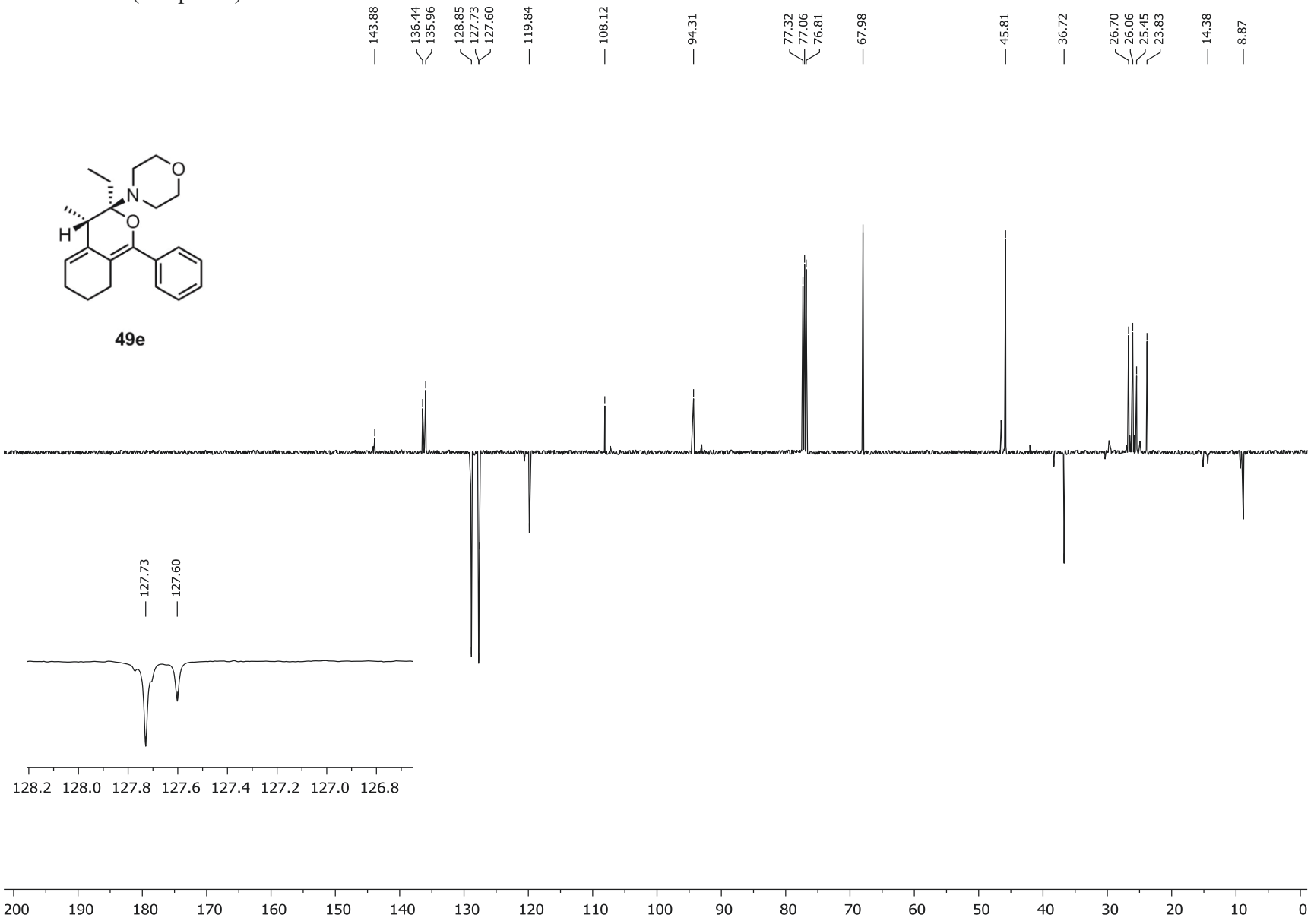

COSY for **49e** (Chapter 3)

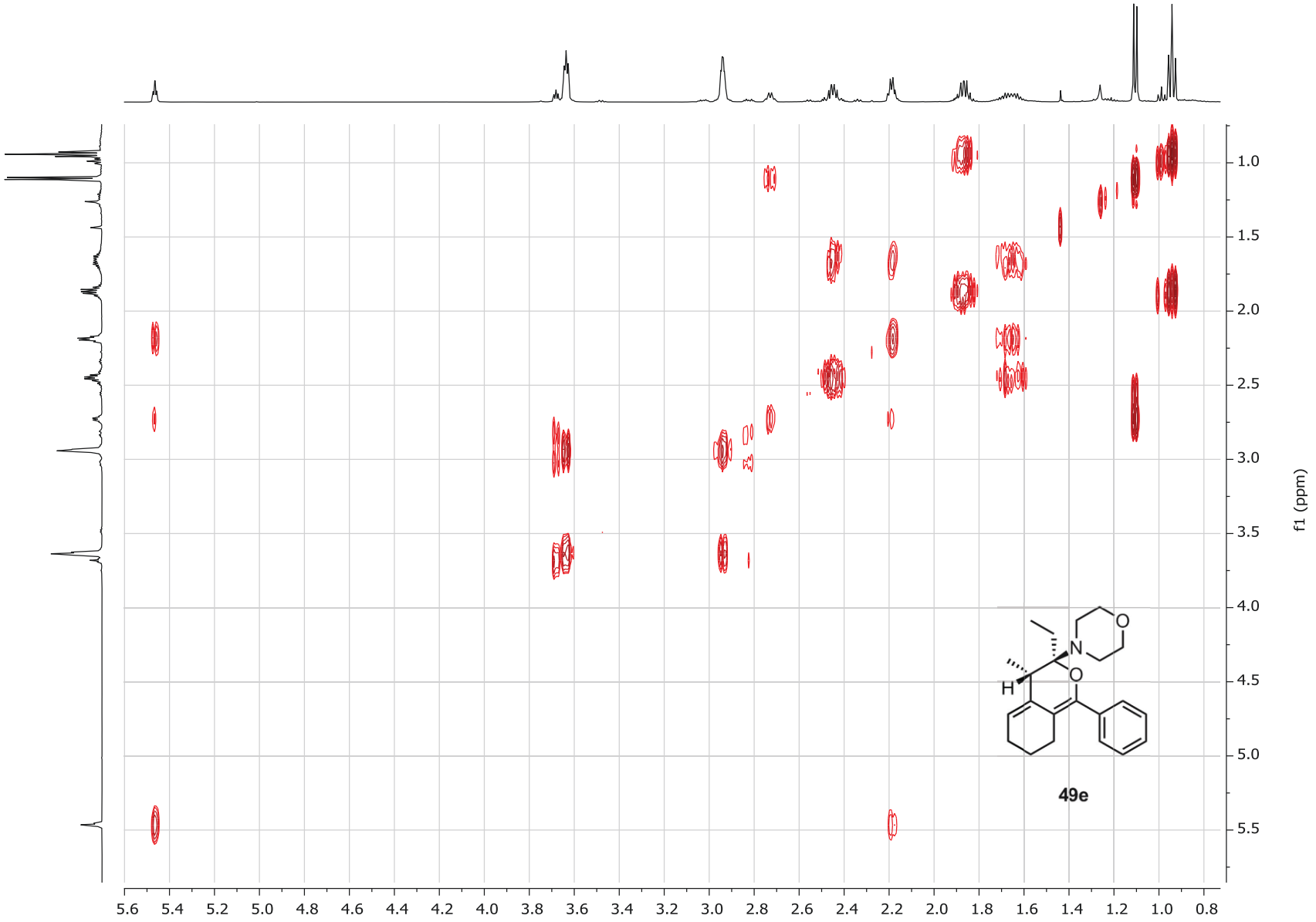

HSQC for **49e** (Chapter 3)

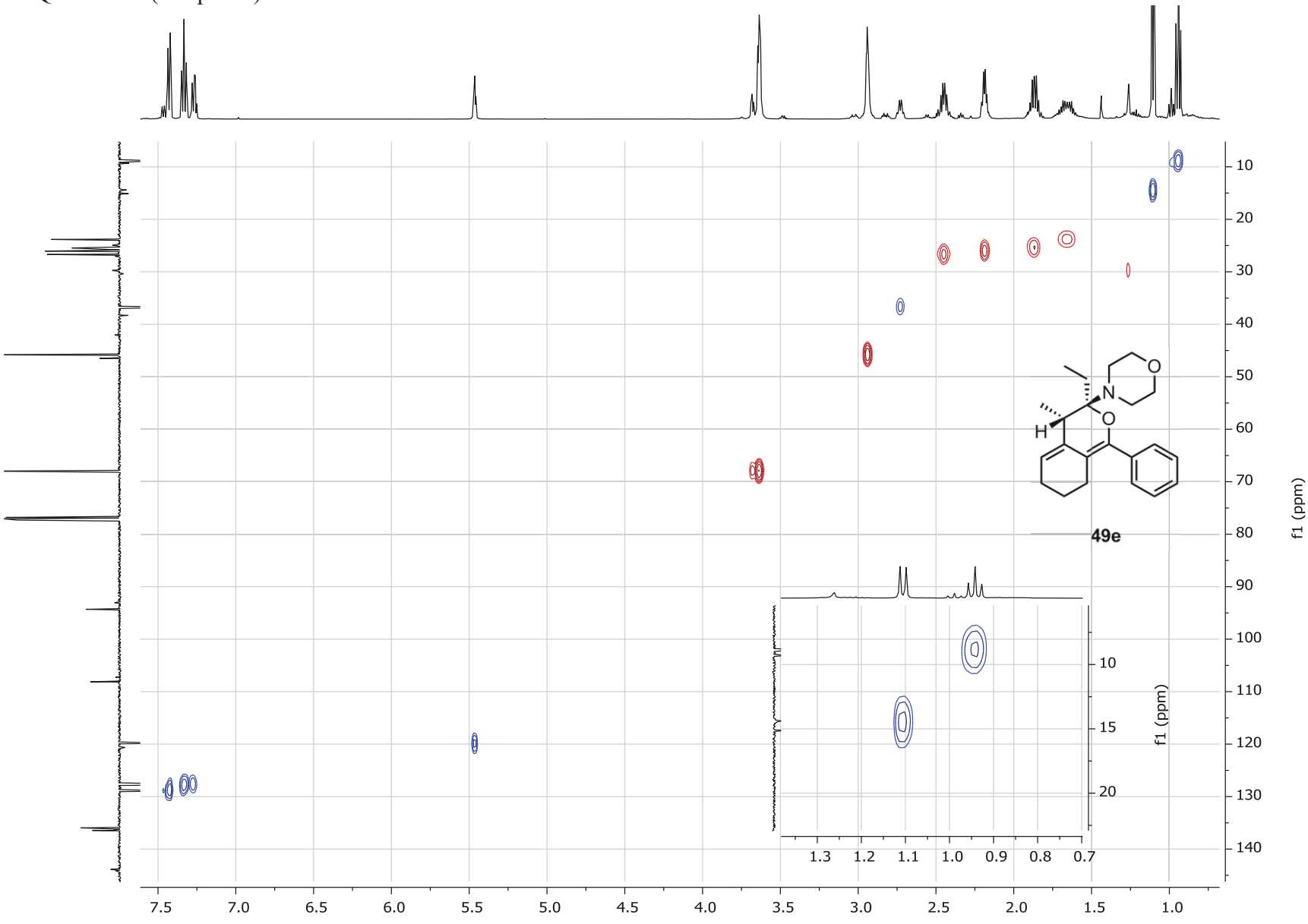

TROESY for **49e** (Chapter 3)

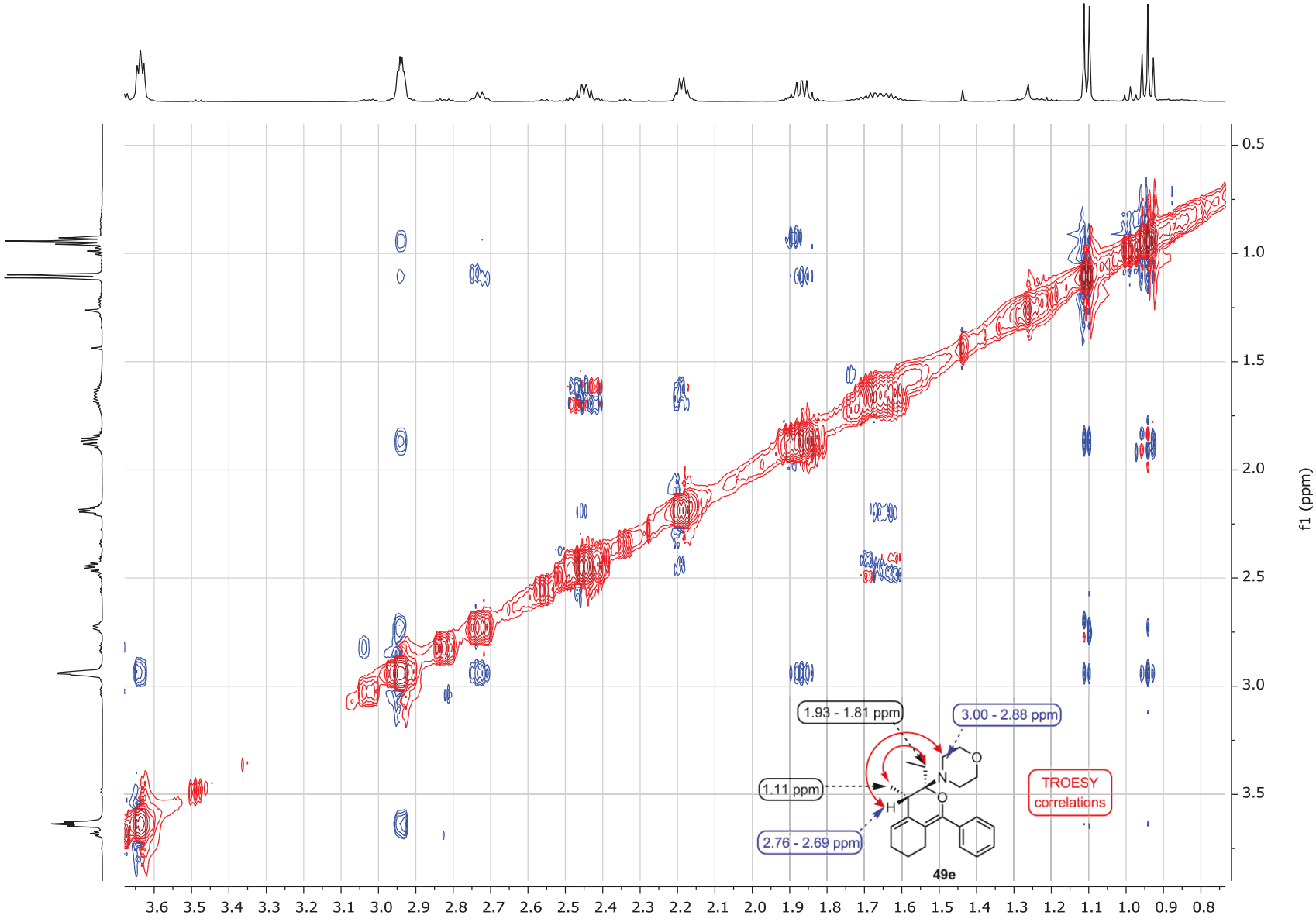


7.43
7.42
7.42
7.41
7.41
7.40
7.40
7.40
7.39
7.38
7.38
7.37
7.36
6.92
6.91
6.90


2.54
2.52
2.51
2.51
2.49
2.48
2.43
2.42
2.42
2.41
2.40
2.27
2.27
2.26
2.25
2.25
2.24
2.03
2.02
2.00
1.99
1.98
1.64
1.63
1.62
1.60
1.59

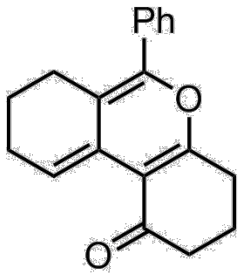
Ph
O
O

50

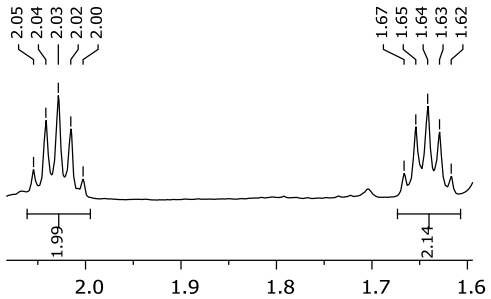
2.05
2.04
2.03
2.02
2.00
1.67
1.65
1.64
1.63
1.62
1.99
2.14
2.0
1.9
1.8
1.7
1.6

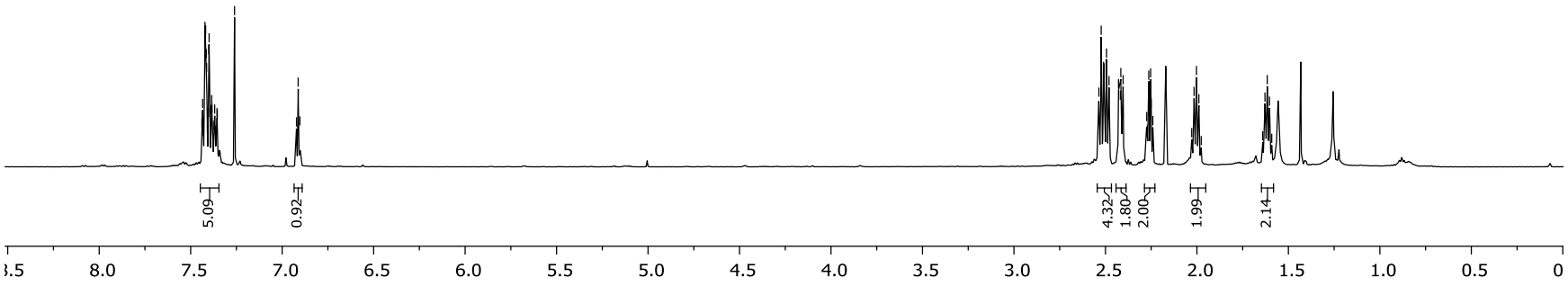
5.09
0.92
4.32
1.80
2.00
1.99
2.14
8.0
7.5
7.0
6.5
6.0
5.5
5.0
4.5
4.0
3.5
3.0
2.5
2.0
1.5
1.0
0.5
0

APT for **50** (Chapter 3)

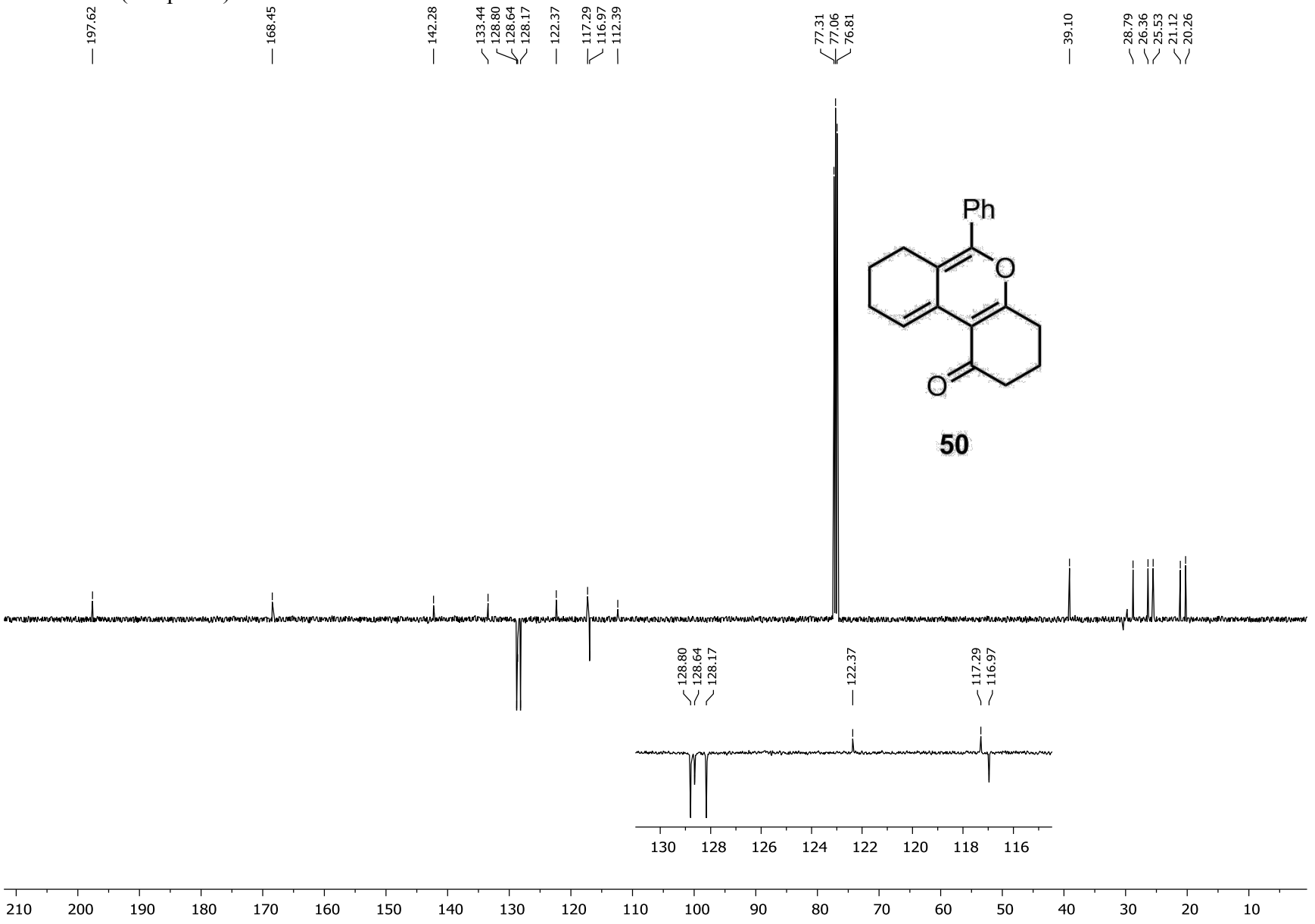

HSQC for **50** (Chapter 3)

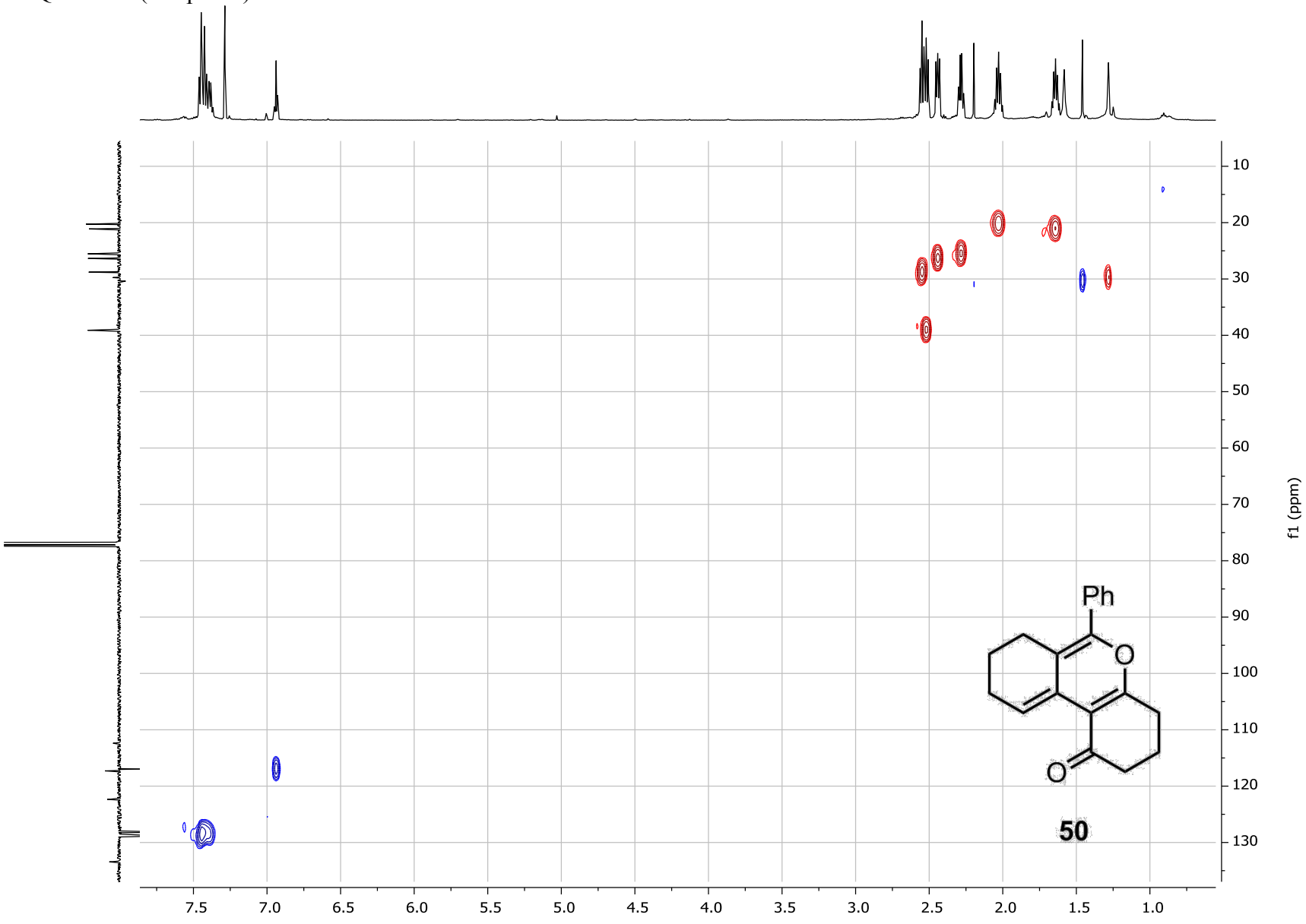

TOCSY for **50** (Chapter 3)

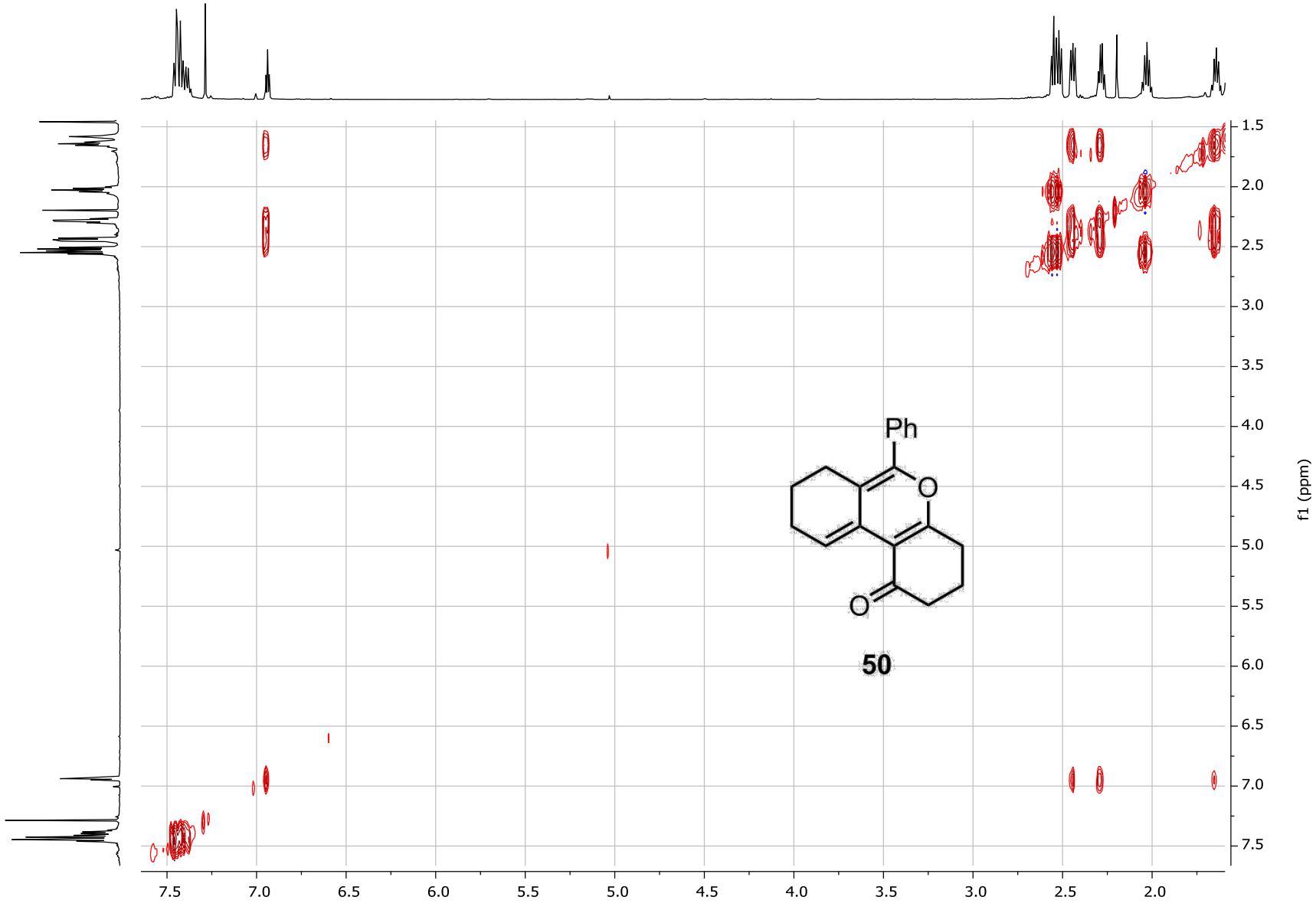

Apendix 1.3 X-ray for compound 49a Chapter 3

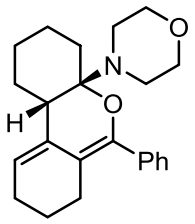

49a

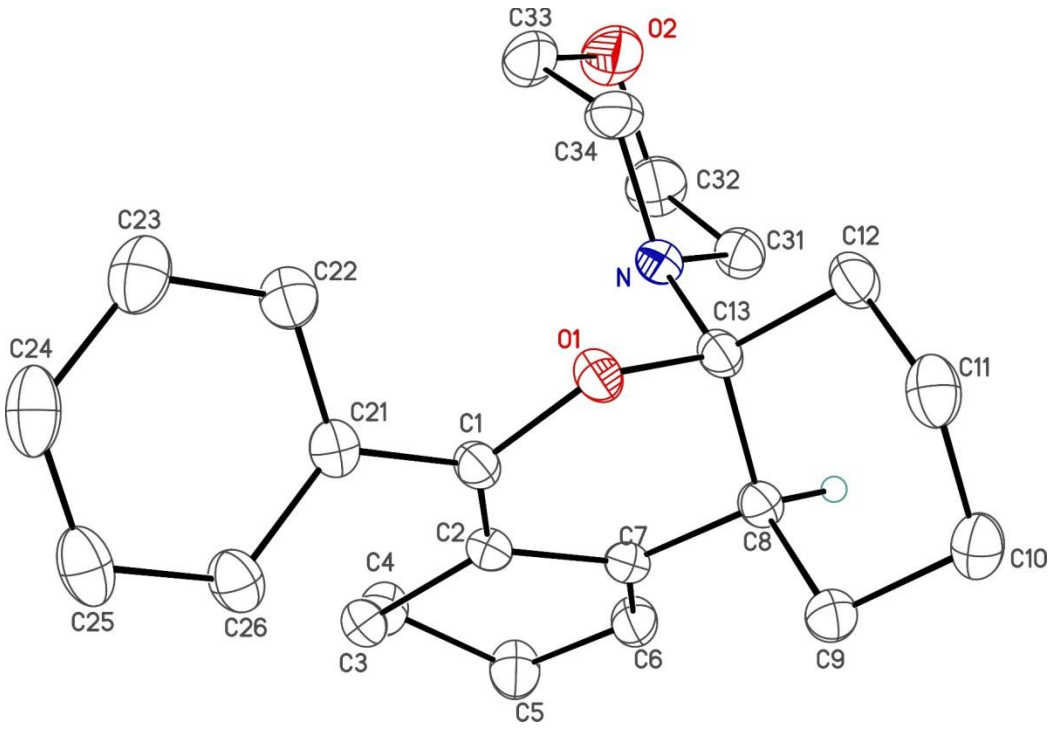

Table 1. Crystallographic Experimental Details

A. Crystal Data	
formula	$C_{23}H_{29}NO_2$
formula weight	351.47
crystal dimensions (mm)	0.36 × 0.27 × 0.26
crystal system	monoclinic
space group	$P2_1/c$ (No. 14)
unit cell parameters[a]	
a (Å)	15.4338(3)
b (Å)	8.3344(2)
c (Å)	16.0463(3)
β (deg)	110.5183(8)
V (Å^3)	1933.12(7)
Z	4
ρ_{calcd} (g cm^{-3})	1.208
μ (mm^{-1})	0.593
B. Data Collection and Refinement Conditions	
diffractometer	Bruker D8/APEX II CCD[b]
radiation (λ [Å])	Cu Kα (1.54178) (microfocus source)
temperature (°C)	–80
scan type	ω and ϕ scans (1.0°) (5 s exposures)
data collection 2θ limit (deg)	149.93
total data collected	66578 (-19 ≤ h ≤ 19, -9 ≤ k ≤ 10, -19 ≤ l ≤ 19)
independent reflections	3902 (R_{int} = 0.0480)
number of observed reflections (*NO*)	3560 [$F_o^2 \geq 2\sigma(F_o^2)$]

structure solution method	intrinsic phasing (*SHELXT-2014*[c])
refinement method	full-matrix least-squares on F^2 (*SHELXL–2017*[d])
absorption correction method	Gaussian integration (face-indexed)
range of transmission factors	0.9621–0.7950
data/restraints/parameters	3902 / 0 / 239
goodness-of-fit (*S*)[e] [all data]	1.103
final *R* indices[f]	
R_1 [$F_o^2 \geq 2\sigma(F_o^2)$]	0.0430
wR_2 [all data]	0.1286
largest difference peak and hole	0.183 and –0.213 e Å^{-3}

[a]Obtained from least-squares refinement of 9802 reflections with 6.12° < 2θ < 148.34°.

[b]Programs for diffractometer operation, data collection, data reduction and absorption correction were those supplied by Bruker.

(continued)

Table 1. Crystallographic Experimental Details (continued)

[c]Sheldrick, G. M. *Acta Crystallogr.* **2015**, *A71*, 3–8. (*SHELXT-2014*)

[d]Sheldrick, G. M. *Acta Crystallogr.* **2015**, *C71*, 3–8. (*SHELXL-2017*)

[e]$S = [\Sigma w(F_o^2 - F_c^2)^2/(n - p)]^{1/2}$ (n = number of data; p = number of parameters varied; $w = [\sigma^2(F_o^2) + (0.0673P)^2 + 0.4530P]^{-1}$ where $P = [\text{Max}(F_o^2, 0) + 2F_c^2]/3$).

[f]$R_1 = \Sigma||F_o| - |F_c||/\Sigma|F_o|$; $wR_2 = [\Sigma w(F_o^2 - F_c^2)^2/\Sigma w(F_o^4)]^{1/2}$.

Table 2. Atomic Coordinates and Equivalent Isotropic Displacement Parameters

Atom	*x*	*y*	*z*	U_{eq}, Å^2
O1	0.71104(5)	0.37267(10)	0.68193(5)	0.0344(2)*
O2	0.53163(9)	-0.12043(17)	0.69359(9)	0.0693(4)*
N	0.64683(7)	0.11503(13)	0.65666(7)	0.0359(3)*
C1	0.78813(8)	0.34536(14)	0.75709(7)	0.0313(3)*
C2	0.84835(8)	0.22543(14)	0.76283(7)	0.0309(3)*
C3	0.92586(8)	0.18042(16)	0.84794(8)	0.0359(3)*
C4	0.93700(10)	-0.00132(17)	0.85492(9)	0.0436(3)*
C5	0.95663(11)	-0.0698(2)	0.77551(9)	0.0513(4)*
C6	0.88951(9)	-0.00518(17)	0.68988(9)	0.0410(3)*
C7	0.83861(8)	0.12677(15)	0.68487(8)	0.0322(3)*
C8	0.76949(8)	0.18703(14)	0.59835(8)	0.0322(3)*
H8	0.7525(9)	0.0988(17)	0.5553(9)	0.032(3)
C9	0.80872(9)	0.32148(17)	0.55623(8)	0.0397(3)*
C10	0.73538(10)	0.38577(17)	0.47183(9)	0.0443(3)*
C11	0.65370(11)	0.45178(17)	0.49318(9)	0.0472(3)*
C12	0.61212(9)	0.32224(17)	0.53497(8)	0.0408(3)*
C13	0.68338(8)	0.24444(14)	0.61675(8)	0.0325(3)*
C21	0.79393(8)	0.46500(14)	0.82682(8)	0.0335(3)*
C22	0.71454(10)	0.51525(16)	0.84195(9)	0.0411(3)*
C23	0.71993(12)	0.62699(18)	0.90769(10)	0.0509(4)*
C24	0.80441(12)	0.68916(16)	0.95970(9)	0.0516(4)*
C25	0.88332(12)	0.64203(17)	0.94491(9)	0.0500(4)*
C26	0.87858(10)	0.53197(16)	0.87855(9)	0.0423(3)*
C31	0.63129(10)	-0.04054(16)	0.61192(9)	0.0424(3)*
C32	0.60945(13)	-0.1643(2)	0.67040(13)	0.0620(4)*
C33	0.54912(12)	0.0305(3)	0.73736(11)	0.0661(5)*
C34	0.56526(10)	0.1582(2)	0.67802(10)	0.0510(4)*

Anisotropically-refined atoms are marked with an asterisk (*). The form of the anisotropic displacement parameter is: $\exp[-2\pi^2(h^2a^{*2}U_{11} + k^2b^{*2}U_{22} + l^2c^{*2}U_{33} + 2klb^*c^*U_{23} + 2hla^*c^*U_{13} + 2hka^*b^*U_{12})]$.

Table 3. Selected Interatomic Distances (Å)

Atom1	Atom2	Distance	Atom1	Atom2	Distance
O1	C1	1.3842(14)	C8	C9	1.5381(17)
O1	C13	1.4510(14)	C8	C13	1.5354(16)
O2	C32	1.424(2)	C8	H8	0.980(14)
O2	C33	1.420(2)	C9	C10	1.5258(18)
N	C13	1.4646(16)	C10	C11	1.521(2)
N	C31	1.4606(17)	C11	C12	1.526(2)
N	C34	1.4608(17)	C12	C13	1.5299(16)
C1	C2	1.3458(17)	C21	C22	1.3944(18)
C1	C21	1.4778(16)	C21	C26	1.3954(18)
C2	C3	1.5139(15)	C22	C23	1.3876(19)
C2	C7	1.4601(16)	C23	C24	1.379(2)
C3	C4	1.5241(19)	C24	C25	1.377(2)
C4	C5	1.5203(19)	C25	C26	1.3878(19)
C5	C6	1.5011(19)	C31	C32	1.510(2)
C6	C7	1.3375(18)	C33	C34	1.506(2)
C7	C8	1.5097(16)			

Table 4. Selected Interatomic Angles (deg)

Atom1	Atom2	Atom3	Angle	Atom1	Atom2	Atom3	Angle
C1	O1	C13	116.92(9)	C8	C9	C10	111.23(10)
C32	O2	C33	108.97(12)	C9	C10	C11	110.04(11)
C13	N	C31	117.44(10)	C10	C11	C12	110.65(11)
C13	N	C34	114.65(11)	C11	C12	C13	112.96(11)
C31	N	C34	109.11(10)	O1	C13	N	106.75(9)
O1	C1	C2	122.94(10)	O1	C13	C8	108.20(9)
O1	C1	C21	110.74(10)	O1	C13	C12	104.33(9)
C2	C1	C21	126.32(11)	N	C13	C8	110.28(10)
C1	C2	C3	123.65(11)	N	C13	C12	114.57(10)
C1	C2	C7	119.90(10)	C8	C13	C12	112.19(10)
C3	C2	C7	116.41(10)	C1	C21	C22	120.72(11)
C2	C3	C4	110.22(10)	C1	C21	C26	121.06(11)
C3	C4	C5	111.21(12)	C22	C21	C26	118.22(12)
C4	C5	C6	110.88(11)	C21	C22	C23	120.78(13)
C5	C6	C7	123.52(12)	C22	C23	C24	120.28(14)
C2	C7	C6	121.99(11)	C23	C24	C25	119.62(13)
C2	C7	C8	115.33(10)	C24	C25	C26	120.58(14)
C6	C7	C8	122.65(11)	C21	C26	C25	120.49(14)
C7	C8	C9	112.73(10)	N	C31	C32	109.56(12)
C7	C8	C13	107.88(9)	O2	C32	C31	112.31(14)
C7	C8	H8	109.1(8)	O2	C33	C34	110.99(13)
C9	C8	C13	110.98(10)	N	C34	C33	108.76(14)
C9	C8	H8	106.6(8)				

Table 5. Torsional Angles (deg)

Atom1	Atom2	Atom3	Atom4	Angle	Atom1	Atom2	Atom3	Atom4	Angle
C13	O1	C1	C2	15.13(16)	C3	C4	C5	C6	-48.56(17)
C13	O1	C1	C21	-165.38(9)	C4	C5	C6	C7	18.1(2)
C1	O1	C13	N	70.33(12)	C5	C6	C7	C2	3.7(2)
C1	O1	C13	C8	-48.36(13)	C5	C6	C7	C8	-178.21(13)
C1	O1	C13	C12	-167.99(10)	C2	C7	C8	C9	80.52(13)
C33	O2	C32	C31	-57.80(19)	C2	C7	C8	C13	-42.37(13)
C32	O2	C33	C34	59.97(19)	C6	C7	C8	C9	-97.66(14)
C31	N	C13	O1	-168.06(10)	C6	C7	C8	C13	139.45(12)
C31	N	C13	C8	-50.74(13)	C7	C8	C9	C10	-176.78(10)
C31	N	C13	C12	76.98(14)	C13	C8	C9	C10	-55.64(13)
C34	N	C13	O1	61.84(12)	C7	C8	C13	O1	60.27(12)
C34	N	C13	C8	179.17(10)	C7	C8	C13	N	-56.15(12)
C34	N	C13	C12	-53.12(14)	C7	C8	C13	C12	174.83(10)
C13	N	C31	C32	170.44(12)	C9	C8	C13	O1	-63.68(12)
C34	N	C31	C32	-56.93(15)	C9	C8	C13	N	179.89(9)
C13	N	C34	C33	-166.63(11)	C9	C8	C13	C12	50.87(13)
C31	N	C34	C33	59.30(14)	C8	C9	C10	C11	59.48(15)
O1	C1	C2	C3	-171.87(10)	C9	C10	C11	C12	-58.15(15)
O1	C1	C2	C7	5.80(18)	C10	C11	C12	C13	54.43(15)
C21	C1	C2	C3	8.72(19)	C11	C12	C13	O1	65.94(13)
C21	C1	C2	C7	-173.61(11)	C11	C12	C13	N	-177.70(10)
O1	C1	C21	C22	39.77(15)	C11	C12	C13	C8	-50.96(14)
O1	C1	C21	C26	-139.53(12)	C1	C21	C22	C23	179.68(12)
C2	C1	C21	C22	-140.76(13)	C26	C21	C22	C23	-1.00(19)
C2	C1	C21	C26	39.94(18)	C1	C21	C26	C25	-178.82(12)
C1	C2	C3	C4	141.23(12)	C22	C21	C26	C25	1.86(19)
C7	C2	C3	C4	-36.51(14)	C21	C22	C23	C24	-0.5(2)
C1	C2	C7	C6	-171.78(12)	C22	C23	C24	C25	1.2(2)
C1	C2	C7	C8	10.02(16)	C23	C24	C25	C26	-0.4(2)
C3	C2	C7	C6	6.05(17)	C24	C25	C26	C21	-1.2(2)
C3	C2	C7	C8	-172.15(10)	N	C31	C32	O2	56.98(17)
C2	C3	C4	C5	58.16(15)	O2	C33	C34	N	-61.69(17)

Table 6. Anisotropic Displacement Parameters (U_{ij}, Å^2)

Atom	U_{11}	U_{22}	U_{33}	U_{23}	U_{13}	U_{12}
O1	0.0314(4)	0.0355(4)	0.0313(4)	-0.0040(3)	0.0049(3)	0.0027(3)
O2	0.0673(7)	0.0807(9)	0.0687(8)	-0.0103(6)	0.0346(6)	-0.0364(7)
N	0.0288(5)	0.0434(6)	0.0340(5)	-0.0046(4)	0.0092(4)	-0.0064(4)
C1	0.0291(5)	0.0332(6)	0.0289(6)	-0.0008(4)	0.0067(4)	-0.0038(4)
C2	0.0265(5)	0.0340(6)	0.0310(6)	-0.0012(4)	0.0086(4)	-0.0033(4)
C3	0.0307(6)	0.0429(7)	0.0308(6)	0.0007(5)	0.0067(5)	0.0003(5)
C4	0.0443(7)	0.0460(7)	0.0384(7)	0.0057(5)	0.0120(6)	0.0129(6)
C5	0.0493(8)	0.0573(9)	0.0437(8)	0.0001(6)	0.0120(6)	0.0222(7)
C6	0.0374(6)	0.0482(7)	0.0363(6)	-0.0051(5)	0.0115(5)	0.0087(5)
C7	0.0260(5)	0.0378(6)	0.0322(6)	-0.0026(5)	0.0095(4)	-0.0019(4)
C8	0.0301(6)	0.0342(6)	0.0305(6)	-0.0034(5)	0.0084(4)	-0.0025(4)
C9	0.0395(6)	0.0438(7)	0.0361(6)	-0.0012(5)	0.0138(5)	-0.0062(5)
C10	0.0560(8)	0.0405(7)	0.0356(7)	0.0015(5)	0.0152(6)	-0.0033(6)
C11	0.0573(8)	0.0428(7)	0.0357(7)	0.0040(6)	0.0091(6)	0.0082(6)
C12	0.0345(6)	0.0489(7)	0.0323(6)	-0.0003(5)	0.0033(5)	0.0054(5)
C13	0.0292(5)	0.0357(6)	0.0286(6)	-0.0036(5)	0.0053(4)	-0.0010(5)
C21	0.0399(6)	0.0275(5)	0.0310(6)	0.0021(4)	0.0097(5)	-0.0003(5)
C22	0.0435(7)	0.0366(6)	0.0413(7)	-0.0013(5)	0.0125(5)	0.0059(5)
C23	0.0669(9)	0.0414(7)	0.0458(8)	-0.0001(6)	0.0214(7)	0.0162(7)
C24	0.0842(11)	0.0301(6)	0.0347(7)	-0.0021(5)	0.0137(7)	0.0084(7)
C25	0.0647(9)	0.0356(7)	0.0390(7)	-0.0046(5)	0.0048(6)	-0.0077(6)
C26	0.0458(7)	0.0365(7)	0.0402(7)	-0.0046(5)	0.0096(6)	-0.0070(5)
C31	0.0426(7)	0.0415(7)	0.0419(7)	-0.0040(6)	0.0132(5)	-0.0080(6)
C32	0.0672(10)	0.0554(9)	0.0659(10)	0.0055(8)	0.0263(8)	-0.0161(8)

C33	0.0552(9)	0.0973(14)	0.0539(9)	-0.0205(9)	0.0295(8)	-0.0341(9)
C34	0.0368(7)	0.0663(9)	0.0536(8)	-0.0184(7)	0.0206(6)	-0.0129(6)

The form of the anisotropic displacement parameter is:

$\exp[-2\pi^2(h^2a^{*2}U_{11} + k^2b^{*2}U_{22} + l^2c^{*2}U_{33} + 2klb^*c^*U_{23} + 2hla^*c^*U_{13} + 2hka^*b^*U_{12})]$

Table 7. Derived Atomic Coordinates and Displacement Parameters for Hydrogen Atoms

Atom	*x*	*y*	*z*	U_{eq}, Å^2
H3A	0.911935	0.221683	0.899722	0.043
H3B	0.984375	0.230072	0.848608	0.043
H4A	0.988509	-0.029007	0.910321	0.052
H4B	0.879726	-0.050090	0.858032	0.052
H5A	1.020473	-0.041585	0.780163	0.062
H5B	0.951860	-0.188206	0.775799	0.062
H6	0.882825	-0.061025	0.636365	0.049
H9A	0.831494	0.410015	0.599556	0.048
H9B	0.861746	0.279582	0.541682	0.048
H10A	0.762351	0.471730	0.445949	0.053
H10B	0.714138	0.298513	0.427430	0.053
H11A	0.605976	0.491397	0.437913	0.057
H11B	0.674382	0.543267	0.534817	0.057
H12A	0.583924	0.238216	0.490014	0.049
H12B	0.562306	0.370314	0.552375	0.049
H22	0.656065	0.472472	0.806844	0.049
H23	0.665197	0.660810	0.916915	0.061
H24	0.808146	0.764063	1.005457	0.062
H25	0.941520	0.685228	0.980449	0.060
H26	0.933365	0.501997	0.868263	0.051
H31A	0.687249	-0.073151	0.599509	0.051
H31B	0.579176	-0.032634	0.554524	0.051
H32A	0.596963	-0.268553	0.638876	0.074
H32B	0.663981	-0.177973	0.725425	0.074

H33A	0.604215	0.022045	0.792324	0.079
H33B	0.495682	0.061024	0.754519	0.079
H34A	0.510609	0.166859	0.622690	0.061
H34B	0.575020	0.263268	0.708693	0.061

Apendix 1.4 Selected ^{1}H NMR and ^{13}C NMR from Chapter 4

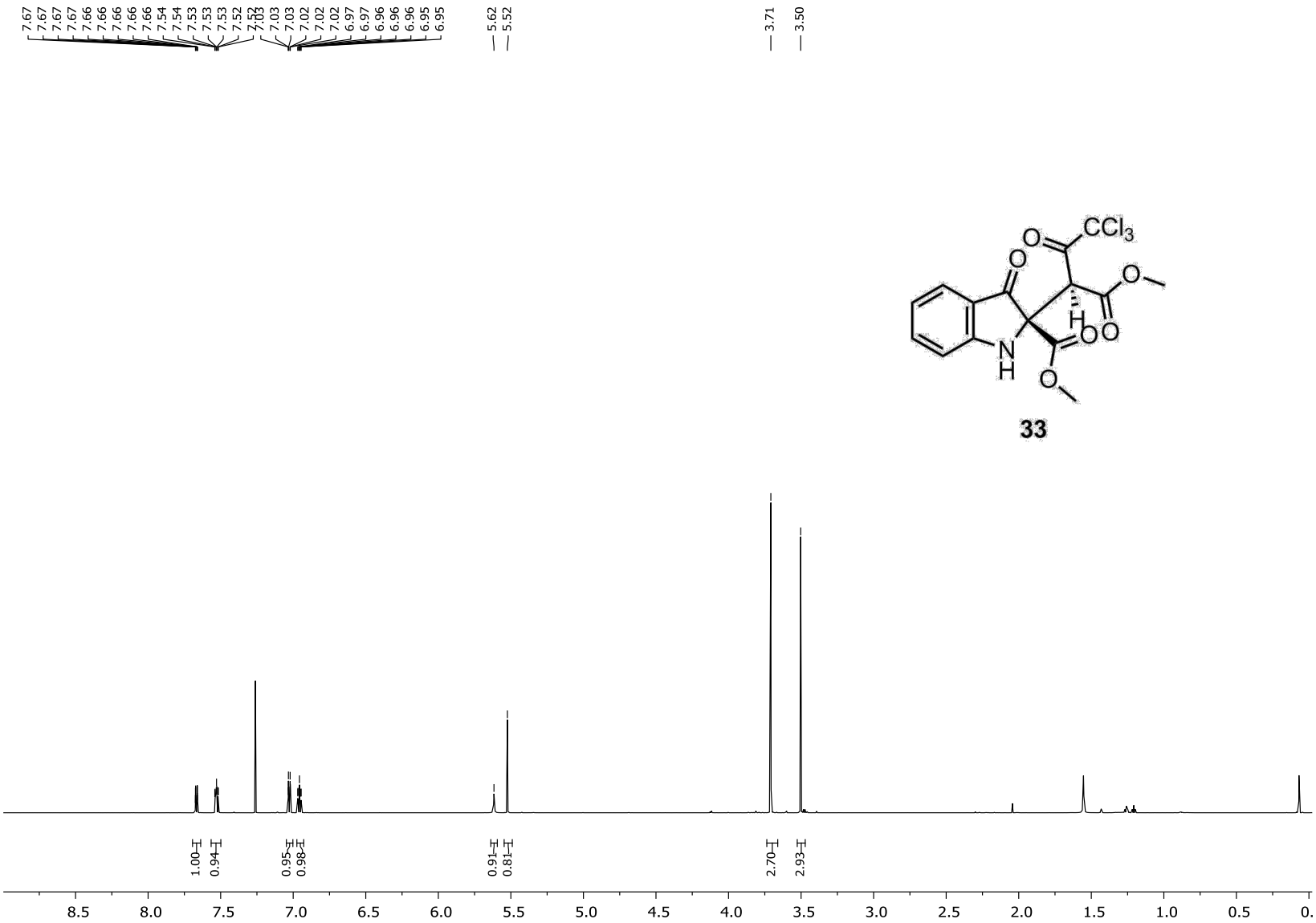
7.67
7.67
7.67
7.67
7.66
7.66
7.66
7.66
7.66
7.54
7.54
7.53
7.53
7.53
7.52
7.52
7.03
7.03
7.03
7.02
7.02
7.02
6.97
6.97
6.96
6.96
6.96
6.95
6.95
5.62
5.52
3.71
3.50
CCl3
O
O
O
O
O
O
H
N
H
O
1.00
0.94
0.95
0.98
0.91
0.81
2.70
2.93
8.5
8.0
7.5
7.0
6.5
6.0
5.5
5.0
4.5
4.0
3.5
3.0
2.5
2.0
1.5
1.0
0.5
0.

33

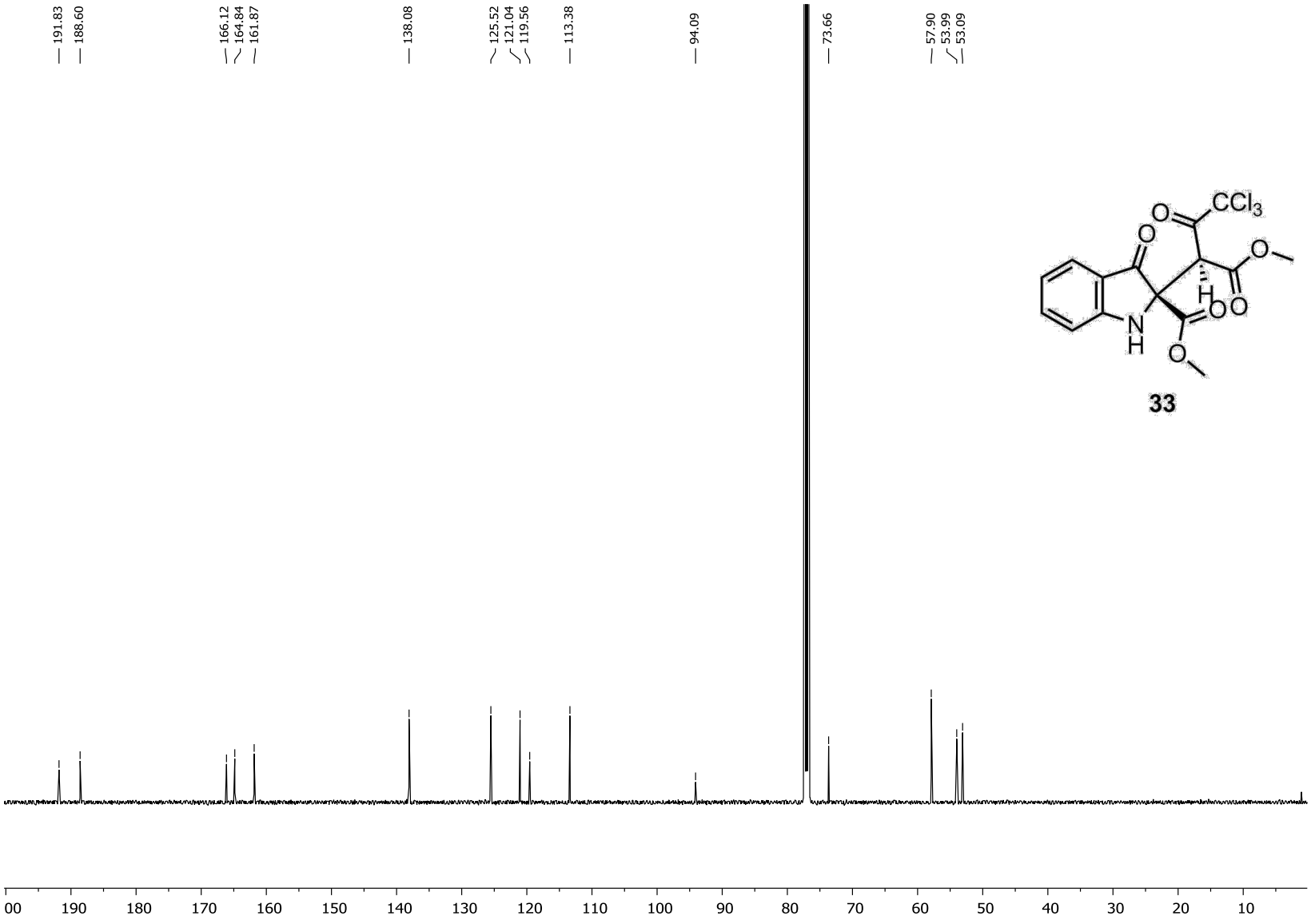
191.83
188.60
166.12
164.84
161.87
138.08
125.52
121.04
119.56
113.38
94.09
73.66
57.90
53.99
53.09
CCl3
O
O
O
O
O
O
H
N
H
O
33
00
190
180
170
160
150
140
130
120
110
100
90
80
70
60
50
40
30
20
10

APT for **33** (Chapter 4)

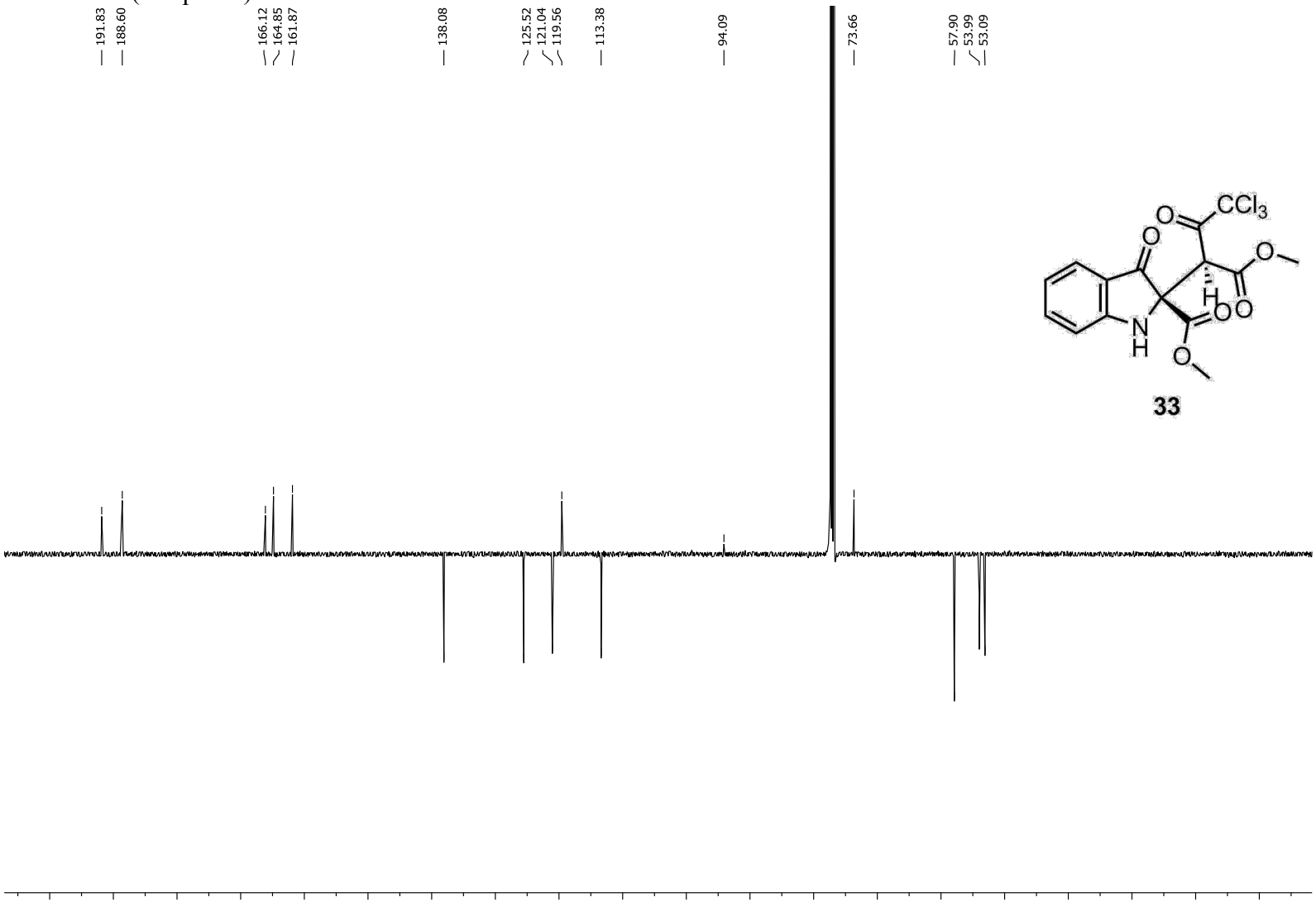

33

Apendix 1.5 X-ray compound 33 from Chapter 4

STRUCTURE REPORT

XCL Code: FGW1505 **Date:** 26 August 2015

Compound: Methyl 3-oxo-2-(4,4,4-trichloro-1-methoxy-1,3-dioxobutan-2-yl)-2,3-dihydro-1*H*-indole-2-carboxylate

Formula: $C_{15}H_{12}Cl_3NO_6$

Supervisor: F. G. West **Crystallographer:** M. J. Ferguson

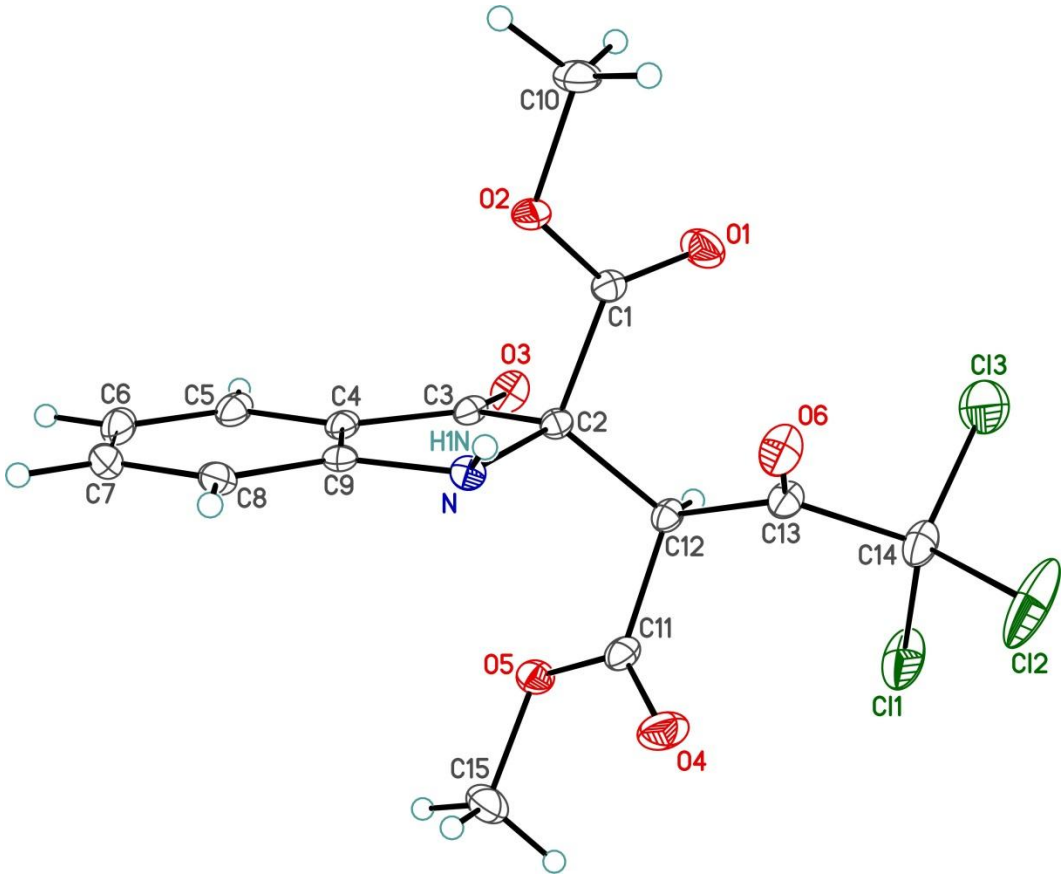

Figure Legends

Figure 1. Perspective view of the methyl 3-oxo-2-(4,4,4-trichloro-1-methoxy-1,3-dioxobutan-2-yl)-2,3-dihydro-1*H*-indole-2-carboxylate molecule showing the atom labelling scheme. Non-hydrogen atoms are represented by Gaussian ellipsoids at the 30% probability level. Hydrogen atoms are shown with arbitrarily small thermal parameters.

Figure 2. Alternate view showing the hydrogen-bonded interactions between inversion related molecules.

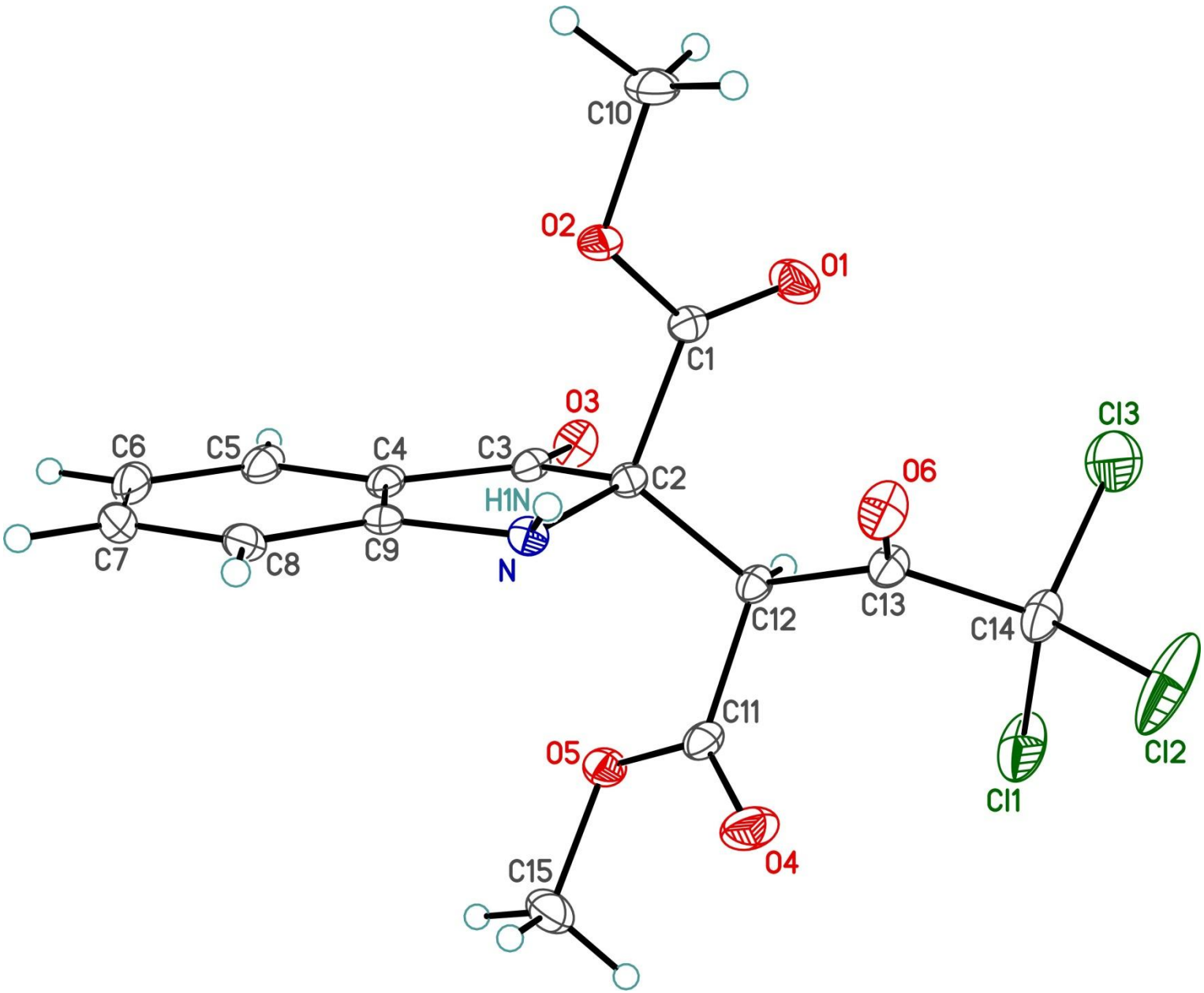
C10
O2
O1
C1
O3
C6
C5
C4
C3
C2
Cl3
O6
H1N
C7
C8
C9
N
C12
C13
C14
C11
O5
Cl2
Cl1
O4
C15

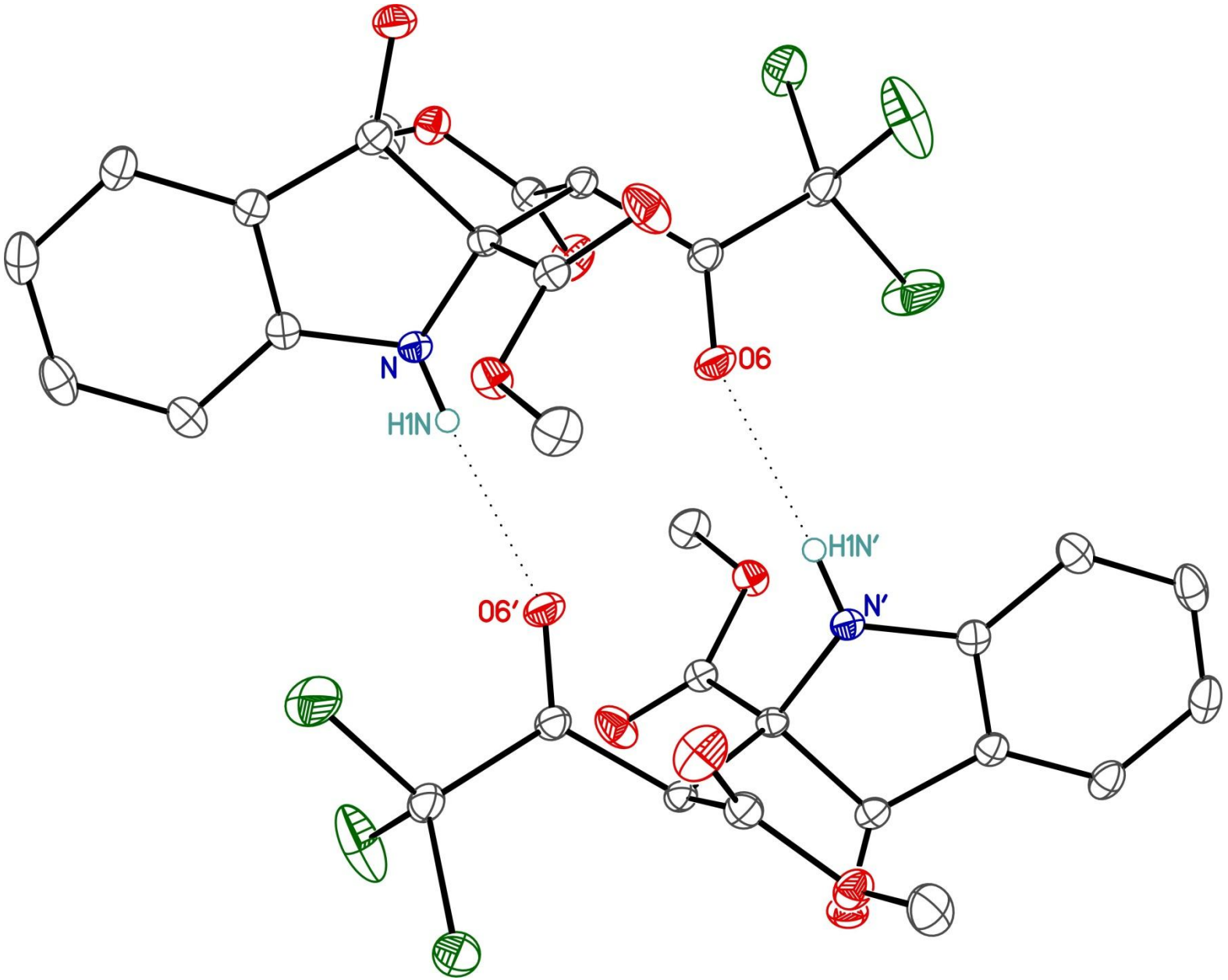
N
H1N
O6
O6′
H1N′
N′

List of Tables

Table 1. Crystallographic Experimental Details

A. Crystal Data	
formula	$C_{15}H_{12}Cl_3NO_6$
formula weight	408.61
crystal dimensions (mm)	$0.32 \times 0.27 \times 0.27$
crystal system	triclinic
space group	$P\bar{1}$ (No. 2)
unit cell parameters[a]	
a (Å)	8.4188 (2)
b (Å)	9.0260 (2)
c (Å)	11.5335 (3)
α (deg)	94.2131 (6)
β (deg)	103.4316 (8)
γ (deg)	93.9818 (7)
V (Å^3)	846.75 (4)
Z	2
ρ_{calcd} (g cm^{-3})	1.603
μ (mm^{-1})	5.214
B. Data Collection and Refinement Conditions	
diffractometer	Bruker D8/APEX II CCD[b]
radiation (λ [Å])	Cu Kα (1.54178) (microfocus source)
temperature (°C)	–100
scan type	ω and ϕ scans (1.0°) (5 s exposures)
data collection 2θ limit (deg)	144.71
total data collected	5917 ($-10 \le h \le 9$, $-11 \le k \le 11$, $-14 \le l \le 14$)

independent reflections	3215 (R_{int} = 0.0166)
number of observed reflections (*NO*)	3182 [$F_o^2 \geq 2\sigma(F_o^2)$]
structure solution method	intrinsic phasing (*SHELXT-2014*[c])
refinement method	full-matrix least-squares on F^2 (*SHELXL–2014*[d])
absorption correction method	Gaussian integration (face-indexed)
range of transmission factors	0.4974–0.2963
data/restraints/parameters	3215 / 0 / 232
goodness-of-fit (*S*)[e] [all data]	1.044
final *R* indices[f]	
R_1 [$F_o^2 \geq 2\sigma(F_o^2)$]	0.0483
wR_2 [all data]	0.1157
largest difference peak and hole	1.120 and –1.068 e Å^{-3}

[a]Obtained from least-squares refinement of 9778 reflections with 9.86° < 2θ < 144.60°.

(continued)

Table 1. Crystallographic Experimental Details (continued)

[b]Programs for diffractometer operation, data collection, data reduction and absorption correction were those supplied by Bruker.

[c]Sheldrick, G. M. *Acta Crystallogr.* **2015**, *A71*, 3–8. (*SHELXT-2014*)

[d]Sheldrick, G. M. *Acta Crystallogr.* **2015**, *C71*, 3–8. (*SHELXL-2014*)

[e]$S = [\Sigma w(F_o^2 - F_c^2)^2/(n-p)]^{1/2}$ (n = number of data; p = number of parameters varied; $w = [\sigma^2(F_o^2) + (0.0472P)^2 + 1.1993P]^{-1}$ where $P = [\mathrm{Max}(F_o^2, 0) + 2F_c^2]/3$).

[f]$R_1 = \Sigma||F_o| - |F_c||/\Sigma|F_o|$; $wR_2 = [\Sigma w(F_o^2 - F_c^2)^2/\Sigma w(F_o^4)]^{1/2}$.

Table 2. Atomic Coordinates and Equivalent Isotropic Displacement Parameters

Atom	*x*	*y*	*z*	U_{eq}, Å^2
Cl1	0.69639(11)	0.22912(9)	0.13862(6)	0.0546(2)*
Cl2	0.73865(16)	0.14357(9)	0.37651(8)	0.0776(4)*
Cl3	0.94429(10)	0.38763(11)	0.32603(11)	0.0748(3)*
O1	0.7777(2)	0.7125(2)	0.38181(16)	0.0372(4)*
O2	0.58105(19)	0.80509(17)	0.46006(13)	0.0254(3)*
O3	0.5634(2)	0.79623(18)	0.12127(14)	0.0297(4)*
O4	0.3452(2)	0.29371(18)	0.18556(17)	0.0394(4)*
O5	0.31951(19)	0.47225(17)	0.05853(13)	0.0269(3)*
O6	0.6137(2)	0.42614(19)	0.42289(14)	0.0332(4)*
N	0.3396(2)	0.63161(19)	0.31055(16)	0.0200(4)*
H1N	0.346(3)	0.614(3)	0.383(3)	0.029(7)
C1	0.6368(3)	0.7246(2)	0.37985(18)	0.0207(4)*
C2	0.4959(2)	0.6504(2)	0.27828(17)	0.0183(4)*
C3	0.4679(3)	0.7665(2)	0.18206(17)	0.0206(4)*
C4	0.3126(3)	0.8245(2)	0.18694(18)	0.0211(4)*
C5	0.2353(3)	0.9410(2)	0.13027(19)	0.0278(5)*
C6	0.0882(3)	0.9751(3)	0.1541(2)	0.0330(5)*
C7	0.0196(3)	0.8936(3)	0.2320(2)	0.0320(5)*
C8	0.0954(3)	0.7785(2)	0.2890(2)	0.0263(5)*
C9	0.2445(3)	0.7446(2)	0.26561(17)	0.0203(4)*
C10	0.7033(3)	0.8728(3)	0.5645(2)	0.0327(5)*
C11	0.3930(3)	0.4090(2)	0.15499(19)	0.0238(4)*
C12	0.5467(3)	0.5041(2)	0.22510(17)	0.0199(4)*
C13	0.6305(3)	0.4111(2)	0.32277(18)	0.0236(4)*
C14	0.7456(3)	0.2943(3)	0.2905(2)	0.0317(5)*
C15	0.1702(3)	0.3881(3)	-0.0113(2)	0.0379(6)*

Anisotropically-refined atoms are marked with an asterisk (*). The form of the anisotropic displacement parameter is: $\exp[-2\pi^2(h^2a^{*2}U_{11} + k^2b^{*2}U_{22} + l^2c^{*2}U_{33} + 2klb^*c^*U_{23} + 2hla^*c^*U_{13} + 2hka^*b^*U_{12})]$.

Table 3. Selected Interatomic Distances (Å)

Atom1	Atom2	Distance	Atom1	Atom2	Distance
Cl1	C14	1.751(2)	C2	C3	1.571(3)
Cl2	C14	1.747(2)	C2	C12	1.544(3)
Cl3	C14	1.764(3)	C3	C4	1.453(3)
O1	C1	1.194(3)	C4	C5	1.398(3)
O2	C1	1.324(3)	C4	C9	1.397(3)
O2	C10	1.453(3)	C5	C6	1.379(4)
O3	C3	1.213(3)	C6	C7	1.401(4)
O4	C11	1.196(3)	C7	C8	1.384(3)
O5	C11	1.330(3)	C8	C9	1.393(3)
O5	C15	1.453(3)	C11	C12	1.524(3)
O6	C13	1.195(3)	C12	C13	1.524(3)
N	C2	1.451(3)	C13	C14	1.563(3)
N	C9	1.396(3)	H1N	O6’	2.25(3)†
C1	C2	1.535(3)	N	O6’	3.095(2)‡

Primed atoms related to unprimed ones by inversion centre located at (0.5, 0.5, 0.5).

†Hydrogen bonded H1N···O6’ interaction.

‡Nonbonded donor-acceptor distance.

Table 4. Selected Interatomic Angles (deg)

Atom1	Atom2	Atom3	Angle	Atom1	Atom2	Atom3	Angle
C1	O2	C10	116.14(18)	C7	C8	C9	117.4(2)
C11	O5	C15	114.07(18)	N	C9	C4	112.38(18)
C2	N	C9	108.63(16)	N	C9	C8	127.1(2)
O1	C1	O2	125.77(19)	C4	C9	C8	120.5(2)
O1	C1	C2	122.83(19)	O4	C11	O5	125.3(2)
O2	C1	C2	111.36(17)	O4	C11	C12	123.4(2)
N	C2	C1	114.16(16)	O5	C11	C12	111.34(17)
N	C2	C3	103.94(16)	C2	C12	C11	108.90(17)
N	C2	C12	113.08(16)	C2	C12	C13	111.67(16)
C1	C2	C3	104.89(15)	C11	C12	C13	106.10(17)
C1	C2	C12	109.98(16)	O6	C13	C12	122.6(2)
C3	C2	C12	110.26(16)	O6	C13	C14	119.08(19)
O3	C3	C2	123.83(19)	C12	C13	C14	118.32(17)
O3	C3	C4	130.86(19)	Cl1	C14	Cl2	109.37(13)
C2	C3	C4	105.30(17)	Cl1	C14	Cl3	108.26(14)
C3	C4	C5	130.3(2)	Cl1	C14	C13	113.39(16)
C3	C4	C9	108.05(18)	Cl2	C14	Cl3	110.46(14)
C5	C4	C9	121.6(2)	Cl2	C14	C13	109.42(16)
C4	C5	C6	117.9(2)	Cl3	C14	C13	105.88(16)
C5	C6	C7	120.3(2)	N	H1N	O6’	175(3)†
C6	C7	C8	122.3(2)				

Primed atoms related to unprimed ones by inversion centre located at (0.5, 0.5, 0.5).

†Includes hydrogen-bonded H1N···O6’ interaction.

Table 5. Torsional Angles (deg)

Atom1	Atom2	Atom3	Atom4	Angle	Atom1	Atom2	Atom3	Atom4	Angle
C10	O2	C1	O1	-5.9(3)	O3	C3	C4	C9	175.4(2)
C10	O2	C1	C2	176.16(17)	C2	C3	C4	C5	172.7(2)
C15	O5	C11	O4	-0.2(3)	C2	C3	C4	C9	-5.5(2)
C15	O5	C11	C12	-178.98(18)	C3	C4	C5	C6	-178.2(2)
C9	N	C2	C1	100.65(19)	C9	C4	C5	C6	-0.2(3)
C9	N	C2	C3	-13.03(19)	C3	C4	C9	N	-2.7(2)
C9	N	C2	C12	-132.61(17)	C3	C4	C9	C8	179.03(18)
C2	N	C9	C4	10.5(2)	C5	C4	C9	N	178.90(18)
C2	N	C9	C8	-171.33(19)	C5	C4	C9	C8	0.6(3)
O1	C1	C2	N	158.8(2)	C4	C5	C6	C7	-0.5(3)
O1	C1	C2	C3	-88.1(2)	C5	C6	C7	C8	0.8(3)
O1	C1	C2	C12	30.5(3)	C6	C7	C8	C9	-0.4(3)
O2	C1	C2	N	-23.2(2)	C7	C8	C9	N	-178.35(19)
O2	C1	C2	C3	89.9(2)	C7	C8	C9	C4	-0.3(3)
O2	C1	C2	C12	-151.56(17)	O4	C11	C12	C2	-112.0(2)
N	C2	C3	O3	-169.59(19)	O4	C11	C12	C13	8.4(3)
N	C2	C3	C4	11.28(19)	O5	C11	C12	C2	66.8(2)
C1	C2	C3	O3	70.3(2)	O5	C11	C12	C13	-172.83(17)
C1	C2	C3	C4	-108.88(18)	C2	C12	C13	O6	21.1(3)
C12	C2	C3	O3	-48.1(3)	C2	C12	C13	C14	-157.53(19)
C12	C2	C3	C4	132.76(17)	C11	C12	C13	O6	-97.4(2)
N	C2	C12	C11	33.1(2)	C11	C12	C13	C14	83.9(2)
N	C2	C12	C13	-83.8(2)	O6	C13	C14	Cl1	155.1(2)
C1	C2	C12	C11	162.00(16)	O6	C13	C14	Cl2	32.7(3)
C1	C2	C12	C13	45.2(2)	O6	C13	C14	Cl3	-86.3(2)
C3	C2	C12	C11	-82.8(2)	C12	C13	C14	Cl1	-26.2(3)
C3	C2	C12	C13	160.36(17)	C12	C13	C14	Cl2	-148.62(17)
O3	C3	C4	C5	-6.3(4)	C12	C13	C14	Cl3	92.3(2)

Table 6. Anisotropic Displacement Parameters (U_{ij}, Å^2)

Atom	U_{11}	U_{22}	U_{33}	U_{23}	U_{13}	U_{12}
Cl1	0.0842(6)	0.0562(4)	0.0256(3)	-0.0054(3)	0.0105(3)	0.0402(4)
Cl2	0.1528(10)	0.0439(4)	0.0644(5)	0.0334(4)	0.0607(6)	0.0559(5)
Cl3	0.0366(4)	0.0637(5)	0.1160(8)	-0.0251(5)	0.0087(4)	0.0167(4)
O1	0.0209(9)	0.0489(10)	0.0385(9)	-0.0109(8)	0.0056(7)	0.0012(7)
O2	0.0251(8)	0.0268(8)	0.0208(7)	-0.0080(6)	0.0019(6)	0.0019(6)
O3	0.0374(9)	0.0281(8)	0.0291(8)	0.0077(6)	0.0168(7)	0.0044(7)
O4	0.0491(11)	0.0230(8)	0.0411(10)	0.0050(7)	0.0032(8)	-0.0067(7)
O5	0.0295(8)	0.0274(8)	0.0203(7)	-0.0008(6)	0.0001(6)	0.0018(6)
O6	0.0495(11)	0.0346(9)	0.0195(8)	0.0065(6)	0.0118(7)	0.0145(8)
N	0.0210(9)	0.0216(8)	0.0174(8)	0.0019(6)	0.0051(7)	0.0013(7)
C1	0.0233(11)	0.0182(9)	0.0202(9)	0.0012(7)	0.0048(8)	0.0006(8)
C2	0.0205(10)	0.0179(9)	0.0166(9)	0.0004(7)	0.0050(7)	0.0011(7)
C3	0.0274(11)	0.0160(9)	0.0172(9)	-0.0004(7)	0.0041(8)	0.0009(8)
C4	0.0258(11)	0.0183(9)	0.0170(9)	-0.0027(7)	0.0018(8)	0.0017(8)
C5	0.0376(13)	0.0222(10)	0.0201(10)	-0.0005(8)	-0.0002(9)	0.0064(9)
C6	0.0355(13)	0.0281(11)	0.0291(11)	-0.0043(9)	-0.0056(10)	0.0127(10)
C7	0.0212(11)	0.0343(12)	0.0348(12)	-0.0109(10)	-0.0019(9)	0.0065(9)
C8	0.0197(10)	0.0281(11)	0.0282(11)	-0.0061(8)	0.0033(8)	-0.0014(8)
C9	0.0212(10)	0.0186(9)	0.0172(9)	-0.0051(7)	-0.0005(7)	0.0002(8)
C10	0.0375(13)	0.0313(12)	0.0228(11)	-0.0075(9)	-0.0016(9)	-0.0017(10)
C11	0.0305(12)	0.0192(10)	0.0211(10)	-0.0023(8)	0.0060(8)	0.0037(8)
C12	0.0260(11)	0.0181(9)	0.0162(9)	0.0013(7)	0.0052(8)	0.0048(8)
C13	0.0305(12)	0.0212(10)	0.0194(10)	0.0021(8)	0.0058(8)	0.0048(8)
C14	0.0467(15)	0.0273(11)	0.0230(11)	0.0046(9)	0.0077(10)	0.0155(10)

C15	0.0258(12)	0.0465(15)	0.0352(13)	-0.0080(11)	-0.0013(10)	0.0014(10)

The form of the anisotropic displacement parameter is:

$\exp[-2\pi^2(h^2a^{*2}U_{11} + k^2b^{*2}U_{22} + l^2c^{*2}U_{33} + 2klb^*c^*U_{23} + 2hla^*c^*U_{13} + 2hka^*b^*U_{12})]$

Table 7. Derived Atomic Coordinates and Displacement Parameters for Hydrogen Atoms

Atom	*x*	*y*	*z*	U_{eq}, Å^2
H5	0.2825	0.9949	0.0770	0.033
H6	0.0332	1.0542	0.1174	0.040
H7	-0.0825	0.9182	0.2463	0.038
H8	0.0476	0.7247	0.3420	0.032
H10A	0.6580	0.9547	0.6031	0.039
H10B	0.8007	0.9115	0.5397	0.039
H10C	0.7335	0.7977	0.6210	0.039
H12	0.6208	0.5268	0.1712	0.024
H15A	0.1177	0.4456	-0.0762	0.046
H15B	0.0952	0.3692	0.0405	0.046
H15C	0.1971	0.2930	-0.0451	0.046